2015

Comprehensive study on the sustainable technology of asphalt rubber for hot mix asphalt binders and mixes

Ka Lai Nieve Ng Puga
Iowa State University

Comprehensive study on the sustainable technology of asphalt rubber for hot mix asphalt binders and mixes

by

Ka Lai Nieve Ng Puga

A dissertation submitted to the graduate faculty

in partial fulfillment of the requirements for the degree of

DOCTOR OF PHILOSOPHY

Major: Civil Engineering (Civil Engineering Materials)

Program of Study Committee:
R. Christopher Williams, Major Professor
Jeramy C. Ashlock
Eric W. Cochran
W. Robert Stephenson
Kejin Wang

Iowa State University

Ames, Iowa

2015

TABLE OF CONTENTS

Page

LIST OF FIGURES

Page

LIST OF TABLES

Page

NOMENCLATURE

AMB	Ambient
AP	Ambient rubber with polyoctenamer
AR	Asphalt rubber
CC	Concentric cylinders
CP	Cryogenic rubber with polyoctenamer
CRYO	Cryogenic
GTR	Ground tire rubber
NMAS	Nominal maximum aggregate size
PO	Polyoctenamer
TOR	Trans-polyoctenamer, same as Polyoctenamer

ACKNOWLEDGMENTS

Firstly I want to thank God, because without all His blessings I would have not been able to finish this dissertation. I would like to thank my major professor, Dr. R. Christopher Williams, for all his support and invaluable advice throughout my graduate studies, and for always believing in me. I would like to acknowledge and thank Dr. W. Robert Stephenson's guidance in the statistical analyses of my research. Thanks to Dr. Eric Cochran who allowed me to use his laboratory facilities. I would also like to Dr. Jeramy Ashlock, and Dr. Kejin Wang, for serving as my committee members and for all the valuable feedback they have provided me not only during the development of this dissertation but also during my graduate studies.

Special thanks to the industry companies who did not hesitate on providing me with the materials needed to perform my doctoral research, especially Seneca Petroleum. I would like to give a special thanks to my family, especially to my sisters, for all their love, support and encouragement, they have being my supporting rocks from the distance. In addition, I would also like to thank my friends, colleagues in the asphalt laboratory, the department faculty and staff for making my time at Iowa State University a wonderful experience.

ABSTRACT

Asphalt rubber (AR) technology is considered a sustainable technology. The high amounts of scrap tires that are in landfills, dumps and stockpiles present an environmental issue. By recycling and reusing ground tire rubber (GTR) in asphalt binders, this environmental issue is not only being addressed but also the overall performance of asphalt pavements is being improved. Although AR technology presents benefits to the fatigue performance of asphalt pavements as reported by the literature, it also presents certain challenges. One of these challenges is its workability, related to the higher viscosities of the binder at conventional mixing and compaction temperatures, leading to having higher mixing and compaction temperatures to obtain the desired workability. The second challenge is related to the rheology characterization of AR binders. While the addition of GTR to asphalt significantly improves the performance of AR mixes, the rheological characterization of AR binders using established performance grade methods for conventional or polymer-modified binders is not suitable to AR binders.

Chemical additives, as polyoctenamer, can be added to AR binders to improve their workability. The effects of polyoctenamer on the performance of AR mixes has not being widely evaluated. The approach of this dissertation is two-fold. The first approach focuses on the low temperature and fatigue performance of laboratory produced AR mixes prepared with AR binders containing polyoctenamer, and the effects and interactions with two types of GTR. The low temperature performance of these mixes was evaluated using the semi-circular bend test; while the fatigue performance was assessed using the four-point bending beam device. Results revealed that the addition of

polyoctenamer does not have detrimental effects on the low temperature performance nor the fatigue performance of AR mixes. Interactions between polyoctenamer and rubber type were found in the fracture energy results. Whereas for the fatigue performance of these mixes, higher fatigue life was observed for mixes containing ambient GTR, but lower rate of damage accumulation was found for mixes containing cryogenic GTR.

The second approach presents a thorough binder study utilizing three different geometries to characterize the rheology of laboratory produced AR binders. The geometries used were 1 and 2 mm gap using parallel plates and concentric cylinders with 5.7 mm gap. Continuous performance grading, master curves, viscosities, mass loss, and storage stability were evaluated. Results demonstrated that the increase in testing gap does not isolate the interference of GTR particles in the rheological characterization of these binders. In general, results obtained with the AR binders that were centrifuged, meaning that rubber particles have been removed by the Binder Accelerated Separation Method, did not have the interference or influence of GTR particles when compared with the results obtained with the non-centrifuged AR binders tested using the aforementioned geometries.

CHAPTER 1. GENERAL INTRODUCTION

Background

The interest in asphalt rubber binders has reemerged in recent years in the United States due to state policies that require the use of ground tire rubber in the pavement projects in certain states. Besides the environmental benefits of reusing scrap tires that are in landfills, the addition of ground tire rubber into asphalt binders has long proved to improve the fatigue and rutting performance of hot mix asphalt, especially in climatic areas where rutting can be a problem.

As with any technology, some challenges are encountered when trying to apply this technology. In the case of asphalt rubber one of these challenges is the workability of the binders, due to the high viscosity that these present which leads to increased mixing and compaction temperatures. Another challenge is the storage stability of the binders after being produced, due to the rubber particles sinking if the binder is not mantain with constant agitation. To overcome these two challenges, chemical modifiers can be added to the binder to improve its workability and storage stability. A third challenge that is related to the rheological characterization of asphalt rubber binders has lead to several researchers finding better ways to determine the rheology of asphalt rubber binders.

Problem Statement

Modification of asphalt rubber binders with chemical additives is made to improve their workability. Polyoctenamer or trans-polyoctenamer is one of the chemical additives used to help reduce the viscosity of asphalt rubber binders without negatively affecting its rheological properties, as established by the author in a previous study (Ng Puga, 2013). Results on moisture susceptibility and rutting performance were promising. However,

aforementioned study did not look at the impact of polyoctenamer on the low temperature and fatigue performance of mixes made with asphalt rubber binders that were modified with polyoctenamer. It neither was an evaluation of the storage stability of the asphalt rubber binders modified with polyoctenamer included.

In the production of asphalt rubber binders, ground tire rubber (GTR) is blended and reacted with liquid asphalt. The GTR particles swell with the lighter fractions of the base binder, therefore increasing in size. The actual testing method for binder performance requires to test the binders using parallel plates with a 1 mm gap in a dynamic shear rheometer. Depending on the mesh size of the GTR and the base asphalt source, it is most likely that the rubber particles will interfere with the geometry during testing with the dynamic shear rheometer. Some researchers advocate the use of concentric cylinders to test the asphalt rubber binders (Gaumgardner and D'Angelo, 2012); whereas others propose to increase the geometry gap from 1 mm to up to 3 mm. Other researchers suggest separating the rubber particles from the liquid asphalt after reacting to evaluate the real changes occurred in the base binder without having the influence of the rubber particles in the parallel plate geometry (Peralta et al., 2012).

Objectives

The objectives of this dissertation are to firstly determine the low temperature performance of hot mix asphalt made with asphalt rubber binders modified with polyoctenamer to establish how the addition of this polymer and two different grinds of GTRs (ambient and cryogenic) influence their thermal cracking performance. Secondly, the fatigue performance of hot mix asphalts with the same type of binders will be determined and compared among them to establish how polyoctenamer and two types of GTRs influence the

fatigue behavior of these mixes. With regards to asphalt rubber binders, the third objective of this dissertation is to execute a thorough comparative rheological study that includes viscosity testing, storage stability, continuous performance grade, and master curve construction and evaluation. The variables that will be considered to carry out the third objective are two types of GTR, the addition of polyoctenamer, two types of curing, two types of aged materials, binders with rubber particles and binders without the rubber particles and three types of testing geometries.

Organization of Dissertation

This dissertation consists of three papers, one of them has being submitted for publication in a scientific journal, and the other two will be submitted to other scientific journals. This dissertation has being divided into five chapters. Chapter 2 provides a general literature review on the sustainable technology of asphalt rubber binders and mixes, it summarizes previous findings on asphalt rubber binders and mixes as a background to the development of the papers presented in this dissertation. Chapter 3 presents the study on low temperature performance of laboratory produced asphalt rubber mixes. Chapter 4 undertakes the study of fatigue performance of laboratory produced asphalt rubber mixes. In Chapter 5, a thorough investigation is presented on the rheological characterization of asphalt rubber binders utilizing different testing geometries, and the differences between testing non-centrifuged and centrifuged asphalt rubber binders. Finally, Chapter 6 summarizes the findings in this dissertation and presents the general conclusions and recommendations for further work.

CHAPTER 2. LITERATURE REVIEW

A general literature review on the asphalt rubber technology will be given in this chapter as a background, most of it as being already presented in the master thesis of the author titled Rheology and performance evaluation of polyoctenamer as asphalt rubber modifier in hot mix asphalt. Literature review specifics on the subjects of the following chapters are given in their respective introduction sections.

Ground Tire Rubber

The generation of scrap tires in the US in 2013 was estimated to be more than 3.7 million tons of tires, which represents approximately one tire per person (Rubber Manufacturers Association, 2014). The generation of scrap tires by Iowans is around 3 million scrap tires annually, this was reported in the website of the Iowa Department of Natural Resources in 2013.

Modern tires are composed of many different components (Figure 2-1). The main components of tires are "vulcanized rubber, rubber filler, rubberized fabric, steel cord, fillers like carbon black or silica gel, sulfur, zinc oxide, processing oil, fabric belts, steel wire, reinforced rubber beads and many other additives". These components make ground tire rubber a great asphalt modifier, because many of these components are rubber components that when reacted with asphalt help modifying the elastic properties of the binder. Table 2-1 presents the typical weight distribution of the components of a tire and it shows that tires are mostly composed of rubbers (Unapumnuk, 2006).

Rubber is a type of elastomer, and as any elastomer it can go under large elastic deformations and return to its original shape. The definition of rubber according with the

ASTM D 6814 (2002) is that rubber is a natural or synthetic elastomer that can be chemically cross-linked/vulcanized to enhance its useful properties. When cross-linked rubber can form a strong three-dimensional chemical network. Rubber will swell in the presence of a solvent, but it will not dissolve and cannot be reprocessed by simply heating it (Hamed, 1992).

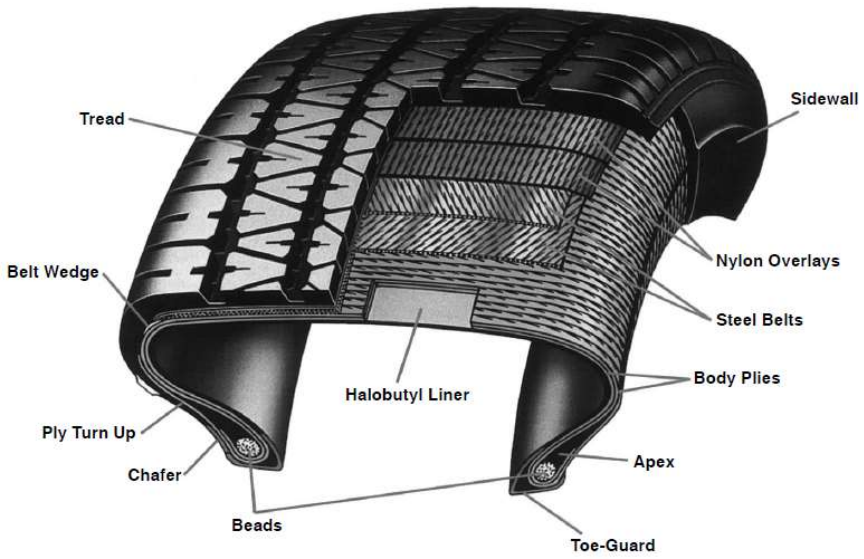

Figure 2-1. Cross section of a high-performance tire
(Mark, 2005)

Table 2-1. Typical weight distribution of the various components of a tire

Tire components	Percentage
Natural rubber	15-19
Carbon black	24-28
Synthetic rubber	25-29
Steel cords	9-13
Textiles cords	9-13
Chemical additives	14-15

From Unapumnuk, (2005)

The amount of rubber that composes scrap tires makes them a potential source of raw material for the rubber industry. Moreover, landfills and legislation are requiring more economical and environmental friendly ways to dispose of scrap tires. There are many technologies to recover the rubber from scrap tires. Some of the methods that these technologies apply include retreading, reclaiming, grinding, pulverization, microwave and

ultrasonic processes, pyrolysis, and incineration. The recycled rubber is generally known as ground tire rubber (GTR) (Isayev, 2005).

Two types of ground tire rubber can be obtained from scrap tire recycling: ambient ground tire rubber (ambGTR) and cryogenic ground tire rubber (cryoGTR) (Figure 2-2). The processes from where these are obtained are different. In general these processes differ in the temperatures used when processing the scrap tires.

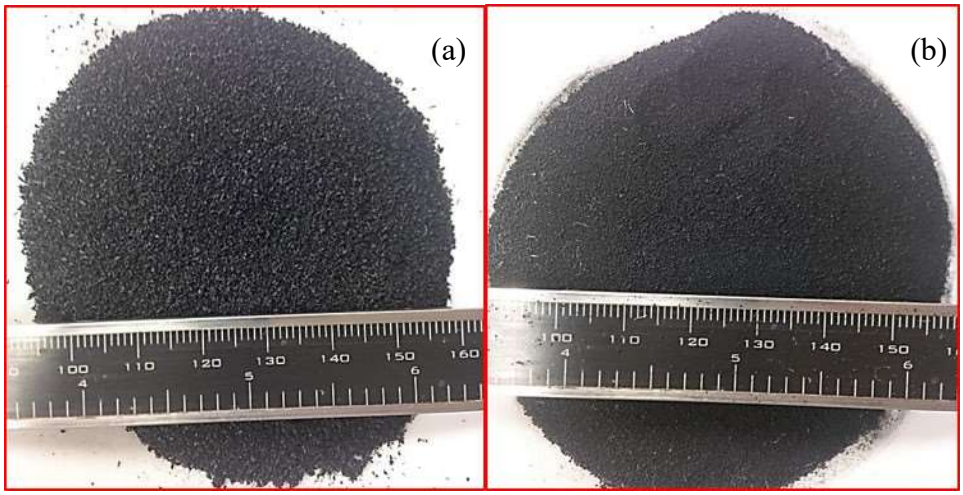

Figure 2-2. Types of GTR (a) Ambient GTR (b) Cryogenic GTR

Ambient GTR is obtained by the grinding of the ground tire rubber at or above ambient temperature, without the use of any cooling system, through either cracker mills or a granulator. The rubber particles of ambient GTR will tend to have cut surface shape and rough texture when processed through granulators. Whereas, if the ambient GTR is ground using cracker mills, its particles will be long and narrow in shape with a high surface area (Recycling Research Institute, 2006).

Figure 2-3 shows the schematic of an ambient rubber processing plant, where the tires are fed into a shredder that will reduce them into two-inch size chips. After that, the chips go into a granulator further reduce the rubber particles to less than 3/8 inches, at this stage most

of the steel and fiber that compose the tires are removed through magnets in the case of the steel, and the fiber is shaken out or wind sifted. When the steel and fibers have been removed, the rubber particles go through finer grinding processes depending on the final size desired, most of the mesh sizes for ambient rubber range from #10 to #30. The usual equipment used to perform this fine grinding are: secondary granulators, high speed rotary mills, extruders or screw presses and cracker mills (Reshner, 2006).

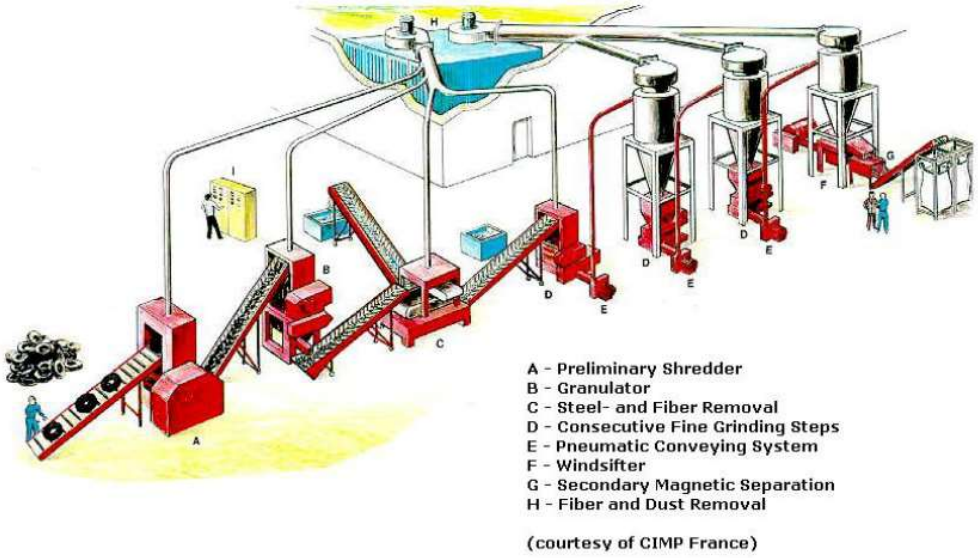

Figure 2-3. Ambient scrap tire processing plant schematics
(Reschner, 2006)

In contrast, cryogenic GTR is obtained through a process where the scrap tires are frozen using liquid nitrogen or other freezing methods to a temperature below the rubber's glass transition temperature to make them brittle, and then the tires are put through a hammermill and reduced to the desired particle size (Reschner, 2006).

Figure 2-4 represents the schematic of a cryogenic scrap tire processing plant, in which the tires are first fed to a shredder reducing the tire to two inch sized chips. These

chips are then cooled through a funnel system using freezing agents, as nitrogen, to approximately -120°C. After being frozen, the rubber is then shattered using a hammer mill system. Steel and fibers are then removed through magnets, aspiration and screening. Next, the rubber is dried and sieved into different particles sizes. The rubber particles obtained from the cryogenic method are smooth and even in size, with a low surface area. (Reschner, 2006).

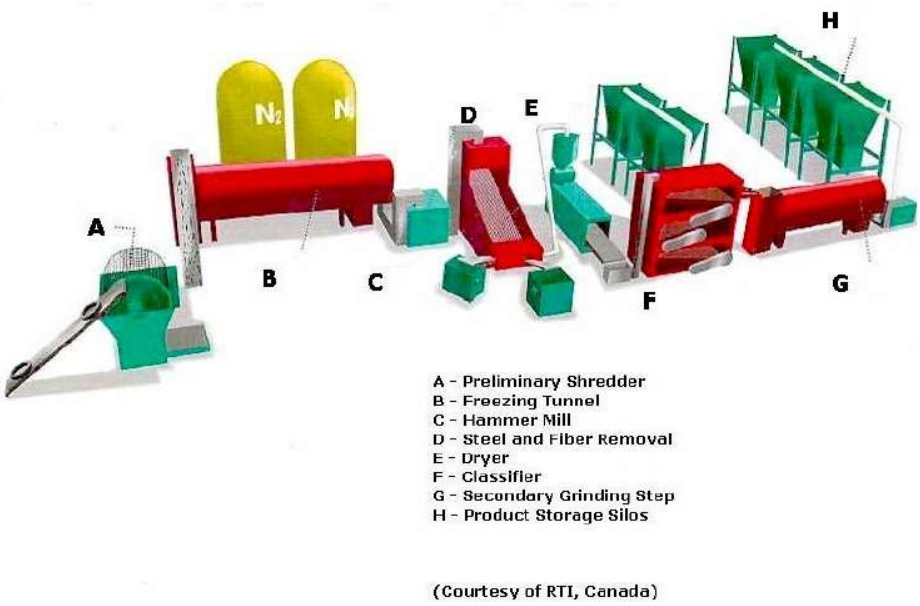

Figure 2-4. Cryogenic scrap tire processing plant schematics
(Reschner, 2006)

Ground tire rubbers are usually used as an asphalt binder modifier due to its elastomeric properties which improves the performance of asphalt mixtures and at the same time it contributes to the reduction of the accumulation of scrap tires in landfills.

Asphalt Rubber Mixtures and Asphalt Rubber Binders

The first uses of asphalt rubber were as binder in chip seals and in dense and open-graded asphalt concrete construction. The asphalt-rubber chip seal, or seal coat, is known as

"asphalt-rubber interlayer", which is placed beneath an asphalt concrete overlay, and it is intended to reduced reflection cracking in overlays. The hot-mix asphalt concrete made with asphalt-rubber binder is known by "asphalt-rubber concrete" in dense-graded mixes and "asphalt-rubber friction course" in open-graded mixes. (Shuler, 1986)

Early applications of asphalt rubber can be categorized as asphalt rubber concrete (ARC), open graded friction courses, stress absorbing membranes (SAM's), stress absorbing membrane interlayers (SAMI's), cape seals, three layer systems and waterproof membranes (FHWA, 2008). Figure 2-5 illustrates some cross-sections of the aforementioned applications of asphalt rubber technology.

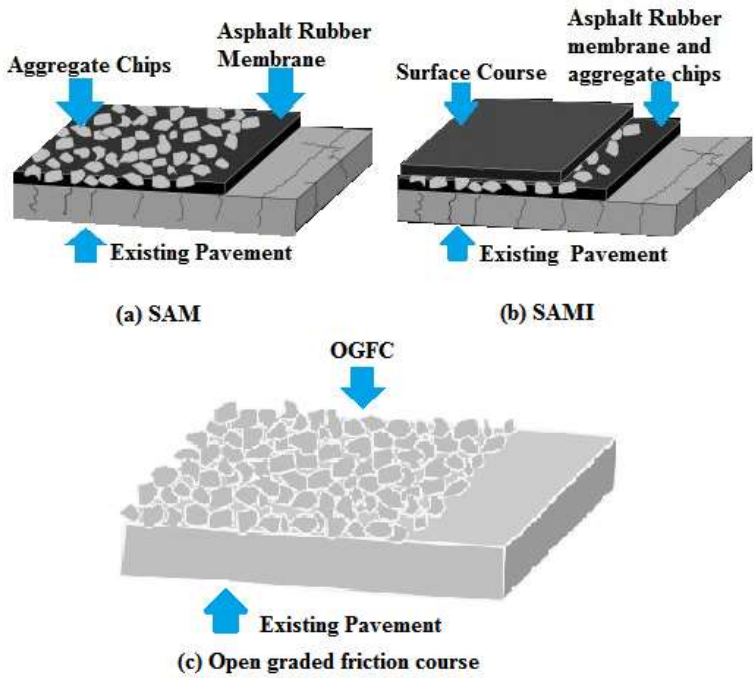

Figure 2-5. Different asphalt rubber applications
(Adopted from ARTS)

Because GTR contains carbon black, which is rich in antioxidants, asphalt rubber mixtures are highly resistant to oxidation and cracking. High viscosities of asphalt rubber

binders help with the rutting resistance of the mixture, while the elastic properties of rubber help with the reflective and thermal cracking resistance of the pavements.

Asphalt rubber mixes can be produced through two processes: the wet process and the dry process. In the first process the crumb rubber or GTR is blended and reacted into the asphalt binder prior to the production of the mixes, whereas, in the second process the rubber is added to the aggregates before mixing it with the asphalt binder. The method used throughout this study focuses only on binders produced utilizing the wet process.

Use of asphalt rubber in the United States

In the mid-1960's, Charles H. McDonald developed the wet process method. In conjunction with Atlos Rubber, the Arizona Department of Transportation (Arizona DOT), and Sahuaro Petroleum and Asphalt Company, he was able to developed commercial binder systems. By the mid-1970's, Arizona Refining Company (ARCO) also developed an asphalt rubber system (Hicks, 2002).

The Arizona DOT carried out comprehensive research on asphalt rubber between the mid-1970's and early 1980's, where they established that the rubber type, rubber gradations, rubber concentration, asphalt type, asphalt concentration, extender oils, reaction times and temperatures influenced the properties of the asphalt rubber binders (Hicks, 2002). Chip seal was the common use of asphalt rubber binder; however, by the beginning of 1990's one-inch thick asphalt-rubber mix overlays were starting to be preferred over the chip seals because the overlays provided a smoother riding surface and produced less traffic noise. Both, chip seals and asphalt-rubber overlays provided retardation of reflection of fatigue cracking and thermal cracking.

The California Department of Transportation (CalTrans) started evaluating asphalt rubber as spray applications (chip seals, interlayers and cape seals) in the 1970's and as hot mix asphalt (dense-graded, open-graded, and gap-graded) in the 1980's using the wet-process. CalTrans has reported that the use of asphalt rubber mixtures usually exhibits less distress, requires less maintenance and handles more deflections than regular dense-graded asphalt concrete and at least forty cities in California have asphalt rubber pavements (Hicks, 2002).

The Texas Department of Transportation (Texas DOT) also started using asphalt rubber in these applications around the same time as Caltrans. After many years of use of asphalt rubber technology Texas DOT have concluded that asphalt rubber chip seals improve the resistance to fatigue cracking and raveling and at the same time the cost of placing is almost half of the cost of repaving, therefore chip seals are the most used application in Texas for asphalt rubber (Estakhri et al, 1992). Dense-graded asphalt rubber hot mixes by the wet-process are also used by the Texas DOT.

At least six asphalt rubber projects using the wet-process were construted in 1979 by the Minnesota Department of Transportation. These projects involved one dense-grade overlay, two SAM's and three SAMI's; however the results obtained for the SAM's were not encouraging, one did not performed well and the other was a success. In the other projects the improvement on the resistance to reflective cracking was not considered enough to overcome the cost related to the technology.

In the 1980's the Kansas Department of Transportation (Kansas DOT) built five projects using asphalt rubber as interlayers, from those five projects only one presented better performance than the control mixes in the reduction of reflective cracking, whereas the others

performed the same as the control mixes, thus the Kansas DOT decided that the extra cost involved in asphalt rubber interlayer did not justify its use.

Between 1989 and 1990, the Florida Department of Transportation (Florida DOT) constructed three asphalt-rubber demonstration projects that included dense graded and open-graded friction courses using the Florida wet-process technology. This was carried as result of a Florida Legislature as part of a Solid Waste Management Act in 1988. Based on the findings of those projects, specifications were developed by the Florida DOT that required asphalt binder with 5% GTR by weight of binder for dense graded friction courses and 12% GTR by weight of binder in open graded friction courses. In 2014, the Florida DOT evaluated and starting implementing a new asphalt rubber binder specifications called PG 76-22 (ARB) that is supposed to address the separation requirements to minimize settlement and to be equivalent in performance to their polymer modified "gold standard" binder PG 76-22 (PMA) (Greene et al., 2014).

In 1990, the Iowa Department of Transportation (Iowa DOT) started studying laboratory asphalt rubber mixes using the wet-process. Five projects were constructed between the years of 1991 and 1992 using asphalt rubber binder in the pavements as chip seals, surface overlays and intermediate layers. The locations of these were in Muscatine, Dubuque, Plymouth, Black Hawk, and Webster Counties. The asphalt rubber pavements performance was better than conventional asphalt pavements in rutting, fatigue cracking, reflective cracking and better winter maintenance in all these projects (Anderson, 1992a, 1992b, 1992c and 1993).

The Federal Highway Administration started several research studies about asphalt rubber in 1992, due to a federal government mandate to reduce the number of used tire

stockpiles in the Intermodal Surface Transportation Efficiency Act (ISTEA) in 1991. The first phase of these research studies was carried by the University of Florida. In the first phase the common practices of the technology were summarized and identification of research needs for a second phase were established. The second phase was developed by Oregon State University from 1994 to 1999. Guidelines for thickness design and construction, and quality control were established, as well as long-term performance of mixes containing crumb rubber and the possibility of recycling mixes containing crumb rubber. The Western Research Institute (WRI) carried out an evaluation study of asphalt rubber on the effect of the asphalt composition and time and temperature of reaction. The National Cooperative Highway Research Program (NCHRP) in 1994 synthesized the state of practice of asphalt rubber including all processes containing crumb rubber. However, before these studies were finalized, the federal mandate on the use of recycled tires in asphalt pavement was revoked by the National Highway System (NHS) Designation act in 1995, but nonetheless the mentioned Act recommended in one of its sections that further research and development of tests and specifications for use of asphalt rubber in conformance with the SuperPave performance-based specifications should be done (FHWA, 2008).

Production of asphalt rubber mixtures and binders

The use of rubber in hot mix asphalt (HMA) is intended to improve the performance of HMA at high service temperatures by increasing its stiffness; also, to modify its performance at intermediate temperatures by increasing its elastic properties, thus improving its resistance to fatigue cracking.

Dry-process

Only a brief description of the dry process will be given in this section, since this technology was not used in any of the methodologies used throughout the development of

this research. Ground tire rubber is added to the aggregates in a 1-3 percentage by weight of aggregate in the dry process. The usual aggregate gradation used in this method is a gap-graded gradation allowing the rubber particles to fit into the aggregate matrix. Coarse ground tire rubber of sizes about 2 mm to 4 mm are generally use in this process. The Swedish Company EnviroTire develop this process in 1960's and commercialize it under the name of PlusRide. Around 1980's and 1990's a generic dry-process technology was developed in the United States where the amount of ground tire rubber did not exceeded 2% by weight of aggregates, this generic process was mainly used in experimental pavement sections by states like Florida, New York and Oregon (FHWA, 2008).

Ice-bonding characteristics of several asphalt paving materials including the ones having rubber, like the PlusRide, where evaluated by the Cold Regions Research and Engineering Laboratory (CRREL) of the U.S. Army Corps of Engineers, as part of the Strategic Highway Research Program. During this evaluation CRREL developed a new technology called the chunk rubber asphalt concrete, where a narrow gradation of aggregates is used, between 4.5 mm and 12mm aggregate size, and larger maximum sizes of crumb rubber compared to the ones used in PlusRide technology (Heitzman, 1992).

Asphalt rubber mixtures using the dry process can be produced by either batch or drum-dryer plants. Production temperatures of this mixtures range between 149°C – 177°C (300°F – 350°F). Laydown temperatures should be at least 121°C (250°F) and continuous compaction with the finishing roller is need until a temperature of at least 60°C (140°F) is reached to avoid swelling of the rubber particles (FHWA, 2008).

Wet-process

The first technology to apply the wet process was developed by Charles H. McDonald and was known as "McDonald Process". In the wet process, rubber is blended with the asphalt at high temperatures. During the reaction process some components of the asphalt migrate due to diffusion into the rubber making it swell, becoming a gel-like material. The components of the asphalt that causes swelling on the rubber are the aromatic oils of the asphalt that form part of the maltenes fraction of the asphalt composition (Figure 2-6) (Heitzman, 1992).

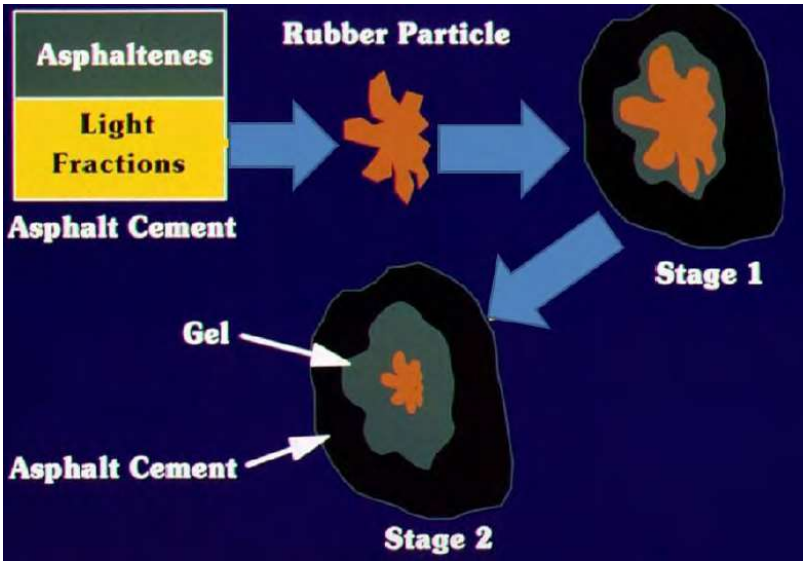

Figure 2-6. Depiction of reaction stages of asphalt and rubber
(RPA, 2011)

The State of Florida developed the continuous blend using an 80 mesh of ground tire rubber in 1980's. The main differences between the McDonald Process and Florida method are in: the percentage of ground tire rubber used, 8-10% in Florida's method, versus 15-26% for the McDonald Process; the size of the ground tire particles; the lower temperatures at which the blend is performed; and the shorter reaction time in Florida method.

The amount of the rubber swelling will depend on the particle's shape, surface area, type and amount of the rubber, type of asphalt, type and amount of shear mixing, blending temperature and time of interaction between the rubber and asphalt. The swelling of the rubber will increase the viscosity of the asphalt binder (Rahman, 2004).

Typical blending temperatures for asphalt rubber range between 160°C-205°C (320°F-400°F) for a minimum blending duration of 45 minutes. Higher temperatures than the aforementioned can lead to rubber depolymerization affecting its physical properties (Hicks and Epps, 2000). Also higher temperatures can lead to an excess of fumes and/or smoke (Hicks, 2002). The addition of petroleum distillates or extender oils or other modifiers are often added to the blend to reduce the viscosity and facilitate spray applications and promote workability.

Three categories of asphalt rubber blending are the batch blending, continuous blending and terminal blending. The batch blending consists of the addition of rubber batches as it is mixed with the asphalt during the production of asphalt rubber. Continuous blending refers to the application of the wet process in a continuous production system developed by the Florida DOT in 1980's as mentioned previously. Terminal blending is performed at asphalt supply terminals using either the batch method or the continuous blending with the advantages of being able to store the asphalt rubber binder for extended periods of time, when compared to the other two methods (Heitzman, 1992 and FHWA, 2008). Some limitations that asphalt rubber mixtures have presented are raveling and flushing, related to construction quality control; fatigue and reflection cracking when the correct thickness has not been used; and tackiness of the asphalt rubber (Hicks, 2002). Typical mixing temperature ranges for asphalt rubber mixes are: 163-191°C (325°F-375°F)

for dense-graded asphalt rubber mixes and 135-163°C (275°F-325°F) for open-graded asphalt rubber mixes (Roberts, 2009).

On-site blending is considered the most efficient and economical way of combining ground tire rubber and asphalt. The on-site blending equipment must have the right components to successfully measure the right amount of rubber and asphalt to accommodate the needs of the in-site project (Figure 2-7 and Figure 2-8).

Figure 2-7. Example of on-site asphalt rubber blending plant
(CEI Enterprises, 2008)

Figure 2-8. Example of asphalt rubber reaction tank
(CEI Enterprises, 2008)

Heated blending tanks are required to have agitation systems to keep the asphalt rubber blend homogenized until it is pumped to the hot plant. Depending on the specific gravity of the rubber components and asphalt, rubber particles can float on top of the tank or settle to the bottom of it. Screw auger systems are the most efficient way of agitation in horizontal blending tanks (Figure 2-9); thanks with this system are preferred due to the high surface area of material that provides better agitation with the screw auger system (RPA, 2011). Vertical storage tanks have the advantages of requiring less square footage than horizontal storage tanks (Figure 2-10). Also, vertical storage tanks have agitations systems consisting of impellers that allows the binder to be recirculate upwards and downwards having better flow patterns that those obtained with horizontal storage tanks (Figure 2-11). Another advantage that vertical storage tanks have over horizontal tanks is that the surface area of the asphalt that is exposed to air is smaller, which reduces the potential for oxidation of the asphalt rubber binder.

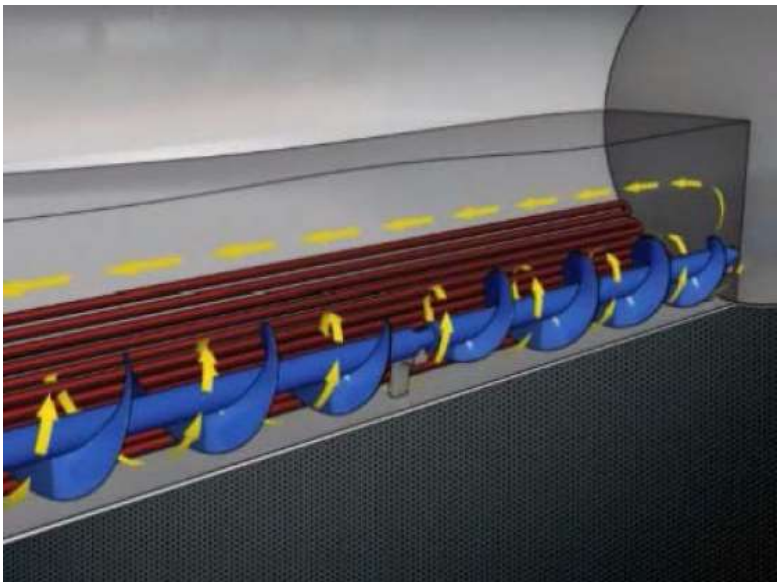

Figure 2-9. Depiction of auger system inside a horizontal blending tank
(RPA, 2011)

Figure 2-10. Vertical storage tanks
(CEI Enterprises, 2008)

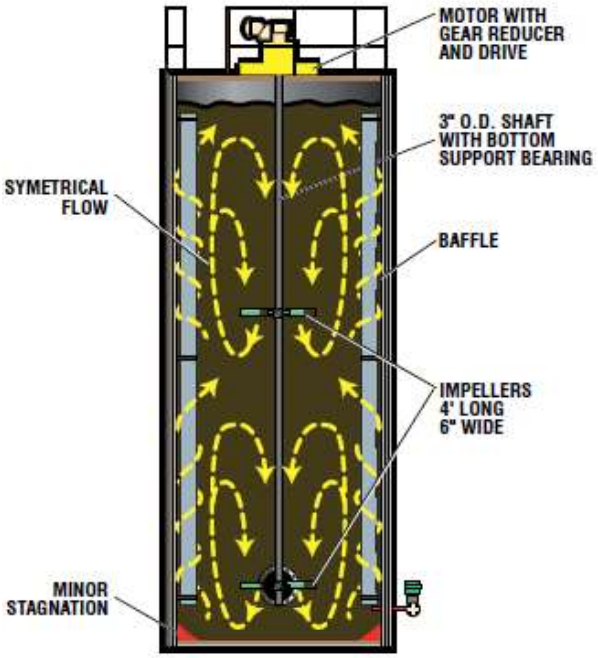

Figure 2-11. Depiction of flow patterns in vertical tanks
(CEI Enterprises, 2008)

Asphalt rubber blending plants consist of many main parts: the ingredient indicators, liquid asphalt meters for measurement and proportioning, a crumb rubber hopper equipped with scales and meters, asphalt rubber binder blending equipment, asphalt rubber binder storage with internal agitation system, temperature control and metering heaters, heat exchangers, additive systems, mixing tank and asphalt rubber reaction tank.

In order to start the asphalt rubber mix production, special heavy-duty pumps, like the one shown in Figure 2-12 are attached from the asphalt rubber binder production equipment to asphalt cement plants, like a drum plant. Asphalt rubber's placing can vary depending on the application that it is being used for, but generally, its laydown temperature should not be less than 121°C (250°F), conventional laydown machinery is used, and immediate rolling with a steel wheel roller is required. The use of rubber tire rollers is prohibited, since the asphalt rubber tends to build up on the roller tires (Way, 2011).

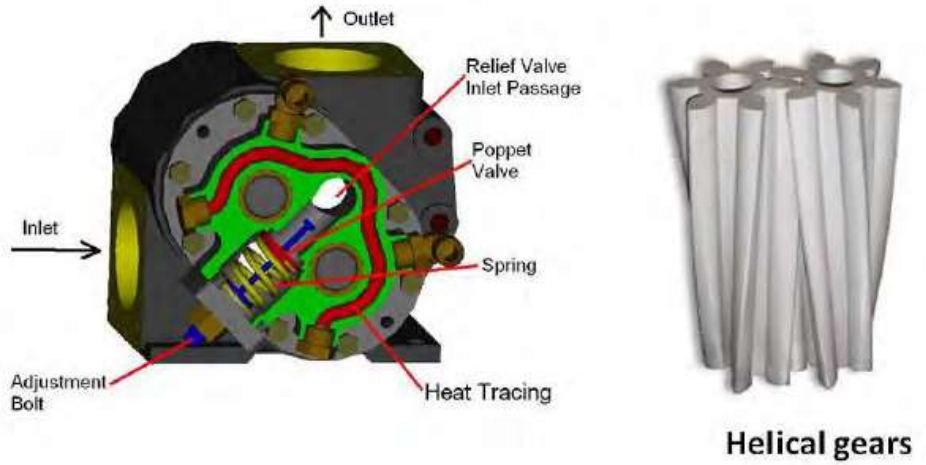

Figure 2-12. Special asphalt rubber pump with special heat tracing and relief valve (Way, 2011)

Polyoctenamer or Trans-polyoctenamer

Polyoctenamer (PO) or trans-polyoctenamer (TOR) is a solid and opaque polymer, obtained from the cyclooctene monomer that is synthesized from 1,3-butadiene via 1,5-

cyclooctadiene. The polymerization of the cyclootadiene is achieved through a metathesis reaction, producing two types of macromolecules, linear and cyclic. The cyclic part of the macromolecules has a crystalline structure that exhibits low viscosity above its melting point. The cyclic part also contains a high amount of double bonds that can serve as cross-linking points and makes a rubbery polymer (Burns, 2000).

The level of crystallinity of PO will depend upon the cis/trans ratio of double bonds; this ratio is controlled by the polymerization conditions; thus the more trans-contents, the higher the crystallinity. Two degrees of crystallinity are usually obtained, one with a trans-content of 80% (cis-content of 20%), and the other with a trans-content of 60% (cis-content of 40%). The melting point of the former is about 54°C (129°F) and for the latter is about 30°C. PO is thermally stable to 271°C (520°F) (Burns, 2000).

The molecular formula of polyoctenamer is $–(C_4H_7=C_4H_7)–_n$ and its synthesis is shown in Figure 2-13. PO is used in the asphalt industry to improve the tackiness of asphalt rubber (Baumgardner and Anderson, 2008). Its macrocyclic molecules, when added to asphalt rubber, will lower the initial viscosity during the initial mixing operation due to its crosslinking of the sulfur associated with the asphaltenes and maltenes in the asphalt and the sulfur in the surface of the ground tire rubber.

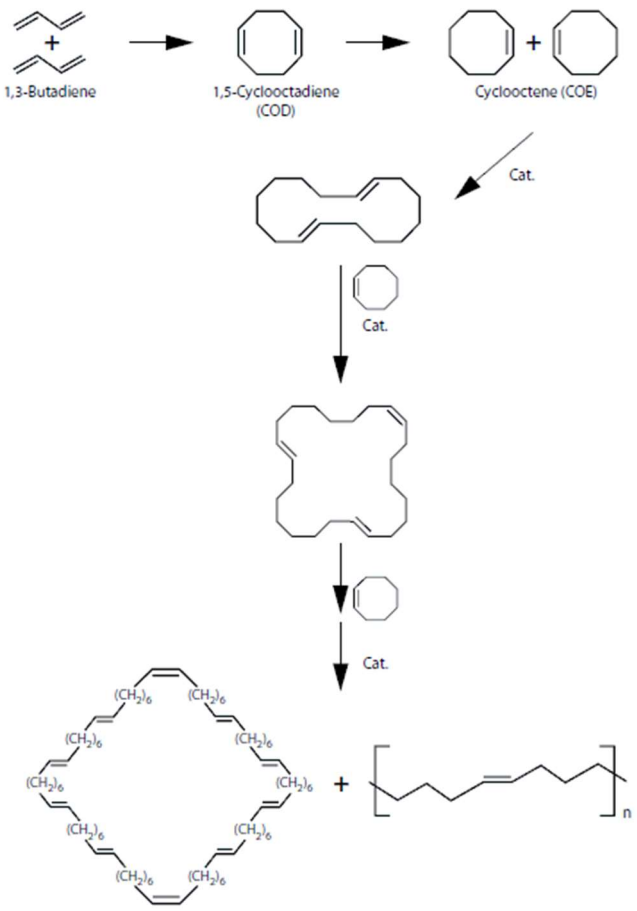

Figure 2-13. Synthesis of trans-polyoctenamer

As the polymerization spreads it will prevent the sinking of the rubber particles by increasing the viscosity. According to Rubber Asphalt Solutions, LLC (2010), this polymer chemically bonds to the ground tire rubber of the asphalt during its blending, it bonds chemically to the aggregate reducing the stripping of the mixtures and will convert the thermoplastic asphalt to a thermoset polymer, that can help reduce cracking and rutting. Among other advantages that are claimed are the mixing gets easier, faster and more uniform, faster paving, a superior surface finish, application at low road-surface temperatures, long service life, elimination of terminal blending and lower cost per mile.

The polyoctenamer is added in a dry particulate form to the heated asphalt cement at a temperature of about 163°C (325° F); however, higher temperatures are also allowed. The GTR can be added to hot asphalt cement with the polyoctenamer pellets (Figure 2-14) or after the polyoctenamer pellets have been mixed, melted and dispersed. The recommended dosage is 4.5% by weight of the GTR (Burns, 2000). Field trials of pavements containing PO were performed during the years of 1998 to 2003 in Canada and United States, and their performance was good as expected. These were located in the province of Ontario and the states of Arizona, New Jersey, Pennsylvania, Illinois, Ohio and Nebraska. (Burns, 2004)

Figure 2-14. Polyoctenamer pellets (80% crystalline)

CHAPTER 3. LOW TEMPERATURE PERFORMANCE OF LABORATORY PRODUCED ASPHALT RUBBER MIXES CONTAINING POLYOCTENAMER

Modified from a paper submitted to *Construction and Building Materials Journal*, published by Elsevier

Ka Lai N. Ng Puga[1] and R. Christopher Williams[2]

Abstract

The research in this paper studies the low temperature performance of laboratory produced asphalt rubber (AR) mixes by means of the semicircular bend geometry test, utilizing two types of ground tire rubber (ambient and cryogenic) at two different percentages of polyoctenamer (PO). Stiffness, fracture toughness and fracture energy for the mixes were obtained in order to statistically evaluate how the variables influence their low temperature performance. Overall, the laboratory test results indicate that the use of PO at the dosage utilized and the rubber types at the percentage employed will not adversely impact the low temperature performance of AR mixes.

Keywords: ground tire rubber, asphalt, mixes, polyoctenamer, low temperature performance, thermal cracking, semicircular bend geometry, fracture energy, stiffness, fracture toughness

[1] Corresponding author. Ph.D. candidate. Department of Civil, Construction and Environmental Engineering, Iowa State University, Ames, IA 50011. E-mail: knnp@iastate.edu
[2] Professor of Civil Engineering, Department of Civil, Construction and Environmental Engineering, Iowa State University, Ames, IA 5001. E-mail: rwilliam@iastate.edu

Introduction

The amount of scrap tires that are collected in landfills, dumps and stockpiles all over the world is overwhelming. For instance, according to the number estimated by Rubber Manufacturers Association in 2013, approximately 3.7 million tons of tires were discarded in the United States. Consequently, much legislation now requires implementing more environmental friendly ways to reuse and recycle scrap tires. This new legislation generally has made the use of ground tire rubber (GTR) a requirement in some states of the United States. GTR, or crumb rubber from scrap tires, has been used since the 1960s to modify conventional asphalt binders, and it has been mostly utilized in chip seals or seal coats. In recent years, new efforts have arisen towards studying the characterization of asphalt rubber (AR) binders and mixes. Extensive research has focused on the high and low temperature performance of AR binders, but only a few studies have investigated the performance of AR mixes [1-11]. From these studies it can be deduced that the high temperature performance of AR binders and mixes is excellent in warm to hot climates, and it has been proven that GTR helps improving the rutting and fatigue performance of asphalt mixes. However, a limited amount of work has been done to evaluate the thermal cracking (low temperature) performance of asphalt rubber mixtures. In geographical areas, where the climate is very hot during summers and very cold during winters, the selection of performance grade binders to be used in the asphalt mixtures for high and low temperature performance, is very important. Due to binder properties, conventional asphalt mixtures that perform very well at hot temperatures are usually not well suited to resist thermal cracking at very low temperatures. In order to withstand rutting and fatigue cracking at high temperatures conventional asphalt mixtures need to have high stiffness. Nevertheless, this high stiffness causes high tensile

stresses when the same conventional asphalt mixture is subjected to very low temperatures, often making it more susceptible to thermal cracking. More so, the working temperature range of conventional asphalt mixtures with conventional unmodified binders is narrower compared to modified asphalt mixtures (e.g. AR and/or polymer modified binders in mixes), often not allowing good performance for very high and very low temperatures at the same time.

One technical challenge that AR mixes presents is the high temperatures required for their mixing and compaction. Therefore, chemical additives are sometimes used in order to improve their workability by reducing their viscosity allowing the use of lower mixing and compaction temperatures. One example of a chemical additive used for this purpose is polyoctenamer (PO), which is also known as trans-polyoctenamer, which is a polymer obtained from the polymerization of cyclootadiene through metathesis reaction [12]. It has been found that the addition of PO in AR binders helps improving their workability by reducing their viscosity without negatively affecting the high temperature performance of AR mixes as well as improving the compatibility of the GTR with the asphalt [1, 13]. However, limited research has been done to see how the addition of PO impacts the low temperature performance of these mixes, more specifically, thermal cracking.

Since it is already known that AR binders and mixes perform very well at high temperatures, the aim of this paper is to determine the low temperature performance of AR mixes by means of the semicircular bend geometry test. To determine the low temperature performance of asphalt mixtures, it is believed in general that the total fracture energy is a good indicator of thermal cracking performance, especially for AR mixes [14]. This is

because fracture energy is an intrinsic material property that should not be affected by the geometry of the specimens tested, size of crack and/or measuring method [15].

The effects of GTR types and the addition of polyoctenamer (PO) on the low temperature performance characteristics of AR mixes, as stiffness, fracture toughness and fracture energy are studied. Thus, in the present paper, the influences of two types of GTR and two levels of PO on the low temperature performance of AR mixes at three low temperatures are studied. Not only the individual effects of these variables, types of GTR and PO dosage, on the low temperature performance of AR mixes are examined, but also any possible interaction between these variables through the analysis of variance (ANOVA) are evaluated.

Materials and Methods

Binder production

The base binder used in this study was performance graded following the standard method established in AASHTO M320-10 [16] as a PG 46-34 and was provided by Flints Hills Resources (Pine Bend, Minnesota). The two types of GTR selected to produce the AR binders were ambient ground (40 mesh) and cryogenic ground (200 mesh), and both were used at 12% by weight of asphalt. These GTR's were supplied by Seneca Petroleum (Crestwood, Illinois) and Lehigh Technologies (Atlanta, Georgia), respectively. The two levels of PO utilized were 0% and 4.5% by weight of GTR [12], and the PO was manufactured by Evonik and provided by Seneca Petroleum.

The base binder was initially mixed in a Silverson L4RT-A high shear mixer at 1000 rpm until reaching 180 °C. Then, the rubber and polyoctenamer were added to the base

binder and the shear was increased to 3000 rpm. The addition of rubber and polyoctenamer (PO) causes a drop in temperature; therefore blending was continued for an additional hour to allow reaction between the rubber, base binder, and polyoctenamer from the moment that 180 °C was reached again [17]. In total, four types of laboratory-produced AR binders were employed to mix and compact four types of AR mixes with the same aggregate gradation. The performance grade of the four AR binders produced were PG 64-34, these results are summarized in Table 3-1.

Table 3-1. Asphalt Rubber binder matrix

Binder ID	Base Binder	Type of GTR[1] by weight of base binder		Polyoctenamer by weight of GTR		Performance grade
		12% Ambient	12% Cryogenic	0%	4.5%	
AMB	PG 46-34	X		X		PG 64-34
AP	PG 46-34	X			X	PG 64-34
CRYO	PG 46-34		X	X		PG 64-34
CP	PG 46-34		X		X	PG 64-34

[1] GTR: ground tire rubber

Mix production and specimen preparation

The gradation of the mixes consisted of a 19 mm NMAS (nominal maximum aggregate size) of five types of aggregates locally obtained in the state of Iowa, in the following proportion: 25% of ¾-in limestone, 12% of $^3/_8$-in limestone, 30% of quartzite, 14% of natural sand and 18% manufactured sand (Figure 3-1). One percent of lime dust was included in the gradation to simulate the breakdown of the limestone aggregates in asphalt plants during mix production [18].

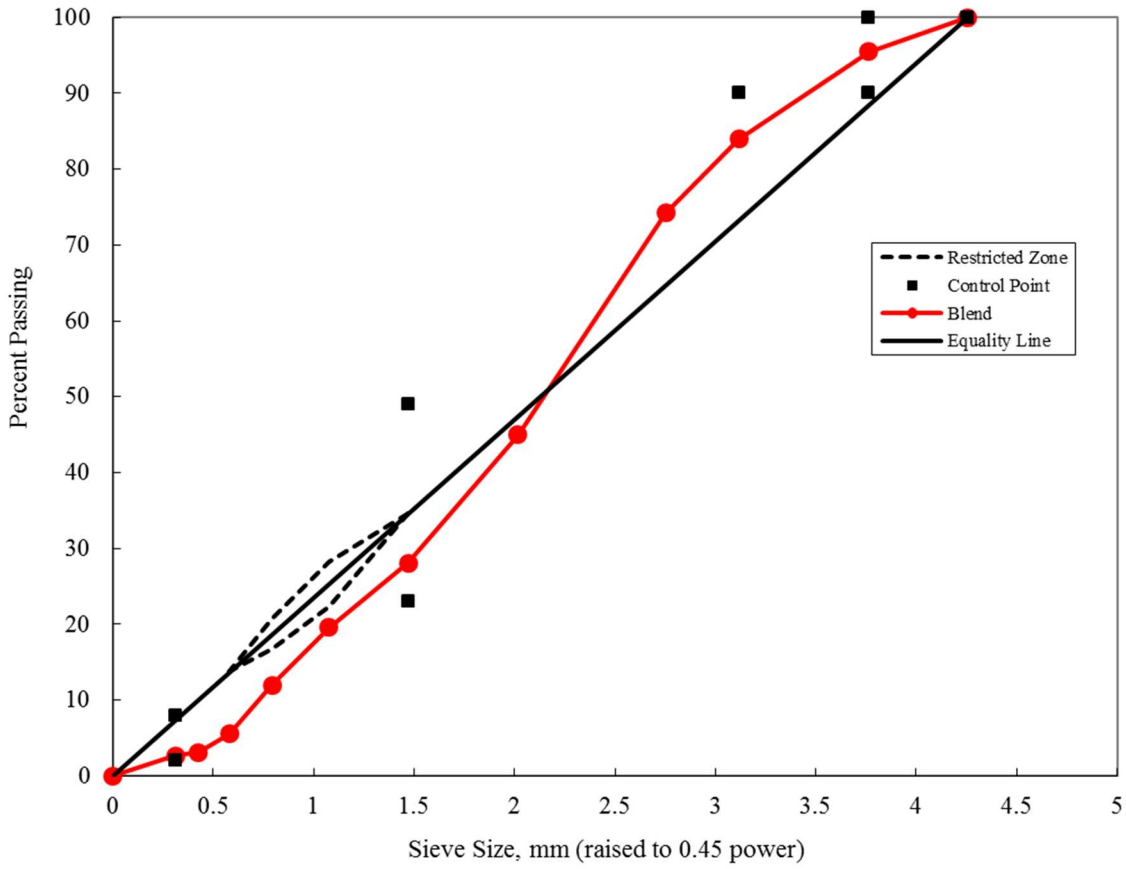

Figure 3-1. Aggregates gradation used in the experimental study (19 mm NMAS)

The optimum binder content for the gradation used in the study was 5.6% based on the Superpave volumetric mix design standard established in AASHTO M323-13 [19]. The mixing temperature and compaction temperatures were 180 °C and 165 °C, respectively. The mixes were cured for 3 hr before compaction. Cylindrical specimens for semicircular bend tests were compacted using a Superpave gyratory compactor. The compacted samples are 150 mm in diameter and 115 mm in height, and volumetric tests were performed to assure that air voids were within 7.0 ± 0.5 %. The standard method, AASHTO TP 105-13 [20], was followed to obtain the semicircular bend test specimens, where three slices with a thickness of 24.7 ± 2 mm were obtained from the center most part of the specimens. The

slices were cut in half, and a notch of 15 ± 0.5 mm in length and no wider than 1.5 mm was cut at the midpoint.

Fracture energy testing and statistical analysis

The protocol used to test the specimens is outlined in AASHTO TP105-13 [20] for determining the fracture energy of the asphalt rubber mixes. Based on the characterization of the binders' performance grade at low temperature, specimens were tested at -12, -24 and -36 °C for fracture energy. Four halves of each AR mix type were randomly assigned to each testing temperature. The samples were conditioned in the chamber before being tested for 2 hr at the testing temperature. A hydraulic universal testing machine of 25 kN capacity and a Epsilon crack mouth opening displacement (CMOD) device was used during testing of the specimens; and a data-acquisition system was used to acquire the data. An initial loading rate of 0.05 mm/s was used until a contact load of 0.3 ± 0.02 kN was obtained, then a seating load up to 0.6 ± 0.02 kN was applied with a loading rate of 0.005 mm/s. The test started when an initial load of 1 ± 0.1 kN was reached with a loading rate of 0.001 mm/s after the seating load was achieved. When the initial load was reached, the CMOD started to control the test by keeping the application of the load at a constant loading rate of 0.0005 mm /s. The test was completed when the load was lower than 0.5 kN or when the CMOD gauge range limited was reached, which ever occurred first. The data were then processed through a MatLab code to compute the stiffness, fracture toughness and fracture energy utilizing the formulas defined in AASHTO TP105-13 [20]. Table 3-2 presents the experimental matrix followed in this study. After these values were computed, averages for each property were calculated for each type of mix at each testing temperature; their standard deviations were also computed, in order to make multiple comparisons. Preliminary full factorial analyses of

variances (ANOVAs) were performed for each parameter at an alpha level of 0.05 to determine the statistically significant factors and interactions for stiffness, fracture toughness and fracture energy. Once these were determined, reduced ANOVAs were performed with the factors and interactions that were found to be significant for each parameter.

Table 3-2. Fracture energy testing experimental matrix

Mix Type	Temperature (°C)		
	-12	-24	-36
AMB	xxxx	xxxx	xxxx
AP	xxxx	xxxx	xxxx
CRYO	xxxx	xxxx	xxxx
CP	xxxx	xxxx	xxxx

where "x" denotes number of samples tested

Results and Discussion

The four types of asphalt rubber produced in this study met the requirements established by the AASHTO standard method for determining the performance grade of asphalt binder, AASHTO M320-10 [16]. A performance grade (PG) of -34 was determined by means of the beam bending rheometer (BBR) following AASHTO T313-10 [21]. The results of the semicircular bend geometry (SCB) test were obtained at three different temperatures: -12 °C, -24 °C and -36 °C; where the two last temperatures are 10 °C above the PG lower limit of the binder and 2 °C below the PG lower limit, respectively, as recommended by AASHTO TP105-13 related to the SCB test, based on the low temperature performance grade of the binder.

Stiffness, S

The stiffness values of the four mixes at three testing temperatures were calculated from the slope of the ascending part of the load-average load line displacement curve for each specimen. Generally, a higher stiffness response is associated with lower temperatures.

The average stiffness per mix type/testing temperature are presented in Figure 3-2. As expected, the average stiffness values for the ambient rubber mixes increased as temperature decreased. The increasing trend was not observed for the cryogenic rubber mixes. The cryogenic rubber showed increasing stiffness at -12 °C and -24 °C, but a decrease in stiffness was observed at -36 °C. It is noticeable that the standard deviations of the results, represented by error bars in Figure 3-2, were smaller at higher temperatures than those at lower temperatures. There were no significant differences in the stiffness when comparing the ambient rubber mixes, as well as within the cryogenic rubber mixes. Also, the addition of polyoctenamer does not statistically significantly affect the stiffness.

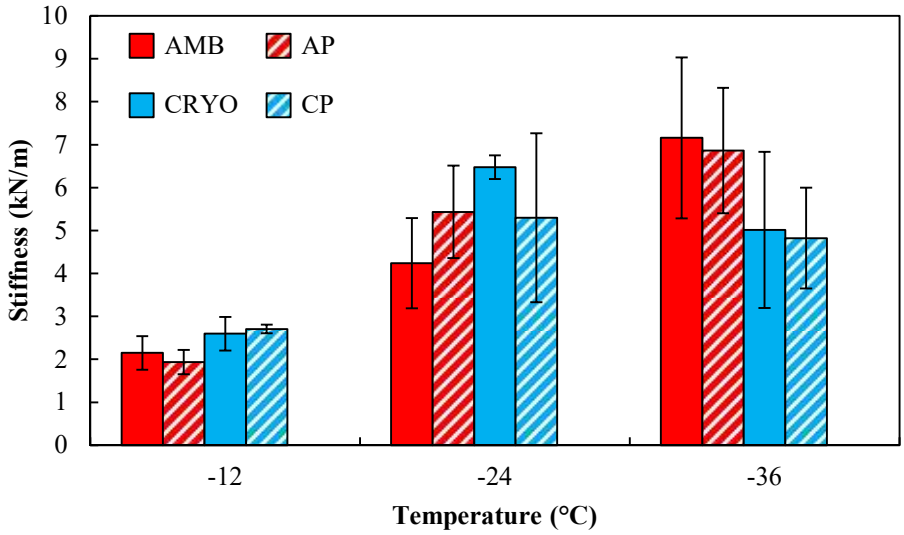

Figure 3-2. Comparison of stiffness of asphalt rubber mixes for ambient rubber (AMB), ambient rubber and polyoctenamer (AP), cryogenic rubber (CRYO), and cryogenic rubber and polyoctenamer (CP) at three different low temperatures.

The preliminary full analysis of variance (ANOVA) for stiffness indicated that the addition polyoctenamer did not have a significant impact in the model, nor were significant any interactions between the polyoctenamer and the other factors. Therefore, a reduced ANOVA was performed considering only the effects of rubber and temperature, and their

interactions. The reduced ANOVA suggests that the stiffness of the AR mixes was not greatly affected by the type of rubber (Table 3-3). However, the test temperature played a role in the determination of the stiffness at low temperatures. Higher stiffness response is linked to lower test temperatures, and this trend was observed in the overall results (Figure 3-3). In addition, the results obtained are in accordance with average stiffness values from the literature for regular hot mix asphalts, warm mix asphalts, and recombined bio-asphalt with asphalt mixes [22-24]. Compared to the results obtained, higher average stiffness values at similar test temperature are reported in the literature. This phenomenon could be due to the presence of the rubber particles, which are likely to maintain some elastic properties at low temperatures, making the mixes less stiff at those temperatures.

Table 3-3. Analysis of Variance for Stiffness, *S.*

Source	DF [1]	Sum of Squares	Mean Square	F Ratio	p-value
Rubber Type	1	0.24898	0.24898	0.1841	0.6701
Test Temperature	2	120.24701	60.12350	44.4472	<.0001*
Rubber Type*Test Temperature	2	23.13445	11.56722	8.5512	0.0008*
Error	42	56.81325	1.3527		
C. Total	47	200.44368			

[1]DF: Degrees of freedom
*Statistical significant different at alpha level = 0.05

Interestingly for this study, there seems to be an interaction between rubber type and test temperature, as presented in Table 3-3. This interaction was observed between -24 °C and -36 °C, where the average stiffness obtained for the cryogenic rubber mixes decreased at the lower test temperature (Figure 3-4). This interaction could be explained by the high standard deviation obtained for the cryogenic rubber mixes at -36 °C, since the least square means using the Tukey-Kramer HSD (Honestly significant difference) test of the AR mixes were not statistically different at -24 °C and -36 °C, as shown in Table 3-4. An increase in standard deviation was observed as the test temperature decreased for all the mixes (Figure

3-2), which is in agreement with Podolsky (2014), Buss (2014) and Peralta (2013) [22-24]. The increase in standard deviation is probably related to either testing device limitations or the natural response of the materials at lower temperatures.

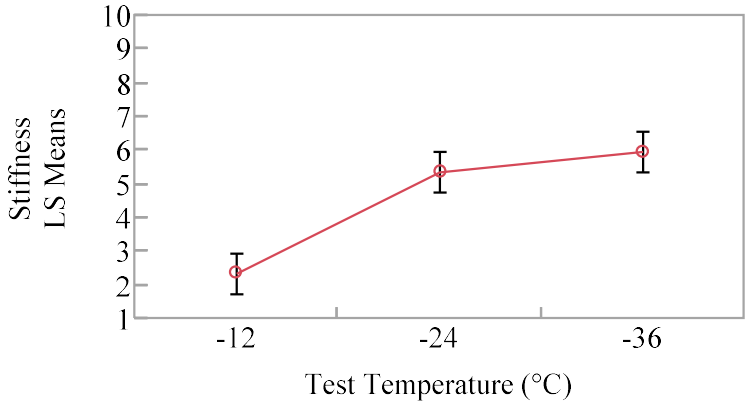

Figure 3-3. Stiffness (kN/m) least square means plot for test temperature. Standard error = 0.2971

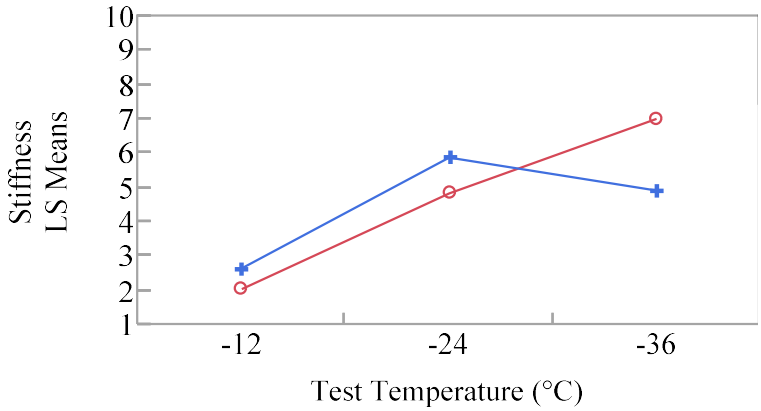

Figure 3-4. Stiffness (kN/m) least square means plot for rubber type and test temperature interaction. o Ambient rubber, + Cryogenic rubber.

Table 3-4. Tukey-Kramer HSD least square means differences of stiffness for rubber type and test temperature interaction.

Level				Least Sq Mean
Ambient,-36	A			7.0108000
Cryogenic,-24	A	B		5.8867750
Cryogenic,-36		B		4.9197625
Ambient,-24		B		4.8366125
Cryogenic,-12			C	2.6512500
Ambient,-12			C	2.0425000

Levels not connected by same letter are significantly different.
Alpha level = 0.05 and Q=2.98525

Fracture toughness, K_{IC}

In order to determine how fracture toughness is affected by the type of rubber and/or addition of polyoctenamer, the average values were compared and are shown in Figure 3-5. The average results for the fracture toughness indicate how the values increase at -12 °C to -24 °C independently of the type of mix. The average fracture decreases from -24 °C to -36 °C for both mixes without polyoctenamer (AMB and CRYO) and shows an increase for the mixes with polyoctenamer (AP and CP), but the standard deviations reveal no significant statistical difference.

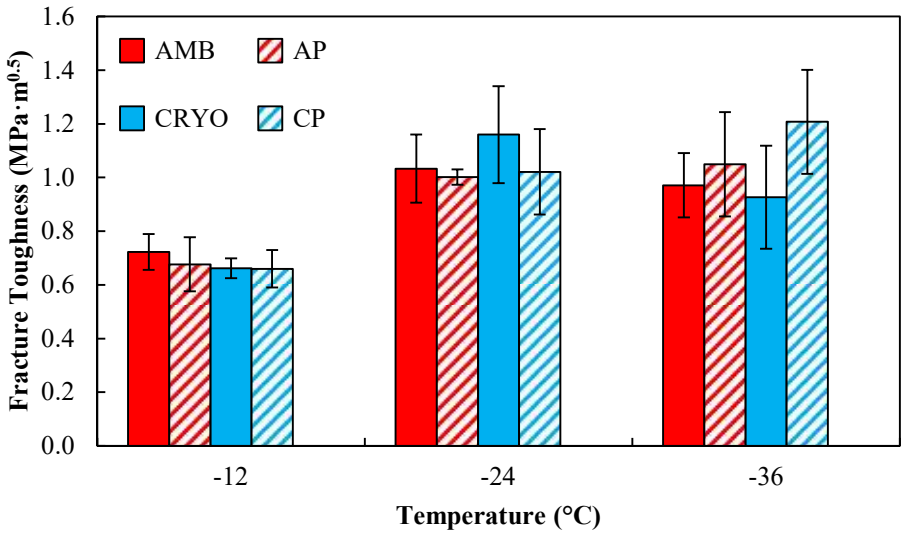

Figure 3-5. Comparison of fracture toughness of asphalt rubber mixes for Ambient rubber (AMB), Ambient rubber and Polyoctenamer (AP), Cryogenic rubber (CRYO), and Cryogenic rubber and Polyoctenamer (CP) at three different low temperatures.

The full ANOVA for fracture toughness showed that the rubber type does not have a significant effect on the fracture toughness of the mixes, nor the interactions between rubber type and the other factors contemplated in the model. From the reduced ANOVA results in Table 3-5, the fracture toughness of the AR mixes was significantly affected by the test temperature. The average fracture toughness at -12 °C was statistically significant different compared to the average fracture toughness at -24 °C and -36 °C (Figure 3-6). There is a

possibility that the fracture toughness of the AR mixes is not sensitive to temperatures lower than -24 °C, as the rubber particles help sustain the local stresses preventing further crack growth.

Table 3-5. Analysis of Variance for Fracture Toughness, K_{IC}.

Source	DF[1]	Sum of Squares	Mean Square	F Ratio	p-value
Polyoctenamer (%)	1	0.0066977	0.0066977	0.3693	0.5466
Test Temperature	2	1.4194714	0.7097357	39.1369	<.0001*
Polyoctenamer (%)*Test Temperature	2	0.1533339	0.0766670	4.2276	0.0212*
Error	42	0.7616576	0.018135		
C. Total	47	2.3411606			

[1]DF: Degrees of freedom
*Statistical significant different at alpha level = 0.05

In comparison with other asphalt technologies, Podolsky et al. (2014) found that the average fracture toughness for mixes prepared with warm mix technology tends to increase and then decrease as test temperatures further decrease [24]. Similarly to this study, the decrease found by Podolsky et al. (2014) was not statistically significant different, due to the high variability of the data at lower temperatures. Overall, the average fracture toughness values obtained are in accordance with values reported by West et al. (2013) on different RAP mixtures and by Buss et al. (2014) on hot mix asphalt and warm mix asphalt mixes at similar test temperatures [22, 25]. Compared to Peralta et al. (2013), the average fracture toughness results were slightly lower than from bio-asphalt with asphalt mixes [23].

In contrast with the stiffness of the mixes, where there was an interaction between rubber type and test temperature, the rubber type did not interact with the test temperatures for fracture toughness. On the other hand, an interaction effect between the percent of polyoctenamer and the test temperature for fracture toughness was found (Figure 3-7). It seems that the presence of polyoctenamer may help retain the fracture toughness of AR mixes at lower test temperatures, whereas the AR mixes without polyoctenamer may

experience a decrease in fracture toughness at the lowest test temperature. It is worth mentioning that the average fracture toughness at -24 °C and -36 °C, for both levels of percent of polyoctenamer, were not significantly different when the least square means test was performed utilizing the Tukey- Kramer HSD (Table 3-6). Therefore, it is not clear how the interaction of the polyoctenamer with test temperature affects the fracture toughness of AR mixes at very low temperatures.

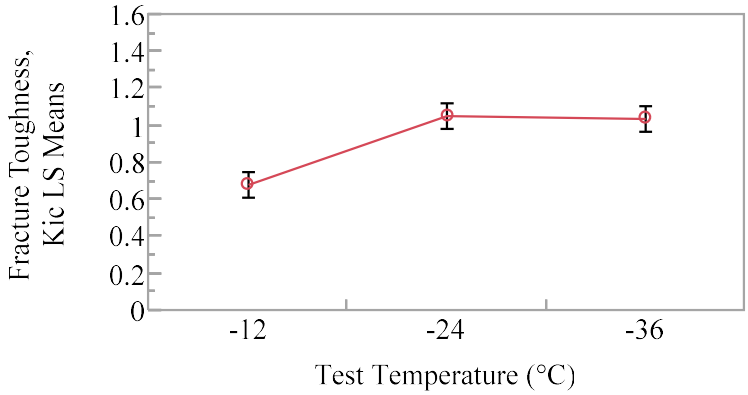

Figure 3-6. Fracture Toughness (MPa·m$^{0.5}$) least square means for test temperature. Standard error = 0.0340

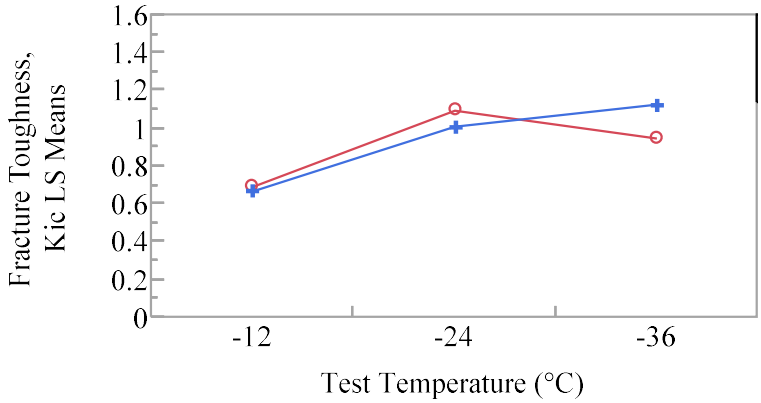

Figure 3-7. Fracture toughness (MPa·m$^{0.5}$) least square means for polyoctenamer (PO) and test temperature interaction. o 0% PO, + 4.5% PO.

Table 3-6. Tukey-Kramer HSD least square means difference of fracture toughness for % polyoctenamer and test temperature interaction

Level			Least Sq Mean
4.5,-36	A		1.1284750
0,-24	A		1.0966000
4.5,-24	A		1.0116875
0,-36	A		0.9489375
0,-12		B	0.6937500
4.5,-12		B	0.6700000

Levels not connected by same letter are significantly different.

Fracture energy, G_f

Figure 3-8 summarizes the results obtained for fracture energy, Gf. It is known that lower fracture energy is required at lower temperatures. In general, the results are consistent with what was expected, decrease in fracture energy as test temperature decreased. The CP mix, however, did not follow this trend. At -36 °C, where a decrease is expected, an increase in the fracture energy was observed, which was similar to the fracture energy obtained at -12 °C. When comparing the average fracture energy for CP at -24 °C to the averages obtained at -12 °C and -36 °C, there was significant difference in the means. This may suggest an interaction between the cryogenic rubber and the polyoctenamer at that specific temperature.

The analysis of variance (Table 3-7) corroborates that test temperature had an effect in the fracture energy and Figure 3-9 illustrates how the average fracture energy diminished as the test temperature decreased. Similar decreasing trends were reported in the literature [22-27]. Furthermore, there may have been possible interactions between the rubber type and the percent of polyoctenamer. This is thought to be a consequence of the particle size of the GTR and the mechanics of how the polyoctenamer interacted with these particles, yet when comparing the means through the Tukey HSD least square, no significant differences were found between rubber type and percent of polyoctenamer (Figure 3-10, Table 3-8).

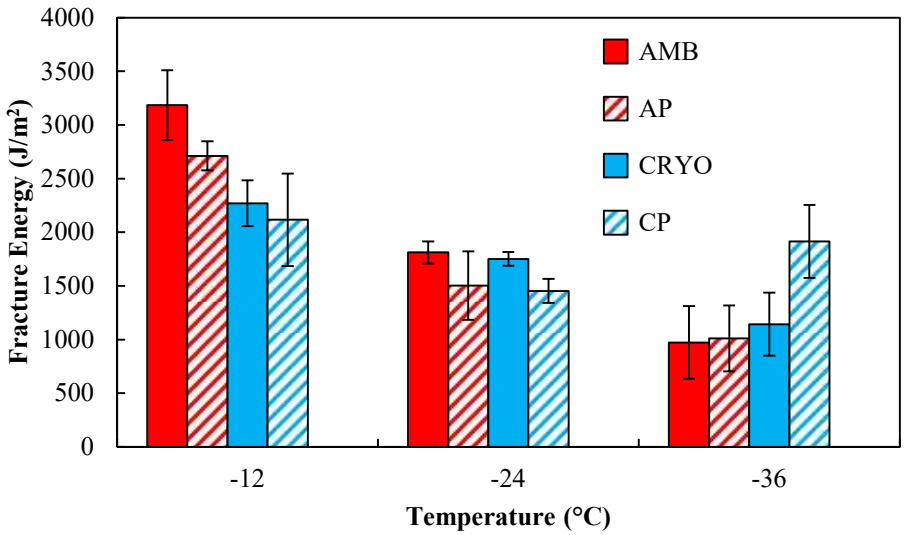

Figure 3-8. Comparison of fracture energy of asphalt rubber mixes for Ambient rubber (AMB), Ambient rubber and Polyoctenamer (AP), Cryogenic rubber (CRYO), and Cryogenic rubber and Polyoctenamer (CP) at three different low temperatures.

Table 3-7. Analysis of variance for fracture energy, G_f.

Source	DF[1]	Sum of Squares	Mean Square	F Ratio	Prob > F
Rubber Type	1	100543	100543	1.3460	0.2536
Polyoctenamer %	1	59956	59956	0.8026	0.3763
Test Temperature (°C)	2	14600482	7300241	97.7299	<.0001*
Rubber Type*Polyoctenamer %	1	375007	375007	5.0203	0.0313*
Rubber Type*Test Temperature (°C)	2	3343833	1671917	22.3823	<.0001*
Polyoctenamer %*Test Temperature (°C)	2	1355275	677638	9.0717	0.0006*
Rubber Type*Polyoctenamer %*Test Temperature (°C)	2	261495	130748	1.7503	0.1882
Error	36	2689132	74698		
Total	47	22785724			

[1]DF: Degrees of freedom
*Statistical significant different at alpha level = 0.05

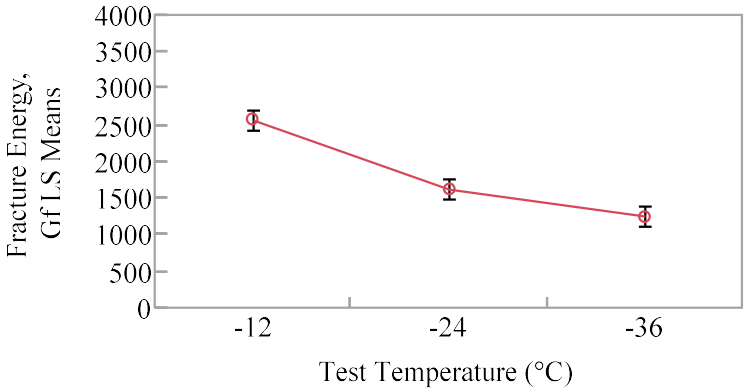

Figure 3-9. Fracture energy (J/m²) least square means for test temperature.
Standard error = 68.33

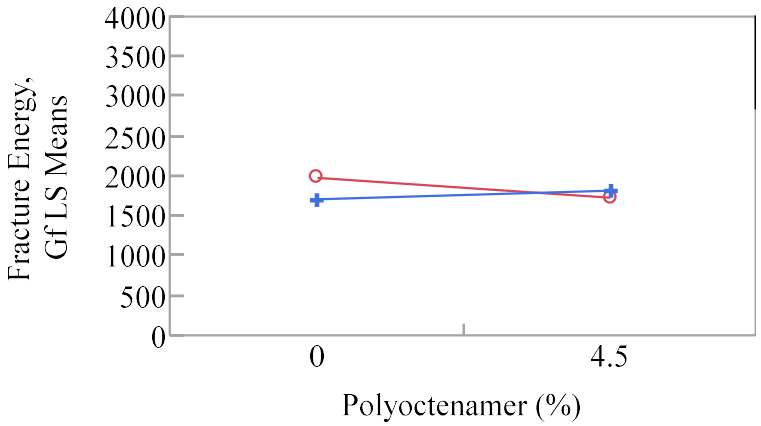

Figure 3-10. Fracture energy (J/m^2) least square means for rubber type and polyoctenamer interaction. o Ambient rubber, + Cryogenic rubber.

Table 3-8. Tukey-Kramer HSD least square means difference of fracture energy for rubber type and % polyoctenamer interaction

Level		Least Sq Mean
Ambient,0	A	1990.0525
Cryogenic,4.5	A	1827.8333
Ambient,4.5	A	1742.5896
Cryogenic,0	A	1721.7394

Levels not connected by same letter are significantly different.

Significant interaction between the rubber type and the temperature were observed in this experiment (Table 3-7). It seems that cryogenic rubber mixes tended to have lower fracture energy when compared to ambient rubber mixes at -12 °C (higher testing temperature); meanwhile at -36 °C (lower testing temperature) the average fracture energy of cryogenic rubber mixes was similar to its average fracture energy at -24 °C (Figure 3-11). This was not observed in the fracture energy of ambient rubber mixes, where its fracture energy decreased as temperature decreased. Ambient rubber mixes at -36 °C presented lower fracture energy than the cryogenic mixes. This is, again, believed to be due to the particle sizes of the rubber types, which makes the ambient rubber mixes slightly more susceptible to thermal cracking than cryogenic rubber mixes. Ambient rubber particles are flat, elongated and bigger in size than cryogenic rubber particles, which in contrast are rounder and smaller.

Additionally, the percent of polyoctenamer and the test temperature seem to interact between the temperatures of -24 °C and -36 °C (p-value = 0.0006), the addition of polyoctenamer appeared to help maintain the fracture energy of the AR mixes of this study at very low temperatures, compared to the AR mixes without polyoctenamer (Figure 3-12).

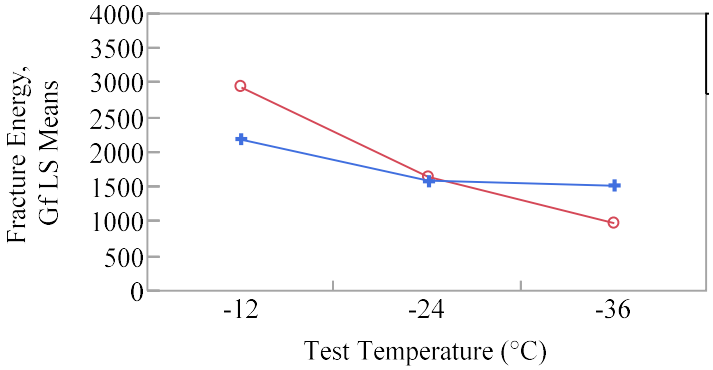

Figure 3-11. Fracture energy (J/m^2) least square means for rubber type and test temperature interaction. o Ambient rubber, + Cryogenic rubber.

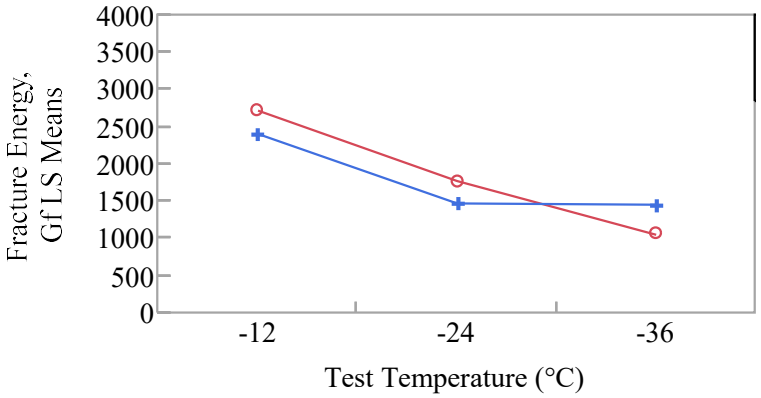

Figure 3-12. Fracture energy (J/m^2) least square means for polyoctenamer (PO) and test temperature interaction. o 0% PO, + 4.5% PO.

Conclusions

In this study, the low temperature performances of four types of AR mixes by means of the semicircular bend (SCB) geometry test were determined. The stiffness, fracture toughness and fracture energy were obtained for these mixes, and their values are very similar to those found in the literature for asphalt mixes using different technologies, as

warm mix asphalt, RAP, and bio-oil asphalts. From the results one can conclude that the rubber type and percent of polyoctenamer may not have significant negative effects on the low temperature performance of the AR mixes at the dosages used in this study. Thus, the use of polyoctenamer to improve the AR mixes workability during mixing and compaction would not be detrimental to their low temperature performance. It has being demonstrated that AR mixes do not only have excellent fatigue and rutting performance, but also, good thermal cracking performance, making it suitable to be used in geographical areas where the seasonal temperatures vary from very hot summers to very cold winters. Future efforts will be performed to corroborate and correlate the SCB test results with the disk-shaped compact tension (DCT) test, mainly because of the high variability presented in the SCB test results, not only in this study but also the results found in the literature. Like the SCB test, the DCT test allows the evaluation of the thermal cracking performance of asphalt mixes. By using the DCT test, it would be possible to cross reference the new results with the SCB results and determine if the high variability obtained at low temperatures for the SCB test is a consequence of a material behavior, or a limitation of the SCB test.

Acknowledgments

The authors would like to thank Seneca Petroleum, Flint Hills and Lehigh Technologies for supplying of us with the materials utilized in this research. Special thanks go to Dr. W. Robert Stephenson from the Department of Statistics at Iowa State University, for providing guidance on the statistical analysis. Also, we would like to provide special acknowledge to Jianhua Yu from the Department of Civil, Construction and Environmental Engineering at Iowa State University for his assistance in sample preparation.

References

[1] Liu H, Chen Z, Wang W, Wang H, Hao P. Investigation of the rheological modification mechanism of crumb rubber modified asphalt (CRMA) containing TOR additive. Construction and Building Materials. 2014;67, Part B(0):225-33.

[2] Xie ZX, Shen JA. Effect of cross-linking agent on the properties of asphalt rubber. Construction and Building Materials. 2014;67:234-8.

[3] Willis JR, Turner P, Plemmons C, Rodezno C, Rosenmayer T, Daranga C, et al. Effect of rubber characteristics on asphalt binder properties. Road Materials and Pavement Design. 2013;14:214-30.

[4] Min KE, Jeong HM. Characterization of air-blown asphalt/trans-polyoctenamer rubber blends. J Ind Eng Chem. 2013;19(2):645-9.

[5] Cong P, Wang J, Li K, Chen S. Physical and rheological properties of asphalt binders containing various antiaging agents. Fuel. 2012;97(0):678-84.

[6] Moreno F, Sol M, Martín J, Pérez M, Rubio MC. The effect of crumb rubber modifier on the resistance of asphalt mixes to plastic deformation. Materials & Design. 2013;47(0):274-80.

[7] Oliveira JRM, Silva HMRD, Abreu LPF, Fernandes SRM. Use of a warm mix asphalt additive to reduce the production temperatures and to improve the performance of asphalt rubber mixtures. Journal of Cleaner Production. 2013;41(0):15-22.

[8] Liu Y, Han S, Zhang Z, Xu O. Design and evaluation of gap-graded asphalt rubber mixtures. Materials & Design. 2012;35(0):873-7.

[9] Peralta J, Silva HMRD, Machado AV, Pais J, Pereira PAA, Sousa JB. Changes in Rubber Due to its Interaction with Bitumen when Producing Asphalt Rubber. Road Materials and Pavement Design. 2010;11(4):1009-31.

[10] Kök BV, Çolak H. Laboratory comparison of the crumb-rubber and SBS modified bitumen and hot mix asphalt. Construction and Building Materials. 2011;25(8):3204-12.

[11] Aflaki S, Memarzadeh M. Using two-way ANOVA and hypothesis test in evaluating crumb rubber modification (CRM) agitation effects on rheological properties of bitumen. Construction and Building Materials. 2011;25(4):2094-106.

[12] Burns B. Rubber-modified asphalt paving binder. Google Patents; 2000.

[13] Ng Puga KLN. Rheology and performance evaluation of Polyoctenamer as Asphalt Rubber modifier in Hot Mix Asphalt. Ames: Digital Repository @ Iowa State University; 2013.

[14] Kaloush KE. Asphalt rubber: Performance tests and pavement design issues. Construction and Building Materials. 2014;67:258-64.

[15] Kinloch AJ. Fracture behaviour of polymers / A.J. Kinlock and R.J. Young. London : New York: London : Applied Science Publishers ; New York : Elsevier Science Publishing Co. distributor; 1983.

[16] AASHTO. M 320-10 - Performance-Graded Asphalt Binder. Standard Specifications for Transportation Materials and Methods of Sampling and Testing (33rd Edition) and AASHTO Provisional Standards, 2013 Edition: American Association of State Highway and Transportation Officials (AASHTO); 2013.

[17] Peralta EJ, Silva HMRD, Pais JC, Machado AV. Rheological and functional evaluation of the interactions between bitumen and rubber. Advanced Testing and Characterisation of Bituminous Materials, Vols 1 and 2. 2009:109-21.

[18] Brown ER, Kandhal PS, Roberts FL, Kim YR, Lee D-Y, Kennedy TW, et al. Hot mix asphalt materials, mixture design, and construction. 3rd ed. Lanham, Md.: NAPA Research and Education Foundation; 2009.

[19] AASHTO. M 323-13 - Superpave Volumetric Mix Design. Standard Specifications for Transportation Materials and Methods of Sampling and Testing (33rd Edition) and AASHTO Provisional Standards, 2013 Edition: American Association of State Highway and Transportation Officials (AASHTO); 2013.

[20] AASHTO. TP 105-13 - Determining the Fracture Energy of Asphalt Mixtures Using the Semicircular Bend Geometry (SCB). Standard Specifications for Transportation Materials and Methods of Sampling and Testing (33rd Edition) and AASHTO Provisional Standards, 2013 Edition: American Association of State Highway and Transportation Officials (AASHTO); 2013.

[21] AASHTO. T 313-12 - Determining the Flexural Creep Stiffness of Asphalt Binder Using the Bending Beam Rheometer (BBR). Standard Specifications for Transportation Materials and Methods of Sampling and Testing (33rd Edition) and AASHTO Provisional Standards, 2013 Edition: American Association of State Highway and Transportation Officials (AASHTO); 2013.

[22] Buss AF. Investigation of sustainable pavement technologies evaluating warm mix asphalt using recycled asphalt materials. Digital Repository @ Iowa State University; 2014.

[23] Peralta E, Silva HMRD, Williams RC, Machado AV. Micro-analysis of Physico-Chemical Interaction between the components of bitumen mixtures with rubber 2013.

[24] Podolsky J. Investigation of bio-derived material and chemical technologies as sustainable warm mix asphalt additives [Doctoral Dissertation]. Ames: Iowa State University; 2014.

[25] West R, Willis JR, Marasteanu MO. Improved mix design, evaluation, and materials management practices for hot mix asphalt with of high reclaimed asphalt pavement content2013.

[26] Li XJ, Marasteanu MO. Using Semi Circular Bending Test to Evaluate Low Temperature Fracture Resistance for Asphalt Concrete. Exp Mech. 2010;50(7):867-76.

[27] Velasquez R, Turos M, Moon KH, Zanko L, Marasteanu M. Using recycled taconite as alternative aggregate in asphalt pavements. Construction and Building Materials. 2009;23(9):3070-8.

CHAPTER 4. FATIGUE PERFORMANCE OF LABORATORY PRODUCED ASPHALT RUBBER MIXES CONTAINING POLYOCTENAMER

A paper to be submitted to *Road Materials and Pavement Design*, published by Taylor and Francis

Ka Lai N. Ng Puga[1] and R. Christopher Williams[2]

Abstract

The fatigue performance of asphalt rubber mixes has proved to be superior to that of conventional asphalt mixes. In this study, the impact in the fatigue performance of laboratory produced asphalt rubber mixes that contained polyoctenamer and two types of ground tire rubber were evaluated. From the results, the laboratory fatigue performance of the mixes containing ambient rubber was significantly higher than of those that were produced with cryogenic rubber. The addition of polyoctenamer proved to help more in the fatigue performance of the mixes containing cryogenic rubber. At low testing micro-strains the laboratory fatigue performance of all the mixes was comparable.

Keywords: ground tire rubber, asphalt, mixes, polyoctenamer, fatigue performance, fatigue cracking, beam fatigue

[1] Corresponding author. Ph.D. candidate. Department of Civil, Construction and Environmental Engineering, Iowa State University, Ames, IA 50011. E-mail: knnp@iastate.edu
[2] Professor of Civil Engineering, Department of Civil, Construction and Environmental Engineering, Iowa State University, Ames, IA 5001. E-mail: rwilliam@iastate.edu

Introduction

Asphalt rubber (AR) has been used in pavement to improve the fatigue performance of asphalt mixtures since the 1960s. Scrap tires are an environmental concern, as evidenced by the generation of approximately 3.7 million tons of scrap tires in 2013 in the United States of America (Association, 2014). Two different types of ground tire rubber (GTR) can be obtained from the processing of scrap tires. Ambient GTR is obtained by processing the scrap tires at ambient temperatures, and cryogenic GTR is obtained when the scrap tires are shredded and processed at cryogenic temperatures. Depending on the type of process, ambient or cryogenic, the particles shape and size distribution will differ. Ambient GTR will tend to have particles with rough surfaces and will have larger particle sizes than cryogenic rubber, usually a #30 mesh. The particle surfaces of cryogenic rubber tend to be smooth, and due to the cryogenic temperatures much smaller particle sizes can be obtained (~#200 mesh).

When the rubber particles react with the asphalt binders during asphalt blending, these particles tend to swell with the lighter components of the asphalt, but they do not melt. Therefore, the presence of the rubber particles have a great effect on the AR binders' viscosity, making the workability of the binders challenging because of a high viscosity. To overcome this, certain additives are added to AR binders to improve their workability (Baumgardner & Anderson, 2008). Polyoctenamer (PO) or trans-polyoctenamer is a polymer that has been used with AR binders to improve their workability by reducing their viscosities. PO is obtained by polymerizing cyclootadiene by means of a metathesis reaction (Burns, 2000).

Baumgardner & Anderson (2008), Liu et al. (2014), Xie & Shen (2014) and Ng Puga (2013) have found that AR binders containing PO present appropriate rheological properties

when compared to control AR binders. Many studies have focused on the fatigue performance of AR mixes (Geng et al., 2014; Kaloush, 2014; Khalid & Artamendi, 2003; Oliveira et al., 2013; Palit, Reddy, & Pandey, 2004; Xiao et al., 2009). However, no studies have been performed on the fatigue performance of AR mixes containing PO. The objective of this paper is to evaluate how the fatigue performance of laboratory produced AR mixtures that contain ambient GTR or cryogenic GTR is affected by the addition of PO.

Materials and Methods

The materials used to make the asphalt rubber mixture beams and the method followed to test the fatigue performance of the asphalt rubber mixes are described in the following section.

Binder production

The asphalt rubber (AR) binders were produced using a base binder PG46-34, provided by Flints Hills Resources (Pine Bend, Minnesota). The base binder was modified using 12 percent of ground tire rubber (GTR) by weight of the base binder. Two types of GTR were utilized in this study: an ambient ground (40 mesh) supplied by Seneca Petroleum (Crestwood, Illinois) and a cryogenic ground (200 mesh) provided by Lehigh Technologies (Atlanta, Georgia). The AR binders were also modified with two levels of trans-polyoctenamer (PO), manufactured by Evonik (Marl, Germany): the control level at 0 percent PO by weight of GTR and the recommended dosage by the manufacturer at 4.5 percent PO by weight of GTR.

The production of the AR binders was as follows. The base binder was preheated covered in an oven at 180 °C and then placed in a heated mantel at the same temperature. A

Silverson L4RT-A high shear mixer was used along with a general purpose disintegrating head to shear the base binder at an initial shear of 1000 rpm. The temperature was monitored using a Model 210 J-Kem Scientific temperature controller probe. The GTR and PO were added to the base binder when the temperature measured by the controller was stabilized at 180 °C. Then, the shear speed was increased to 3000 rpm. The temperature of the overall binder decreases after the addition of GTR and PO, mainly due to the differences in temperature between the base binder and the GTR, being the latest at room temperature. Therefore, time was allowed for the temperature to reattain 180 °C. Once this was achieved, blending was continued for an additional hour to allow reaction between the rubber, polyoctenamer and base binder.

The experimental matrix of the production of AR binders is presented in Table 4-1. Four AR binders were laboratory produced in total, these binders were then performance graded following the standard method AASHTO M320-10 (AASHTO, 2013a). The four laboratory produced AR binders graded as PG64-34.

Table 4-1. Experimental plan of laboratory produced asphalt rubber binders

Binder ID	Type of GTR[1] by weight of base binder[2]		Trans-polyoctenamer by weight of GTR	
	12% ambient	12% cryogenic	0%	4.5%
AMB	x		x	
AMB+PO	x			x
CRYO		x	x	
CRYO+PO		x		x

[1]GTR: Ground tire rubber
[2]Base binder: PG46-34

Mix production and specimen preparation

A coarse-graded 19 mm NMAS (nominal maximum aggregate size) gradation was used to produce the AR mixes. The gradation was comprised of five types of aggregates

locally obtained in the State of Iowa. The proportions of the gradation was as follows: 25 percent of ¾-in limestone, 12 percent of $^{3}/_{8}$-in limestone, 30 percent of quartzite, 14 percent of natural sand and 18 percent of manufactured sand. To account for the breakage of the limestone aggregates during asphalt plant production, one percent of lime dust was also considered in the gradation. Figure 4-1 summarizes the mix gradation used in this study.

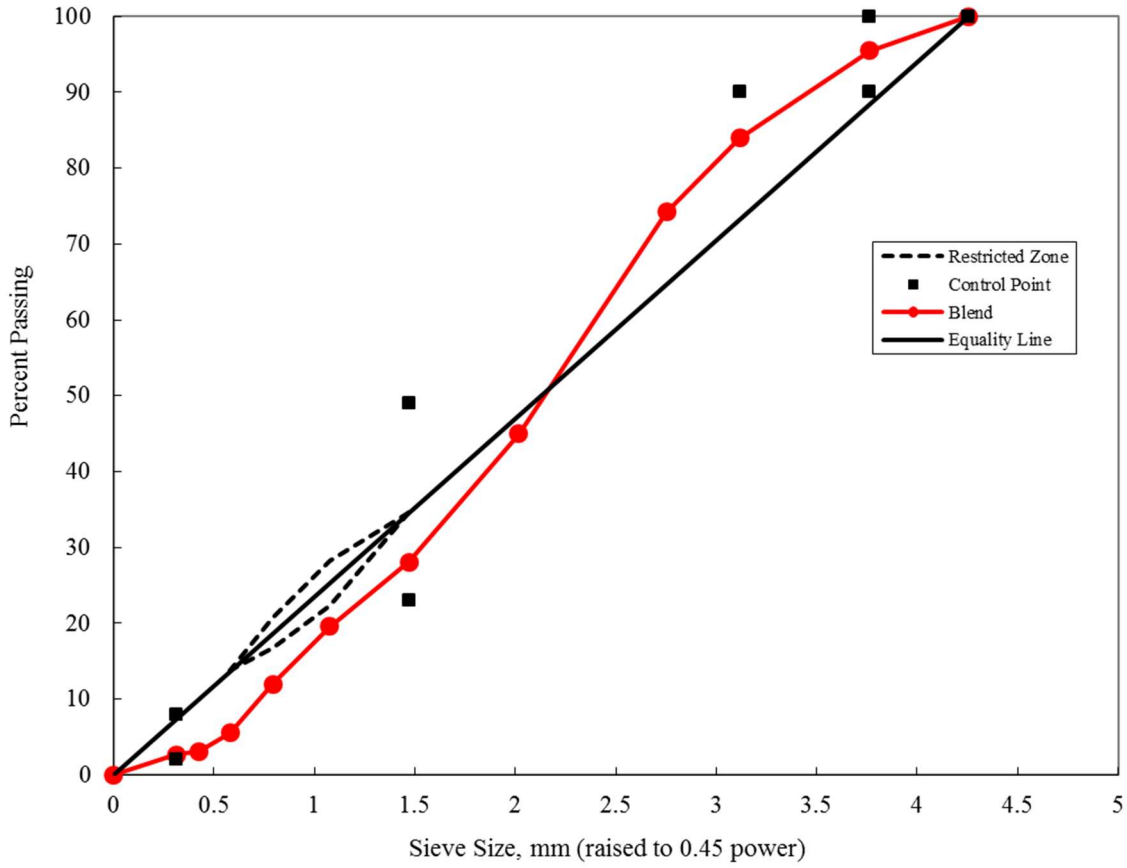

Figure 4-1. Aggregates gradation used in the experimental study (19 mm NMAS)

The Superpave volumetric mix design standard described in AASHTO M323-13 (AASHTO, 2013b) was followed to obtain the optimum binder content for the asphalt rubber mixes. The AR mixes were produced using an optimum binder content of 5.6%. The mixing and compaction temperatures of the mixes were 180 °C and 165 °C, respectively. The curing

time of the mixes before compaction was for 3 hrs at 165 °C. Slabs were compacted using a Precision Machine Welding rolling wheel compactor to a 7 percent target air voids. After compaction, volumetrics were checked on the slabs the following day to ensure the target air voids were met with a tolerance of ±1 percent air voids.

Three beams were saw cut from each slab. Following the AASHTO T321-07 standard procedure (AASHTO, 2013c), the dimensions of the cut beams were 380 ± 6 mm long, 63 ± 6 mm wide and 50 ± 6 mm height. Once cut, volumetrics on each beam were checked to ensure that the target air voids of 7 ± 1 percent were still being met. A total of six beams were obtained for each type of mix.

Beam fatigue testing

The repeated flexural bending test run in a four point beam fatigue machine produces a constant bending moment over the center one-third of a beam. The sinusoidal load applied to produce the bending moment induces the beam to return to its original position producing in this way reversal stresses, meaning that the external portions of the beam are being subjected to tensile and compressive stresses. Basic engineering equations are used to calculate the stresses and strains produced in the beam due to the sinusoidal load.

The maximum tensile stress, σ_t, at each load cycle interval can be computed using equation 1.

$$\sigma_t = \frac{0.357P}{bh^2} \quad \text{(Eq. 1)}$$

where:

σ_t = tensile stress (psi),

P = load applied by actuator (N),

b = average specimen width (m), and

h = average specimen height (m).

The maximum tensile strain, ε_t, can be computed using the equation 2 presented below.

$$\varepsilon_t = \frac{12\delta h}{3L^2 - 4a^2} = \frac{12\delta h}{0.325703} \quad \text{(Eq. 2)}$$

ε_t = maximum tensile strain (m/m),

δ = maximum deflection at center of beam (m),

a = space between inside clamps (0.119 m), and

L = length of beam between outside clamps (0.357 m).

The flexural stiffness, S, is then computed by the ratio of the maximum tensile stress and the maximum tensile strain, as showed in equation 3.

$$S = \frac{\sigma_t}{\varepsilon_t} \quad \text{(Eq. 3)}$$

The repeated flexural bending test was performed using a control and data acquisition system (CDAS) that has as a servo-feedback loading control electronics and, a transducer data acquisition and timing functionality. The servo controlled apparatus allows control and measurement from a load cell and a linear variable displacement transducer (LVDT) that was mounted onto the specimen. This servo controlled apparatus also allows the monitoring of the actuator position. The test was run in strain controlled mode, and the sinusoidal load frequency applied was 10 Hz.

The beam specimens were conditioned in an environmental chamber at the testing temperature 20.0 ± 0.5 °C at least two hours prior to testing. The beams were tested at different constant strain levels. The constant strain levels chosen in this study were 375, 450, 525, 600, 675 and 750 microstrain (με). The initial stiffness of each beam was determined at the 50th load cycle and the termination stiffness was computed as 50 percent of the initial stiffness. When the beam achieved the termination stiffness the number of cycles to failure, N_f was recorded. Table 4-2 summarizes the experimental matrix for the beam fatigue test.

Table 4-2. Beam fatigue test experimental plan

Mix ID	Microstrain (με)					
	375	450	525	600	675	750
AMB	X	X	X	X	X	X
AMB+PO	X	X	X	X	X	X
CRYO	X	X	X	X	X	X
CRYO+PO	X	X	X	X	X	X

Since the tests was run using the controlled strain approach as the mode of loading, the fatigue life of the mixtures can be computed using the power law relationship represented in equation 4 (Brown et al., 2009).

$$N_f = K_1\left(\frac{1}{\varepsilon_t}\right)^{K_2} \quad \text{(Eq. 4)}$$

N_f = number of cycles to failure

ε_t = flexural strain

K_1, K_2 = regression constants

The flexural modulus is characterized in the fatigue life model by K_1, whereas the rate of damage accumulation in the sample is indicated by K_2 in the model.

Results and Discussion

The results obtained from the four-point bending beam fatigue test of the AR mixes for the initial flexural stiffness and cycles to failure are summarize in Table 4-3. The AMB+PO and CRYO+PO beams tested at 375 με, passed 3 million cycles without failing. Therefore, only five data points were used for these mixtures to obtain the experimental fatigue coefficients. Figure 4-2 presents the fatigue curves obtained for the AR mixes. From it, it can be stated that at higher micro-strain levels (600 – 750 με), the mixes with ambient rubber presented a higher load cycles to failure. At lower micro-strain levels, the mix containing cryogenic rubber with polyoctenamer presented a higher load cycles to failure than the other three mixes. The mixes containing ambient GTR only, presented lower cycles to failure than their counterpart with polyoctenamer at all the tested micro-strain levels.

Table 4-3. Four-point bending beam fatigue test results

Mix type	Microstrain (με)	Initial Flexural Stiffness (MPa)	50% of Initial Flexural Stiffness (MPa)	Flexural Stiffness at end of test (MPa)	Cycles to Failure (N_f)	Cumulative dissipated energy (MJ/m^3)
AMB	750	1447	723	660	115810	106.8
	675	1911	955	861	172390	172.3
	600	1946	973	967	250290	203.7
	525	1557	778	768	245220	140.4
	450	1782	891	887	680940	295.5
	375	1669	835	821	2163410	581.5
AMB+PO	750	1827	825	914	152670	201.5
	675	1978	989	975	187640	182.6
	600	1750	875	873	668940	475.0
	525	1520	760	593	1328790	726.6
	450	1852	926	926	913580	427.6
	375	1587	793	1025	> 3000000	—

Table 4-3. Four-point bending beam fatigue test results - continued

Mix type	Microstrain (με)	Initial Flexural Stiffness (MPa)	50% of Initial Flexural Stiffness (MPa)	Flexural Stiffness at end of test (MPa)	Cycles to Failure (Nf)	Cumulative dissipated energy (MJ/m3)
CRYO	750	1854	927	896	41190	50.3
	675	1955	978	960	116960	105.6
	600	1827	914	888	501570	324.6
	525	1937	969	936	477160	307.7
	450	1695	848	842	637410	298.1
	375	1966	983	975	896100	292.8
CRYO+PO	750	2284	1142	1142	17240	325.9
	675	1767	884	880	87260	76.9
	600	1967	984	938	582410	444.4
	525	1513	765	764	3388230	1726.1
	450	1884	942	937	642600	302.1
	375	1493	747	868	> 3000000	---

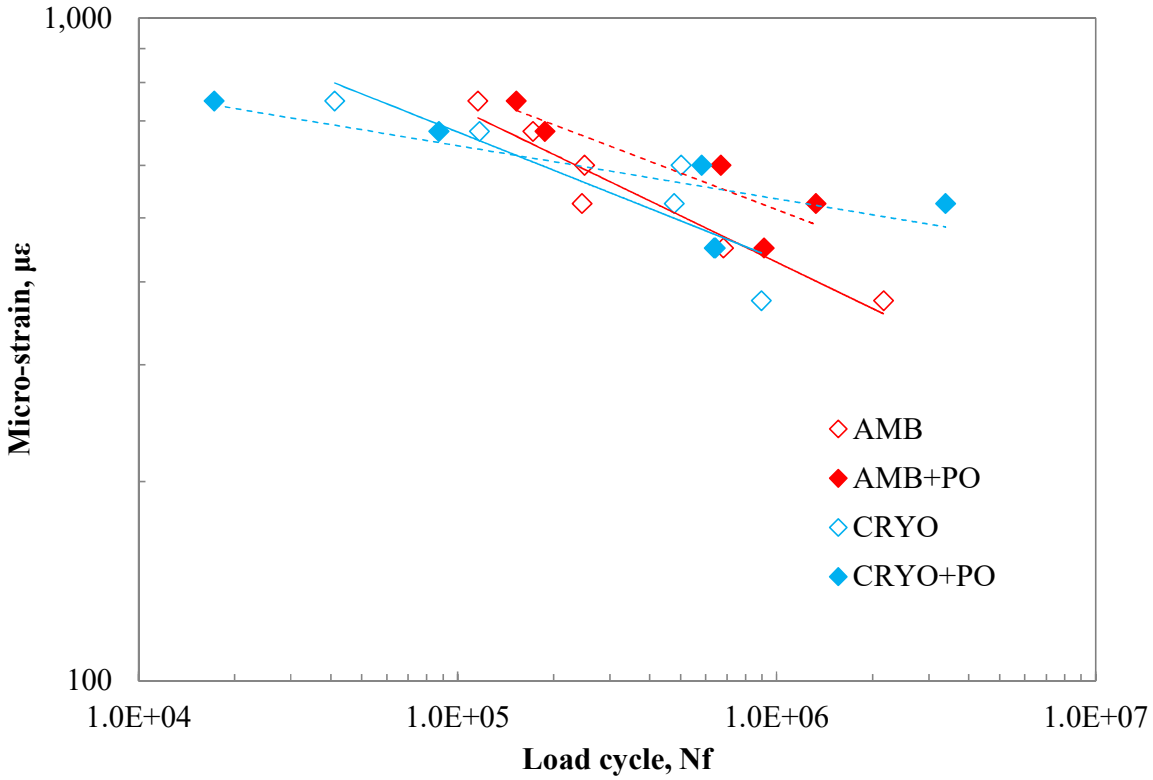

Figure 4-2. Four point bending beam fatigue curves

Table 4-4 presents the experimental fatigue coefficients obtained for the four mixes. Ranges of K1 values for conventional asphalt mixtures found by Williams et al (2011) point to values in between 2.497E-17 and 1.398 E-7; Ghuzlan and Carpenter (2003) have reported values in the range of 3.98E-15 – 1.25E-7; whereas, Pais et al (2009) reported values of 3.04E-12 to 3.81E-7. Based on the values reported by the literature, the coefficient values obtained for the flexural modulus of the four asphalt rubber mixes fall on the higher side of the ranges described previously. Which means that the fatigue life of these mixtures is comparable or better than conventional asphalt mixtures. As seen in the results, the K2 values obtained for the AMB, AMB+PO and CRYO mixes are around the suggested values by the literature. The Asphalt Institute recommends a K2 value of 4.477; Shell (1978) recommends 4.0; The University of Nottingham (Huang, 2004) suggests a value of 3.571; and the Illinois Department of Transportation (S. H. Carpenter, 2006) points to a range of 3.5 to 4.5 for K2. The CRYO+PO presented the highest coefficient for the rate of damage accumulation, which means that the accumulation of fatigue damage is lower for this mixture.

Table 4-4. Experimental fatigue coefficients for asphalt rubber mixes with 7 % air voids

Mix ID	K1	K2	R^2
AMB	3.652E-08	3.980	0.926
AMB+PO	1.062E-08	4.227	0.883
CRYO	1.782E-08	4.053	0.777
CRYO+PO	1.297E-16	8.159	0.695

It is not clear what chemical and physical interactions the polyoctenamer has with the cryogenic rubber that led to lower fatigue performance at higher micro-strain, but to higher fatigue performance at lower micro-strain. When comparing the fatigue life of the two types

of rubber, it is noticeable that the fatigue life of the ambient rubber is usually higher than the fatigue life of the cryogenic rubber, this could be due to the larger particle sizes of the rubber that interact better in the matrix of the mixes. Also, cryogenic rubber presents a smoother particle surface; whereas, the particle surface of ambient rubber is very rough. It could be that the addition of polyoctenamer provides a better network or matrix for the cryogenic rubber at lower micro-strains.

Conclusions

The fatigue testing results of the laboratory produced AR mixes demonstrate the good fatigue life that AR mixes have in general. In this study, mixes containing ambient GTR tend to present a higher fatigue life than the mixes containing cryogenic GTR. Regardless of this, the four AR mixes presented good fatigue performance compared to conventional asphalt mixes. The addition of polyoctenamer have a greater effect on the fatigue performance of AR mixes containing cryogenic GTR than for those that contain ambient GTR. In sum, the results of this study are in accordance with results from the literature of AR mixes that do not contain polyoctenamer.

Acknowledgments

The authors would like to thank Seneca Petroleum, Flint Hills and Lehigh Technologies for supplying the materials utilized in this research. The authors would like to acknowledge the help in mixing and compaction of slabs to Jesse Studer, and the help in test specimen preparation to Paul Ledtje.

References

AASHTO. (2013a). M 320-10 - Performance-Graded Asphalt Binder *Standard Specifications for Transportation Materials and Methods of Sampling and Testing (33rd Edition)*

and AASHTO Provisional Standards, 2013 Edition: American Association of State Highway and Transportation Officials (AASHTO).

AASHTO. (2013b). M 323-13 - Superpave Volumetric Mix Design *Standard Specifications for Transportation Materials and Methods of Sampling and Testing (33rd Edition) and AASHTO Provisional Standards, 2013 Edition*: American Association of State Highway and Transportation Officials (AASHTO).

AASHTO. (2013c). T 321-07 (2011) - Determining the Fatigue Life of Compacted Hot Mix Asphalt (HMA) Subjected to Repeated Flexural Bending *Standard Specifications for Transportation Materials and Methods of Sampling and Testing (33rd Edition) and AASHTO Provisional Standards, 2013 Edition*: American Association of State Highway and Transportation Officials (AASHTO).

Association, R. M. (2014). 2013 U.S. Scrap Tire Management Summary, from http://www.rma.org/download/scrap-tires/market-reports/US_STMarket2013.pdf

Baumgardner, G., & Anderson, D. (2008). *Trans-polyoctenamer reactive polymer/recycled tire rubber modified asphalt: processing, compatibility and binder properties.* Paper presented at the Proceedings: 5th international transport conference, Wuppertal, Germany.

Brown, E. R., Kandhal, P. S., Roberts, F. L., Kim, Y. R., Lee, D.-Y., Kennedy, T. W., . . . National Center for Asphalt Technology (U.S.). (2009). *Hot mix asphalt materials, mixture design, and construction* (3rd ed.). Lanham, Md.: NAPA Research and Education Foundation.

Burns, B. (2000). *Rubber-modified asphalt paving binder* (Vol. EP 0994161 A2): Google Patents.

Carpenter, S., Ghuzlan, K., & Shen, S. (2003). Fatigue endurance limit for highway and airport pavements. *Transportation Research Record: Journal of the Transportation Research Board*(1832), 131-138.

Carpenter, S. H. (2006). Fatigue performance of IDOT mixtures.

Geng, L., Wang, X., Ren, R., Chen, F., & Yang, X. (2014). Performance evaluation of dense mixtures with stabilised rubber modified asphalt. *Road Materials and Pavement Design, 15*(4), 953-965.

Huang, Y. H. (2004). *Pavement analysis and design* (2nd ed.). Upper Saddle River, NJ: Pearson/Prentice Hall.

Kaloush, K. E. (2014). Asphalt rubber: Performance tests and pavement design issues. *Construction and Building Materials, 67*, 258-264. doi: DOI 10.1016/j.conbuildmat.2014.03.020

Khalid, H. A., & Artamendi, I. (2003). Performance based characterisation of crumb rubber asphalt modified using the wet process. *Road Materials and Pavement Design, 4*(4), 385-399.

Liu, H., Chen, Z., Wang, W., Wang, H., & Hao, P. (2014). Investigation of the rheological modification mechanism of crumb rubber modified asphalt (CRMA) containing TOR additive. *Construction and Building Materials, 67, Part B*(0), 225-233. doi: http://dx.doi.org/10.1016/j.conbuildmat.2013.11.031

Ng Puga, K. L. N. (2013). Rheology and performance evaluation of Polyoctenamer as Asphalt Rubber modifier in Hot Mix Asphalt: Digital Repository @ Iowa State University.

Oliveira, J. R. M., Silva, H. M. R. D., Abreu, L. P. F., & Fernandes, S. R. M. (2013). Use of a warm mix asphalt additive to reduce the production temperatures and to improve the performance of asphalt rubber mixtures. *Journal of Cleaner Production, 41*(0), 15-22. doi: http://dx.doi.org/10.1016/j.jclepro.2012.09.047

Pais, J. C., Pereira, P. A., Minhoto, M. J., Fontes, L. P., Kumar, D., & Silva, B. (2009). *The prediction of fatigue life using the k1-k2 relationship.* Paper presented at the 2nd Workshop on Four Point Bending.

Palit, S., Reddy, K., & Pandey, B. (2004). Laboratory Evaluation of Crumb Rubber Modified Asphalt Mixes. *Journal of Materials in Civil Engineering, 16*(1), 45-53. doi: 10.1061/(ASCE)0899-1561(2004)16:1(45)

Shell International Petroleum Company, l. (1978). *Shell Pavement Design Manual: Asphalt Pavements and Overlays for Road Traffic*: Shell International Petroleum.

Williams, R. C., Cascione, A., Haugen, D. S., Buttlar, W. G., Bentsen, R., & Behnke, J. (2011). Characterization of hot mix asphalt containing post-consumer recycled asphalt shingles and fractionated reclaimed asphalt pavement. *Final report for the Illinois State Toll Highway Authority*.

Xiao, F., Amirkhanian, S. N., Shen, J., & Putman, B. (2009). Influences of crumb rubber size and type on reclaimed asphalt pavement (RAP) mixtures. *Construction and Building Materials, 23*(2), 1028-1034. doi: http://dx.doi.org/10.1016/j.conbuildmat.2008.05.002

Xie, Z. X., & Shen, J. A. (2014). Effect of cross-linking agent on the properties of asphalt rubber. *Construction and Building Materials, 67*, 234-238. doi: DOI 10.1016/j.conbuildmat.2014.03.039

CHAPTER 5. RHEOLOGY STUDY OF ASPHALT RUBBER BINDERS USING DIFFERENT GEOMETRIES

A paper to be submitted to International Journal of Pavement Engineering, published by Taylor and Francis

Ka Lai N. Ng Puga[1] and R. Christopher Williams[2]

Abstract

Crumb rubber from waste tires is mostly used to improve the rheological characteristics of asphalt binders due to its elastomeric characteristics and thus improve mix performance. However, it is suspected that the swelled crumb rubber particles, depending upon the crumb rubber grind size, can interfere in the assessment of the rheological properties of the modified asphalts due to the 1 mm gap in the parallel plate geometry of the dynamic shear rheometer (DSR) used during testing procedures. Some researchers have proposed to increase the gap geometry to 2 mm to avoid the interference of the crumb rubber particles with the plates of the DSR; whereas, others proposed to use the concentric cylinder geometry. Meanwhile, some advocate for separating the rubber particles from the liquid part of the binders using a binder accelerated separation method. The objective of this paper is to determine if the results obtained using these different gaps, geometries and/or separation methods are any different amongst them. For this, four different asphalt rubber binders have been studied; the unaged and rolling thin film oven aged materials were tested in dynamic

[1] Corresponding author. Ph.D. candidate. Department of Civil, Construction and Environmental Engineering, Iowa State University, Ames, IA 50011. E-mail: knnp@iastate.edu
[2] Professor of Civil Engineering, Department of Civil, Construction and Environmental Engineering, Iowa State University, Ames, IA 5001. E-mail: rwilliam@iastate.edu

shear rheometers. The continuous performance grade of the binders were determined and master curves constructed. Rotational viscosities, specific gravities and storage stability were also measured.

Keywords: ground tire rubber, asphalt, binder, polyoctenamer, rheology, dynamic shear rheometer, parallel plate, concentric cylinders

Introduction

The rheological characterization of asphalt rubber (AR) binders have regain attention in the past few years. The established standardized performance grading protocol for asphalt binders have been questioned on whether or not the correct rheological characteristics of AR binders are being measured. In 1994 and 1995, Bahia and Davies performed rheological testing in asphalt rubber binders containing different types and percentages of ground tire rubber using a 2 mm gap parallel plate; however, these results were not compared with other testing geometries. Tayebali et al. (1997) studied the applicability of the Superpave protocols for dynamic shear rheometer (DSR) testing using ambient ground rubber, they deduced that the differences in the results obtained with 1 mm and 2 mm gap was within the natural variability of the results and the specimen setup (operator related). However, Putman and Armirkhanian (2006) separated the rubber particles from the binders, and compared the results obtained from the drained binders and the binders with the rubber particles finding that the rubber particles had two types of effects: an interaction effect and a filler effect. These effects dependent on the crude source and rubber content. More recently, Baumgardner & D'Angelo (2012) developed a proposed crumb rubber PG binder specification utilizing concentric cylinders in the DSR, in order to allow larger size rubber particles in the binders; however the effects of ground tire rubber particles was not evaluated.

The use of concentric cylinders to determine rheological properties had been used before by Polacco (2003) in order to construct master curves of SBS - polymer modified asphalts at temperatures from 60 °C to 90 °C obtaining good overlapping with results obtained with parallel plate geometry. In 2012, Peralta et al. proposed a new separation method for AR binders that allows testing of the liquid part of the binder without the interference of the rubber particles, while keeping a 1 mm gap in the parallel plate geometry of the DSR. Despite all the efforts and studies that have been carried out, a comprehensive comparison of different factors that can affect the rheological properties of AR binders has not been performed. Factors as the different testing geometries, materials types (such as binders non-centrifuged or centrifuged), AR binders with modifiers, AR binders unaged and RTFO aged, and AR binders that have undergo curing in the oven for 72 hrs have not been studied altogether.

This paper has several objectives. The first objective is to evaluate the viscosities of different types of AR binders subjected to different treatments and compare the results among them in order to determine though an analysis of variance which factors are statistically significant. The second objective is to evaluate the storage stability of AR binders subjected to different treatments. The third objective is to determine specific gravities and mass losses of the different types of AR binders. The fourth objective is to performance grade the different types of AR binders using different dynamic shear rheometer geometries. The fifth objective is to construct master curves from those binders in order to fit two models used to describe the rheology of binders in the asphalt industry, and compare their predictions with the true rheological behavior of the AR binders. Lastly, the final objective is to compare the master curves of the AR binders that were tested using different

geometries in the dynamic shear rheometer among each category of binder type, in order to determine which geometry is able to segregate the effects of the rubber particles during testing.

Materials and Methods

A base binder PG52-34 from Flint Hills Resources (Pine Bend, Minessota) was used to laboratory blend asphalt rubber binders. Two types of crumb rubber from waste tires or ground tire rubber (GTR) were selected at a dosage of 12 percent by weight of base binder. The types of GTR utilized were ambient grind (30 mesh) and cryogenic grind (200 mesh). The GTR were provided by Seneca Petroleum (Crestwood, Illinois) and Lehigh Technologies (Atlanta, Georgia), respectively. Polyoctenamer was also used to produce the asphalt rubber binders, this polyoctenamer was manufactured by Evonik (Germany). The dosages of polyoctenamer selected were 0 percent (control group) and 4.5 percent. Four types of asphalt rubber binders were blended in total; Table 5-1 shows the blending matrix.

Table 5-1. Laboratory produced asphalt rubber binders matrix

Binder ID	Base Binder	Type of GTR by weight of base binder		Polyoctenamer by weight of GTR	
		12% Ambient	12% Cryogenic	0%	4.5%
AMB	PG 52-34	X		X	
AP	PG 52-34	X			X
CRYO	PG 52-34		X	X	
CP	PG 52-34		X		X

The binders were shear blended using a Silverson L4RT shear mixer in conjunction with a general purpose disintegrating head. The base binder was heated to 180 °C while being slowly sheared at 1000 rpm before adding the ground tire rubber and polyoctenamer. After adding the ground tire rubber and polyoctenamer; the shear speed was increased to

3000 rpm. Since the ground tire rubber and the polyoctenamer are at room temperature before being added to the base binder, a decrease in temperature of the sheared binder was observed. Therefore, shear blending was done at 3000 rpm until the temperature returned to 180 °C and from there the blend was kept for an hour.

Figure 5-1 summarizes the procedure followed after blending each of the four types of asphalt rubber binders before collecting samples for testing. The centrifuged materials were obtained right after blending the binders (no cure) or after 72 hours of curing by using the Binder Accelerated Separation (BAS) method develop by Peralta (2012). The BAS method consists of centrifuging the asphalt rubber binders using a device that it is inserted in a one-gallon can. The device consists of a wire mesh basket covered by a cotton cloth. The basket is contained inside a metal circular frame. A part of the device called the "weight" is use to keep the circular frame with the basket in place and allows them to spin inside the one-gallon can.

An IKA RW 20 digital overhead stirrer is use to exert the centrifuge power, a special fixture is used with the overhead stirrer. This fixture has three notches that couples perfectly with the metal circular frame. An hour prior to centrifuging, the device is placed in a one-gallon can and kept heated in an oven at the blending temperature. Prior to centrifuging, the device is filled with the binder, approximately a quart to a little less of a third of its capacity. The fixture is then interlocked and the centrifugal force is applied, a maximum 1500 rpm were applied, care was taken to avoid spillage of the binder due to the action of the centrifugal force. After centrifuging, the ground tire rubber particles are trapped inside the basket and the liquid part of the binder remains in the one-gallon can.

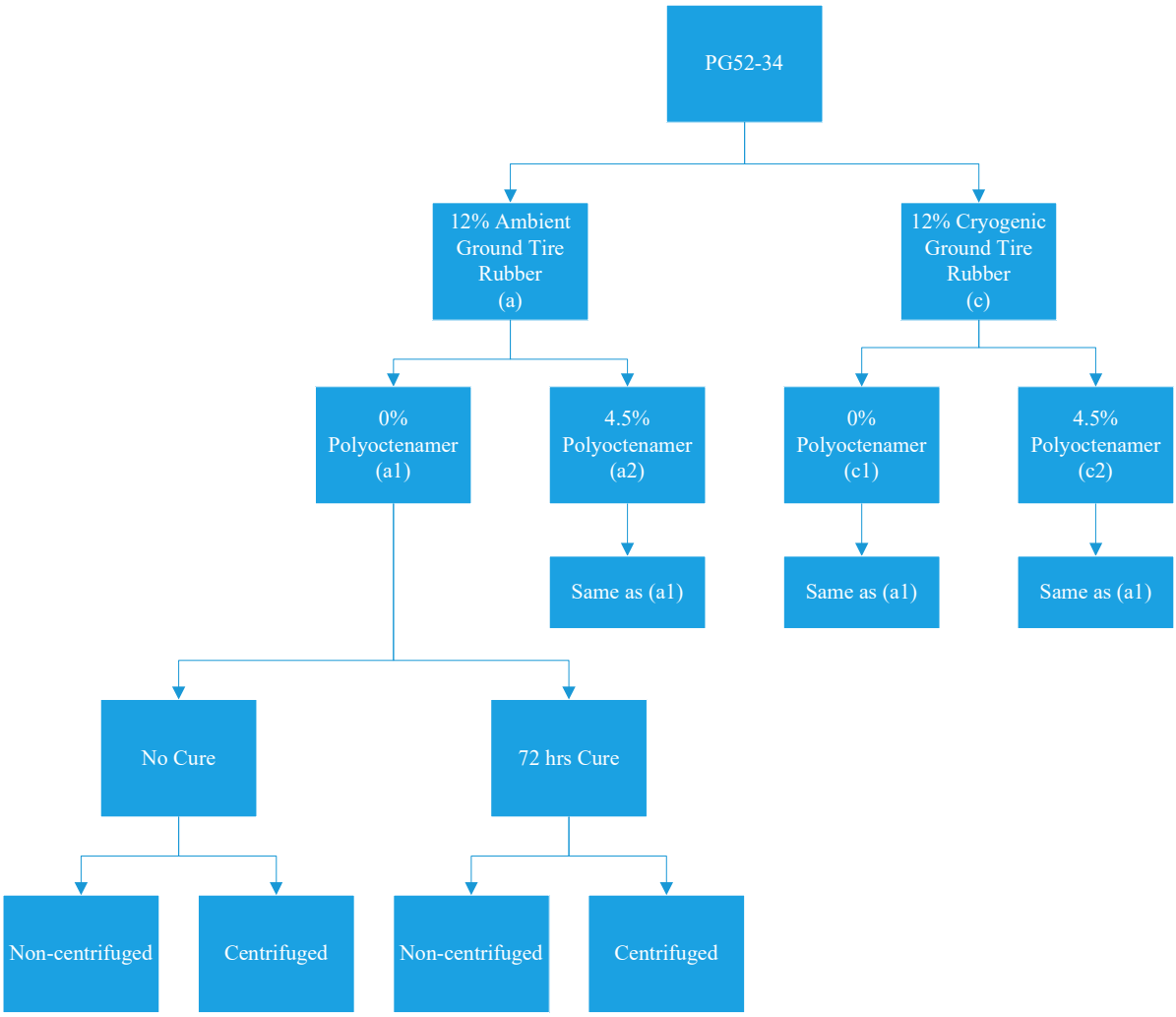

Figure 5-1. Flow chart of laboratory asphalt rubber binder production

Samples of the non-centrifuged and centrifuged unaged asphalt rubber binders were then collected to be tested in the dynamic shear rheometer. Rotational viscosity, specific gravity and storage stability tests (for non-centrifuged binders) were also performed. The remains of the unaged materials were then RTFO aged and samples were collected to perform rotational viscosity tests, and other rheology tests in the dynamic shear rheometer.

Rotational viscosity and specific gravity

Rotational viscosities were measured following ASTM D4402-13 *Standard Test Method for Viscosity Determination of Asphalt at Elevated Temperatures Using a Rotational Viscometer*. The unaged and RTFO aged non-centrifuged binders were tested at 20 rpm at 135 °C, 165 °C, 180 °C and 195 °C using a S27 spindle size in a Brookfield DVII+ Pro Rotational Viscometer. Whereas, the unaged and RTFO aged of the base binder and the centrifuged binders were tested at 20 rpm at 135 °C, 150 °C, 165 °C and 180 °C using a S21 spindle size. The lower testing temperatures and bigger spindle size selection for the base binder and centrifuged materials was due to the expected lower viscosities when compared to their non- centrifuged counterparts and to maintain torque values between 2% to 98%.

An analysis of variance using a split plot design was performed at an alpha level of 0.05, in order to establish the statistical differences of the binders' viscosities.

Specific gravities of the unaged binders non-centrifuged and centrifuged were determined using ASTM D70-09 *Standard Test Method for Density of Semi-Solid Bituminous Materials (Pycnometer Method)* in order to quantify the change in specific gravities due to the addition of rubber, type of rubber, addition of polyoctenamer or 72 hrs of curing. The experimental plan for rotational viscosity and specific gravity evaluation is summarized in Table 5-2.

Table 5-2. Rotational viscosity and specific gravity experimental plan for asphalt rubber binders

Binder Type	Curing	Type of material	Rotational viscosity		Specific gravity
			Unaged	RTFO aged	Unaged
PG52-34	None	N/A	XXX	XXX	XXX
AMB	None	Non-Centrifuged	XXX	XXX	XXX
		Centrifuged	XXX	XXX	XXX
	72 hrs cured	Non-Centrifuged	XXX	XXX	XXX
		Centrifuged	XXX	XXX	XXX
AP	None	Non-Centrifuged	XXX	XXX	XXX
		Centrifuged	XXX	XXX	XXX
	72 hrs cured	Non-Centrifuged	XXX	XXX	XXX
		Centrifuged	XXX	XXX	XXX
CRYO	None	Non-Centrifuged	XXX	XXX	XXX
		Centrifuged	XXX	XXX	XXX
	72 hrs cured	Non-Centrifuged	XXX	XXX	XXX
		Centrifuged	XXX	XXX	XXX
CP	None	Non-Centrifuged	XXX	XXX	XXX
		Centrifuged	XXX	XXX	XXX
	72 hrs cured	Non-Centrifuged	XXX	XXX	XXX
		Centrifuged	XXX	XXX	XXX

Master curves and model fitting

Master curves of the unaged and RTFO aged materials were obtained by using dynamic shear rheometers. Two dynamic shear rheometers were used in the experiment. A TA Instruments rheometer, model AR 1500ex was used to test the binders using parallel plate geometry at 1 and 2 mm gaps. A second TA Instruments rheometer, model ARES G2, was used to obtain master curves using concentric cylinders geometry (cup and bob). The cup used on the ARES G2 had a diameter of 30 mm, whereas the conical bob had a diameter of 18.6 mm, allowing a gap between walls of 5.7 mm. In total, three different geometries were used to obtain the master curves of the materials.

The unaged and RTFO aged samples that were tested using the parallel plate geometries were tested at the following temperatures: 20, 30, 40, 46, 52, 58, 64, 70, 76 and 82 °C. Whereas, the unaged and RTFO aged samples that were tested using the concentric cylinders geometry were tested at the following temperatures: 52, 58, 64, 70, 76, 82, 88, 95, 105, 115 and 135 °C, higher temperatures were chosen for the concentric cylinders because of the high viscosity of the samples at lower temperatures. All the unaged and RTFO aged samples were tested at the same frequencies ranging from 0.1 Hz to 100 Hz. The summarized experimental plan for the dynamic shear rheometer testing is presented in Table 5-3.

Table 5-3. Dynamic shear rheometer experimental testing plan for asphalt rubber binders

Binder Type	Curing	Type of material	DSR Unaged Master Curve			DSR RTFO-Aged Master Curve		
			Gap		CC	Gap		CC
			1mm	2mm		1mm	2mm	
AMB	None	Non-Centrifuged	XXX	XXX	X	XXX	XXX	X
		Centrifuged	XXX			XXX		
	72 hrs cured	Non-Centrifuged	XXX	XXX	X	XXX	XXX	X
		Centrifuged	XXX			XXX		
AP	None	Non-Centrifuged	XXX	XXX	X	XXX	XXX	X
		Centrifuged	XXX			XXX		
	72 hrs cured	Non-Centrifuged	XXX	XXX	X	XXX	XXX	X
		Centrifuged	XXX			XXX		
CRYO	None	Non-Centrifuged	XXX	XXX	X	XXX	XXX	X
		Centrifuged	XXX			XXX		
	72 hrs cured	Non-Centrifuged	XXX	XXX	X	XXX	XXX	X
		Centrifuged	XXX			XXX		
CP	None	Non-Centrifuged	XXX	XXX	X	XXX	XXX	X
		Centrifuged	XXX			XXX		
	72 hrs cured	Non-Centrifuged	XXX	XXX	X	XXX	XXX	X
		Centrifuged	XXX			XXX		

The Williams-Landel-Ferry (WLF) empirical equation (Eq. 5) was used to find the shift factors (a_T) to shift the curves for each binder type and testing geometry by applying the time-temperature superposition principle.

$$\log(a_T) = \frac{-C_1\left(T - T_{ref}\right)}{C_2 + \left(T - T_{ref}\right)} \quad \text{(Eq. 5)}$$

where:

a_T = shift factor,
T = temperature (K),
T_{ref} = reference temperature (K), and
C_1 and C_2 = empirical constants.

The same reference temperature T_{ref} was used to build all the master curves at 64 °C. With the aid of the Microsoft Excel Solver function a minimizing sum of square error (SSE_{a_T}) between the manually shift factors and the equation-based shift factors (from Eq. 5) was performed in order to find the empirical constants, C_1 and C_2.

$$SSE_{a_T} = \sum \frac{\left(\log a_{Tmanual} - \log a_{Tequation-based}\right)^2}{\left(\log a_{Tmanual}\right)^2} \quad \text{(Eq. 6)}$$

where:

$\log a_{Tmanual}$ = logarithm of the manually adjusted a_T, and
$\log a_{Tequation-based}$ = logarithm of the a_T obtained with Eq. 5.

After obtaining the empirical constants (C_1 and C_2) and the reduced frequencies, the master curves for the complex modulus (|G*|) were fitted to the empirical equations of the

Christensen-Anderson-Marasteanu (CAM) model and the Sigmoidal model. The CAM model defines the complex modulus (|G*|) and the phase angle (δ) as follows.

$$\left|G^*\right| = Gg\left[1+\left(\frac{\omega_c}{\omega}\right)^{\frac{\log 2}{R}}\right]^{-\frac{wR}{\log 2}} \quad \text{(Eq. 7)}$$

$$\delta = \frac{90w}{\left[1+\left(\frac{\omega_c}{\omega}\right)^{\frac{\log 2}{R}}\right]} \quad \text{(Eq. 8)}$$

where:

$\left|G^*\right|$ = Complex modulus (Pa),

δ = phase angle (degrees),

Gg = Glassy modulus (1E9 Pa),

ω_c = cross-over frequency

R = rheological index,

w = empirical parameter that takes into account how $\left|G^*\right|$ converges into two asymptotes as the frequency goes to zero or infinity, and

ω = reduced frequency (Hz).

Whereas, the Sigmoidal model defines the complex modulus with the following equation.

$$\log\left|G^*\right| = \upsilon + \frac{\alpha}{1+e^{\beta+\gamma\left[\log(\omega)\right]}} \quad \text{(Eq. 9)}$$

where:

$\left|G^*\right|$ = Complex modulus (Pa),

υ = lower asymptote,

α = difference between the values of the upper and lower asymptote,

β and γ = define the shape between the asymptotes and the location of the inflection point, and

$\log \omega$ = logarithm of the reduced frequency (Hz)

The minimization of sum of square error (SSE_{model}) for both models was performed with the aid of the Microsoft Excel Solver function in order to obtain the different parameters of each model.

$$SSE_{\text{model}} = \sum \frac{\left(\log\left|G^*_{observed}\right| - \log\left|G^*_{\text{model}}\right|\right)^2}{\left(\log\left|G^*_{observed}\right|\right)^2}$$

where:

$\log\left|G^*_{observed}\right|$ = logarithm of the measured complex modulus from the DSR, and

$\log\left|G^*_{\text{model}}\right|$ = logarithm of the predicted complex modulus obtained using either model.

Storage stability tests

Storage stability tests were performed by following the procedures in ASTM standard D7173-11 *Determining the separation tendency of polymer from polymer modified asphalt*. The binders of the top and bottom part of the tube were performance graded and the percent difference between the corresponding top and bottom were computed.

Results and Discussion

Viscosities

The average viscosities of the non-centrifuged laboratory produced binders are summarized from Table 5-4 to 5-6. The aging indexes for the binders were obtained by the ratio of the RTFO aged viscosities and the unaged viscosities. The values from Table 5-4 demonstrate that the presence of rubber particles have a significant influence on the rotational viscosity measurements. As seen, the non-cured laboratory produced binders meet the performance grade asphalt binder criteria for the maximum viscosity allowed at 135 °C, this values is 3.0 Pa·s, as required by AASHTO M320-10. As expected, the non-centrifuged binders with ambient rubber presented higher rotational viscosities compared with the non-centrifuged binders with cryogenic rubber. The higher viscosity readings for the unaged and RTFO aged materials of the non-centrifuged binders with ambient rubber is due to the bigger particle sizes of the ambient ground tire rubber when compared with the particle sizes of the cryogenic ground tire rubber. Also from Table 5-4, the addition of polyoctenamer increases the rotational viscosity at 135 °C of all the unaged binders, the opposite is observed for all the RTFO aged binders. The non-centrifuged RTFO aged binders without polyoctenamer present a higher viscosity than their counterpart with polyoctenamer, except for the CP binder. Whereas, the viscosities of the centrifuged RTFO binders without polyoctenamer were lower than the centrifuged RTFO binders with polyoctenamer at 135 °C. Table 5-5 shows how the viscosities of the non-centrifuged materials is lower for the unaged binders without polyoctenamer compared to the unaged with polyoctenamer between temperatures of 165 °C and 195 °C. In contrast, the viscosities of the non-centrifuged RTFO aged binders without polyoctenamer are higher than the RTFO aged binders with polyoctenamer at the aforementioned temperature range. As seen in Table 5-6, the same is not observed for the

centrifuged binders, the viscosities of the unaged and RTFO aged binders without polyoctenamer were lower when compared with their counterpart with polyoctenamer.

These differences in the average viscosities between the non-centrifuged and centrifuged binders show how the rubber particles interfere with the viscosity readings obtained during the tests. In general, the binders with ambient rubber presented higher viscosities than the binders with cryogenic rubber. This is expected because of the particle size differences between both types of GTR. Also, in general, the centrifuged binders without polyoctenamer presented lower viscosities than the centrifuged binders with polyoctenamer.

Figure 5-2 to 5-4 present a visual comparison of the average viscosities of the binders tested at 135, 150, 165, 180 and 195 °C at 20 rpm. The viscosities for the base binder PG46-34 are shown as a reference. From Figure 5-2 and 5-4 it is noticeable how the viscosities of the centrifuged unaged and RTFO aged CP binder cured for 72 hrs are significantly higher compared with the other centrifuged binders. This could be explained by the swelling of the cryogenic rubber particles during the curing process, the smaller particles of the cryogenic rubber swelled to their maximum capacity, somehow helped by the polyoctenamer, until they broke into smaller particles size due to the swelling. These smaller particles, less than #200 mesh, were then able to go through the cloth mesh used during centrifuging. This phenomenon was not observed for the centrifuged AP binders, it is believed that due to the bigger particles sizes of the ambient rubber their capacity of swelling is higher, and if they do indeed break into smaller particle sizes, these new smaller particles sizes for the ambient rubber will not be as small as the ones obtained with the cryogenic rubber. Therefore the new smaller ambient particles will still be retained in the cloth mesh used for centrifuging.

To really capture the statistical differences of the binders, an analysis of variance (ANOVA) was performed. The binders' viscosities at 135, 165 and 180 °C were chosen to perform the ANOVA. When performing an ANOVA, care should be taken to ensure that the data meet Fisher's assumption about equal variances. Figure 5-6 presents the non-transformed viscosity data, as it can be seen the variances are not equal, with the viscosities obtained at 135 °C having a largest variance compared to 165 and 180 °C. Therefore a logarithmic transformation was performed in order to meet Fisher's assumption, as seen in Figure 5-7.

The viscosity results at the aforementioned temperatures were statistically analyzed using a split-plot repeated measures design. The viscosity test is a repeated measures test because there are multiple viscosities measures over a range of temperatures in the same sample. In the split plot design the whole plot factors evaluated are the different types of binders (rubber type, polyoctenamer %, curing, centrifuging, aging) for each sample and the sub plot factor will be the testing temperatures at three different levels (135, 165 and 180 °C).

As established by ASTM D4402-13, repeated measurements of viscosities at the same temperatures are performed within a minute a part each. For ease of the statistical analysis, time was not taken as a second sub plot factor. Instead, the average of the viscosities at each temperature was taken into account for the split plot repeated measures design. It was considered that the variation in the viscosity readings within a minute apart were not significantly different. The summarized ANOVA table at an alpha level of 0.05 is presented in Table 5-7, where the F-ratios and p-values for each factor and interaction are presented. The significant different factors and interactions are marked with an asterisk. The complete statistical output can be found in **Error! Reference source not found.**.

Table 5-4. Asphalt rubber binders' average rotational viscosities at 135 °C and 20 rpm

	PG52-34	AMB		AP		CRYO		CP	
		No cure	72 hrs cure	No cure	72 hrs cure	No cure	72 hrs cure	No cure	72 hrs cure
Temperature 135 °C									
Unaged materials									
Non-centrifuged	0.205	1.759	2.658	2.211	3.051	1.315	1.732	1.450	1.813
Centrifuged	—	0.270	0.488	0.374	0.509	0.341	0.466	0.381	1.055
RTFO aged materials									
Non-centrifuged	0.276	3.956	3.856	3.666	3.769	2.482	2.613	2.329	2.807
Centrifuged	—	0.479	0.720	0.561	0.725	0.502	0.666	0.572	2.262
Aging index									
Non-centrifuged	1.347	2.530	1.450	1.655	1.235	1.887	1.508	1.606	1.549
Centrifuged	—	1.773	1.475	1.499	1.425	1.472	1.429	1.503	2.144

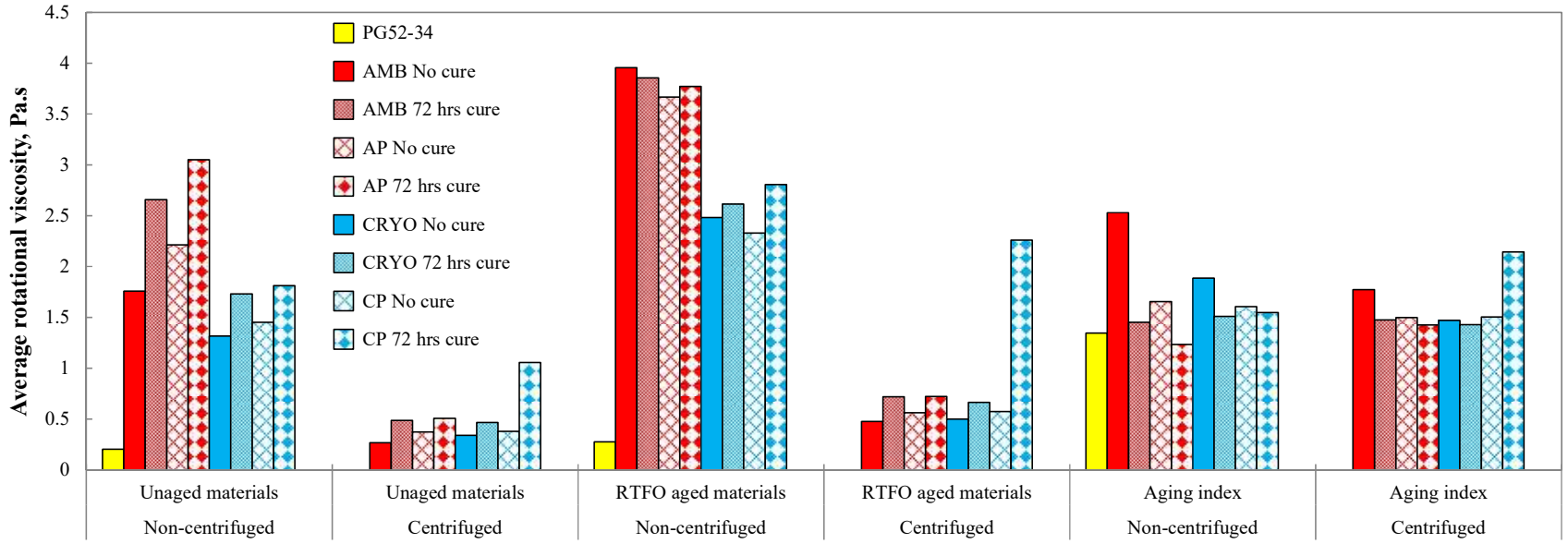

Figure 5-2. Average rotational viscosities measured at 135 °C and 20 rpm

Table 5-5. Non-centrifuged asphalt rubber binders' average rotational viscosities at 20 rpm

	PG52-34	AMB		AP		CRYO		CP	
		No cure	72 hrs cure	No cure	72 hrs cure	No cure	72 hrs cure	No cure	72 hrs cure
Temperature 165 °C									
Unaged materials	0.130	0.635	0.996	0.707	1.100	0.585	0.782	0.631	0.949
RTFO aged materials	0.159	1.333	1.399	1.208	1.260	0.951	1.021	0.806	1.028
Aging index	1.223	2.101	1.404	1.709	1.145	1.627	1.306	1.278	1.083
Temperature 180 °C									
Unaged materials	0.104	0.413	0.589	0.458	0.653	0.450	0.582	0.482	0.679
RTFO aged materials	0.112	0.722	0.803	0.703	0.799	0.667	0.747	0.594	0.703
Aging index	1.075	1.751	1.363	1.533	1.223	1.481	1.284	1.233	1.035
Temperature 195 °C									
Unaged materials	0.091	0.357	0.451	0.410	0.507	0.371	0.444	0.401	0.519
RTFO aged materials	0.092	0.517	0.585	0.489	0.639	0.532	0.554	0.431	0.558
Aging index	1.006	1.447	1.295	1.193	1.260	1.434	1.247	1.073	1.075

Table 5-6. Centrifuged asphalt rubber binders' average rotational viscosities at 20 rpm

	PG52-34	AMB		AP		CRYO		CP	
		No cure	72 hrs cure	No cure	72 hrs cure	No cure	72 hrs cure	No cure	72 hrs cure
Temperature 150 °C									
Unaged materials	0.130	0.185	0.262	0.211	0.273	0.194	0.256	0.212	0.564
RTFO aged materials	0.159	0.255	0.361	0.288	0.365	0.255	0.311	0.293	0.808
Aging index	1.223	1.377	1.379	1.363	1.339	1.317	1.215	1.386	1.434
Temperature 165 °C									
Unaged materials	0.104	0.126	0.166	0.141	0.171	0.131	0.166	0.137	0.346
RTFO aged materials	0.112	0.161	0.213	0.172	0.214	0.159	0.189	0.177	0.441
Aging index	1.075	1.278	1.281	1.219	1.254	1.209	1.143	1.293	1.277
Temperature 180 °C									
Unaged materials	0.091	0.098	0.117	0.108	0.120	0.103	0.122	0.103	0.233
RTFO aged materials	0.092	0.121	0.143	0.118	0.141	0.111	0.131	0.121	0.277
Aging index	1.006	1.237	1.226	1.092	1.176	1.087	1.070	1.170	1.191

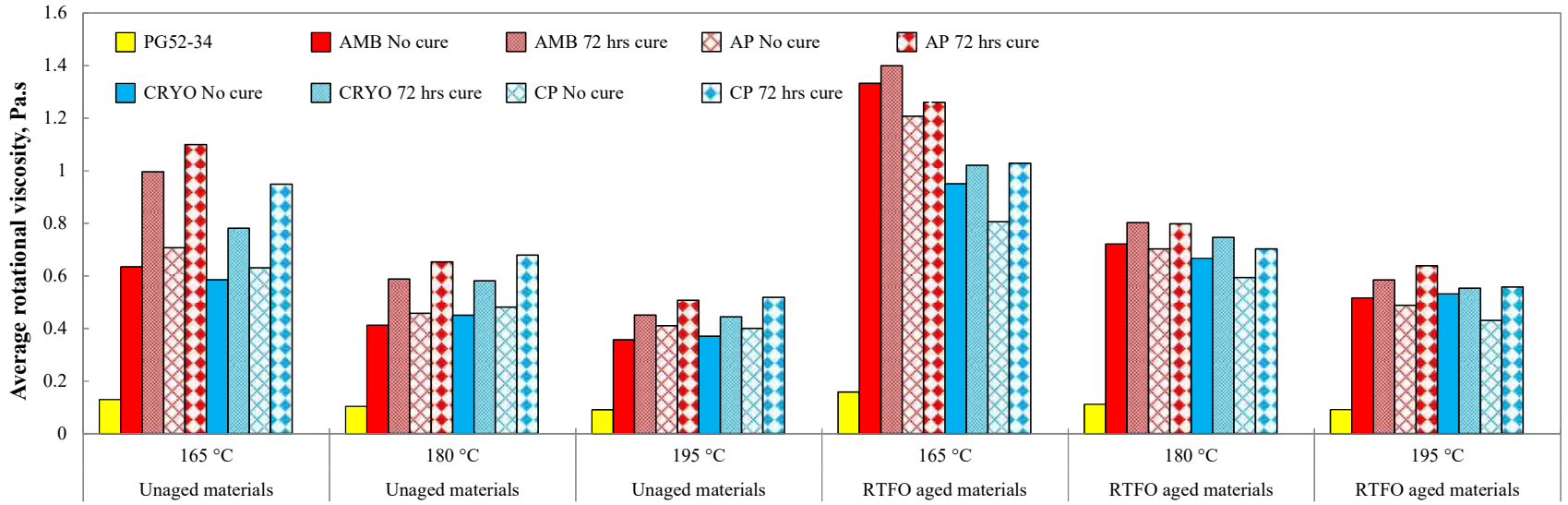

Figure 5-3. Average rotational viscosities of non-centrifuged asphalt rubber binders

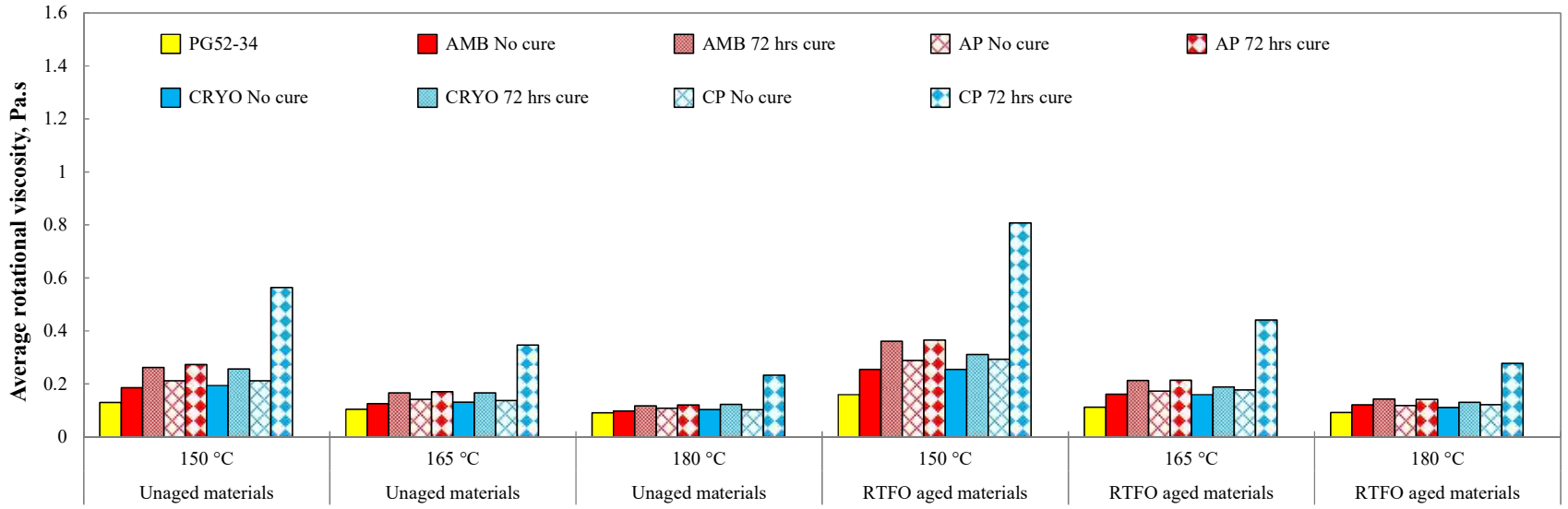

Figure 5-4. Average rotational viscosities of centrifuged asphalt rubber binders

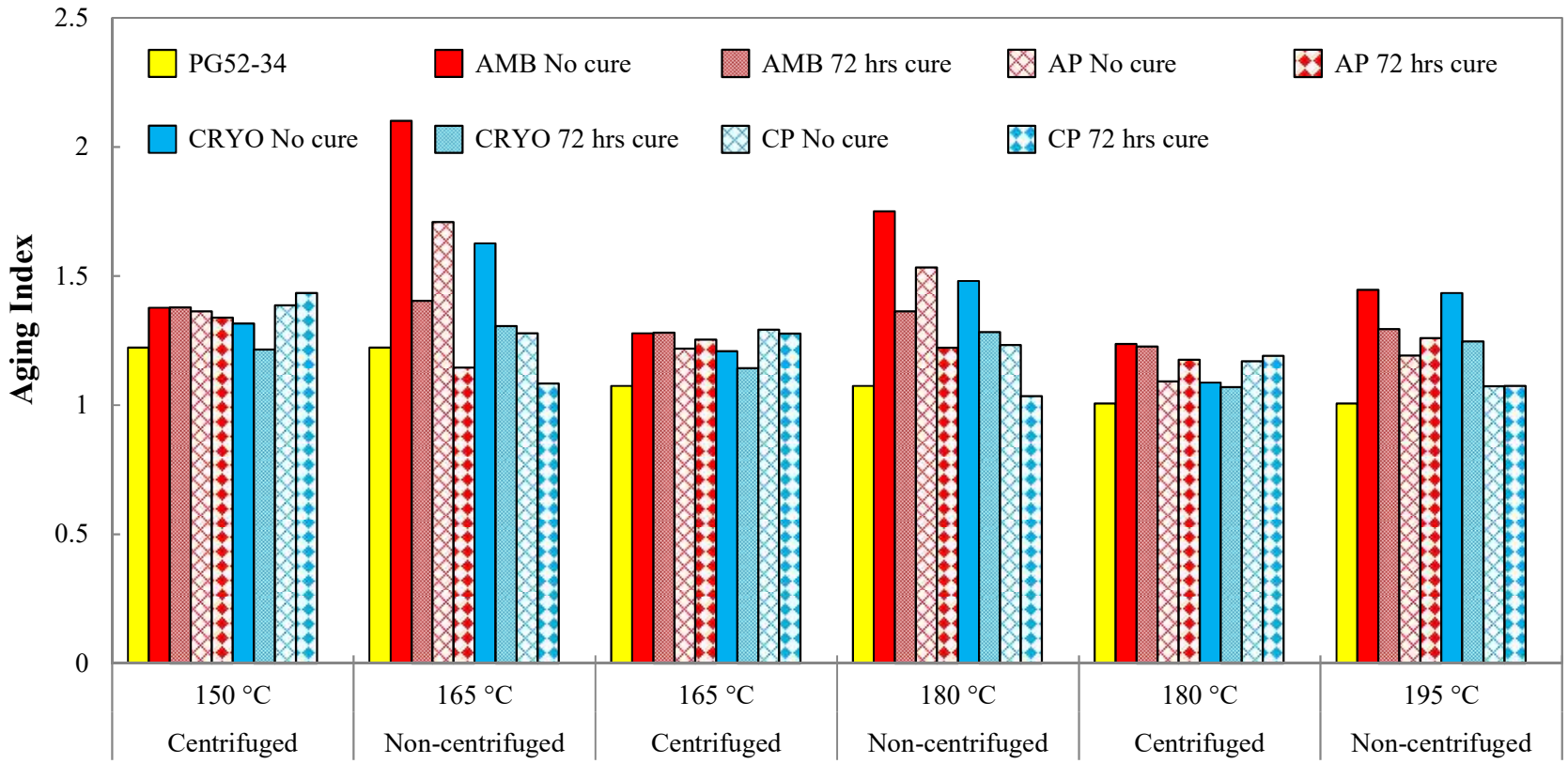

Figure 5-5. Aging indexes for asphalt rubber binders

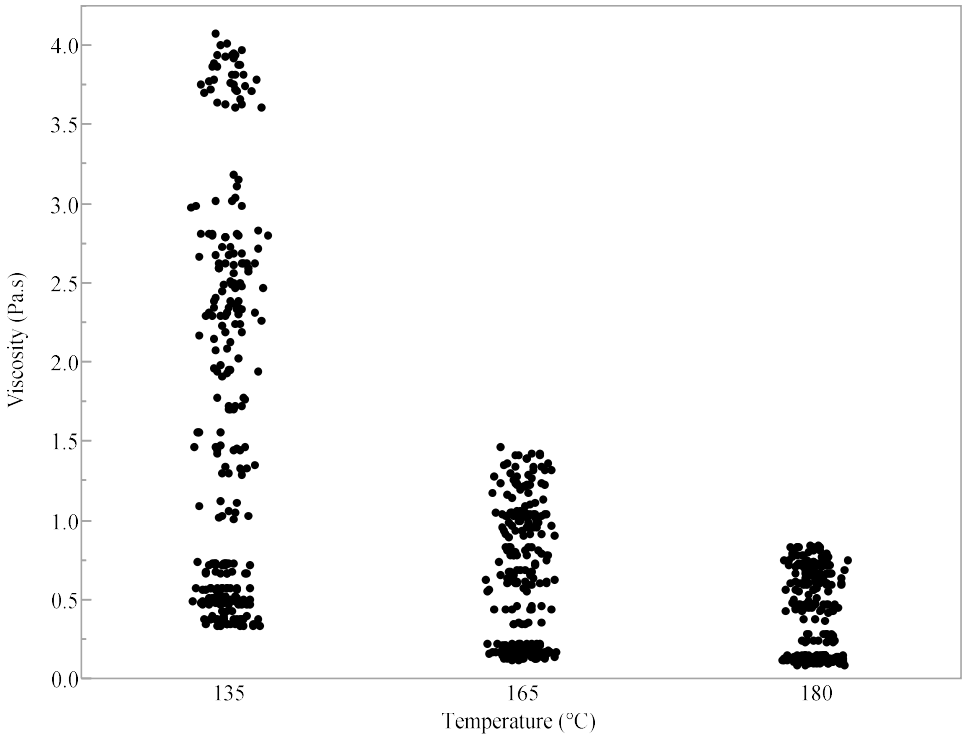

Figure 5-6. Non transformed viscosity data

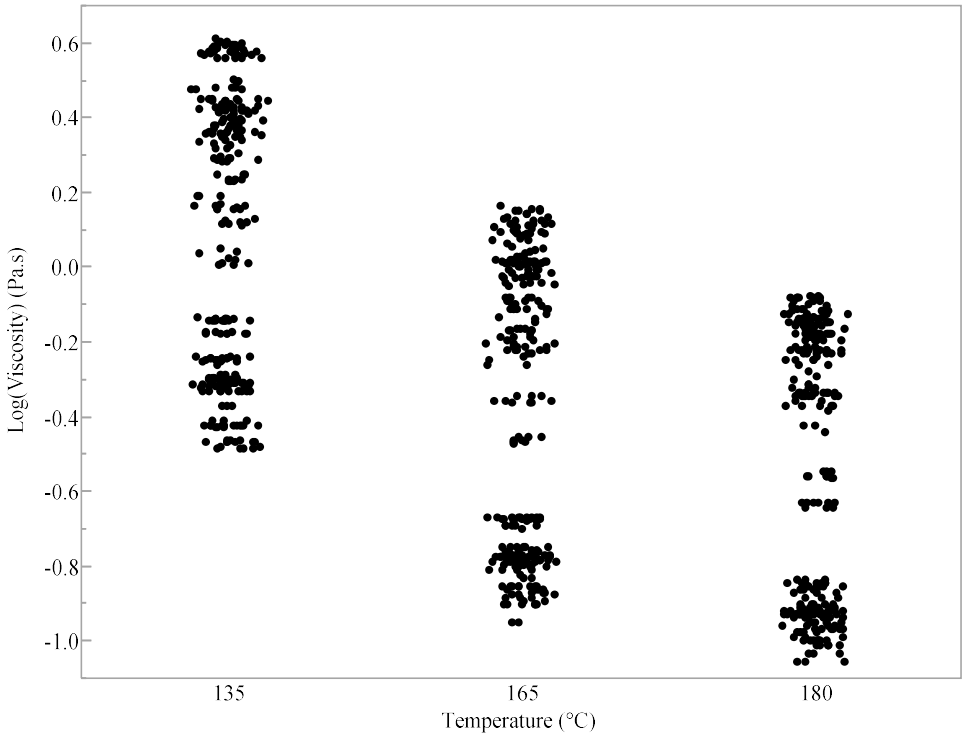

Figure 5-7. Viscosity data with a $\log_{10}$ transformation

Table 5-7. Summarized ANOVA table

	Source	DF	F Ratio	p-value
Whole Plot	Treatment	**31**		
	Rubber Type (Ambient/Cryogenic)	1	20.1453	<.0001*
	Polyoctenamer (0% / 4,5%)	1	519.6964	<.0001*
	Curing (None/72hrs)	1	2754.714	<.0001*
	Centrifuging (Non-centrifuged/Centrifuged)	1	66643.04	<.0001*
	Aging (Unaged/RTFOaged)	1	2741.679	<.0001*
	Rubber Type*Polyoctenamer	1	299.7700	<.0001*
	Rubber Type*Curing	1	243.8454	<.0001*
	Polyoctenamer*Curing	1	282.7029	<.0001*
	Rubber Type*Polyoctenamer*Curing	1	328.9107	<.0001*
	Rubber Type*Centrifuging	1	1213.724	<.0001*
	Polyoctenamer*Centrifuging	1	382.3472	<.0001*
	Rubber Type*Polyoctenamer*Centrifuging	1	270.0537	<.0001*
	Curing*Centrifuging	1	316.4190	<.0001*
	Rubber Type*Curing*Centrifuging	1	196.2950	<.0001*
	Polyoctenamer*Curing*Centrifuging	1	134.9868	<.0001*
	Rubber Type*Polyoctenamer*Curing*Centrifuging	1	267.3651	<.0001*
	Rubber Type*Aging	1	8.1938	0.0057*
	Polyoctenamer*Aging	1	18.1327	<.0001*
	Rubber Type*Polyoctenamer*Aging	1	9.7482	0.0027*
	Curing*Aging	1	67.8623	<.0001*
	Rubber Type*Curing*Aging	1	11.1247	0.0014*
	Polyoctenamer*Curing*Aging	1	4.4374	0.0391*
	Rubber Type*Polyoctenamer*Curing*Aging	1	7.0391	0.0100*
	Centrifuging*Aging	1	74.6921	<.0001*
	Rubber Type*Centrifuging*Aging	1	13.6182	0.0005*
	Polyoctenamer*Centrifuging*Aging	1	67.2371	<.0001*
	Rubber Type*Polyoctenamer*Centrifuging*Aging	1	15.2355	0.0002*
	Curing*Centrifuging*Agingd	1	109.1338	<.0001*
	Rubber Type*Curing*Centrifuging*Aging	1	4.1940	0.0447*
	Polyoctenamer*Curing*Centrifuging*Aging	1	1.7462	0.1911
	Rubber Type*Polyoctenamer*Curing*Centrifuging*Aging	1	0.1617	0.6889
	Tube[Rubber Type,Polyoctenamer,Curing,Centrifuging,Aging]&Random	**64**	1.3679	0.0681
Sub Plot	Temperature	**2**	28202.07	<.0001*
Whole Plot and Sub Plot interactions	**WP*SP Interactions**	**62**		
	Rubber Type*Temperature	2	93.2302	<.0001*
	Polyoctenamer*Temperature	2	9.1851	0.0002*
	Rubber Type*Polyoctenamer*Temperature	2	11.7220	<.0001*
	Curing*Temperature	2	13.5713	<.0001*
	Rubber Type*Curing*Temperature	2	8.2510	0.0004*
	Polyoctenamer*Curing*Temperature	2	4.8417	0.0094*
	Rubber Type*Polyoctenamer*Curing*Temperature	2	1.8127	0.1674
	Centrifuging*Temperature	2	76.1350	<.0001*
	Rubber Type*Centrifuging*Temperature	2	176.5381	<.0001*
	Polyoctenamer*Centrifuging*Temperature	2	12.9559	<.0001*
	Rubber Type*Polyoctenamer*Centrifuging*Temperature	2	3.1895	0.0445*
	Curing*Centrifuging*Temperature	2	71.3393	<.0001*
	Rubber Type*Curing*Centrifuging*Temperature	2	0.6205	0.5393
	Polyoctenamer*Curing*Centrifuging*Temperature	2	1.5650	0.2131
	Rubber Type*Polyoctenamer*Curing*Centrifuging*Temperature	2	10.8718	<.0001*
	Aging*Temperature	2	145.8871	<.0001*

Table 5-7. Summarized ANOVA table - continued

	Source	DF	F Ratio	p-value
Whole Plot and Sub Plot interactions	Rubber Type*Aging*Temperature	2	44.1230	<.0001*
	Polyoctenamer*Aging*Temperature	2	13.3307	<.0001*
	Rubber Type*Polyoctenamer*Aging*Temperature	2	0.4246	0.6550
	Curing*Aging*Temperature	2	10.8769	<.0001*
	Rubber Type*Curing*Aging*Temperature	2	1.5721	0.2116
	Polyoctenamer*Curing*Aging*Temperature	2	0.3496	0.7056
	Rubber Type*Polyoctenamer*Curing*Aging*Temperature	2	13.7521	<.0001*
	Centrifuging*Aging*Temperature	2	13.7024	<.0001*
	Rubber Type*Centrifuging*Aging*Temperature	2	2.1589	0.1196
	Polyoctenamer*Centrifuging*Aging*Temperature	2	1.0432	0.3553
	Rubber Type*Polyoctenamer*Centrifuging*Aging*Temperature	2	0.9753	0.3799
	Curing*Centrifuging*Aging*Temperature	2	1.1036	0.3348
	Rubber Type*Curing*Centrifuging*Aging*Temperature	2	3.9715	0.0212*
	Polyoctenamer*Curing*Centrifuging*Aging*Temperature	2	0.2214	0.8017
	Rubber Type*Polyoctenamer*Curing*Centrifuging*Aging*Temperature	2	1.0442	0.3549
	Error	**128**		
	Corrected Total	**287**		

As expected, the statistical analysis shows that the viscosities are statistically different with regards to the testing temperatures. The whole plot factors were all statistically different and almost all their interactions were significant, except for the four-way interaction between polyoctenamer, curing, aging, centrifuging and aging and for the only five-way interaction.

To further examine the differences presented for the whole plot factors interactions, least square means plot were generated for those significant whole plot factors interactions that were of interest to the researchers. Figure 5-8 to 5-12 illustrate the least square means for the interactions that were of interest to the researchers.

Figure 5-8 shows how the viscosity of the ambient and cryogenic binders increases with the addition of polyoctenamer. Figure 5-9 shows the interaction between rubber type, polyoctenamer, and curing it is clear that the curing process influenced greatly the viscosity of binders with cryogenic rubber and polyoctenamer.

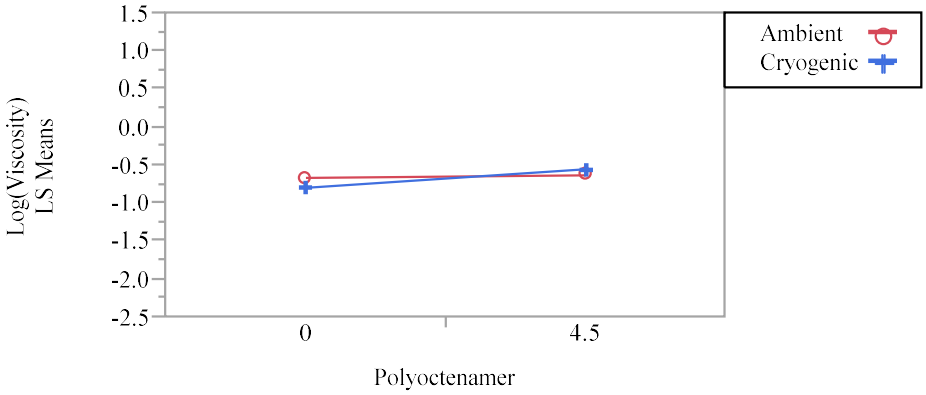

Figure 5-8. Least square means for rubber type and polyoctenamer interaction

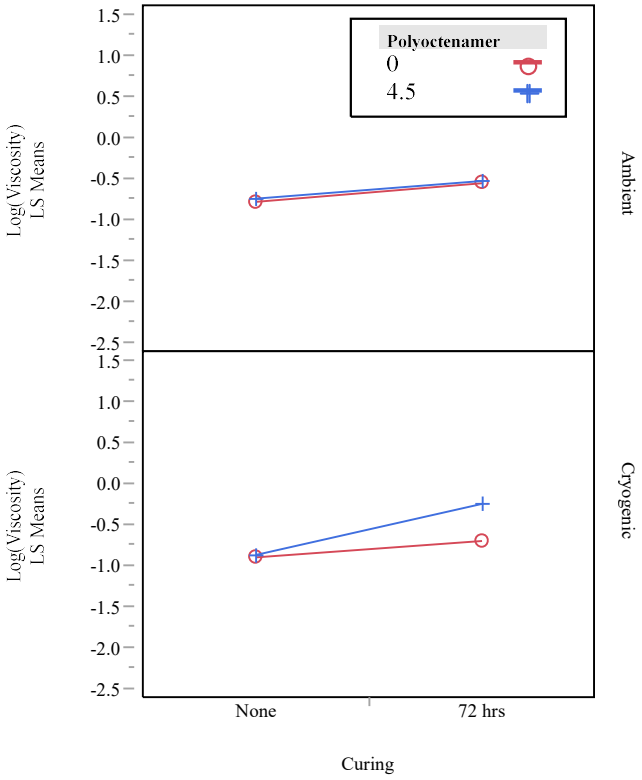

Figure 5-9. Least square means plot for rubber type, polyoctenamer and curing.

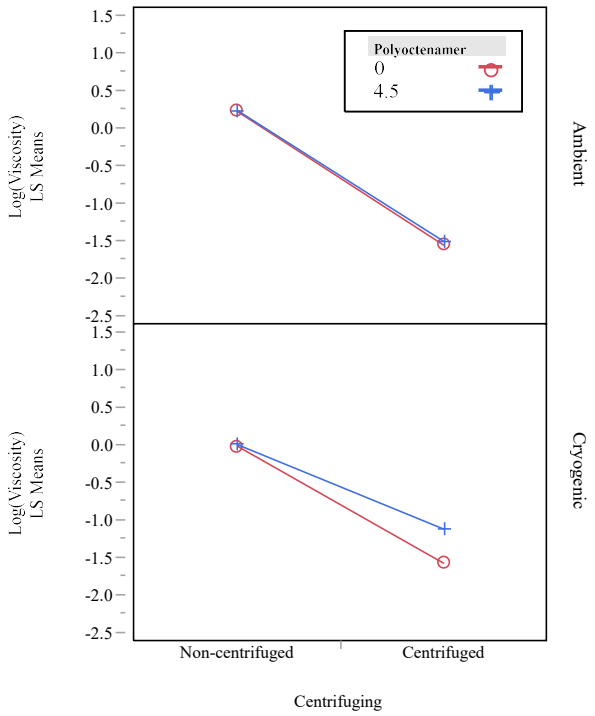

Figure 5-10. Least square means plot for rubber type, polyoctenamer and centrifuging

When looking at the interaction between rubber type, polyoctenamer and centrifuging (Figure 5-10), it is noticeable that the viscosities of the centrifuged materials are lower compared to the non-centrifuged binders, which was expected. Also, the centrifuged cryogenic binder with polyoctenamer has viscosity least square means significantly higher than the centrifuged binder without polyoctenamer.

The interaction between rubber type, polyoctenamer and aging (Figure 5-11) demonstrate how the cryogenic binder containing polyoctenamer had consistent higher viscosity values regardless of the aging stage. It seem that the viscosity for the ambient binders with and without polyoctenamer for the RTFO aged materials were somewhat similar.

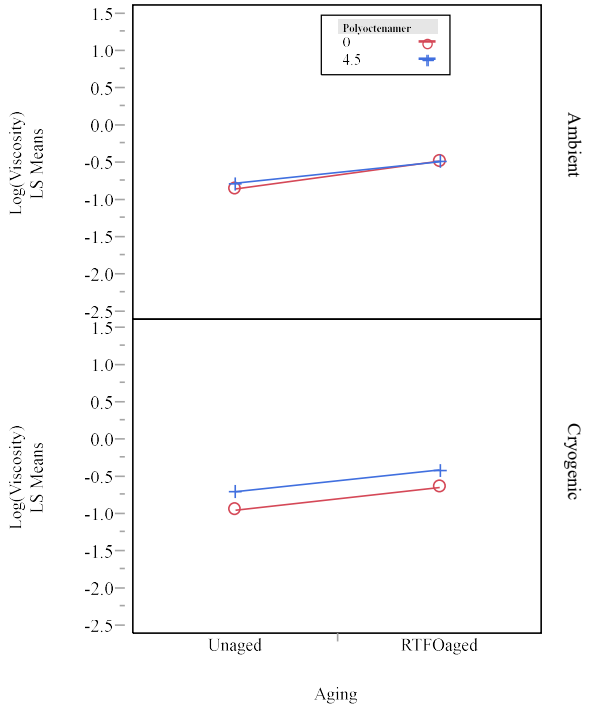

Figure 5-11. Least square means plot for rubber type, polyoctenamer and aging

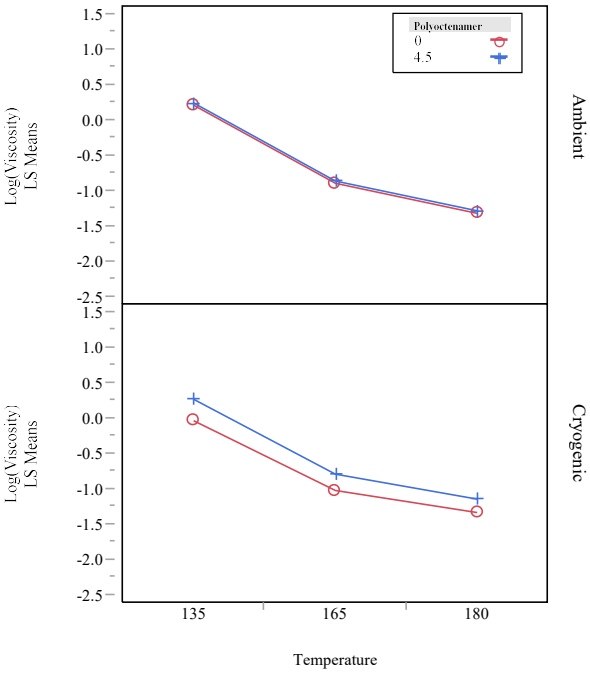

Figure 5-12. Least square means plot for rubber type, polyoctenamer and temperature

The last interaction of interest for the researchers shows again that the viscosities of the cryogenic binders containing polyoctenamer was consistently higher compared with the cryogenic binder without polyoctenamer (Figure 5-12).

Specific gravity

The specific gravities of the binders produced were determined by the Pycnometer Method. The results are summarized in Table 5-8. It can be seen how the addition of polyoctenamer increased the specific gravity of the binders containing ambient rubber for both cure and no cure, whereas, the specific gravity is decreased for the cryogenic rubber binders cure and no cure containing polyoctenamer. The specific gravities of the 72 hrs centrifuged binders AP, CRYO and CP were not determined due to shortage in the amount of centrifuged material to perform the test. The authors do not expect the specific gravities of the aforementioned binders to be higher than their non-centrifuged counterpart.

In general the specific gravity of the binders is reduced after 72 hrs of curing. This can be explained because of the breaking into smaller rubber particles sizes that the rubber suffers after being swelled to its maximum extend.

Table 5-8. Specific gravity results

Binder Type	Curing	Type of material	Specific gravity
AMB	None	Non-Centrifuged	1.040
		Centrifuged	1.029
	72 hrs cured	Non-Centrifuged	1.037
		Centrifuged	1.031
AP	None	Non-Centrifuged	1.042
		Centrifuged	1.023
	72 hrs cured	Non-Centrifuged	1.038
		Centrifuged	n/a

Table 5-8. Specific gravity results - continued

Binder Type	Curing	Type of material	Specific gravity
CRYO	None	Non-Centrifuged	1.039
		Centrifuged	1.029
	72 hrs cured	Non-Centrifuged	1.035
		Centrifuged	n/a
CP	None	Non-Centrifuged	1.034
		Centrifuged	1.026
	72 hrs cured	Non-Centrifuged	1.033
		Centrifuged	n/a

Mass loss

The results of mass loss are summarized in Table 5-9. It is noticeable that higher percent of mass loss was obtained for the binders containing ambient rubber. In general the percent of mass loss was somewhat higher for the non-centrifuged binders when compared to their centrifuged counterpart. This was not observed for the centrifuged CP 72 hrs cure binder, but the small difference in mass loss can be due to the natural variability in the results, since the standard deviation of the results for centrifuged CP 72 hrs cure binder was 0.28.

Table 5-9. Mass loss results

Binder Type	Curing	Type of material	Mass Loss (%)
PG52-34	None	Not applicable	0.58
AMB	None	Non-Centrifuged	1.26
		Centrifuged	0.87
	72 hrs cured	Non-Centrifuged	1.45
		Centrifuged	0.29
AP	None	Non-Centrifuged	1.40
		Centrifuged	0.72
	72 hrs cured	Non-Centrifuged	1.52
		Centrifuged	0.86

Table 5-9. Mass loss results - continued

Binder Type	Curing	Type of material	Mass Loss (%)
CRYO	None	Non-Centrifuged	0.79
		Centrifuged	0.72
	72 hrs cured	Non-Centrifuged	0.94
		Centrifuged	0.72
CP	None	Non-Centrifuged	1.01
		Centrifuged	0.94
	72 hrs cured	Non-Centrifuged	0.90
		Centrifuged	0.94

Storage stability

Storage stability tests were run on all of the AR binders in order to determine if the addition of polyoctenamer improved the storage stability of the AR binders. Also, the effects of the curing process (72 hrs) on the storage stability was determined. The storage stability in this study was define as the percent difference in the average continuous grades obtained between the top third of the storage stability tubes and the bottom third of the tubes, since the continuous grade for each type of binder is determined for a G*/sin δ value of 1.0. Table 5-10 presents the storage stability results of the AR binders, negative percent differences means that separation is occurring by sinking of rubber particles, as observed with the lower continuous grade values obtained from the top parts of the tubes in comparison with the values from the bottom parts of the tubes.

The addition of polyoctenamer reduced the percent difference in the AR binders containing ambient GTR for both, no cure and 72 hrs cure. The opposite was observed for the AR binders containing cryogenic GTR, an increase in the percent difference was observed for both types of curing when comparing the binders with and without polyoctenamer. What is noticeable is that the curing process helped in some way to reduce

the percent difference for all the AR binders when comparing the same binder types and the curing process. Also, the results obtained from the AR binders containing ambient GTR showed a higher standard deviation than the standard deviation from the cryogenic GTR binders. It should be noted that the storage stability tests were performed by using the 1 mm gap with the parallel plate geometry in a DSR.

Table 5-10. Storage stability results for AR binders

Binder Type	Curing	Average continuous grade Top	Std. dev. Top	Average continuous grade Bottom	Std. dev. Bottom	Percent difference in continuous grade (%)
AMB	No Cure	68.06	0.41	80.15	3.29	-17.76
	72 hrs cure	68.43	0.58	79.95	0.51	-16.83
AP	No Cure	68.24	0.19	78.62	0.25	-15.21
	72 hrs cure	71.95	0.36	79.04	0.62	-9.84
CRYO	No Cure	62.09	0.10	76.16	0.84	-22.66
	72 hrs cure	65.18	0.13	76.32	0.56	-17.09
CP	No Cure	62.45	0.08	78.88	0.12	-26.31
	72 hrs cure	65.09	0.17	77.95	0.54	-19.77

Continuous performance grade

The continuous performance grade (PG) of the laboratory produced asphalt rubber binders was determined and the results are summarized in Table 5-11. In general, as observed in Figure 5-13 to 5-16, the continuous PG of the binders that were tested with the 1 mm and 2 mm gap geometries are very similar within each specific binder, and within each specific type of aged binder. The continuous PG obtained from the results of the test with concentric cylinders were higher for all the binder types, except for the RTFO aged non-centrifuged CRYO binder, for which its continuous PG was very similar from those obtained from the tests with 1 mm and 2 mm gaps. The continuous PG of the centrifuged materials was lower for all the binders when compared to their non-centrifuged counterparts, in general the difference was between one to two performance grades between centrifuged and non-centrifuged binders.

The continuous PG obtained for all the binders corroborate the fact that increasing the testing gap from 1 to 2 mm will lead to results where the influence of the rubber particles is still present in the testing results. A further gap increase can cause the binder to start flowing out of the parallel plates as testing temperature increases during the test leading to sample loss and non-conformance of test geometry. Samples are not able to sustain its superficial tension as testing temperature rises, especially if the base binder is a soft binder, as the one used in the study. By testing the centrifuged binder one can truly measure the benefits of blending asphalt binder with GTR without having the rubber particles influence the testing results. In this specific study, the results obtained using the concentric cylinders geometry did not seem to isolate the effect of the rubber particles, even though the gap between walls was 5.7 mm.

Table 5-11. Continuous performance grading of asphalt rubber binders

Binder Type	Curing	Type of material	Unaged continuous PG grading						RTFO aged continuous PG grading					
			Gap				CC		Gap				CC	
			1 mm		2 mm				1 mm		2mm			
			Average	Std. dev.	Average	Std. dev.	Average	Std. dev.	Average	Std. dev.	Average	Std. dev.	Average	Std. dev.
PG52-34			52.71	0.11	—	—	—	—	58.54	0.06	—	—	—	—
AMB	None	Non-Centrifuged	68.48	0.71	68.56	0.62	74.29	—	81.20	6.92	80.98	0.42	83.07	—
		Centrifuged	59.02	0.50	—	—	—	—	66.09	0.07	—	—	—	—
	72 hrs cured	Non-Centrifuged	71.03	0.68	71.93	0.29	75.07	—	82.88	0.96	81.78	1.32	84.37	—
		Centrifuged	64.51	0.25	—	—	—	—	71.59	0.14	—	—	—	—
AP	None	Non-Centrifuged	71.63	0.58	71.82	0.21	70.13	—	82.39	0.73	82.74	0.18	87.72	—
		Centrifuged	60.49	0.19	—	—	—	—	67.70	0.24	—	—	—	—
	72 hrs cured	Non-Centrifuged	73.78	0.12	73.77	0.36	79.21	—	83.91	0.62	84.62	0.32	88.79	—
		Centrifuged	64.03	0.27	—	—	—	—	70.86	0.08	—	—	—	—

Table 5-11. Continuous performance grading of asphalt rubber binders - continued

Binder Type	Curing	Type of material	Unaged continuous PG grading						RTFO aged continuousPG grading					
			Gap				CC		Gap				CC	
			1 mm		2 mm				1 mm		2mm			
			Average	Std. dev.	Average	Std. dev.	Average	Std. dev.	Average	Std. dev.	Average	Std. dev.	Average	Std. dev.
CRYO	None	Non-Centrifuged	66.64	0.45	66.41	0.56	72.29	—	77.16	0.38	77.21	0.78	77.18	—
		Centrifuged	59.65	0.30	—	—	—	—	66.48	0.19	—	—	—	—
	72 hrs cured	Non-Centrifuged	68.77	0.29	69.70	0.65	75.66	—	78.02	0.54	77.91	0.42	82.61	—
		Centrifuged	63.18	0.21	—	—	—	—	69.89	0.14	—	—	—	—
CP	None	Non-Centrifuged	67.90	1.14	68.80	0.32	71.56	—	79.09	0.19	78.94	0.45	84.33	—
		Centrifuged	60.91	0.08	—	—	—	—	67.95	0.17	—	—	—	—
	72 hrs cured	Non-Centrifuged	70.35	0.39	70.31	0.09	72.69	—	78.97	0.38	78.37	0.78	81.27	—
		Centrifuged	68.75	0.20	—	—	—	—	76.66	0.14	—	—	—	—

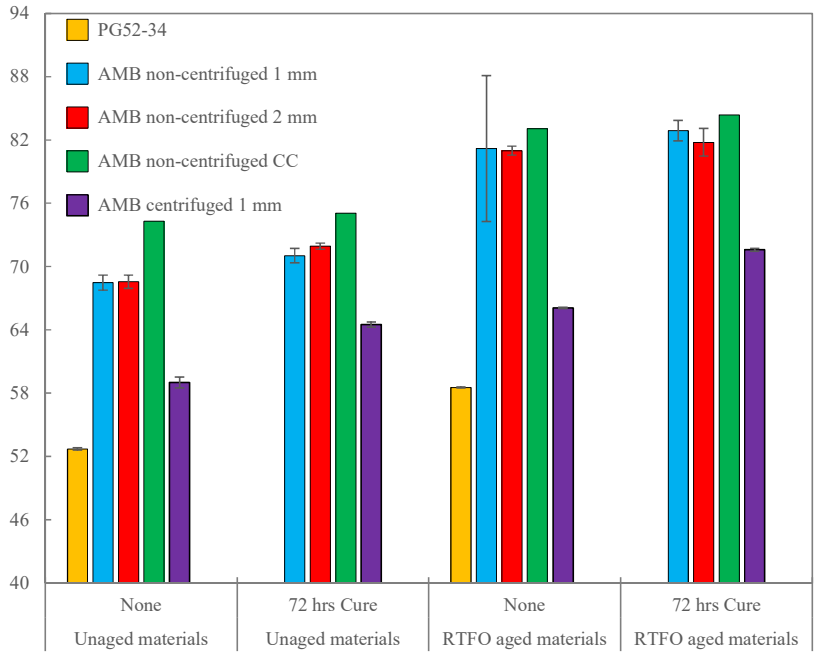

Figure 5-13. Continuous PG grading of AMB binder tested with different geometries

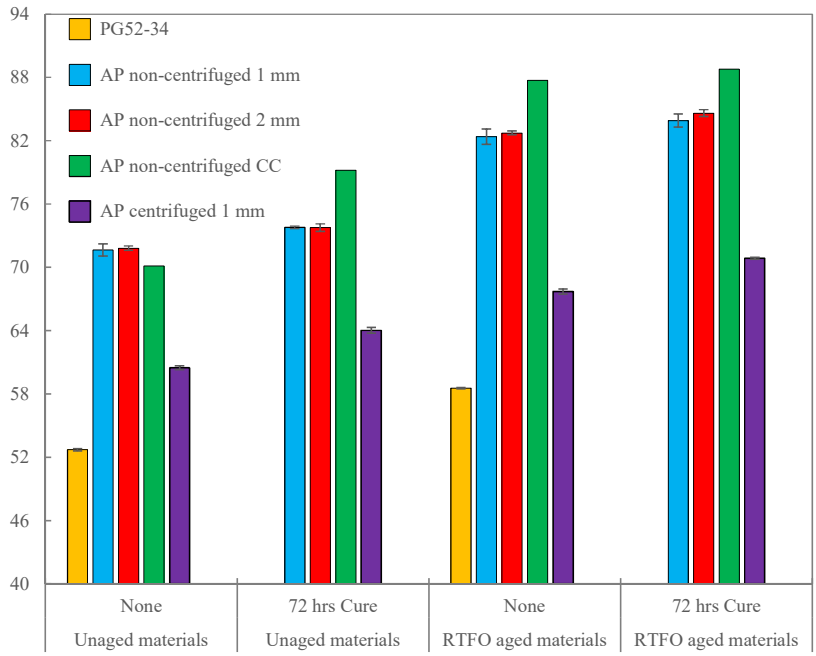

Figure 5-14. Continuous PG grading of AP binder tested with different geometries

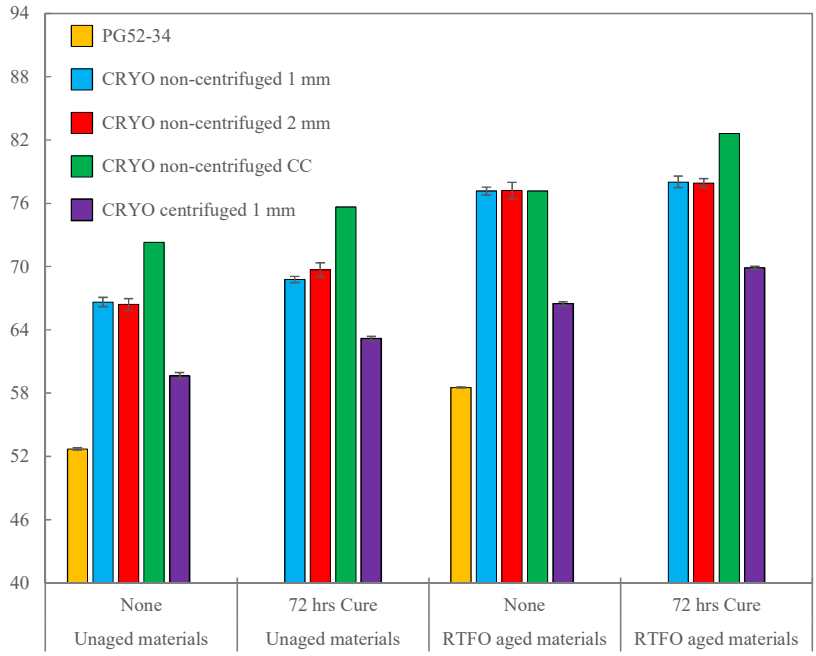

Figure 5-15. Continuous PG grading of CRYO binder tested with different geometries

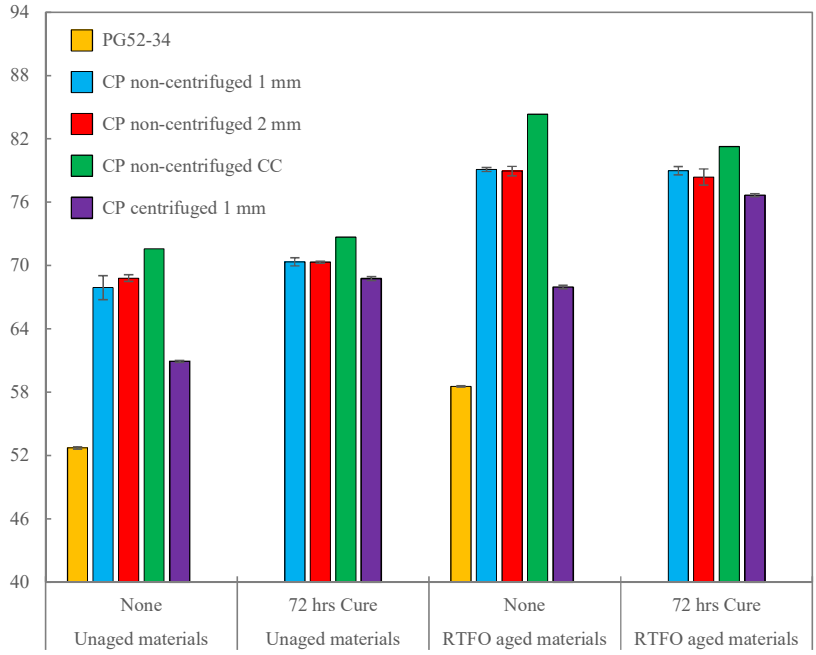

Figure 5-16. Continuous PG grading of CP binder tested with different geometries

Model fitting of master curves

The empirical constants obtained for each binder type are summarized in Table 5-12. The CAM model parameters obtained from fitting the data to the model are presented in Table 5-13 and the Sigmoidal model parameters obtained are summarized in Table 5-14.

The C_1 and C_2 values obtained with the parallel plate geometry for the different types of binders were very consistent. In general, C_1 values in the range of 6.7 – 7.5 were obtained for the unaged binders when using the parallel plate geometry regardless of the gap. The values obtained from the concentric cylinders geometry presented a wider range in between 5.5 – 17.1. The range of C_2 values were to vary from 126.5 – 147.3 for the parallel plate geometry; a wider range was found for the concentric cylinders, 94.2 – 422.5. Values found for C_1 and C_2 of the RTFO aged materials of cryogenic GTR without polyoctenamer binder tested with the parallel plate were the same regardless of the curing type. Similar C_1 values were obtained for the RTFO aged binder with ambient GTR without polyoctenamar, whereas their C_2 values were slightly different. Slightly similar C_1 values between the RTFO aged binders containing polyoctenamer were seen within each rubber type tested with parallel plates, the same was not observed for the C_2 values, which differ more between them. Again, for the C_1 and C_2 values obtained for the RTFO aged materials tested with concentric cylinders did not presented similarities when compared to the values obtained with the parallel plates. It is noticeable that all the C_1 and C_2 values obtained from the centrifuged materials were higher than their non-centrifuged counterpart tested in 1 mm gap.

Table 5-12. WLF empirical constants, C_1 and C_2

Binder Type	Curing	Type of material	Empirical constants	Unaged Master Curve			RTFO-Aged Master Curve		
				Gap		CC	Gap		CC
				1 mm	2 mm		1 mm	2 mm	
PG52-34	None	None	C_1	6.8	---	---	7.3	---	---
			C_2	141.0	---	---	141.2	---	---
AMB	None	Non-Centrifuged	C_1	6.2	6.8	7.1	7.9	7.6	7.8
			C_2	126.5	135.2	140.8	146.9	140.7	143.1
		Centrifuged	C_1	7.5	---	---	8.5	---	---
			C_2	147.3	---	---	151.7	---	---
	72 hrs cured	Non-Centrifuged	C_1	6.8	7.10	6.8	7.9	7.6	9.2
			C_2	136.3	140.4	126.7	146.9	139.9	173.9
		Centrifuged	C_1	7.3	---	---	8.5	---	---
			C_2	136.2	---	---	144.5	---	---
AP	None	Non-Centrifuged	C_1	6.9	6.7	5.5	11.9	10.5	11.4
			C_2	136.6	132.4	94.2	206.0	180.6	226.7
		Centrifuged	C_1	7.1	---	---	8.3	---	---
			C_2	138.3	---	---	147.7	---	---
	72 hrs cured	Non-Centrifuged	C_1	6.7	6.7	17.1	10.5	9.08	10.1
			C_2	131.5	131.2	422.5	180.6	160.9	192.3
		Centrifuged	C_1	7.1	---	---	8.0	---	---
			C_2	138.3	---	---	141.6	---	---
CRYO	None	Non-Centrifuged	C_1	6.7	6.7	6.1	7.5	7.5	7.5
			C_2	134.9	133.8	118.2	137.7	137.7	136.8
		Centrifuged	C_1	7.1	---	---	8.6	---	---
			C_2	138.3	---	---	150.5	---	---
	72 hrs cured	Non-Centrifuged	C_1	6.7	7.0	7.1	7.5	7.5	8.2
			C_2	133.9	137.4	142.5	137.7	137.7	154.6
		Centrifuged	C_1	7.1	---	---	8.6	---	---
			C_2	138.3	---	---	150.5	---	---
CP	None	Non-Centrifuged	C_1	7.0	7.0	8.7	9.2	9.2	10.0
			C_2	137.4	137.4	196.5	167.8	163.8	195.4
		Centrifuged	C_1	7.1	---	---	8.6	---	---
			C_2	138.3	---	---	150.5	---	---
	72 hrs cured	Non-Centrifuged	C_1	7.0	7.0	6.8	9.4	8.4	7.3
			C_2	137.4	137.4	137.6	166.4	151.7	129.1
		Centrifuged	C_1	7.1	---	---	9.5	---	---
			C_2	136.4	---	---	167.2	---	---

The CAM model parameters found for the binders ranged from 1.05 to 1.20 for the Rheological Index, R. Lower or the same rheological index values were consistently found for the RTFO aged materials for all the testing geometries. The rheological indexes found for the unaged materials tested with the concentric cylinders were higher when compared to those found for the unaged materials tested with the parallel plate geometries. The opposite is observed for the rheological indexes of the RTFO aged materials tested with concentric cylinders, the indexes are lower when compared to the ones found for the RTFO aged binders tested with parallel plates. Overall, higher rheological indexes were found for the centrifuged binders when compared to their non-centrifuged counterparts. As noted by Huang et al. (2014), the rheological index is related to the width of the relaxation spectrum of the binder. Usually, a higher rheological index belong to master curves that are flatter in shape. In general, binders with higher rheological indexes tend to present large elastic modulus values. The empirical parameter, w, for all the binders are very similar for all the unaged binders tested with the three geometries and for the RTFO aged binders tested with the parallel plates. Higher values of w were found for the RTFO aged materials tested with the concentric cylinders. The cross-over frequency value found for all the binders was 3.27E6 Hz, the cross-over frequency parameter is defined as the frequency where tan δ is equal to one.

The parameters values found for the Sigmoidal model for the lower asymptote (υ), the difference between upper and lower asymptote (α) and one of the parameters that defines the shape between the asymptotes and the location of the inflection point (β) were higher for the RTFO aged materials than for the unaged materials; whereas the other parameter that defines the shape between the asymptotes and the location of the inflection point (γ) was lower for

the RTFO aged materials than for the unaged materials. Overall, all the υ and α parameter values found for the unaged centrifuged materials were significantly lower than those found for the unaged non-centrifuged materials. The opposite trend was observed for the RTFO aged centrifuged materials when compared to their non-centrifuged counterparts.

Table 5-13. CAM model parameters for the binders

Binder Type	Curing	Type of material	Empirical constants	Unaged Master Curve			RTFO-Aged Master Curve		
				Gap		CC	Gap		CC
				1 mm	2 mm		1 mm	2 mm	
PG52-34	None	None	ω_c	3.27e6	---	---	3.27e6	---	---
			w	1.03	---	---	0.99	---	---
			R	1.16	---	---	1.18	---	---
AMB	None	Non-Centrifuged	ω_c	3.27e6	3.27e6	3.27e6	3.27e6	3.27e6	0.14
			w	0.90	0.90	0.89	0.81	0.82	1.58
			R	1.13	1.13	1.20	1.10	1.10	1.06
		Centrifuged	ω_c	3.27e6	---	---	3.27e6	---	---
			w	0.98	---	---	0.93	---	---
			R	1.19	---	---	1.18	---	---
	72 hrs cured	Non-Centrifuged	ω_c	3.27e6	3.27e6	3.27e6	3.27e6	3.27e6	0.98
			w	0.87	0.87	0.88	0.81	0.81	1.42
			R	1.11	1.11	1.15	1.10	1.10	1.06
		Centrifuged	ω_c	3.27e6	---	---	3.27e6	---	---
			w	0.94	---	---	0.89	---	---
			R	1.16	---	---	1.16	---	---
AP	None	Non-Centrifuged	ω_c	3.27e6	3.27e6	3.27e6	3.27e6	3.27e6	0.12
			w	0.88	0.88	0.91	0.81	0.80	1.51
			R	1.13	1.12	1.16	1.11	1.10	1.05
		Centrifuged	ω_c	3.27e6	---	---	3.27e6	---	---
			w	0.97	---	---	0.92	---	---
			R	1.18	---	---	1.18	---	---
	72 hrs cured	Non-Centrifuged	ω_c	3.27e6	3.27e6	3.27e6	3.27e6	3.27e6	0.12
			w	0.86	0.86	0.86	0.80	0.80	1.51
			R	1.11	1.11	1.14	1.10	1.10	1.05
		Centrifuged	ω_c	3.27e6	---	---	3.27e6	---	---
			w	0.95	---	---	0.89	---	---
			R	1.18	---	---	1.16	---	---

Table 5-13. CAM model parameters for the binders - continued

Binder Type	Curing	Type of material	Empirical constants	Unaged Master Curve			RTFO-Aged Master Curve		
				Gap		CC	Gap		CC
				1 mm	2 mm		1 mm	2 mm	
CRYO	None	Non-Centrifuged	ω_c	3.27e6	3.27e6	3.27e6	3.27e6	3.27e6	905.2
			w	0.92	0.92	0.91	0.84	0.84	1.19
			R	1.14	1.14	1.25	1.11	1.11	1.07
		Centrifuged	ω_c	3.27e6	---	---	3.27e6	---	---
			w	0.98	---	---	0.90	---	---
			R	1.18	---	---	1.17	---	---
	72 hrs cured	Non-Centrifuged	ω_c	3.27e6	3.27e6	3.27e6	3.27e6	3.27e6	13.87
			w	0.89	0.89	0.88	0.83	0.83	1.35
			R	1.11	1.12	1.18	1.10	1.11	1.06
		Centrifuged	ω_c	3.27e6	---	---	3.27e6	---	---
			w	0.95	---	---	0.93	---	---
			R	1.18	---	---	1.17	---	---
CP	None	Non-Centrifuged	ω_c	3.27e6	3.27e6	3.27e6	3.27e6	3.27e6	316.8
			w	0.91	0.90	0.91	0.83	0.83	1.20
			R	1.13	1.13	1.18	1.11	1.11	1.07
		Centrifuged	ω_c	3.27e6	---	---	3.27e6	---	---
			w	0.97	---	---	0.91	---	---
			R	1.17	---	---	1.17	---	---
	72 hrs cured	Non-Centrifuged	ω_c	3.27e6	3.27e6	3.27e6	3.27e6	3.27e6	0.06
			w	0.88	0.88	0.88	0.83	0.83	1.66
			R	1.11	1.11	1.13	1.11	1.11	1.05
		Centrifuged	ω_c	3.27e6	---	---	3.27e6	---	---
			w	0.90	---	---	0.85	---	---
			R	1.13	---	---	1.12	---	---

Table 5-14. Sigmoidal model parameter for the binders

Binder Type	Curing	Type of material	Empirical constants	Unaged Master Curve			RTFO-Aged Master Curve		
				Gap		CC	Gap		CC
				1 mm	2 mm		1 mm	2 mm	
PG52-34	None	None	υ	-6.2	---	---	-6.4	---	---
			α	16.1	---	---	16.0	---	---
			β	-0.08	---	---	-0.23	---	---
			γ	-0.25	---	---	-0.25	---	---
AMB	None	Non-Centrifuged	υ	-42.1	-48.0	-53.1	-25.2	-51.2	-69.2
			α	52.5	58.5	77.7	36.2	62.6	80.0
			β	-1.80	-1.93	-0.96	-1.34	-1.92	-2.30
			γ	-0.14	-0.14	-0.06	-0.12	-0.11	-0.11
		Centrifuged	υ	-5.8	---	---	-63.7	---	---
			α	15.6	---	---	77.9	---	---
			β	-0.15	---	---	-1.78	---	---
			γ	-0.25	---	---	-0.10	---	---
	72 hrs cured	Non-Centrifuged	υ	-47.4	-49.6	-63.9	-26.7	-51.5	-71.8
			α	58.5	61.2	76.9	38.5	63.9	83.1
			β	-1.84	-1.84	-1.92	-1.28	-1.82	-2.27
			γ	-0.12	-0.11	-0.09	-0.11	-0.09	-0.10
		Centrifuged	υ	-9.9	---	---	-62.1	---	---
			α	19.7	---	---	73.9	---	---
			β	-0.60	---	---	-2.04	---	---
			γ	-0.21	---	---	-0.12	---	---
AP	None	Non-Centrifuged	υ	-48.9	-50.4	-52.1	-48.5	-49.9	-71.6
			α	59.5	60.4	79.3	63.1	63.0	82.2
			β	-1.94	-2.06	-0.82	-1.55	-1.72	-2.37
			γ	-0.13	-0.14	-0.05	-0.08	-0.09	-0.11
		Centrifuged	υ	-6.1	---	---	-60.4	---	---
			α	15.7	---	---	74.0	---	---
			β	-0.23	---	---	-1.79	---	---
			γ	-0.25	---	---	-0.10	---	---
	72 hrs cured	Non-Centrifuged	υ	-49.5	-49.3	-44.5	-49.2	-50.0	-71.6
			α	61.6	60.3	66.4	62.8	63.3	82.2
			β	-1.90	-1.90	-0.94	-1.65	-1.70	-2.37
			γ	-0.12	-0.12	-0.06	-0.08	-0.09	-0.11
		Centrifuged	υ	-7.3	---	---	-61.5	---	---
			α	16.7	---	---	73.7	---	---
			β	-0.42	---	---	-1.97	---	---
			γ	-0.24	---	---	-0.11	---	---

Table 5-14. Sigmoidal model parameter for the binders - continued

Binder Type	Curing	Type of material	Empirical constants	Unaged Master Curve			RTFO-Aged Master Curve		
				Gap		CC	Gap		CC
				1 mm	2 mm		1 mm	2 mm	
CRYO	None	Non-Centrifuged	υ	-47.8	-46.7	-45.2	-53.2	-69.4	-66.5
			α	58.4	56.9	76.4	63.4	79.7	80.2
			β	-1.90	-1.91	-0.54	-2.12	-2.35	-1.90
			γ	-0.14	-0.14	-0.05	-0.13	-0.13	-0.09
		Centrifuged	υ	-6.3	---	---	-76.8	---	---
			α	15.9	---	---	90.9	---	---
			β	-0.24	---	---	-1.97	---	---
			γ	-0.25	---	---	-0.09	---	---
	72 hrs cured	Non-Centrifuged	υ	-49.1	-47.3	-61.3	-63.8	-71.0	-69.3
			α	59.7	58.2	78.4	74.2	81.8	80.8
			β	-1.93	-1.86	-1.53	-2.25	-2.30	-2.21
			γ	-0.13	-0.12	-0.07	-0.12	-0.11	-0.10
		Centrifuged	υ	-7.4	---	---	-70.8	---	---
			α	17.0	---	---	83.7	---	---
			β	-0.39	---	---	-2.03	---	---
			γ	-0.24	---	---	-0.11	---	---
CP	None	Non-Centrifuged	υ	-47.0	-48.7	-35.1	-71.5	-75.0	-68.5
			α	57.6	59.0	78.4	82.3	86.0	81.5
			β	-1.89	-1.96	0.06	-2.30	-2.33	-2.04
			γ	-0.13	-0.14	-0.05	-0.11	-0.11	-0.09
		Centrifuged	υ	-6.1	---	---	-63.2	---	---
			α	15.6	---	---	76.7	---	---
			β	-0.26	---	---	-1.85	---	---
			γ	-0.25	---	---	-0.10	---	---
	72 hrs cured	Non-Centrifuged	υ	-49.3	-48.3	-57.1	-71.6	-75.0	-71.7
			α	60.1	59.1	75.7	83.1	86.0	82.1
			β	-1.91	-1.89	-1.36	-2.23	-2.33	-2.37
			γ	-0.12	-0.12	-0.07	-0.11	-0.11	-0.11
		Centrifuged	υ	-30.0	---	---	-65.7	---	---
			α	40.6	---	---	77.5	---	---
			β	-1.46	---	---	-2.11	---	---
			γ	-0.14	---	---	-0.11	---	---

Master curves of unaged materials

The master curves of the unaged binders are presented in APPENDIX B. Table 5-15 summarizes the comparison of the models' prediction for the unaged materials. Over prediction on the behavior was represented by a red cell and the word "over", under prediction of the behavior was represented by a yellow cell and the word "under", and two shades of green were used for "good" and "fair" predictions by the models. In general, the Sigmoidal model is able to describe better the behavior of the unaged asphalt rubber binders than the CAM model, at intermediate frequencies. This behavior looks like a lump in frequencies ranging between 1 Hz and 10 Hz in most of the non-centrifuged/no cure binders tested with parallel plates. The CAM model under predicts the complex modulus values for the binders in this region. The aforementioned lump is less noticeable in the non-centrifuged binders that were subjected to a 72 hr cure. This lump is not present in the master curves of the centrifuged materials. Therefore, it can be said that this behavior at intermediate temperatures is caused by the interaction of the rubber particles and the geometries.

The CAM model over predicts the complex modulus for the non-centrifuged binders at higher frequencies and lower frequencies for the non-centrifuged no cure binders tested with parallel plates. However, the CAM model is able to predict the complex modulus at higher frequencies for the non-centrifuged 72 hr cured binders tested with parallel plates. Whereas, the Sigmoidal model falls short in the prediction of the complex modulus values at high frequencies for those binders, but it is able to capture the behavior of those binders at lower frequencies.

The models are not able to capture the behavior of the binders with no cure and those that were tested using the concentric cylinders geometry at higher frequencies or lower

testing temperatures, the predicted values are higher than the measured values. The behavior of the 72 hr cured binders containing polyoctenamer and tested with the concentric cylinders is captured by both models. However, the Sigmoidal model does a better job at predicting the complex modulus of the binders at higher frequencies than the CAM model

At low frequencies related to higher temperatures, the Sigmoidal model is able in general to describe better the behavior of the binders than the CAM model. The CAM model tends to over predict the complex modulus of the binders at low frequencies.

Both models describe well the behavior of the centrifuged/no cure binders at low frequencies. The Sigmoidal model is able to capture the behavior of those same binders at higher frequencies, where the CAM model over predicts their behavior. For the centrifuged 72 hrs cure binders, the CAM model over predicts at higher and lower frequencies. In general, the Sigmoidal models is able to capture better the behavior of the centrifuged 72 hr cured binders.

Table 5-15. CAM and Sigmoidal Models prediction's comparison for unaged materials

Binder Type	Testing geometry	CAM model			Sigmoidal Model		
		Low Freq	Inter Freq	High Freq	Low Freq	Inter Freq	High Freq
AMB No Cure	1 mm	Over	Under	Over	Good	Good	Under
	2 mm	Over	Under	Over	Good	Good	Under
	CC	Good	Under	Over	Good	Under	Over
	Centrifuged	Good	Good	Over	Good	Good	Good
AMB 72 hrs Cure	1 mm	Over	Fair	Good	Good	Good	Under
	2 mm	Over	Fair	Good	Good	Good	Under
	CC	Good	Under	Over	Good	Good	Good
	Centrifuged	Over	Fair	Over	Good	Good	Under
AP No Cure	1 mm	Over	Under	Over	Good	Good	Under
	2 mm	Over	Under	Over	Good	Good	Under
	CC	Good	Under	Over	Good	Under	Over
	Centrifuged	Good	Fair	Over	Good	Good	Fair
AP 72 hrs Cure	1 mm	Over	Fair	Good	Good	Good	Under
	2 mm	Over	Fair	Good	Good	Good	Under
	CC	Fair	Under	Fair	Fair	Under	Fair
	Centrifuged	Fair	Under	Over	Good	Good	Good

Table 5-15. CAM and Sigmoidal Models prediction's comparison for unaged materials – continued

Binder Type	Testing geometry	CAM model			Sigmoidal Model		
		Low Freq	Inter Freq	High Freq	Low Freq	Inter Freq	High Freq
CRYO No Cure	1 mm	Over	Under	Over	Good	Good	Under
	2 mm	Over	Under	Over	Good	Good	Under
	CC	Good	Under	Over	Good	Under	Over
	Centrifuged	Good	Good	Over	Good	Good	Fair
CRYO 72 hrs Cure	1 mm	Over	Under	Fair	Good	Good	Under
	2 mm	Over	Under	Over	Good	Fair	Under
	CC	Good	Under	Over	Good	Under	Over
	Centrifuged	Fair	Under	Over	Good	Good	Good
CP No Cure	1 mm	Over	Under	Over	Good	Good	Under
	2 mm	Over	Under	Over	Good	Good	Under
	CC	Good	Under	Good	Good	Under	Over
	Centrifuged	Good	Good	Over	Good	Good	Fair
CP 72 hrs Cure	1 mm	Over	Under	Good	Good	Good	Under
	2 mm	Over	Fair	Good	Good	Good	Under
	CC	Good	Good	Over	Good	Good	Over
	Centrifuged	Over	Under	Good	Good	Good	Under

Master curves of RTFO aged materials

The master curves of the RTFO aged materials are presented in APPENDIX C. The RTFO master curve for the base binder was better described by the Sigmoidal model; the CAM model fit well for intermediate and low frequencies but over predicts the behavior at high frequencies or low temperatures.

Similarly to Table 5-15, Table 5-16 summarizes the comparison of the behavior predictions made by the CAM and Sigmoidal Models. For the RTFO master curves of the AMB no cure binder (Figures C-2 to C-5), it can be said that the Sigmoidal model describes well the behavior of the non-centrifuged materials tested using the parallel plates at low and intermediate frequencies, whereas the CAM model over predicts the behavior at low frequencies. However, at high frequencies the CAM model is able to better describe the behavior of the binders, when the Sigmoidal under predicts their behavior. For the materials tested with concentric cylinders, both models describe well the behavior, except at intermediate frequencies, where both are not able to capture the hump in the curve, both models under predict this behavior. The Sigmoidal model fits better the master curve of the centrifuged material than the CAM model does. The CAM model over predicts the behavior of the centrifuged material at low and high frequencies and under predicts it at intermediate frequencies.

The model fitting of the master curves of the RTFO AMB 72 hr cured binders (Figures C-6 to C-9) showed that for the non-centrifuged binders tested with the parallel plates at 1 and 2 mm gaps, the Sigmoidal model is capable of describing the behavior of these materials at low and intermediate frequencies. The CAM model tends to over predict the behavior of these materials at low frequencies, both are capable of describing the

behavior at intermediate frequencies. Both models under predict the behavior of the materials tested with those geometries approximately after 1E4 Hz.

The master curve of the RTFO AMB 72 hr cured binder tested with concentric cylinders is well described by both the Sigmoidal and CAM models except after approximately the 1E2 Hz frequency, where both models under predict the behavior of the binder (. For the RTFO centrifuged materials of that same binder, the Sigmoidal model is able to capture the whole behavior of the binder; whereas, the CAM model does not capture the behavior of the binder, it over predicts at lower and higher frequencies, and under predicts at intermediate frequencies.

For the behavior of the AP no cured binder, the Sigmoidal and CAM models fit the master curve of the non-centrifuged binder tested with 1 mm gap parallel plate geometry. The non-centrifuged binder tested with the 2 mm gap is well described at lower and intermediate frequencies by the Sigmoidal model. At high frequencies approximately after 1E4 Hz, both models underestimate the behavior of the binder. The CAM model over estimates the behavior at low frequencies, at intermediate frequencies the model fits the data. For the master curves obtained from the binder tested with concentric cylinders both models describe the data except for after the frequency of 1E2, where the data values are higher than the prediction of the models. The behavior of the centrifuged binder is captured well by the Sigmoidal model, and as for the other RTFO centrifuged binders the CAM model does not fit the data.

The Sigmoidal and CAM model describe the behavior of RTFO AP 72 hr cured binder tested with different geometries (Figures C-14 to C-17)in a similar way as the behavior of the RTFO AP no cure binder, except for the non-centrifuged binder tested with 1

mm gap parallel plate geometry. The behavior described for this binder is similar to the one described for the 2 mm gap RTFO AP no cured.

The Sigmoidal model is only able to describe the rheological behavior of the RTFO aged non-centrifuged CRYO no cure binders tested with parallel plate at 1 and 2 mm gaps, at low and intermediate frequencies (Figures C-18 and C-19). The CAM model is not able to describe its behavior at low and intermediate frequencies, but at frequencies higher than 1E4 Hz, the CAM model predicts the behavior of the binders. For the binders tested with the concentric cylinders (Figure C-20), none of the models are able to capture the hump present by the data at intermediate frequencies. The behavior of the centrifuged binder (Figure C-21) is better captured by the Sigmoidal model; the CAM model is not able to fit the master curve shape.

The model's curves for RTFO aged materials for the CRYO 72 hr cured binder tested with the parallel plate geometry at 1 mm and 2 mm gaps describe in similar fashion the behavior of each binder (Figures C-22 and C-23). In sum, the Sigmoidal model fits the data at low and intermediate frequencies, at those same frequencies the CAM model over predicts and under predicts the G* of the binders, respectively. However, the CAM model fits the data at high frequencies well; whereas, the Sigmoidal does present lower predicted G*. Both models are able to predict the G* of the non-centrifuged binders tested with concentric cylinders (Figure C-24). For the centrifuged binders tested with parallel plates, the Sigmoidal model has a better fit than the CAM model (Figure C-25). The latter over predicts at low and high frequencies and under predicts at intermediate frequencies.

For the RTFO aged materials of the CP no cure binders, similar to the previous binder types, the Sigmoidal model is able to predict G* at low and intermediate frequencies, but not

so much at high frequencies for the non-centrifuged binders tested at 1 and 2 mm gap (Figures C-26 and C-27). While the CAM model fails to predict G* accurately at those same frequencies, at higher frequencies from 1E4 Hz the CAM model is able to capture the behavior of those binders. The results from the binder tested with concentric cylinders present a hump at intermediate frequencies, neither of the two models is capable of capturing this behavior (Figure C-28). For the master curve of the centrifuged material tested with parallel plates the Sigmoidal model fits the behavior of the binder (Figure C-29). As it happened with the other types of centrifuged materials, the CAM model does not describe the rheological behavior of these centrifuged materials.

Finally for this section Figures C-30 to C-33 presents the master curves of RTFO aged materials of the CP 72 hr cured binder. The Sigmoidal model is able to describe the G* of the non-centrifuged binders tested with parallel plates at 1 and 2 mm gaps at low and intermediate frequencies, whereas at high frequencies the CAM model better describes this behavior. The master curves obtained for the material tested using the concentric cylinders is well described by the Sigmoidal and CAM models. For the centrifuged material tested with parallel plates, the Sigmoidal model fits the data better at low and intermediate frequencies; at higher frequencies the CAM model fits the data better.

Table 5-16. CAM and Sigmoidal Models prediction's comparison for RTFO aged materials

Binder Type	Testing geometry	CAM model			Sigmoidal Model		
		Low Freq	Inter Freq	High Freq	Low Freq	Inter Freq	High Freq
AMB No Cure	1 mm	Over	Good	Under	Over	Good	Under
	2 mm	Over	Good	Under	Over	Good	Under
	CC	Good	Good	Good	Good	Good	Good
	Centrifuged	Over	Under	Over	Good	Good	Good
AMB 72 hrs Cure	1 mm	Over	Good	Under	Over	Good	Under
	2 mm	Over	Good	Under	Over	Good	Under
	CC	Good	Good	Under	Good	Good	Under
	Centrifuged	Over	Under	Over	Good	Good	Good
AP No Cure	1 mm	Good	Good	Good	Good	Good	Good
	2 mm	Good	Good	Under	Good	Good	Under
	CC	Good	Good	Under	Good	Good	Under
	Centrifuged	Over	Under	Over	Good	Good	Good
AP 72 hrs Cure	1 mm	Good	Good	Under	Good	Good	Under
	2 mm	Good	Good	Under	Good	Good	Under
	CC	Good	Good	Under	Good	Good	Under
	Centrifuged	Over	Under	Over	Good	Good	Good

Table 5-16. CAM and Sigmoidal Models prediction's comparison for RTFO aged materials – continued

Binder Type	Testing geometry	CAM model			Sigmoidal Model		
		Low Freq	Inter Freq	High Freq	Low Freq	Inter Freq	High Freq
CRYO No Cure	1 mm	Over	Fair	Good	Good	Good	Under
	2 mm	Over	Fair	Good	Good	Good	Under
	CC	Good	Under	Good	Good	Under	Over
	Centrifuged	Over	Under	Over	Good	Good	Good
CRYO 72 hrs Cure	1 mm	Over	Fair	Good	Good	Good	Under
	2 mm	Over	Fair	Good	Good	Good	Under
	CC	Good	Good	Good	Good	Good	Good
	Centrifuged	Over	Under	Over	Good	Good	Good
CP No Cure	1 mm	Over	Under	Fair	Good	Good	Under
	2 mm	Over	Fair	Fair	Good	Good	Under
	CC	Good	Under	Good	Good	Under	Good
	Centrifuged	Over	Under	Over	Good	Good	Good
CP 72 hrs Cure	1 mm	Over	Fair	Fair	Good	Good	Under
	2 mm	Over	Fair	Good	Good	Good	Under
	CC	Good	Good	Good	Good	Good	Good
	Centrifuged	Over	Good	Over	Good	Good	Under

Master curves comparison of different geometries results

The master curves obtained for each type of binder with each geometry are compared among each other in the same figure. As a reference the master curve of the base binder PG 52-34 is presented in each figure. Figure 5-17 through 5-24 present these comparisons for the unaged materials of the AR binders. Then, from Figure 5-25 through 5-32, the comparison of the master curves of the RTFO aged materials is depicted.

For the unaged master curves of the AR binders with ambient GTR (Figure 5-17 to 5-20) it can be seen that master curves obtained from the testing results of the non-centrifuged binders tested in the parallel plate geometries are overlapping each other. The master curve obtained for the centrifuged materials of these binders are parallel to the master curve of the base binder PG52-34. The parallel distance for the 72 hr cured centrifuged binders seems to be farther from the base binder when compared to the parallel distance of the no cure centrifuged binders from the base binder. Overlapping of the master curve from the materials tested with the concentric cylinders was only found for the unaged AP no cure binder. Some overlapping at intermediate frequencies were observed for the AMB no cure binder. Overlapping of the master curves was not observed for the AMB no cure and AP 72 hr cured binders. At higher frequencies or lower temperatures, the G* values obtained for the unaged non-centrifuged AR binders containing ambient GTR tested with parallel plates were similar to the G* values obtained for the base binder. The G* values observed for the centrifuged binders tested at higher frequencies or lower temperatures were higher when compared with the G*s of the ones for the non-centrifuged and base binders. At lower frequencies or higher temperatures, the G* values for the non-centrifuged materials are higher than those of the centrifuged ones.

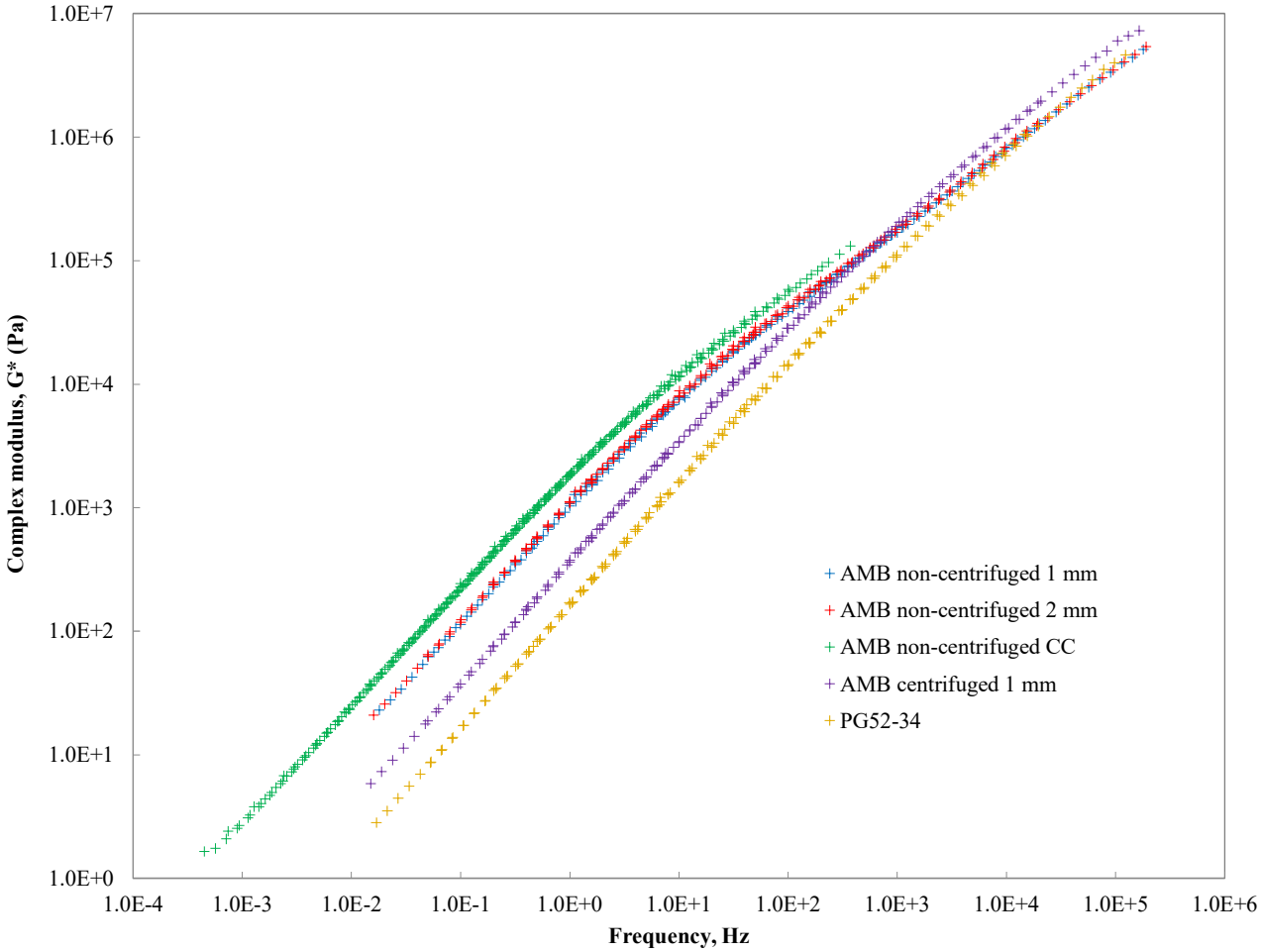

Figure 5-17. Master curve comparison of unaged AMB binder tested with different geometries, T_{ref} = 64 °C

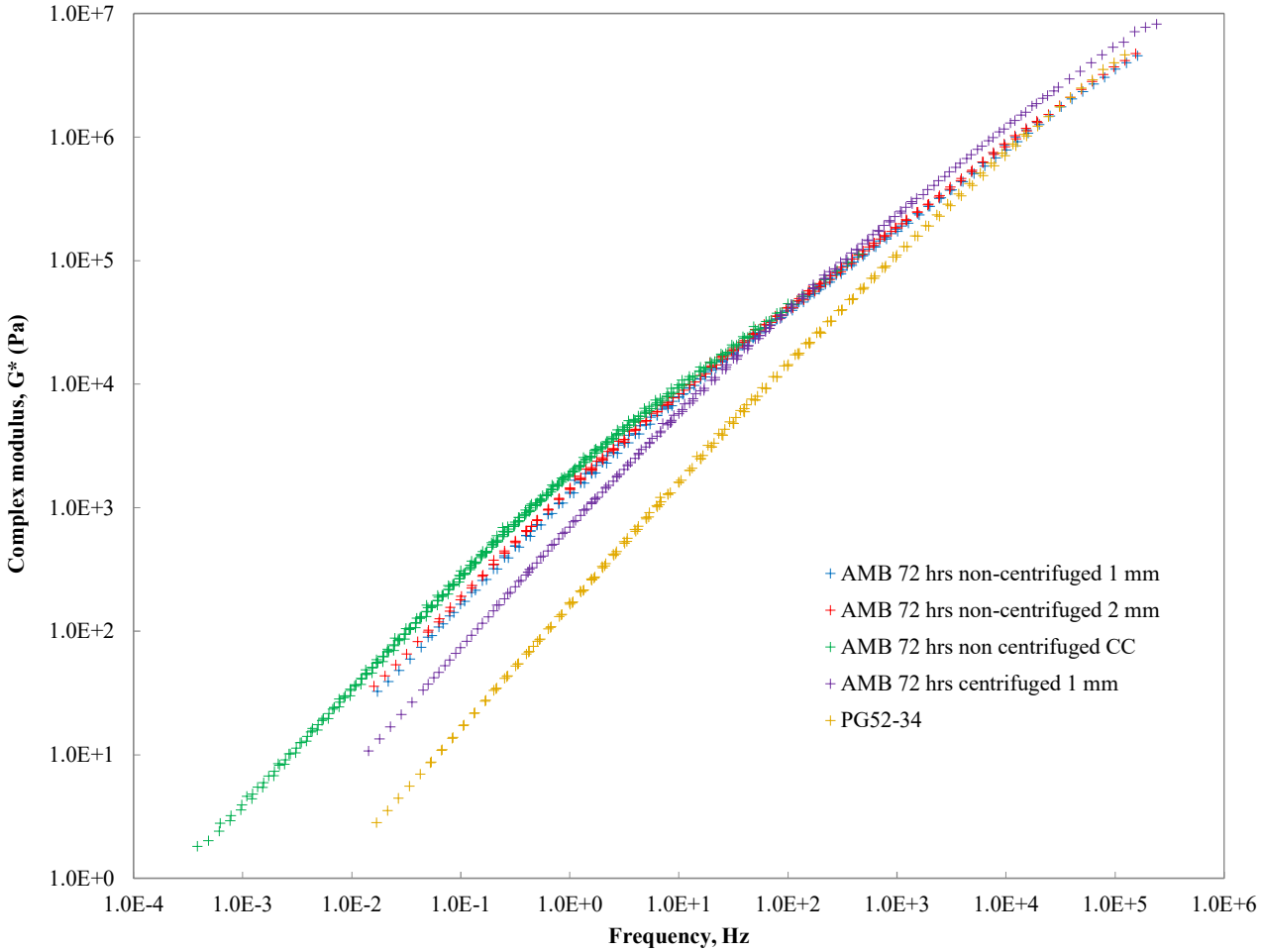

Figure 5-18. Master curve comparison of unaged AMB 72 hrs cure binder tested with different geometries, T_{ref} = 64 °C

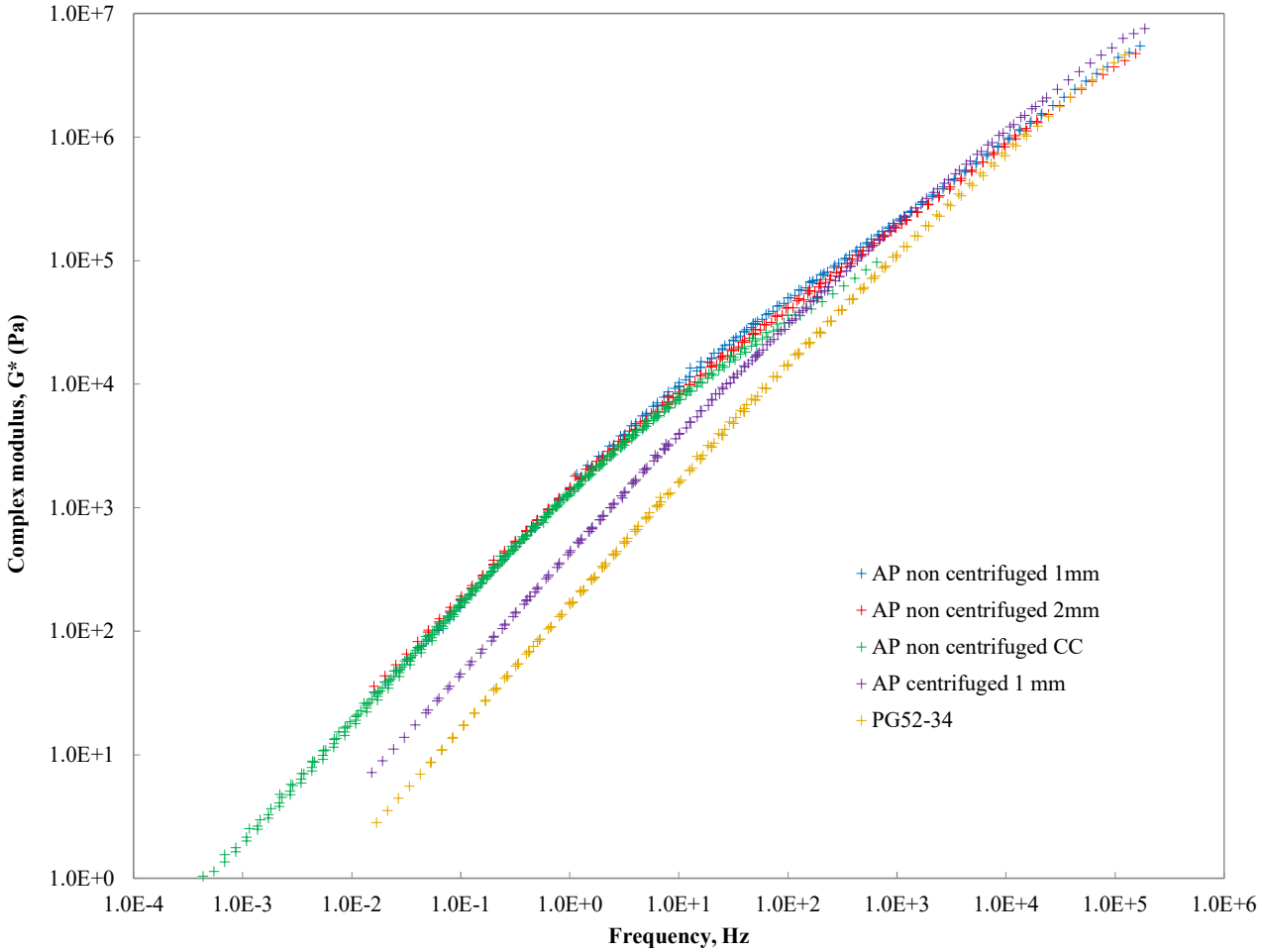

Figure 5-19. Master curve comparison of unaged AP binder tested with different geometries, T_{ref} = 64 °C

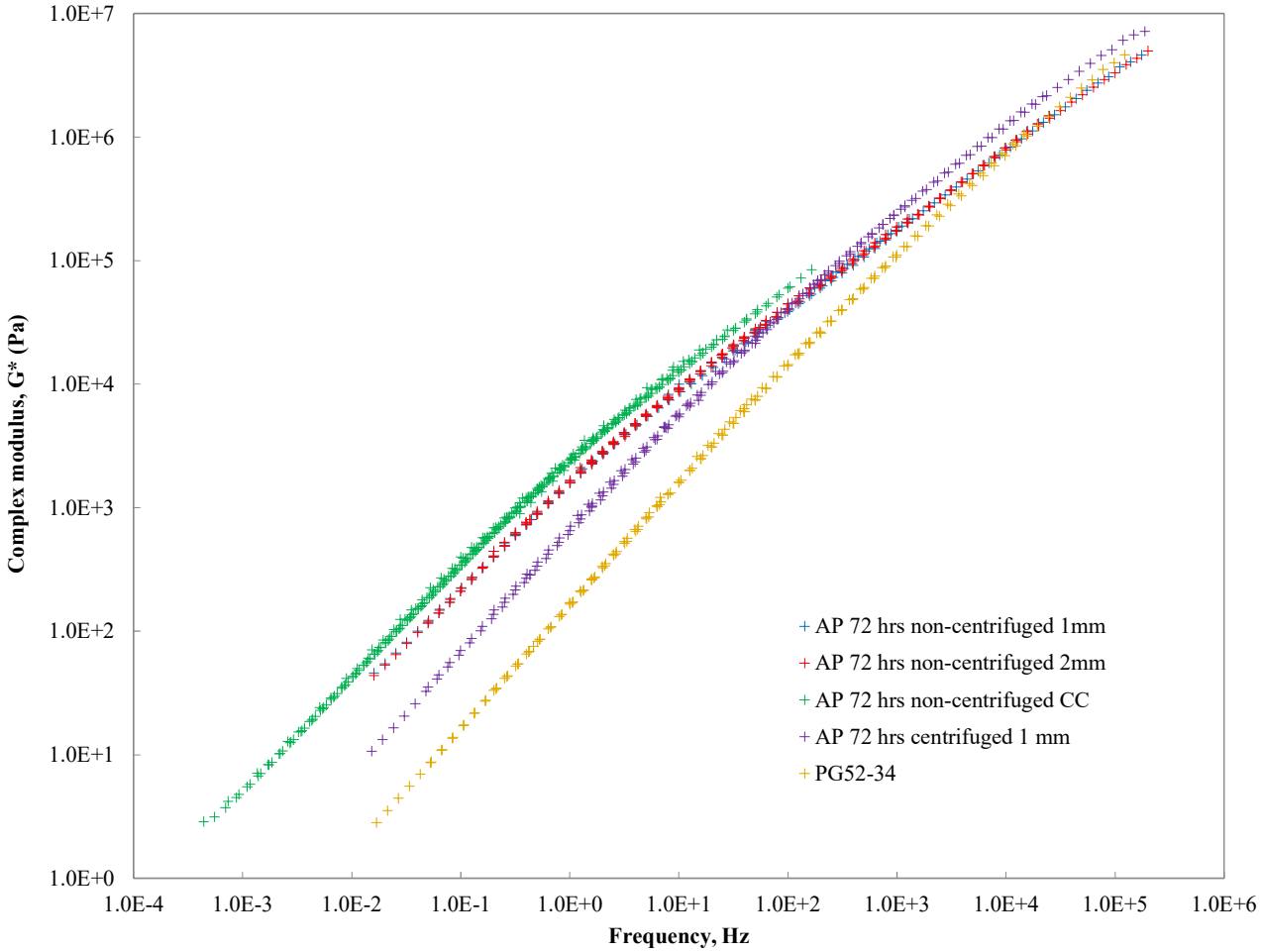

Figure 5-20. Master curve comparison of unaged AP 72 hrs cure binder tested with different geometries, T_{ref} = 64 °C

For the unaged master curves comparison of the AR binders containing cryogenic GTR (Figure 5-21 to 5-24), one can observe that the master curves obtained from the non-centrifuged materials tested with parallel plates overlap with each other. The master curves of the centrifuged materials are parallel to the base binder's mater curve, except for the CP 72 hr cured binder. As mentioned before, it is suspected that the curing had a great influence in the AR binder containing cryogenic rubber and polyoctenamer, making the rubber particles swell to its maximum capacity and then began to break down into smaller particles that the cloth mesh was not able to retain. At higher frequencies the G* values were higher for the centrifuged materials than for the non-centrifuged ones. This behavior changes at intermediate and lower frequencies, where higher G* values are observed for the non-centrifuged binders tested with parallel plates. With respect to the G* values from the concentric cylinders testing geometry, these were higher than the ones obtained with parallel plate geometry. Some overlapping between the master curves from concentric cylinders results is observed at intermediate frequencies with the parallel plate results for the non-centrifuged binders.

The RTFO aged master curves of the non-centrifuged binders containing ambient GTR tested with parallel plates (Figure 5-25 to 5-28) overlap with each other for those binder types, except for the AP binder, where the G* values observed where higher for the 1 mm gap. The master curves of the centrifuged binders are parallel to the master curve of the base binder. The parallel distance between these curves and the base binder is greater for the 72 hr cured centrifuged binders. No overlapping was observed for the curves obtained from the materials tested using the concentric cylinders with the master curves of the non-centrifuged materials tested with parallel plates.

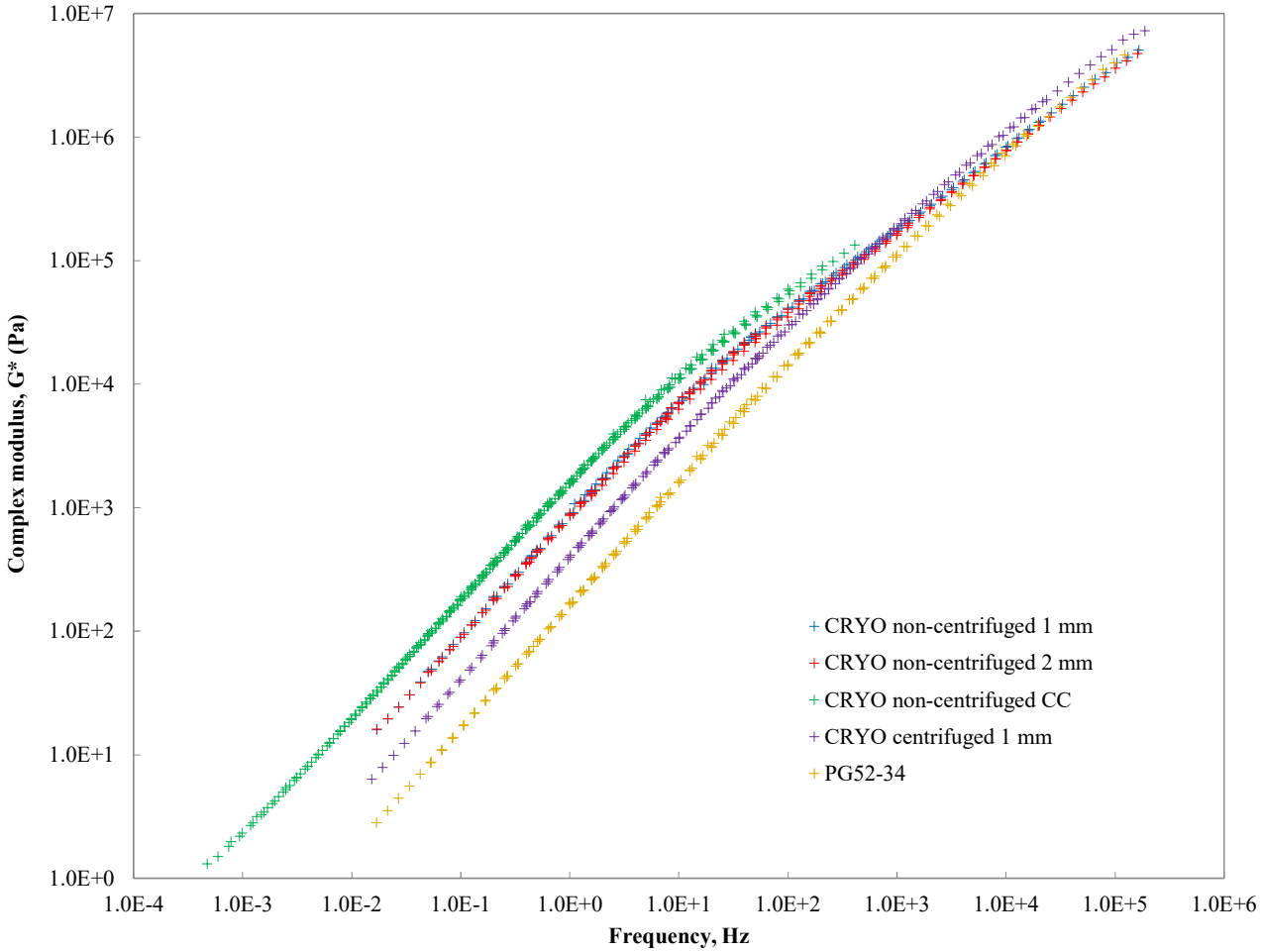

Figure 5-21. Master curve comparison of unaged CRYO binder tested with different geometries, T_{ref} = 64 °C

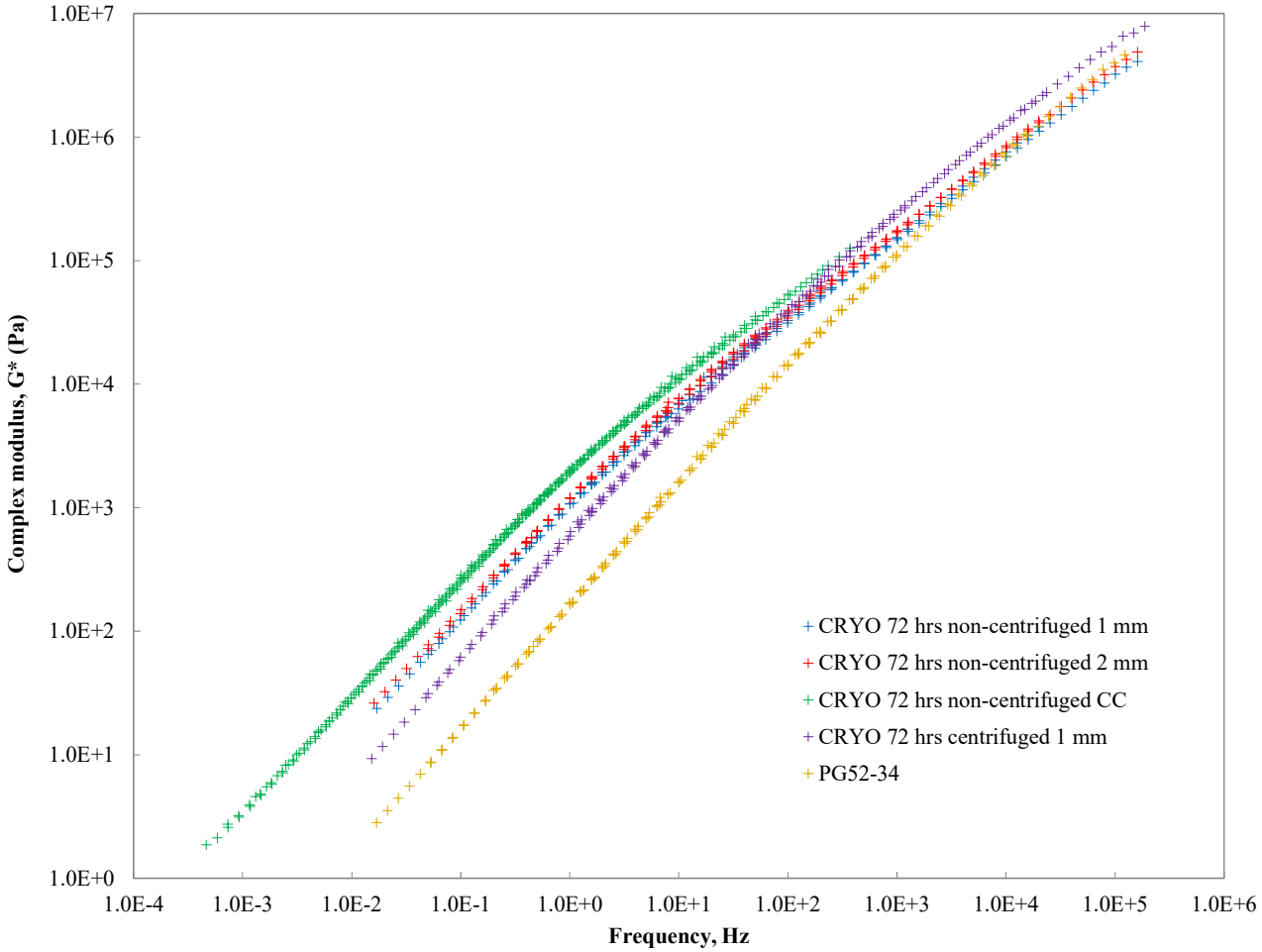

Figure 5-22. Master curve comparison of unaged CRYO 72 hrs binder tested with different geometries, T_{ref} = 64 °C

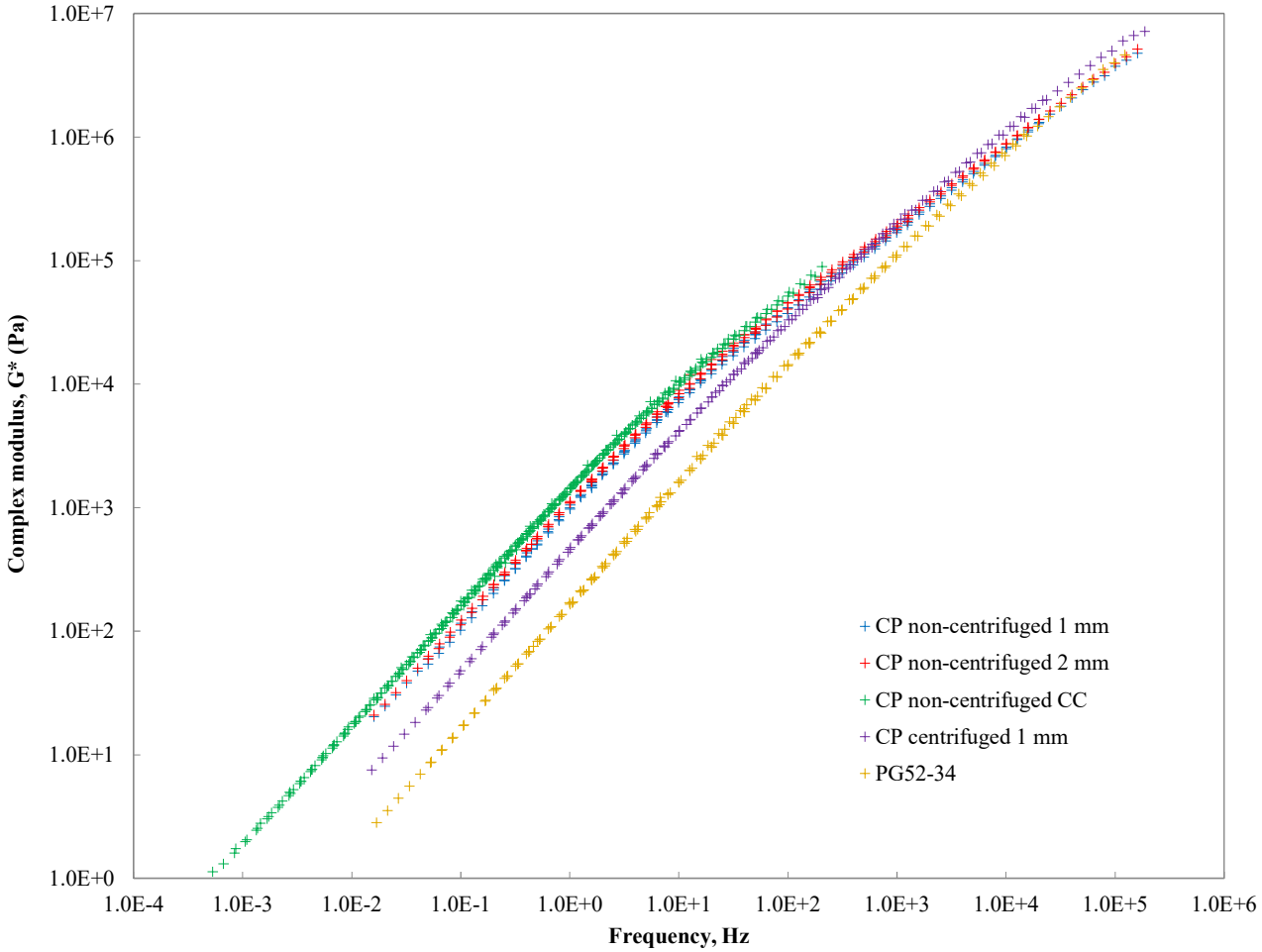

Figure 5-23. Master curve comparison of unaged CP binder tested with different geometries, T_{ref} = 64 °C

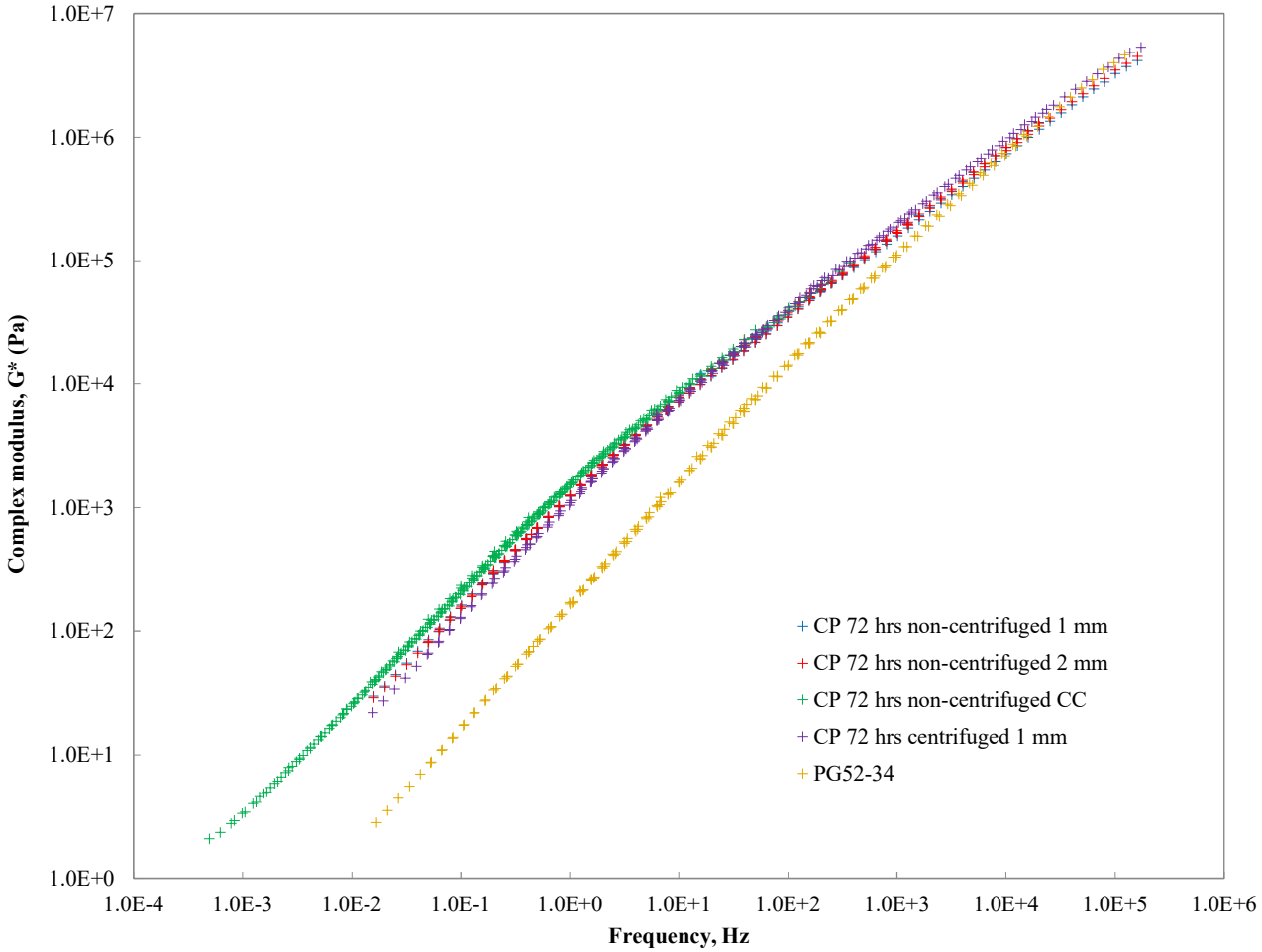

Figure 5-24. Master curve comparison of unaged CP 72 hrs cure binder tested with different geometries, T_{ref} = 64 °C

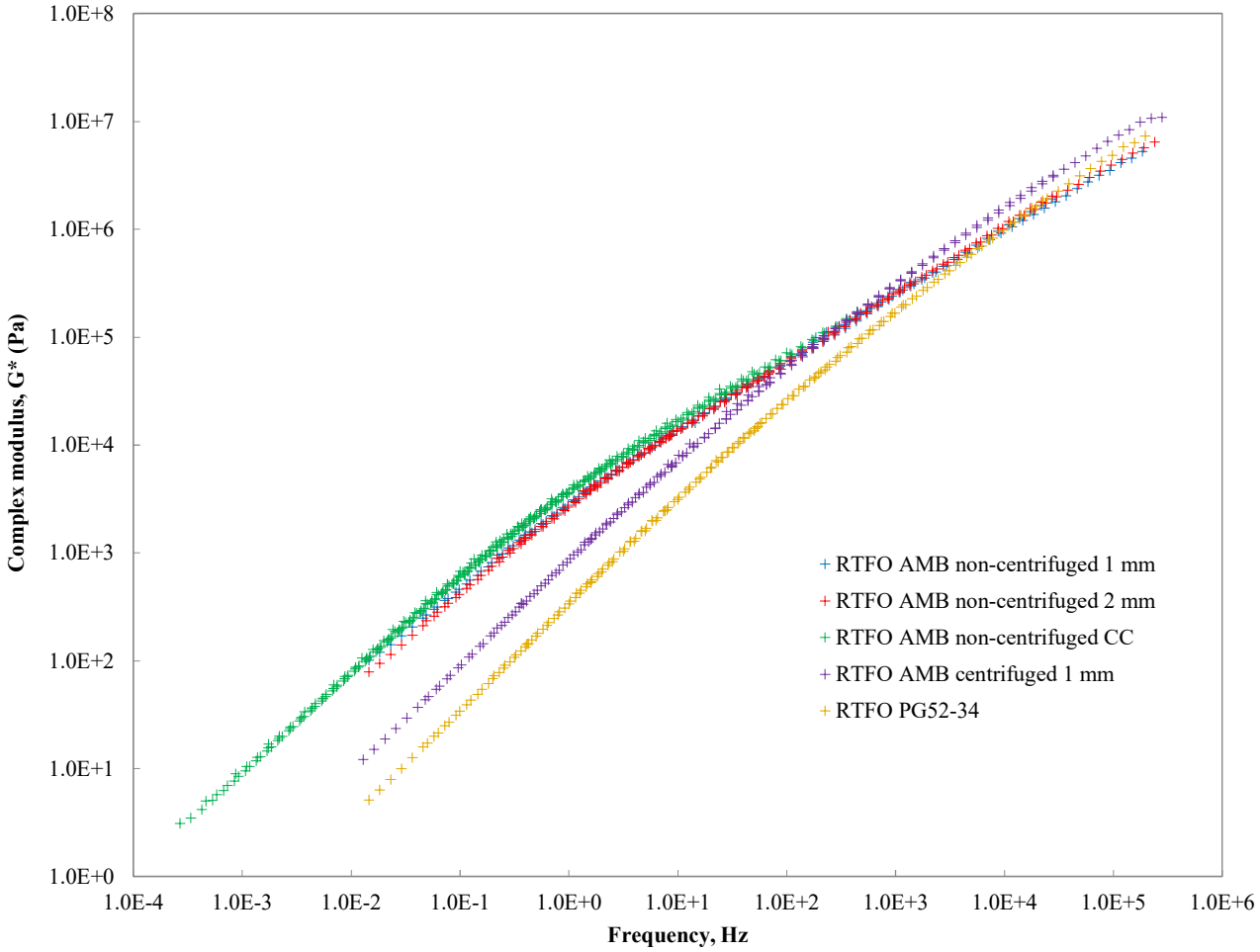

Figure 5-25. Master curve comparison of RTFO aged AMB binder tested with different geometries, T_{ref} = 64 °C

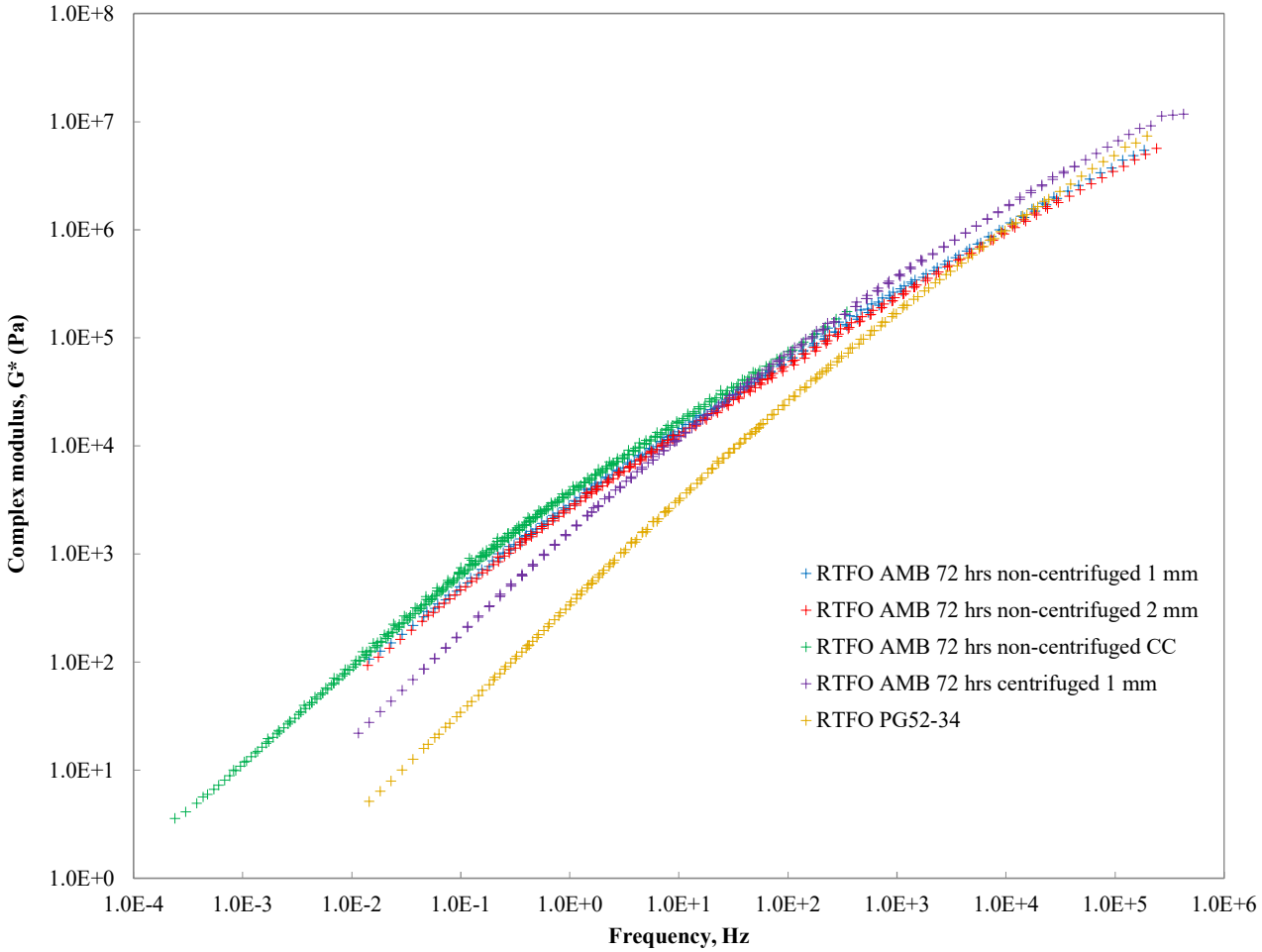

Figure 5-26. Master curve comparison of RTFO aged AMB 72 hrs cure binder tested with different geometries, T_{ref} = 64 °C

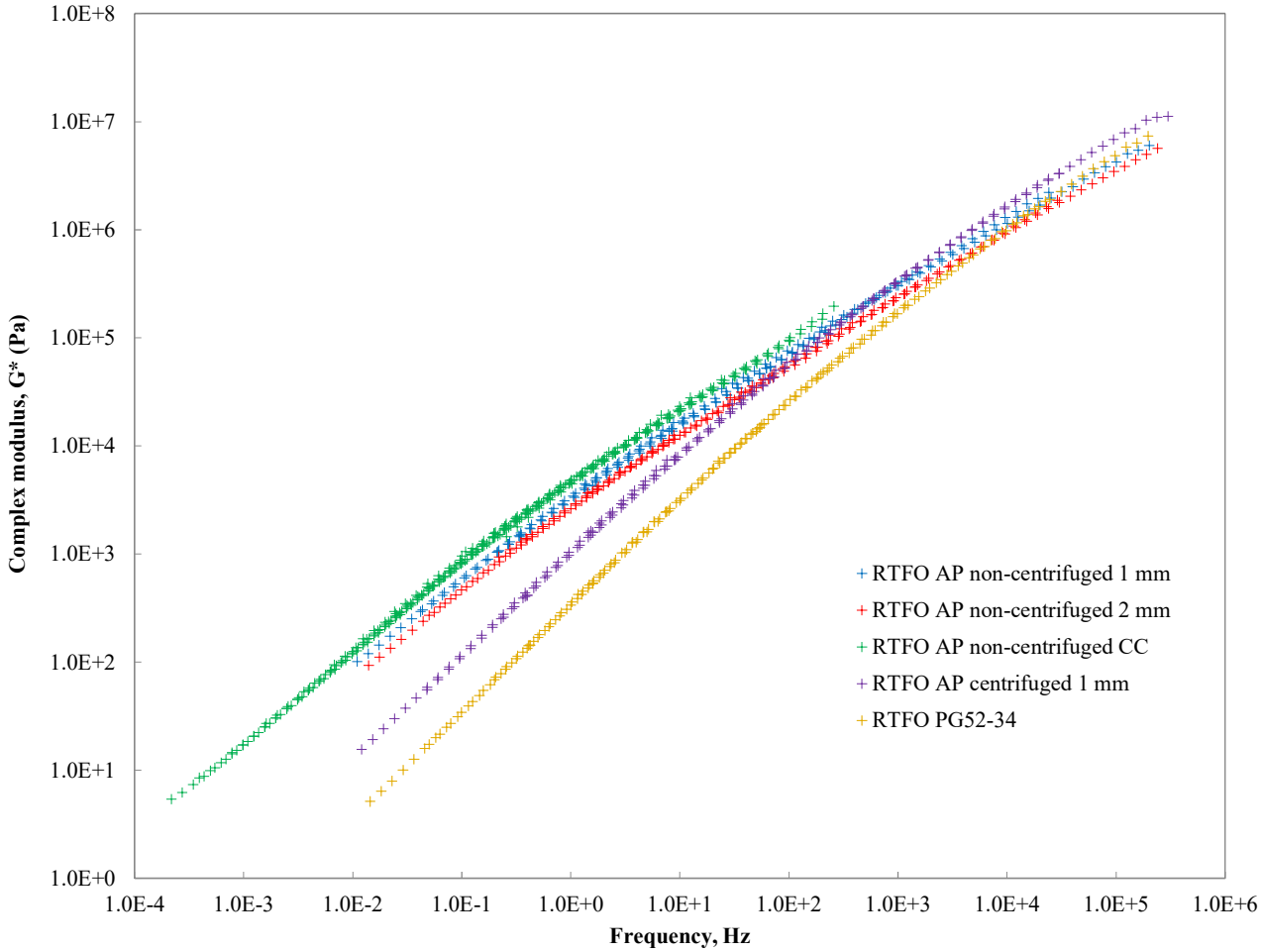

Figure 5-27. Master curve comparison of RTFO aged AP binder tested with different geometries, T_{ref} = 64 °C

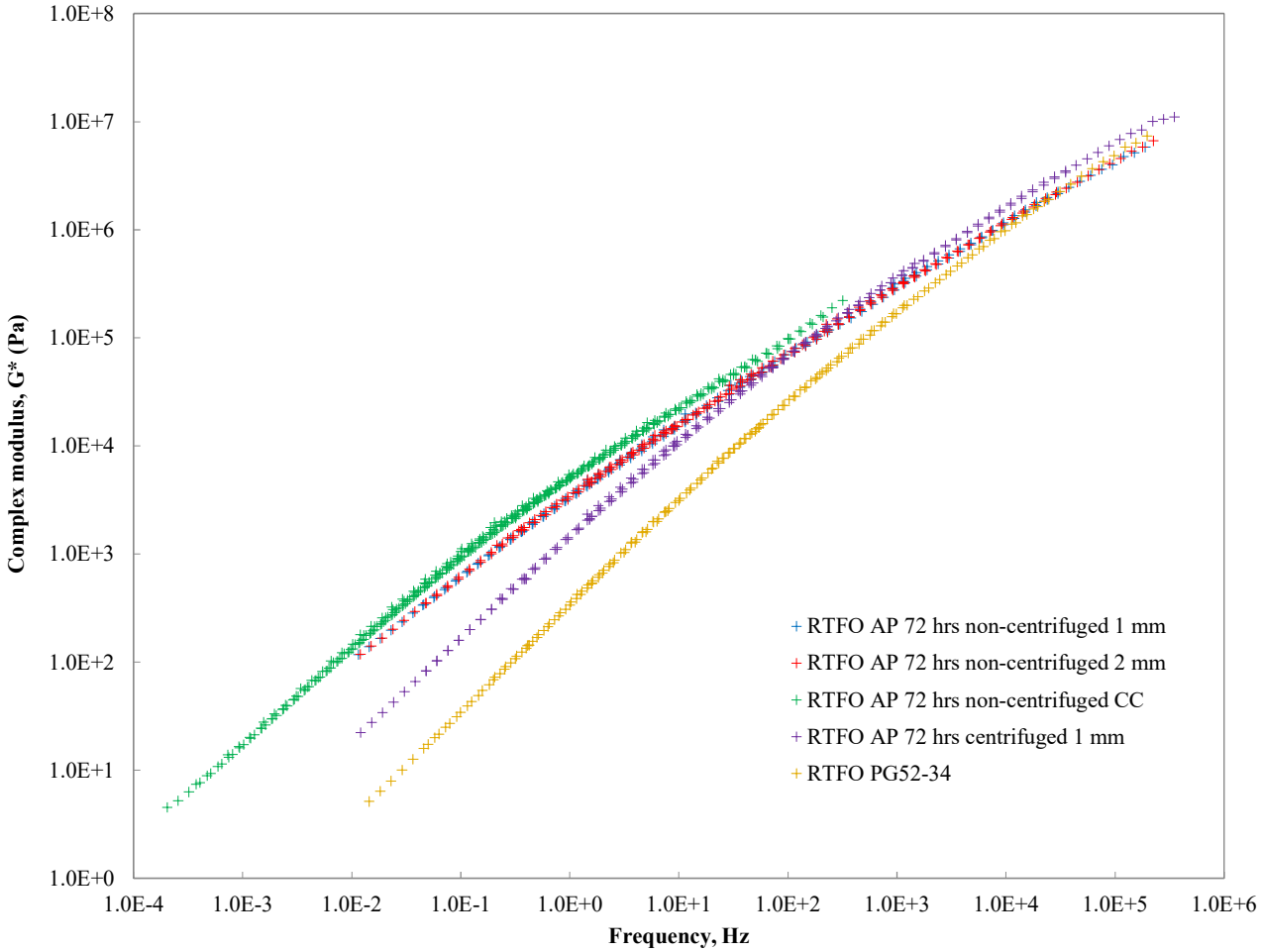

Figure 5-28. Master curve comparison of RTFO aged AP 72 hrs cure binder tested with different geometries, T_{ref} = 64 °C

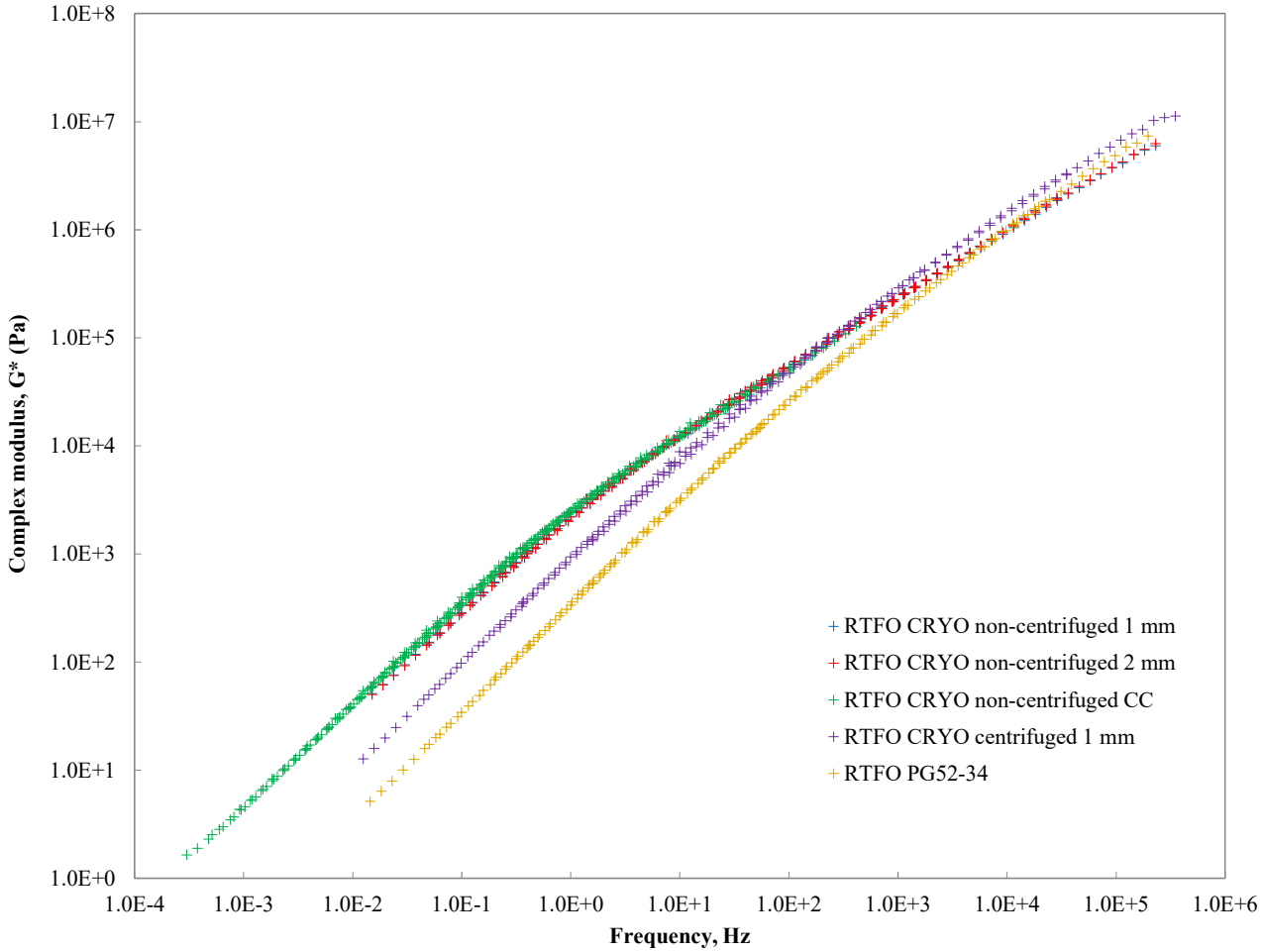

Figure 5-29. Master curve comparison of RTFO aged CRYO binder tested with different geometries, T_{ref} = 64 °C

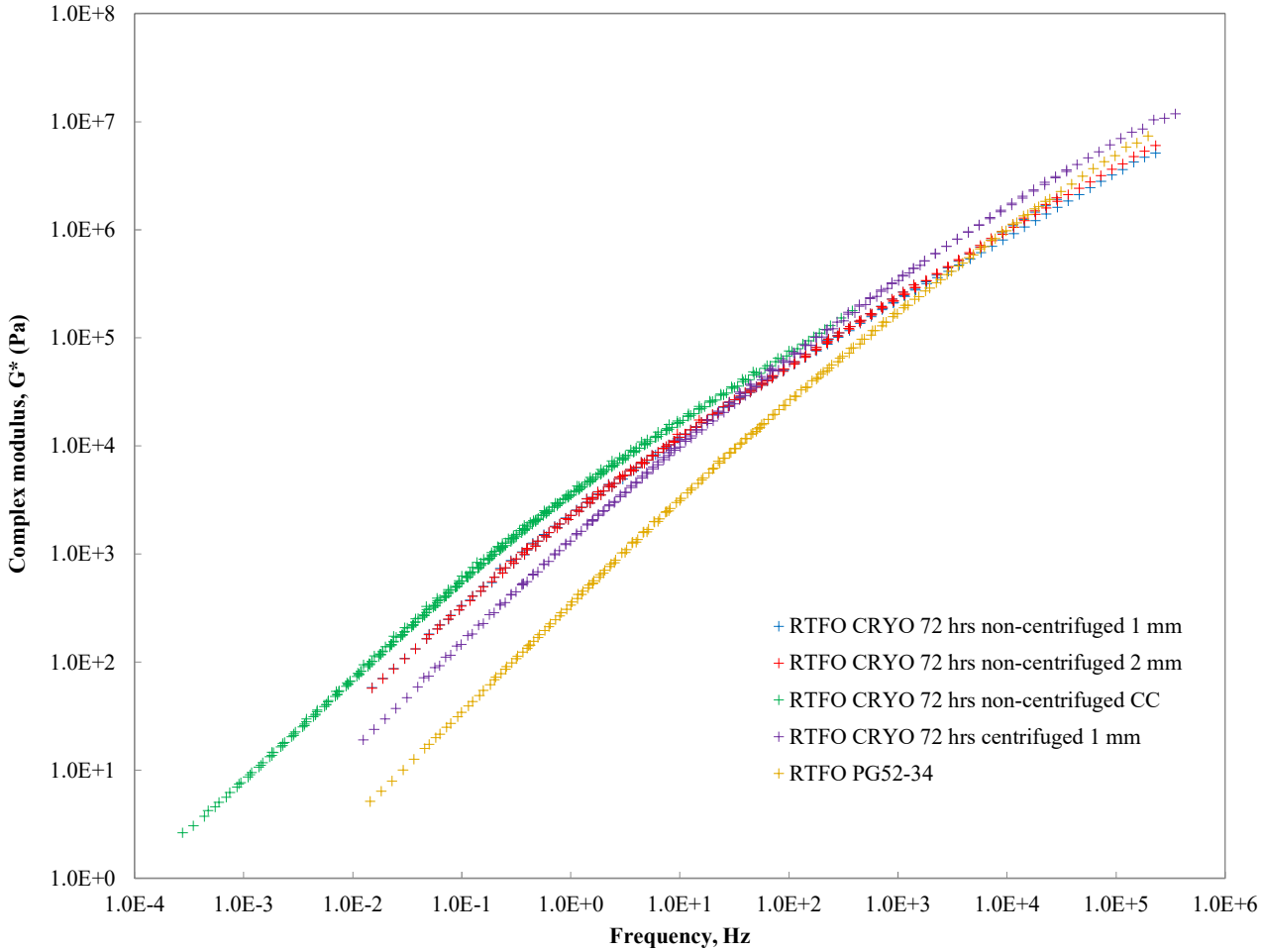

Figure 5-30. Master curve comparison of RTFO aged CRYO 72 hrs cure binder tested with different geometries, T_{ref} = 64 °C

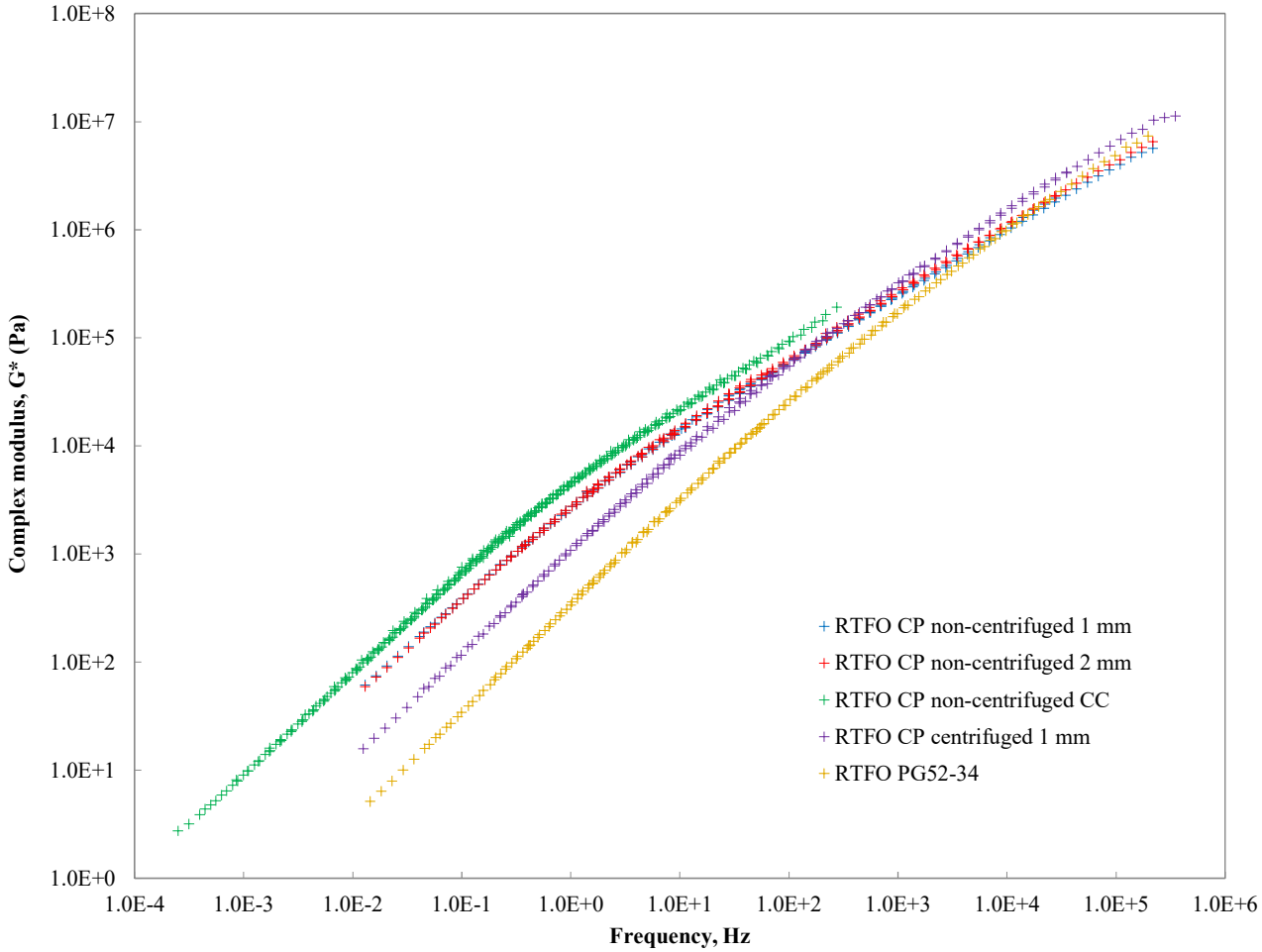

Figure 5-31. Master curve comparison of RTFO aged CP binder tested with different geometries, T_{ref} = 64 °C

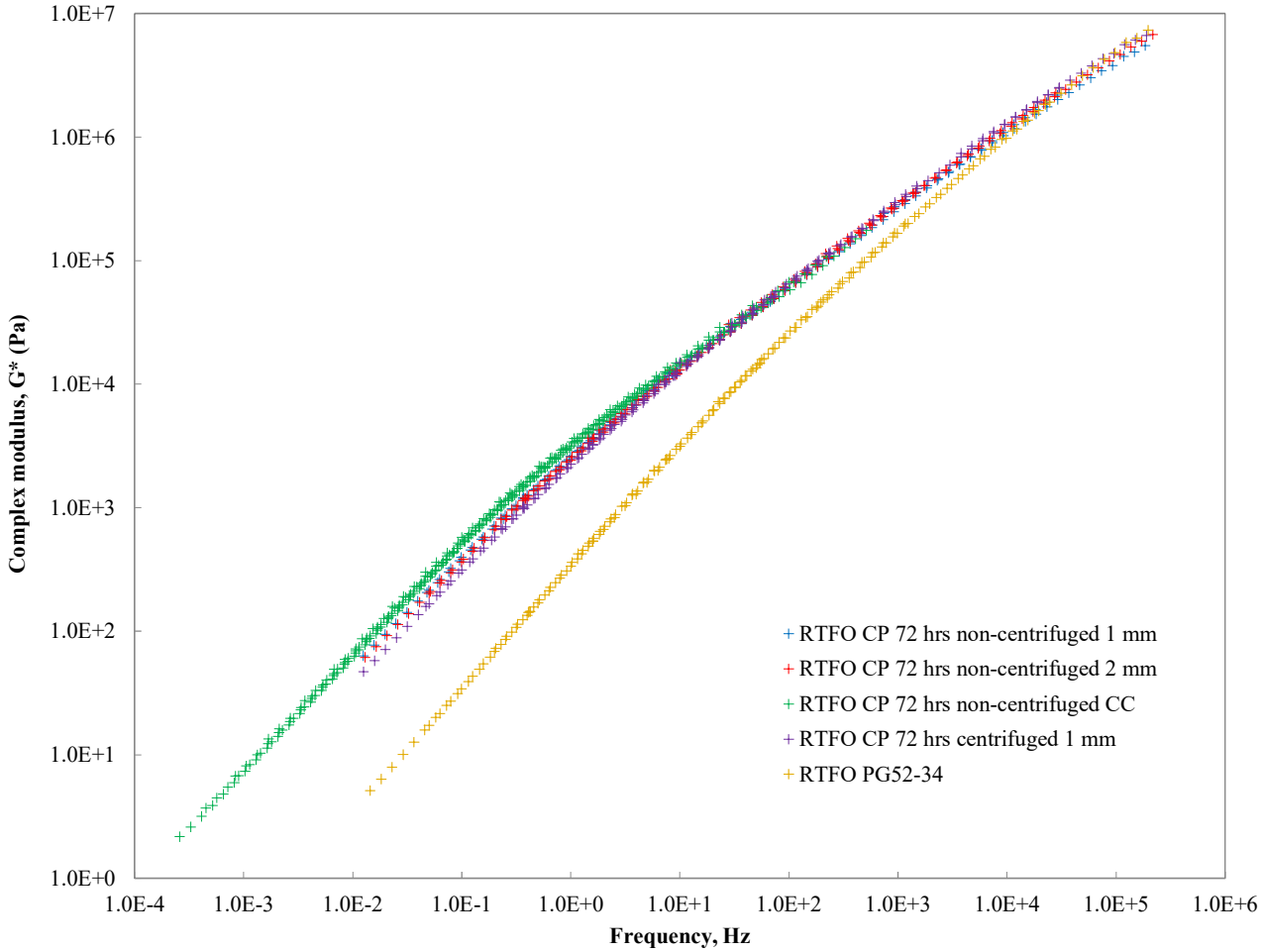

Figure 5-32. Master curve comparison of RTFO aged CP 72 hrs cure binder tested with different geometries, T_{ref} = 64 °C

The master curves obtained for the RTFO aged materials of the AR binders containing cryogenic GTR and tested with the different geometries (Figure 5-29 to 5-32) presented similar behavior as those observed with the RTFO aged binders with ambient GTR, except for the RTFO aged CP 72 hr cured binder. Excluding the CP 72 hr cured binder, overall, the curves for the centrifuged materials were parallel to the base binder. At higher frequencies the curves for the non-centrifuged materials had lower G* values than the curve for the centrifuged materials, this starts to shift at intermediate frequencies, and at lower frequencies the G* values for the non-centrifuged binders are higher than the centrifuged binders. Some overlapping of curves occurs at intermediate frequencies between the binders tested with concentric cylinders and the non-centrifuged binders tested with parallel plates for the CRYO no cure binder and the CP 72 hr cured binder.

Conclusions

The addition of polyoctenamer increased the viscosity of the unaged asphalt rubber binders used in this study regardless of the type of rubber that the binder contains. After RTFO aging, the asphalt rubber binders containing polyoctenamer presented lower viscosities than the control binders. The former is true only for the non-centrifuged asphalt rubber binders; however, the centrifuged materials containing polyoctenamer did not presented lower viscosities than the control binders. Thus, for the base binder type used in this study, polyoctenamer did not necessarily improves the workability of the asphalt rubber binders.

The asphalt rubber binders containing polyoctenamer had, in general, higher specific gravities that the asphalt rubber binders without polyoctenamer. In sum, slightly higher mass loss was obtained for the asphalt rubber binders containing polyoctenamer; slightly higher

mass loss was also observed for the non-centrifuged binders compared to the centrifuged materials. The curing process seem to increase somewhat the mass loss of the asphalt rubber binders containing ambient GTR, but slightly reduces the mass loss of those containing cryogenic GTR.

From the storage stability results one can conclude that curing the binders will help to some degree with the storage stability of the asphalt rubber binders. The addition of polyoctenamer in this study was only beneficial to the storage stability of the asphalt rubber binders containing ambient GTR.

The continuous grade of the asphalt rubber binders and the master curves comparisons corroborate the findings of the author in a previous study that demonstrate that increasing the gap size to 2 mm does not avoid the interference of the rubber particles in the dynamic shear rheometer testing. It also corroborates findings made by Alavi (2015), where the continuous grades obtained with the concentric cylinder geometry were higher than those obtained with parallel plates. It was proved that better and sounder results are obtained by using the centrifuged materials of the asphalt rubber binders. By centrifuging the asphalt rubber binders, one can isolate the rubber particles effect and really capture the modification made by the GTR without having the interaction of the rubber particles. This method does not require the acquisition nor retro-fitting of costly dynamic shear rheometer accessories, and the testing can still be performed using the parallel plate geometry with 1 mm gap, without concern of losing the integrity of the sample when testing with greater gap sizes.

With regards to the models used in this study to model the master curves constructed for the asphalt rubber binders, it is noticeable that the Sigmoidal model could predict better the behavior of the complex modulus of the asphalt rubber binders because is able to capture

the hump in the master curves at intermediate temperatures that was characteristic for the asphalt rubber binders tested in this study. The flatter shape of the CAM model did not allow proper fitting for the master curves at intermediate and higher temperatures; however, it does predict the complex modulus of the RTFO aged asphalt rubber binders at low temperatures well.

It is recommended to evaluate the rubber particles of the cryogenic GTR binders under a special microscope (Scanning Electron microscopy or/and Fluorescence microscopy) to measure the particle sizes of the cryogenic rubber in the binder with no cure and 72 hrs of cure and compare them to corroborate that indeed the particles sizes of the 72 hr cured binder are smaller than the no cure binder. Since master curves are constructed in a log-log scale, a split-plot statistical analysis is recommended to evaluate in detail the statistical differences between master curves; a statistical analysis of this nature will be able to capture details that are lost due to the use of a log-log scale.

Acknowledgments

The authors would like to acknowledge the following companies Seneca Petroleum, Flint Hills and Lehigh Technologies for supplying of us with the materials utilized in this research. And, would also like to acknowledge Dr. Eric Cochran from the Department of Chemical and Biological Engineering at Iowa State University for making available his laboratory facilities to the researchers to carry out tests for this study.

References

ASTM Standard D70 (2009). Standard Test Method For Specific Gravity And Density Of Semi Solid Bituminous Materials (Pycnometer Method). ASTM International, West Conshohocken, PA, 2009

ASTM Standard D4402 (2013). Standard Test Method for Viscosity Determination of Asphalt at Elevated Temperatures Using a Rotational Viscometer. ASTM International, West Conshohocken, PA, 2013

ASTM Standard D7173 (2011). Determining the separation tendency of polymer from polymer modified asphalt. ASTM International, West Conshohocken, PA, 2011

Bahia, H. U., & Davies, R. (1994). Effect of crumb rubber modifiers (CRM) on performance related properties of asphalt binders. Asphalt paving technology, 63, 414-414.

Bahia, H. U., & Davies, R. (1995). Factors Controlling The Effect Of Crumb Rubber On Critical Properties of Asphalt Binders (With Discussion). Journal of the Association of Asphalt paving Technologists, 64.

Baumgardner, G., & D'Angelo, J. A. (2012). Development of a Crumb Rubber Modified (CRM) PG binder Specification. In Asphalt Rubber International Conference AR.

Huang, S.-C., Pauli, A. T., Grimes, R. W., & Turner, F. (2014). Ageing characteristics of RAP binder blends – what types of RAP binders are suitable for multiple recycling? *Road Materials and Pavement Design, 15*(sup1), 113-145. doi:10.1080/14680629.2014.926625

Peralta, J., Silva, H. M. R. D., Hilliou, L., Machado, A. V., Pais, J., & Christopher Williams, R. (2012). Mutual changes in bitumen and rubber related to the production of asphalt rubber binders. *Construction and Building Materials, 36*, 557-565. doi:http://dx.doi.org/10.1016/j.conbuildmat.2012.06.030

Polacco, G., Vacin, O. J., Biondi, D., Stastna, J., & Zanzotto, L. (2003). Dynamic master curves of polymer modified asphalt from three different geometries. *Applied Rheology, 13*(3), 118-124.

Putman, B. J., & Amirkhanian, S. N. (2006, October). Crumb rubber modification of binders: interaction and particle effects. In Proceedings of the Asphalt Rubber 2006 Conference (Vol. 3, pp. 655-677).

Tayebali, A. A., Vyas, B. B., & Malpass, G. A. (1997). Effect of crumb rubber particle size and concentration on performance grading of rubber modified asphalt binders. ASTM Special Technical Publication, 1322, 30-47.

CHAPTER 6. GENERAL CONCLUSIONS

This research involved the study of asphalt rubber mixtures and asphalt rubber binders that were laboratory produced. The performance of four asphalt rubber mixtures at low temperatures prove to be suitable when compared to other asphalt technologies. The addition of polyoctenamer to improve the workability of asphalt rubber binders prove to not adversely affect the low temperature performance of these mixtures. The behavior at low temperature of the mixes containing polyoctenamer were very similar to their counterpart without polyoctenamer.

The fatigue performance of asphalt rubber mixes containing polyoctenamer was also evaluated. The laboratory mixes containing ambient rubber presented in general better fatigue life than the mixes containing cryogenic rubber. However, the mix containing cryogenic rubber and polyoctenamer had the lower rate of damage accumulation compared to the other three mixes. In sum, asphalt rubber mixes not only have excellent rutting and low temperature performance but also adequate fatigue performance.

The addition of polyoctenamer does not necessarily improve the storage stability of all the asphalt rubber binders. In this study it worked better with ambient GTR binders than with cryogenic GTR. Curing the asphalt rubber binders after blending can improve the storage stability of the binders; however, the viscosity of the cured binders is higher than the ones that do not undergo curing. The rheological study of asphalt rubber binders has demonstrated that increasing the testing gap does not isolate the influence of the rubber particles in the parallel plate geometry. It also demonstrated that the use of concentric cylinders for asphalt rubber binders led to higher testing results than those obtained with parallel plate geometry. It has been proved that better rheological results are obtained when

the binders are centrifuged and only the liquid part is tested using parallel plate geometry. The main advantage of this method is that the acquisition of expensive equipment is not required. The centrifuge system necessary is very simple and economical when compared to retrofitting an existing rheometer with the concentric cylinder accessories or to getting a new rheometer. As result of this study, the next step is to elaborate and propose a standard practice on the centrifuging of asphalt rubber binders.

REFERENCES

Anderson, C., & Iowa. Highway Research Board. (1992a). Evaluation of recycled rubber in asphalt concrete, Black Hawk County / by Chris Anderson. Ames, Iowa: Office of Materials, Highway Division, Iowa Dept. of Transportation.

Anderson, C., & Iowa. Highway Division. (1992b). Evaluation of recycled rubber in asphalt concrete, Plymouth County construction report for Iowa Highway Research Board project HR-330A / Chris Anderson. Ames, Iowa: Iowa Dept. of Transportation, Highway Division.

Anderson, C., & Iowa. Highway Division. (1992c). Evaluation of recycled rubber in asphalt concrete, Dubuque County construction report for Iowa Highway Research Board project HR-330C / Chris Anderson. Ames, Iowa: Iowa Dept. of Transportation, Highway Division.

Anderson, C., & Iowa. Highway Division. (1993). Asphalt rubber cement concrete, Webster County construction report for Iowa Department of Transportation project HR-555 / by Chris Anderson. Ames, Iowa: Iowa Dept. of Transportation, Highway Division.

Baumgardner, G., & Anderson, D. (2008). Trans-polyoctenamer reactive polymer/recycled tire rubber modified asphalt: processing, compatibility and binder properties. Paper presented at the Proceedings: 5th international transport conference, Wuppertal, Germany.

Burns, B. (2000). Rubber-mod*ified asphalt paving binder*. EP 0994161 A2, filed Oct 13 1999, and issued Apr 19, 2000.

Burns, B. (2004). *Modification of rubberized asphalt with polyoctenamer*. Symposium, Cheyenne, June 23-25 Wyoming, 2004.

CEI (2008). CEI Enterprises [online] Available at: http://www.ceienterprises.com/downloads/cei_tankline.pdf [Accessed: 18 Nov 2015]

Caltrans. (2003). *Asphalt Rubber Usage Guide*. Caltrans, State of California Department of Transportation, Sacramento, California, USA.

Estakhri, C. K. et al (1992). *Use, Availability, and Cost-Effectiveness of Asphalt Rubber in Texas.* Transportation Research Record No. 1339, Transportation Research Board, Washington, DC, 1992.

Greene, J. et al. (2014). Evaluation and Implementation of PG 76-22 Asphalt Rubber Binder in Florida. FHWA (2008). *User Guidelines for Byproduct and Secondary Use Materials in Pavement Construction. FHWA-RD-97-148*. Washington, D.C. Federal Highway Administration.

Hamed, G.R. (1992). *"Materials and Compounds" Engineering with Rubber - How to Design Rubber Components (2nd edition)*, from Alan N. Gent, Hanser Publishers.

Heitzman, M. (1992). *State of the practice: design and construction of asphalt paving materials with crumb rubber modifier.* Publication No. FHWA-SA-92-022, US Dept. of Transportation, Federal Highway Administration

Hicks, R.G. (2002). *Asphalt Rubber Design and Construction Guidelines. Volume I – Design Guidelines*. Northern California Asphalt Concrete Technology Center. California Integrated Waste Management Board. January 2002

Isayev, A.I. (2005). *"Recycling of Rubbers"* Science and Technology of Rubber (3rd Edition). Elsevier.

Ng Puga, K.L.N. (2013). *Rheology and performance evaluation of Polyoctenamer as Asphalt Rubber modifier in Hot Mix Asphalt*. Ames: Digital Repository @ Iowa State University; 2013.

Peralta, J. et al. (2012). Mutual changes in bitumen and rubber related to the production of asphalt rubber binders. *Construction and Building Materials, 36*, 557-565. doi:http://dx.doi.org/10.1016/j.conbuildmat.2012.06.030

Putman, B. J., & Amirkhanian, S. N. (2006). *Crumb rubber modification of binders: interaction and particle effects.* In Proceedings of the Asphalt Rubber 2006 Conference (Vol. 3, pp. 655-677).

Rahman, M.M. (2004). *Characterization of Dry Process Crumb Rubber Modified Asphalt Mixtures.* School of Civil Engineering, University of Nottingham

Recycling Research Institute (2006). Rubber Recycling. Scrap Tire News. Recycling Research Institute. Leesburg, Virginia, USA

Reschner, K. (2006). *Scrap Tire Recycling – A summary of Prevalent Disposal and Recycling Methods.* Berlin, Germany. 2006

Roberts, F. et al (2009). *Hot mix asphalt materials, mixture design and construction.* Lanham, Md. Napa Educational Foundation

Rubberasphaltsolutions.com (2010) Rubber Asphalt Solutions LLC. [online] Available at: http://rubberasphaltsolutions.com/reference.htm [Accessed: 15 Feb 2013].

Unapumnuk, K. (2006). *A study of the pyrolysis of tire derived fuels and an analysis of derived chars and oils.* Department of Civil and Environmental Engineering, College of Engineering, Division of Research and Advanced Studies of the University of Cincinnati.

Way, G. B. (2011). Asphalt Rubber Standard Practice Guide. Rubber Pavements Association. Final Report October 17, 2011. First Edition.

APPENDIX A. STATISTICAL ANALYSIS OUTPUT OF VISCOSITIES

Summary of Fit

RSquare	0.999217
RSquare Adj	0.998245
Root Mean Square Error	0.043643
Mean of Response	-0.6588
Observations (or Sum Wgts)	288

Analysis of Variance

Source	DF	Sum of Squares	Mean Square	F Ratio
Model	159	311.15288	1.95694	1027.428
Error	128	0.24380	0.00190	Prob > F
C. Total	287	311.39668		<.0001*

Tests wrt Random Effects

Source	SS	MS Num	DF Num	F Ratio	Prob > F
Rubber Type	0.05249	0.05249	1	20.1453	<.0001*
Polyoctenamer	1.35406	1.35406	1	519.6964	<.0001*
Rubber Type*Polyoctenamer	0.78104	0.78104	1	299.7700	<.0001*
Curing	7.17734	7.17734	1	2754.714	<.0001*
Rubber Type*Curing	0.63533	0.63533	1	243.8454	<.0001*
Polyoctenamer*Curing	0.73658	0.73658	1	282.7029	<.0001*
Rubber Type*Polyoctenamer*Curing	0.85697	0.85697	1	328.9107	<.0001*
Centrifuging	173.637	173.637	1	66643.04	<.0001*
Rubber Type*Centrifuging	3.16233	3.16233	1	1213.724	<.0001*
Polyoctenamer*Centrifuging	0.9962	0.9962	1	382.3472	<.0001*
Rubber Type*Polyoctenamer*Centrifuging	0.70362	0.70362	1	270.0537	<.0001*
Curing*Centrifuging	0.82442	0.82442	1	316.4190	<.0001*
Rubber Type*Curing*Centrifuging	0.51144	0.51144	1	196.2950	<.0001*
Polyoctenamer*Curing*Centrifuging	0.3517	0.3517	1	134.9868	<.0001*
Rubber Type*Polyoctenamer*Curing*Centrifuging	0.69661	0.69661	1	267.3651	<.0001*
Aging	7.14337	7.14337	1	2741.679	<.0001*
Rubber Type*Aging	0.02135	0.02135	1	8.1938	0.0057*
Polyoctenamer*Aging	0.04724	0.04724	1	18.1327	<.0001*
Rubber Type*Polyoctenamer*Aging	0.0254	0.0254	1	9.7482	0.0027*
Curing*Aging	0.17681	0.17681	1	67.8623	<.0001*
Rubber Type*Curing*Aging	0.02899	0.02899	1	11.1247	0.0014*
Polyoctenamer*Curing*Aging	0.01156	0.01156	1	4.4374	0.0391*
Rubber Type*Polyoctenamer*Curing*Aging	0.01834	0.01834	1	7.0391	0.0100*
Centrifuging*Aging	0.19461	0.19461	1	74.6921	<.0001*
Rubber Type*Centrifuging*Aging	0.03548	0.03548	1	13.6182	0.0005*
Polyoctenamer*Centrifuging*Aging	0.17518	0.17518	1	67.2371	<.0001*
Rubber Type*Polyoctenamer*Centrifuging*Aging	0.0397	0.0397	1	15.2355	0.0002*
Curing*Centrifuging*Aging	0.28435	0.28435	1	109.1338	<.0001*
Rubber Type*Curing*Centrifuging*Aging	0.01093	0.01093	1	4.1940	0.0447*
Polyoctenamer*Curing*Centrifuging*Aging	0.00455	0.00455	1	1.7462	0.1911
Rubber Type*Polyoctenamer*Curing*Centrifuging*Aging	0.00042	0.00042	1	0.1617	0.6889
Temperature	107.433	53.7163	2	28202.07	<.0001*
Rubber Type*Temperature	0.35515	0.17758	2	93.2302	<.0001*
Polyoctenamer*Temperature	0.03499	0.01749	2	9.1851	0.0002*
Rubber Type*Polyoctenamer*Temperature	0.04465	0.02233	2	11.7220	<.0001*
Curing*Temperature	0.0517	0.02585	2	13.5713	<.0001*
Rubber Type*Curing*Temperature	0.03143	0.01572	2	8.2510	0.0004*
Polyoctenamer*Curing*Temperature	0.01844	0.00922	2	4.8417	0.0094*
Rubber Type*Polyoctenamer*Curing*Temperature	0.00691	0.00345	2	1.8127	0.1674
Centrifuging*Temperature	0.29003	0.14501	2	76.1350	<.0001*
Rubber Type*Centrifuging*Temperature	0.6725	0.33625	2	176.5381	<.0001*
Polyoctenamer*Centrifuging*Temperature	0.04935	0.02468	2	12.9559	<.0001*
Rubber Type*Polyoctenamer*Centrifuging*Temperature	0.01215	0.00608	2	3.1895	0.0445*
Curing*Centrifuging*Temperature	0.27176	0.13588	2	71.3393	<.0001*
Rubber Type*Curing*Centrifuging*Temperature	0.00236	0.00118	2	0.6205	0.5393
Polyoctenamer*Curing*Centrifuging*Temperature	0.00596	0.00298	2	1.5650	0.2131
Rubber Type*Polyoctenamer*Curing*Centrifuging*Temperature	0.04141	0.02071	2	10.8718	<.0001*
Aging*Temperature	0.55574	0.27787	2	145.8871	<.0001*
Rubber Type*Aging*Temperature	0.16808	0.08404	2	44.1230	<.0001*

Source	SS	MS Num	DF Num	F Ratio	Prob > F
Polyoctenamer*Aging*Temperature	0.05078	0.02539	2	13.3307	<.0001*
Rubber Type*Polyoctenamer*Aging*Temperature	0.00162	0.00081	2	0.4246	0.6550
Curing*Aging*Temperature	0.04143	0.02072	2	10.8769	<.0001*
Rubber Type*Curing*Aging*Temperature	0.00599	0.00299	2	1.5721	0.2116
Polyoctenamer*Curing*Aging*Temperature	0.00133	0.00067	2	0.3496	0.7056
Rubber Type*Polyoctenamer*Curing*Aging*Temperature	0.05239	0.02619	2	13.7521	<.0001*
Centrifuging*Aging*Temperature	0.0522	0.0261	2	13.7024	<.0001*
Rubber Type*Centrifuging*Aging*Temperature	0.00822	0.00411	2	2.1589	0.1196
Polyoctenamer*Centrifuging*Aging*Temperature	0.00397	0.00199	2	1.0432	0.3553
Rubber Type*Polyoctenamer*Centrifuging*Aging*Temperature	0.00372	0.00186	2	0.9753	0.3799
Curing*Centrifuging*Aging*Temperature	0.0042	0.0021	2	1.1036	0.3348
Rubber Type*Curing*Centrifuging*Aging*Temperature	0.01513	0.00756	2	3.9715	0.0212*
Polyoctenamer*Curing*Centrifuging*Aging*Temperature	0.00084	0.00042	2	0.2214	0.8017
Rubber Type*Polyoctenamer*Curing*Centrifuging*Aging*Temperature	0.00398	0.00199	2	1.0442	0.3549
Tube[Rubber Type,Polyoctenamer,Curing,Centrifuging,Aging]&Random	0.16675	0.00261	64	1.3679	0.0681

Residual by predicted plot

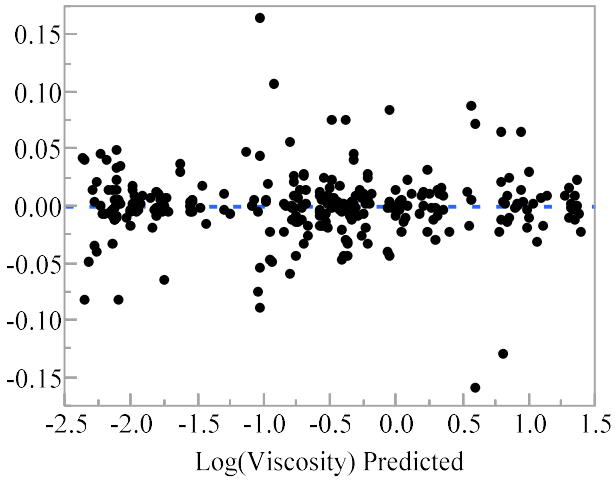

Effect Details

Rubber Type

Effect Test

Sum of Squares	F Ratio	DF	Prob > F
0.05248805	20.1453	1	<.0001*

Denominator MS Synthesis:
Tube[Rubber Type,Polyoctenamer,Curing,Centrifuging,Aging]&Random

Least Squares Means Table

Level	Least Sq Mean	Std Error	Mean
Ambient	-0.6453014	0.00425365	-0.64530
Cryogenic	-0.6723015	0.00425365	-0.67230

LS Means Plot

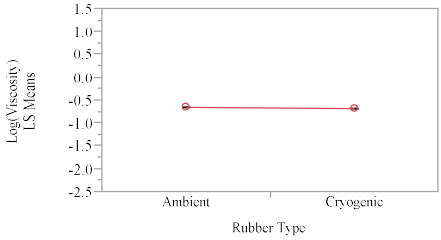

Polyoctenamer

Effect Test

Sum of Squares	F Ratio	DF	Prob > F
1.3540554	519.6964	1	<.0001*

Denominator MS Synthesis:
Tube[Rubber Type,Polyoctenamer,Curing,Centrifuging,Aging]&Random

Least Squares Means Table

Level	Least Sq Mean	Std Error	Mean
0	-0.7273695	0.00425365	-0.72737
4.5	-0.5902334	0.00425365	-0.59023

LS Means Plot

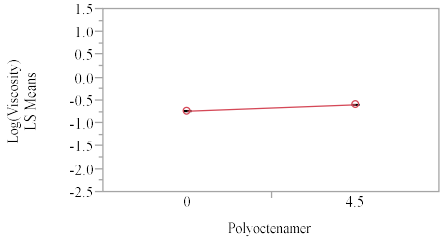

Rubber Type*Polyoctenamer

Effect Test

Sum of Squares	F Ratio	DF	Prob > F
0.78104297	299.7700	1	<.0001*

Denominator MS Synthesis:
Tube[Rubber Type,Polyoctenamer,Curing,Centrifuging,Aging]&Random

Least Squares Means Table

Level	Least Sq Mean	Std Error
Ambient,0	-0.6617931	0.00601557
Ambient,4.5	-0.6288098	0.00601557
Cryogenic,0	-0.7929460	0.00601557
Cryogenic,4.5	-0.5516569	0.00601557

LS Means Plot

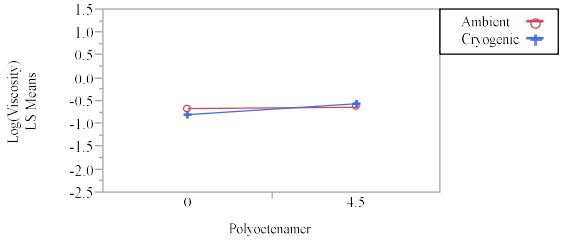

Curing

Effect Test

Sum of Squares	F Ratio	DF	Prob > F
7.1773359	2754.714	1	<.0001*

Denominator MS Synthesis:
Tube[Rubber Type,Polyoctenamer,Curing,Centrifuging,Aging]&Random

Least Squares Means Table

Level	Least Sq Mean	Std Error	Mean
None	-0.8166663	0.00425365	-0.81667
72 hrs	-0.5009366	0.00425365	-0.50094

LS Means Plot

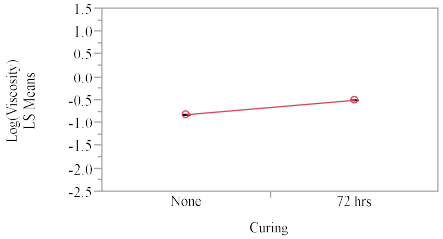

Rubber Type*Curing
Effect Test

Sum of Squares	F Ratio	DF	Prob > F
0.63533287	243.8454	1	<.0001*

Denominator MS Synthesis:
Tube[Rubber Type,Polyoctenamer,Curing,Centrifuging,Aging]&Random

Least Squares Means Table

Level	Least Sq Mean	Std Error
Ambient,None	-0.7561980	0.00601557
Ambient,72 hrs	-0.5344049	0.00601557
Cryogenic,None	-0.8771345	0.00601557
Cryogenic,72 hrs	-0.4674684	0.00601557

LS Means Plot

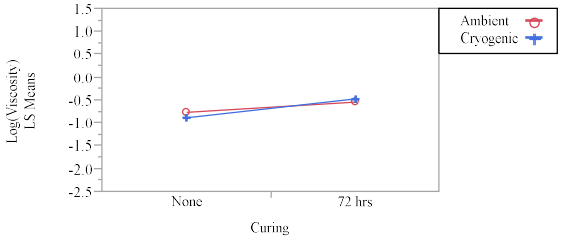

Polyoctenamer*Curing
Effect Test

Sum of Squares	F Ratio	DF	Prob > F
0.73657503	282.7029	1	<.0001*

Denominator MS Synthesis:
Tube[Rubber Type,Polyoctenamer,Curing,Centrifuging,Aging]&Random

Least Squares Means Table

Level	Least Sq Mean	Std Error
0,None	-0.8346621	0.00601557
0,72 hrs	-0.6200769	0.00601557
4.5,None	-0.7986704	0.00601557
4.5,72 hrs	-0.3817963	0.00601557

LS Means Plot

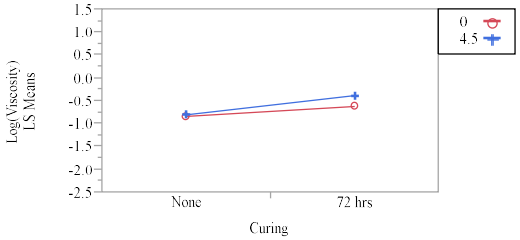

Rubber Type*Polyoctenamer*Curing
Effect Test

Sum of Squares	F Ratio	DF	Prob > F
0.85696832	328.9107	1	<.0001*

Denominator MS Synthesis:
Tube[Rubber Type,Polyoctenamer,Curing,Centrifuging,Aging]&Random

Least Squares Means Table

Level	Least Sq Mean	Std Error
Ambient,0,None	-0.7766663	0.00850731
Ambient,0,72 hrs	-0.5469198	0.00850731
Ambient,4.5,None	-0.7357297	0.00850731
Ambient,4.5,72 hrs	-0.5218899	0.00850731
Cryogenic,0,None	-0.8926579	0.00850731
Cryogenic,0,72 hrs	-0.6932340	0.00850731
Cryogenic,4.5,None	-0.8616112	0.00850731
Cryogenic,4.5,72 hrs	-0.2417027	0.00850731

LS Means Plot

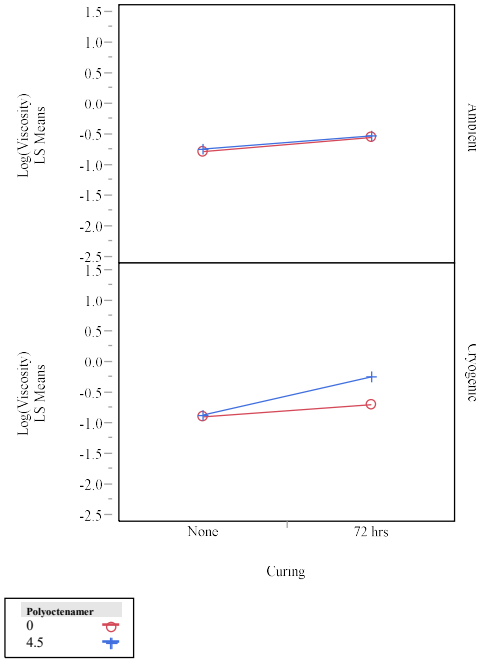

Centrifuging
Effect Test

Sum of Squares	F Ratio	DF	Prob > F
173.63671	66643.04	1	<.0001*

Denominator MS Synthesis:
Tube[Rubber Type,Polyoctenamer,Curing,Centrifuging,Aging]&Random

Least Squares Means Table

Level	Least Sq Mean	Std Error	Mean
Non-centrifuged	0.117668	0.00425365	0.1177
Centrifuged	-1.435271	0.00425365	-1.4353

LS Means Plot

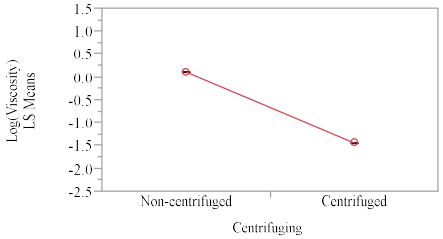

Rubber Type*Centrifuging
Effect Test

Sum of Squares	F Ratio	DF	Prob > F
3.1623269	1213.724	1	<.0001*

Denominator MS Synthesis:
Tube[Rubber Type,Polyoctenamer,Curing,Centrifuging,Aging]&Random

Least Squares Means Table

Level	Least Sq Mean	Std Error
Ambient,Non-centrifuged	0.235955	0.00601557
Ambient,Centrifuged	-1.526558	0.00601557
Cryogenic,Non-centrifuged	-0.000619	0.00601557
Cryogenic,Centrifuged	-1.343984	0.00601557

LS Means Plot

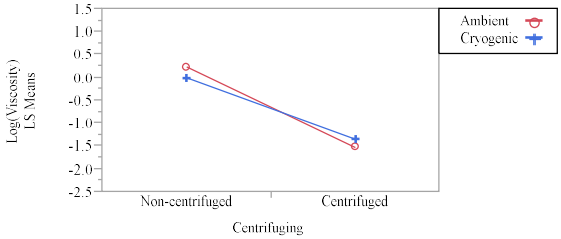

Polyoctenamer*Centrifuging
Effect Test

Sum of Squares	F Ratio	DF	Prob > F
0.99619573	382.3472	1	<.0001*

Denominator MS Synthesis:
Tube[Rubber Type,Polyoctenamer,Curing,Centrifuging,Aging]&Random

Least Squares Means Table

Level	Least Sq Mean	Std Error
0,Non-centrifuged	0.107914	0.00601557
0,Centrifuged	-1.562653	0.00601557
4.5,Non-centrifuged	0.127423	0.00601557
4.5,Centrifuged	-1.307890	0.00601557

LS Means Plot

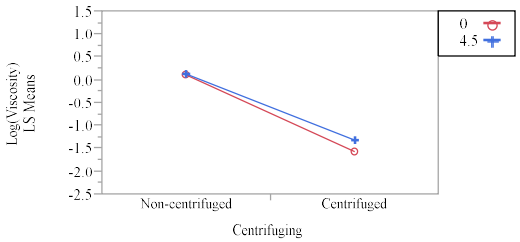

Rubber Type*Polyoctenamer*Centrifuging
Effect Test

Sum of Squares	F Ratio	DF	Prob > F
0.70361801	270.0537	1	<.0001*

Denominator MS Synthesis:
Tube[Rubber Type,Polyoctenamer,Curing,Centrifuging,Aging]&Random

Least Squares Means Table

Level	Least Sq Mean	Std Error
Ambient,0,Non-centrifuged	0.228849	0.00850731
Ambient,0,Centrifuged	-1.552435	0.00850731
Ambient,4.5,Non-centrifuged	0.243061	0.00850731
Ambient,4.5,Centrifuged	-1.500681	0.00850731
Cryogenic,0,Non-centrifuged	-0.013022	0.00850731
Cryogenic,0,Centrifuged	-1.572870	0.00850731
Cryogenic,4.5,Non-centrifuged	0.011785	0.00850731
Cryogenic,4.5,Centrifuged	-1.115098	0.00850731

LS Means Plot

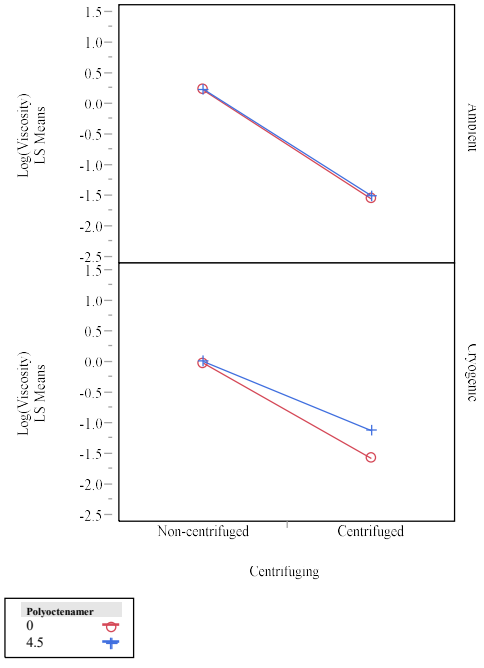

Curing*Centrifuging
Effect Test

Sum of Squares	F Ratio	DF	Prob > F
0.82442147	316.4190	1	<.0001*

Denominator MS Synthesis:
Tube[Rubber Type,Polyoctenamer,Curing,Centrifuging,Aging]&Random

Least Squares Means Table

Level	Least Sq Mean	Std Error
None,Non-centrifuged	0.013306	0.00601557
None,Centrifuged	-1.646639	0.00601557
72 hrs,Non-centrifuged	0.222030	0.00601557
72 hrs,Centrifuged	-1.223903	0.00601557

LS Means Plot

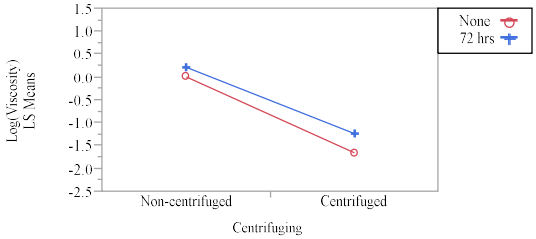

Rubber Type*Curing*Centrifuging
Effect Test

Sum of Squares	F Ratio	DF	Prob > F
0.51144153	196.2950	1	<.0001*

Denominator MS Synthesis:
Tube[Rubber Type,Polyoctenamer,Curing,Centrifuging,Aging]&Random

Least Squares Means Table

Level	Least Sq Mean	Std Error
Ambient,None,Non-centrifuged	0.136421	0.00850731
Ambient,None,Centrifuged	-1.648817	0.00850731
Ambient,72 hrs,Non-centrifuged	0.335489	0.00850731
Ambient,72 hrs,Centrifuged	-1.404299	0.00850731
Cryogenic,None,Non-centrifuged	-0.109808	0.00850731
Cryogenic,None,Centrifuged	-1.644461	0.00850731
Cryogenic,72 hrs,Non-centrifuged	0.108571	0.00850731
Cryogenic,72 hrs,Centrifuged	-1.043507	0.00850731

LS Means Plot

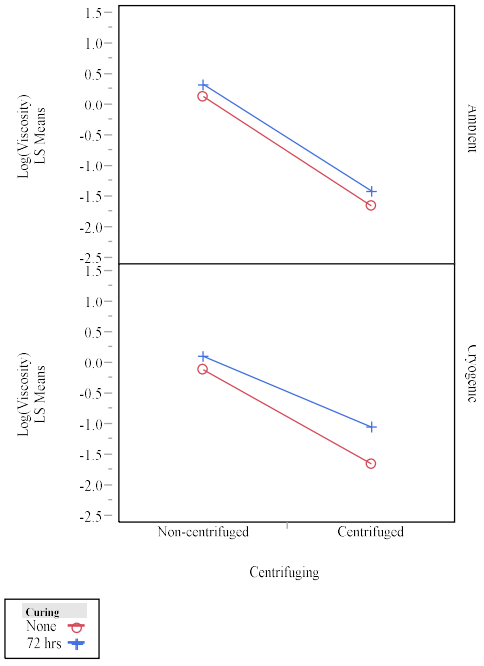

Polyoctenamer*Curing*Centrifuging
Effect Test

Sum of Squares	F Ratio	DF	Prob > F
0.35170468	134.9868	1	<.0001*

Denominator MS Synthesis:
Tube[Rubber Type,Polyoctenamer,Curing,Centrifuging,Aging]&Random

Least Squares Means Table

Level	Least Sq Mean	Std Error
0,None,Non-centrifuged	0.019178	0.00850731
0,None,Centrifuged	-1.688503	0.00850731
0,72 hrs,Non-centrifuged	0.196649	0.00850731
0,72 hrs,Centrifuged	-1.436803	0.00850731
4.5,None,Non-centrifuged	0.007435	0.00850731
4.5,None,Centrifuged	-1.604775	0.00850731
4.5,72 hrs,Non-centrifuged	0.247411	0.00850731
4.5,72 hrs,Centrifuged	-1.011004	0.00850731

LS Means Plot

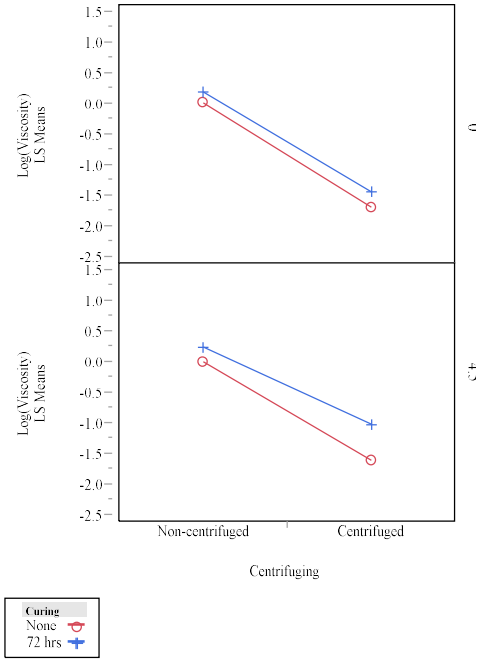

Rubber Type*Polyoctenamer*Curing*Centrifuging Effect Test

Sum of Squares	F Ratio	DF	Prob > F
0.69661271	267.3651	1	<.0001*

Denominator MS Synthesis:
Tube[Rubber Type,Polyoctenamer,Curing,Centrifuging,Aging]&Random

LS Means Plot

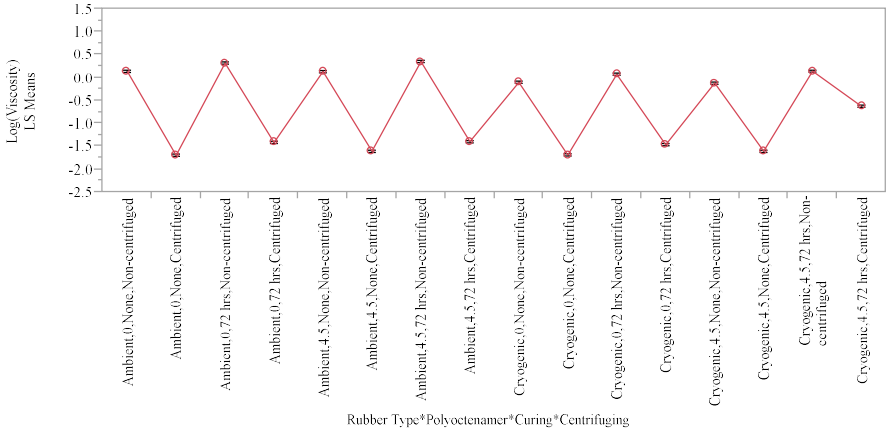

Aging

Effect Test

Sum of Squares	F Ratio	DF	Prob > F
7.1433731	2741.679	1	<.0001*

Denominator MS Synthesis:
Tube[Rubber Type,Polyoctenamer,Curing,Centrifuging,Aging]&Random

Least Squares Means Table

Level	Least Sq Mean	Std Error	Mean
Unaged	-0.8162923	0.00425365	-0.81629
RTFOaged	-0.5013106	0.00425365	-0.50131

LS Means Plot

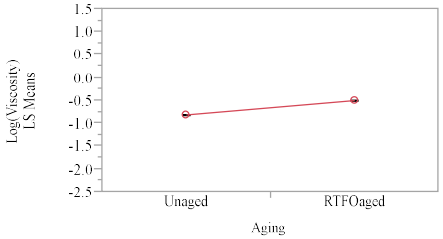

Rubber Type*Aging

Effect Test

Sum of Squares	F Ratio	DF	Prob > F
0.02134864	8.1938	1	0.0057*

Denominator MS Synthesis:
Tube[Rubber Type,Polyoctenamer,Curing,Centrifuging,Aging]&Random

Least Squares Means Table

Level	Least Sq Mean	Std Error
Ambient,Unaged	-0.8114020	0.00601557
Ambient,RTFOaged	-0.4792008	0.00601557
Cryogenic,Unaged	-0.8211826	0.00601557
Cryogenic,RTFOaged	-0.5234203	0.00601557

LS Means Plot

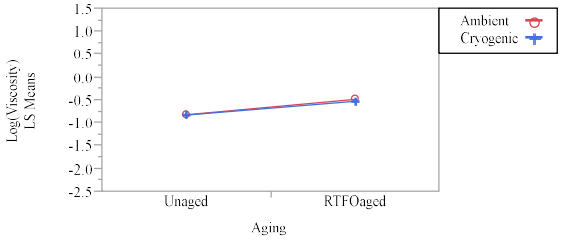

Polyoctenamer*Aging
Effect Test

Sum of Squares	F Ratio	DF	Prob > F
0.04724420	18.1327	1	<.0001*

Denominator MS Synthesis:
Tube[Rubber Type,Polyoctenamer,Curing,Centrifuging,Aging]&Random

Least Squares Means Table

Level	Least Sq Mean	Std Error
0,Unaged	-0.8976683	0.00601557
0,RTFOaged	-0.5570707	0.00601557
4.5,Unaged	-0.7349164	0.00601557
4.5,RTFOaged	-0.4455504	0.00601557

LS Means Plot

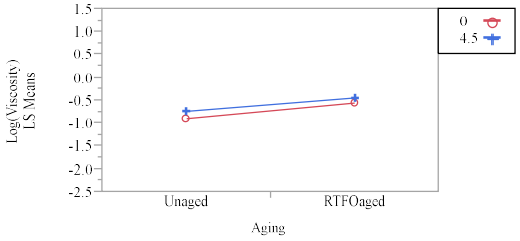

Rubber Type*Polyoctenamer*Aging
Effect Test

Sum of Squares	F Ratio	DF	Prob > F
0.02539862	9.7482	1	0.0027*

Denominator MS Synthesis:
Tube[Rubber Type,Polyoctenamer,Curing,Centrifuging,Aging]&Random

Least Squares Means Table

Level	Least Sq Mean	Std Error
Ambient,0,Unaged	-0.8500925	0.00850731
Ambient,0,RTFOaged	-0.4734936	0.00850731
Ambient,4.5,Unaged	-0.7727116	0.00850731
Ambient,4.5,RTFOaged	-0.4849080	0.00850731
Cryogenic,0,Unaged	-0.9452441	0.00850731
Cryogenic,0,RTFOaged	-0.6406478	0.00850731
Cryogenic,4.5,Unaged	-0.6971211	0.00850731
Cryogenic,4.5,RTFOaged	-0.4061927	0.00850731

LS Means Plot

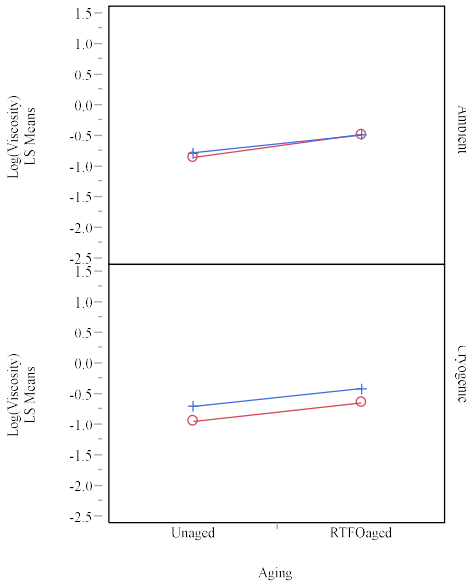

Curing*Aging
Effect Test

Sum of Squares	F Ratio	DF	Prob > F
0.17681344	67.8623	1	<.0001*

Denominator MS Synthesis:
Tube[Rubber Type,Polyoctenamer,Curing,Centrifuging,Aging]&Random

Least Squares Means Table

Level	Least Sq Mean	Std Error
None,Unaged	-0.9989349	0.00601557
None,RTFOaged	-0.6343977	0.00601557
72 hrs,Unaged	-0.6336498	0.00601557
72 hrs,RTFOaged	-0.3682235	0.00601557

LS Means Plot

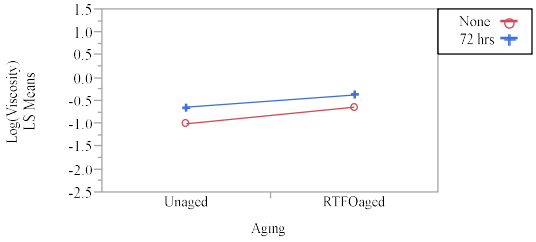

Rubber Type*Curing*Aging
Effect Test

Sum of Squares	F Ratio	DF	Prob > F
0.02898524	11.1247	1	0.0014*

Denominator MS Synthesis:
Tube[Rubber Type,Polyoctenamer,Curing,Centrifuging,Aging]&Random

Least Squares Means Table

Level	Least Sq Mean	Std Error
Ambient,None,Unaged	-0.957108	0.00850731

Level	Least Sq Mean	Std Error
Ambient,None,RTFOaged	-0.555288	0.00850731
Ambient,72 hrs,Unaged	-0.665696	0.00850731
Ambient,72 hrs,RTFOaged	-0.403114	0.00850731
Cryogenic,None,Unaged	-1.040761	0.00850731
Cryogenic,None,RTFOaged	-0.713508	0.00850731
Cryogenic,72 hrs,Unaged	-0.601604	0.00850731
Cryogenic,72 hrs,RTFOaged	-0.333333	0.00850731

LS Means Plot

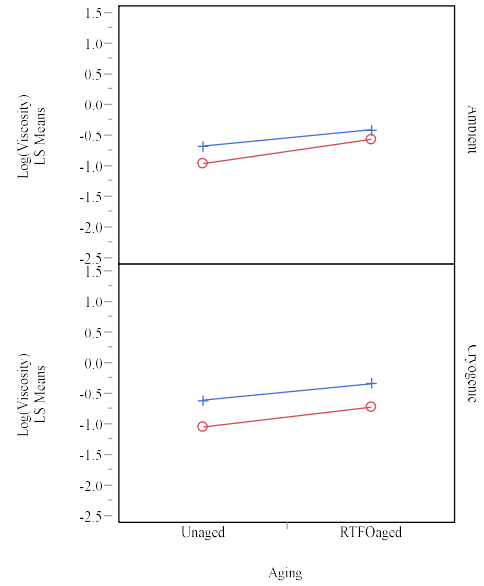

Polyoctenamer*Curing*Aging
Effect Test

Sum of Squares	F Ratio	DF	Prob > F
0.01156146	4.4374	1	0.0391*

Denominator MS Synthesis:
Tube[Rubber Type,Polyoctenamer,Curing,Centrifuging,Aging]&Random

Least Squares Means Table

Level	Least Sq Mean	Std Error
0,None,Unaged	-1.036075	0.00850731
0,None,RTFOaged	-0.633250	0.00850731
0,72 hrs,Unaged	-0.759262	0.00850731
0,72 hrs,RTFOaged	-0.480892	0.00850731
4.5,None,Unaged	-0.961795	0.00850731
4.5,None,RTFOaged	-0.635546	0.00850731
4.5,72 hrs,Unaged	-0.508037	0.00850731
4.5,72 hrs,RTFOaged	-0.255555	0.00850731

LS Means Plot

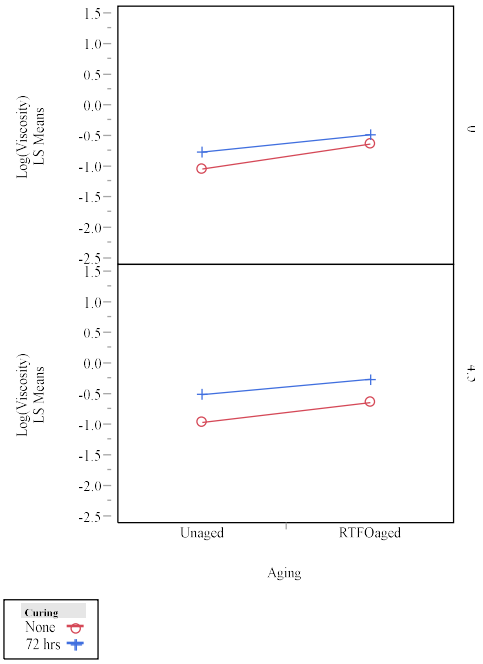

Rubber Type*Polyoctenamer*Curing*Aging
Effect Test

Sum of Squares	F Ratio	DF	Prob > F
0.01834031	7.0391	1	0.0100*

Denominator MS Synthesis:
Tube[Rubber Type,Polyoctenamer,Curing,Centrifuging,Aging]&Random

LS Means Plot

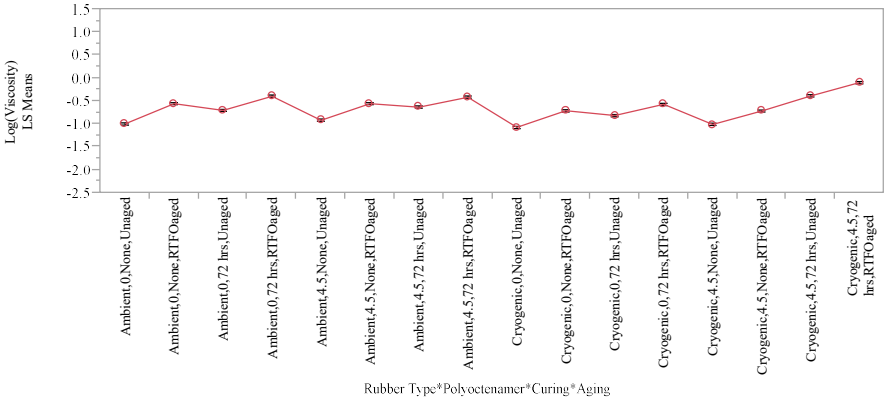

Centrifuging*Aging
Effect Test

Sum of Squares	F Ratio	DF	Prob > F
0.19460843	74.6921	1	<.0001*

Denominator MS Synthesis:
Tube[Rubber Type,Polyoctenamer,Curing,Centrifuging,Aging]&Random

Least Squares Means Table

Level	Least Sq Mean	Std Error
Non-centrifuged,Unaged	-0.065817	0.00601557
Non-centrifuged,RTFOaged	0.301154	0.00601557
Centrifuged,Unaged	-1.566767	0.00601557
Centrifuged,RTFOaged	-1.303775	0.00601557

LS Means Plot

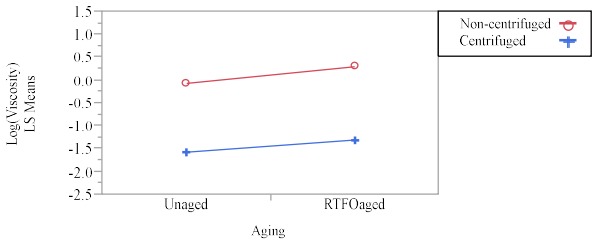

Rubber Type*Centrifuging*Aging Effect Test

Sum of Squares	F Ratio	DF	Prob > F
0.03548197	13.6182	1	0.0005*

Denominator MS Synthesis:
Tube[Rubber Type,Polyoctenamer,Curing,Centrifuging,Aging]&Random

Least Squares Means Table

Level	Least Sq Mean	Std Error
Ambient,Non-centrifuged,Unaged	0.032760	0.00850731
Ambient,Non-centrifuged,RTFOaged	0.439150	0.00850731
Ambient,Centrifuged,Unaged	-1.655564	0.00850731
Ambient,Centrifuged,RTFOaged	-1.397552	0.00850731
Cryogenic,Non-centrifuged,Unaged	-0.164395	0.00850731
Cryogenic,Non-centrifuged,RTFOaged	0.163158	0.00850731
Cryogenic,Centrifuged,Unaged	-1.477970	0.00850731
Cryogenic,Centrifuged,RTFOaged	-1.209998	0.00850731

LS Means Plot

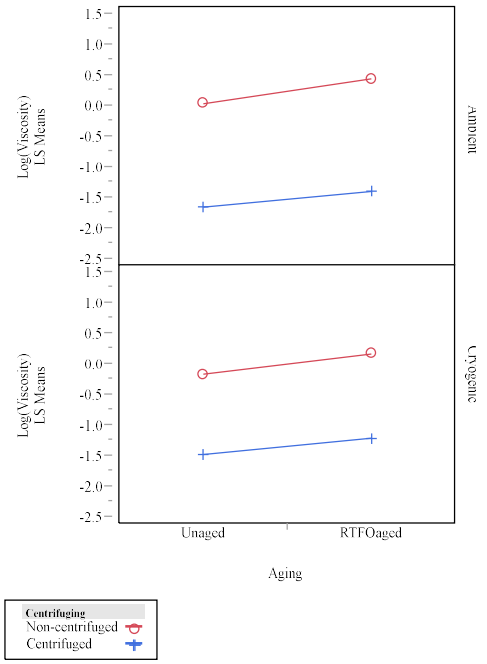

Polyoctenamer*Centrifuging*Aging
Effect Test

Sum of Squares	F Ratio	DF	Prob > F
0.17518445	67.2371	1	<.0001*

Denominator MS Synthesis:
Tube[Rubber Type,Polyoctenamer,Curing,Centrifuging,Aging]&Random

Least Squares Means Table

Level	Least Sq Mean	Std Error
0,Non-centrifuged,Unaged	-0.113043	0.00850731
0,Non-centrifuged,RTFOaged	0.328870	0.00850731
0,Centrifuged,Unaged	-1.682293	0.00850731
0,Centrifuged,RTFOaged	-1.443012	0.00850731
4.5,Non-centrifuged,Unaged	-0.018591	0.00850731
4.5,Non-centrifuged,RTFOaged	0.273437	0.00850731
4.5,Centrifuged,Unaged	-1.451241	0.00850731
4.5,Centrifuged,RTFOaged	-1.164538	0.00850731

LS Means Plot

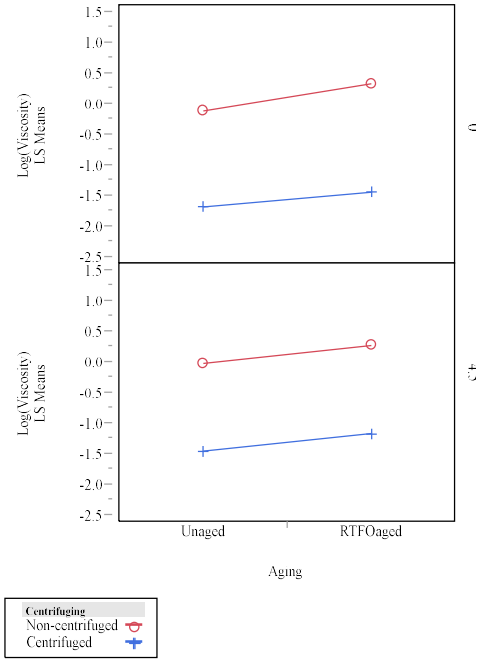

Rubber Type*Polyoctenamer*Centrifuging*Aging
Effect Test

Sum of Squares	F Ratio	DF	Prob > F
0.03969560	15.2355	1	0.0002*

Denominator MS Synthesis:
Tube[Rubber Type,Polyoctenamer,Curing,Centrifuging,Aging]&Random

LS Means Plot

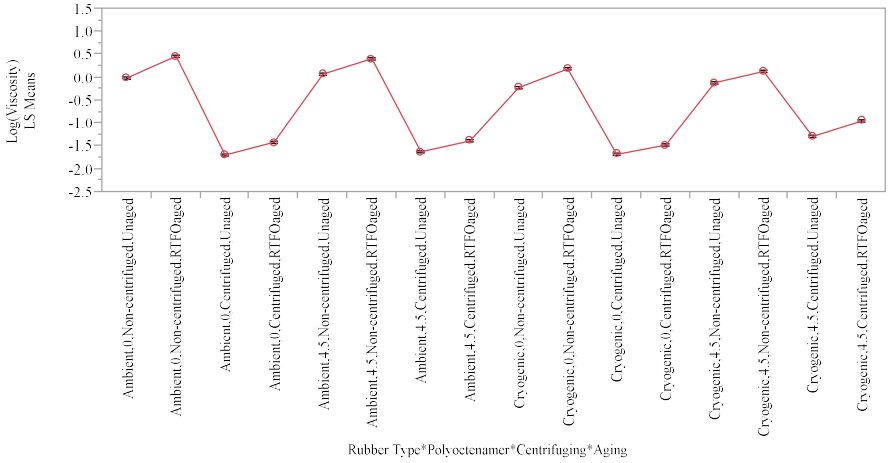

Curing*Centrifuging*Aging
Effect Test

Sum of Squares	F Ratio	DF	Prob > F
0.28434523	109.1338	1	<.0001*

Denominator MS Synthesis:
Tube[Rubber Type,Polyoctenamer,Curing,Centrifuging,Aging]&Random

Least Squares Means Table

Level	Least Sq Mean	Std Error
None,Non-centrifuged,Unaged	-0.226378	0.00850731
None,Non-centrifuged,RTFOaged	0.252991	0.00850731
None,Centrifuged,Unaged	-1.771491	0.00850731
None,Centrifuged,RTFOaged	-1.521787	0.00850731
72 hrs,Non-centrifuged,Unaged	0.094744	0.00850731
72 hrs,Non-centrifuged,RTFOaged	0.349316	0.00850731
72 hrs,Centrifuged,Unaged	-1.362043	0.00850731
72 hrs,Centrifuged,RTFOaged	-1.085763	0.00850731

LS Means Plot

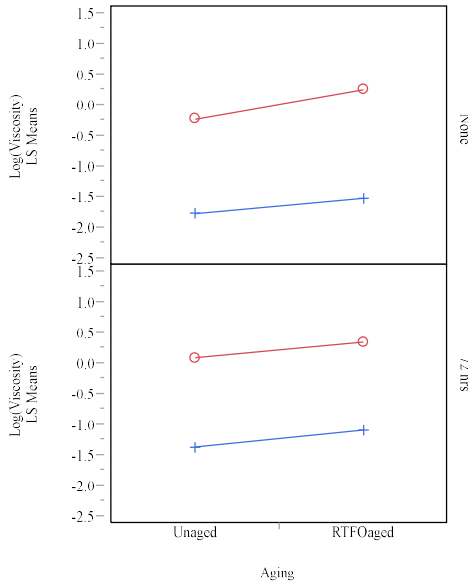

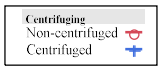

Rubber Type*Curing*Centrifuging*Aging
Effect Test

Sum of Squares	F Ratio	DF	Prob > F
0.01092735	4.1940	1	0.0447*

Denominator MS Synthesis:
Tube[Rubber Type,Polyoctenamer,Curing,Centrifuging,Aging]&Random

LS Means Plot

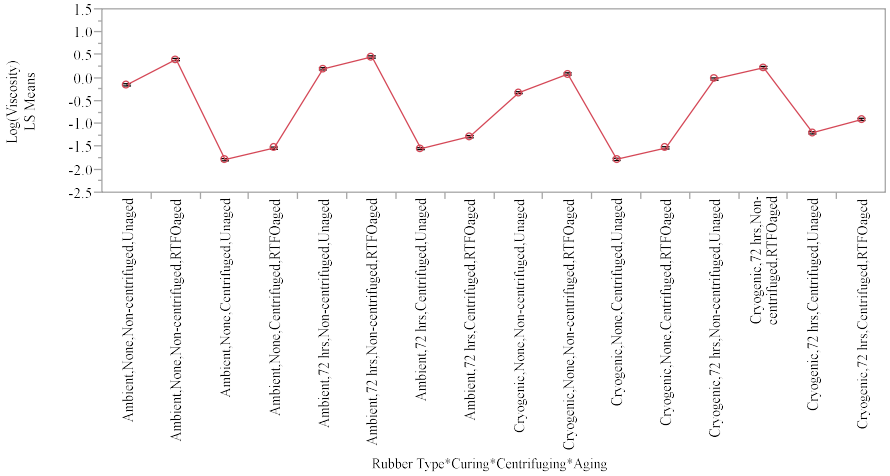

Temperature
Effect Test

Sum of Squares	F Ratio	DF	Prob > F
107.43258	28202.07	2	<.0001*

Denominator MS Synthesis:
Residual

Least Squares Means Table

Level	Least Sq Mean	Std Error	Mean
135	0.176985	0.00445427	0.1770
165	-0.887909	0.00445427	-0.8879
180	-1.265481	0.00445427	-1.2655

LS Means Plot

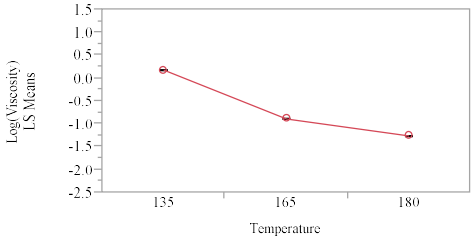

Rubber Type*Temperature
Effect Test

Sum of Squares	F Ratio	DF	Prob > F
0.35515005	93.2302	2	<.0001*

Denominator MS Synthesis: Residual

Least Squares Means Table

Level	Least Sq Mean	Std Error
Ambient,135	0.232589	0.00629929
Ambient,165	-0.872652	0.00629929
Ambient,180	-1.295841	0.00629929
Cryogenic,135	0.121382	0.00629929
Cryogenic,165	-0.903166	0.00629929
Cryogenic,180	-1.235121	0.00629929

LS Means Plot

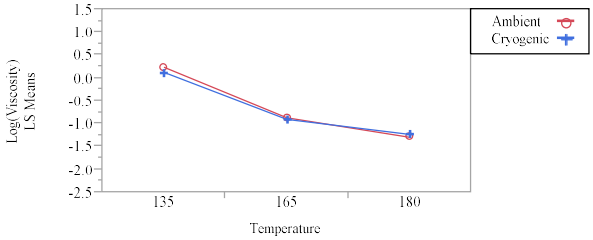

LSMeans Differences Tukey HSD

α=
0.050 Q=
2.89336
LSMean[i] By LSMean[j]

Mean[i]-Mean[j] Std Err Dif Lower CL Dif Upper CL Dif	Ambient,135	Ambient,165	Ambient,180	Cryogenic,135	Cryogenic,165	Cryogenic,180
Ambient,135	0 0 0 0	1.10524 0.00891 1.07947 1.13102	1.52843 0.00891 1.50265 1.5542	0.11121 0.00891 0.08543 0.13698	1.13575 0.00891 1.10998 1.16153	1.46771 0.00891 1.44193 1.49348
Ambient,165	-1.1052 0.00891 -1.131 -1.0795	0 0 0 0	0.42319 0.00891 0.39741 0.44896	-0.994 0.00891 -1.0198 -0.9683	0.03051 0.00891 0.00474 0.05629	0.36247 0.00891 0.33669 0.38824
Ambient,180	-1.5284 0.00891 -1.5542 -1.5027	-0.4232 0.00891 -0.449 -0.3974	0 0 0 0	-1.4172 0.00891 -1.443 -1.3914	-0.3927 0.00891 -0.4185 -0.3669	-0.0607 0.00891 -0.0865 -0.0349
Cryogenic,135	-0.1112 0.00891 -0.137 -0.0854	0.99403 0.00891 0.96826 1.01981	1.41722 0.00891 1.39145 1.443	0 0 0 0	1.02455 0.00891 0.99877 1.05032	1.3565 0.00891 1.33073 1.38228
Cryogenic,165	-1.1358 0.00891 -1.1615 -1.11	-0.0305 0.00891 -0.0563 -0.0047	0.39267 0.00891 0.3669 0.41845	-1.0245 0.00891 -1.0503 -0.9988	0 0 0 0	0.33195 0.00891 0.30618 0.35773
Cryogenic,180	-1.4677 0.00891 -1.4935 -1.4419	-0.3625 0.00891 -0.3882 -0.3367	0.06072 0.00891 0.03494 0.0865	-1.3565 0.00891 -1.3823 -1.3307	-0.332 0.00891 -0.3577 -0.3062	0 0 0 0

Level						Least Sq Mean
Ambient,135	A					0.232589
Cryogenic,135		B				0.121382
Ambient,165			C			-0.872652
Cryogenic,165				D		-0.903166
Cryogenic,180					E	-1.235121
Ambient,180						F	-1.295841

Levels not connected by same letter are significantly different.

Polyoctenamer*Temperature
Effect Test

Sum of Squares	F Ratio	DF	Prob > F
0.03498957	9.1851	2	0.0002*

Denominator MS Synthesis:
Residual

Least Squares Means Table

Level	Least Sq Mean	Std Error
0,135	0.093633	0.00629929
0,165	-0.953363	0.00629929
0,180	-1.322378	0.00629929
4.5,135	0.260338	0.00629929
4.5,165	-0.822455	0.00629929
4.5,180	-1.208583	0.00629929

LS Means Plot

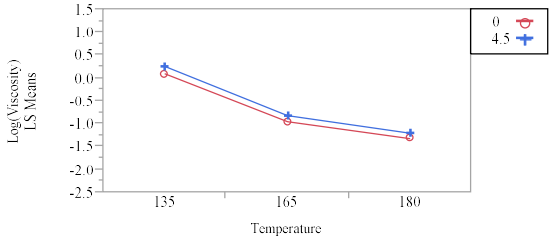

LSMeans Differences Tukey HSD

α=
0.050 Q=
2.89336
LSMean[i] By LSMean[j]

Mean[i]-Mean[j] Std Err Dif Lower CL Dif Upper CL Dif	0,135	0,165	0,180	4.5,135	4.5,165	4.5,180
0,135	0	1.047	1.41601	-0.1667	0.91609	1.30222
	0	0.00891	0.00891	0.00891	0.00891	0.00891
	0	1.02122	1.39024	-0.1925	0.89031	1.27644
	0	1.07277	1.44179	-0.1409	0.94186	1.32799
0,165	-1.047	0	0.36902	-1.2137	-0.1309	0.25522
	0.00891	0	0.00891	0.00891	0.00891	0.00891
	-1.0728	0	0.34324	-1.2395	-0.1567	0.22944
	-1.0212	0	0.39479	-1.1879	-0.1051	0.281
0,180	-1.416	-0.369	0	-1.5827	-0.4999	-0.1138
	0.00891	0.00891	0	0.00891	0.00891	0.00891
	-1.4418	-0.3948	0	-1.6085	-0.5257	-0.1396
	-1.3902	-0.3432	0	-1.5569	-0.4741	-0.088
4.5,135	0.1667	1.2137	1.58272	0	1.08279	1.46892
	0.00891	0.00891	0.00891	0	0.00891	0.00891
	0.14093	1.18793	1.55694	0	1.05702	1.44315
	0.19248	1.23948	1.60849	0	1.10857	1.4947
4.5,165	-0.9161	0.13091	0.49992	-1.0828	0	0.38613
	0.00891	0.00891	0.00891	0.00891	0	0.00891
	-0.9419	0.10513	0.47415	-1.1086	0	0.36035
	-0.8903	0.15668	0.5257	-1.057	0	0.4119
4.5,180	-1.3022	-0.2552	0.1138	-1.4689	-0.3861	0
	0.00891	0.00891	0.00891	0.00891	0.00891	0
	-1.328	-0.281	0.08802	-1.4947	-0.4119	0
	-1.2764	-0.2294	0.13957	-1.4431	-0.3604	0

Level			Least Sq Mean
4.5,135	A		0.260338
0,135		B	0.093633
4.5,165		C	-0.822455

Level		Least Sq Mean
0,165	D	-0.953363
4.5,180	E	-1.208583
0,180	F	-1.322378

Levels not connected by same letter are significantly different.

Rubber Type*Polyoctenamer*Temperature
Effect Test

Sum of Squares	F Ratio	DF	Prob > F
0.04465369	11.7220	2	<.0001*

Denominator MS Synthesis:
Residual

LS Means Plot

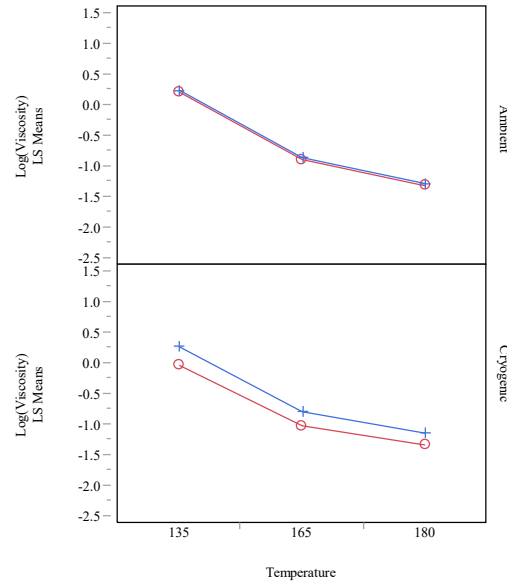

Curing*Temperature
Effect Test

Sum of Squares	F Ratio	DF	Prob > F
0.05169834	13.5713	2	<.0001*

Denominator MS Synthesis:
Residual

Least Squares Means Table

Level	Least Sq Mean	Std Error
None,135	0.006370	0.00629929
None,165	-1.051536	0.00629929
None,180	-1.404832	0.00629929
72 hrs,135	0.347601	0.00629929
72 hrs,165	-0.724282	0.00629929
72 hrs,180	-1.126129	0.00629929

LS Means Plot

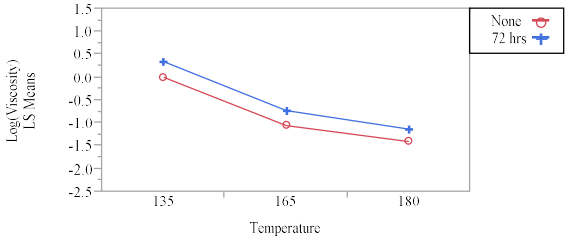

Rubber Type*Curing*Temperature
Effect Test

Sum of Squares	F Ratio	DF	Prob > F
0.03143120	8.2510	2	0.0004*

Denominator MS Synthesis:
Residual

LS Means Plot

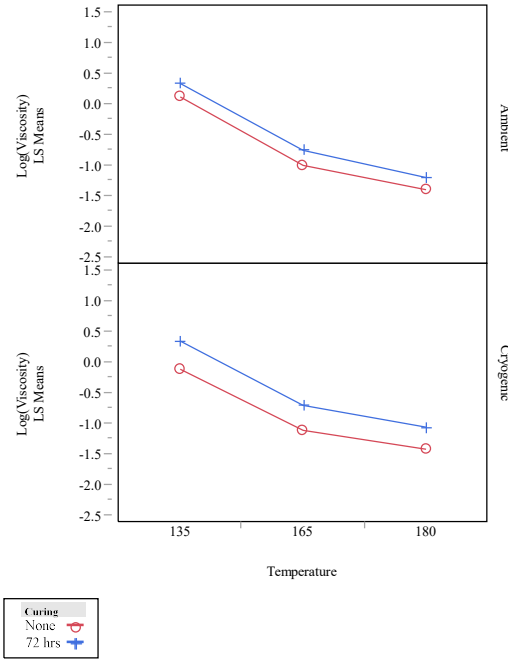

Polyoctenamer*Curing*Temperature
Effect Test

Sum of Squares	F Ratio	DF	Prob > F
0.01844382	4.8417	2	0.0094*

Denominator MS Synthesis:
Residual

LS Means Plot

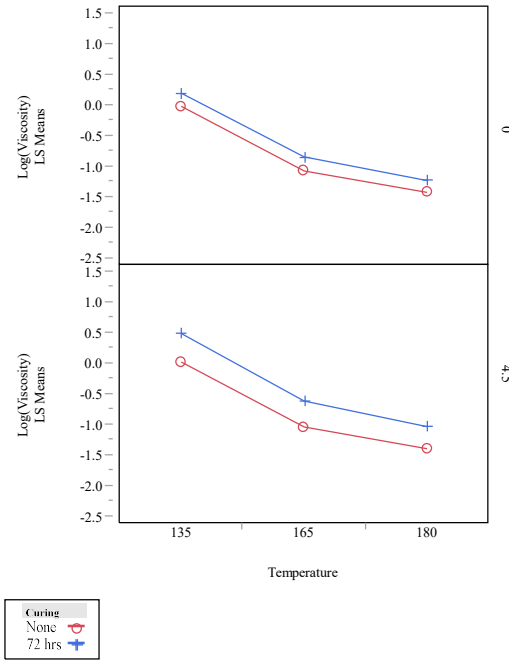

Centrifuging*Temperature
Effect Test

Sum of Squares	F Ratio	DF	Prob > F
0.29002785	76.1350	2	<.0001*

Denominator MS Synthesis:
Residual

Least Squares Means Table

Level	Least Sq Mean	Std Error
Non-centrifuged,135	0.913186	0.00629929
Non-centrifuged,165	-0.074148	0.00629929
Non-centrifuged,180	-0.486033	0.00629929
Centrifuged,135	-0.559215	0.00629929
Centrifuged,165	-1.701670	0.00629929
Centrifuged,180	-2.044928	0.00629929

LS Means Plot

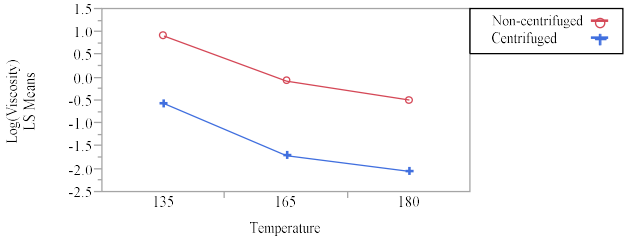

Rubber Type*Centrifuging*Temperature
Effect Test

Sum of Squares	F Ratio	DF	Prob > F
0.67250214	176.5381	2	<.0001*

Denominator MS Synthesis:
Residual

LS Means Plot

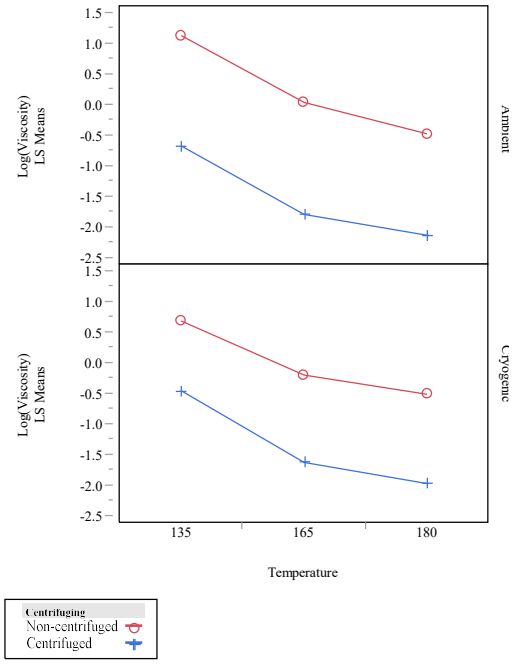

Polyoctenamer*Centrifuging*Temperature Effect Test

Sum of Squares	F Ratio	DF	Prob > F
0.04935420	12.9559	2	<.0001*

Denominator MS Synthesis:
Residual

LS Means Plot

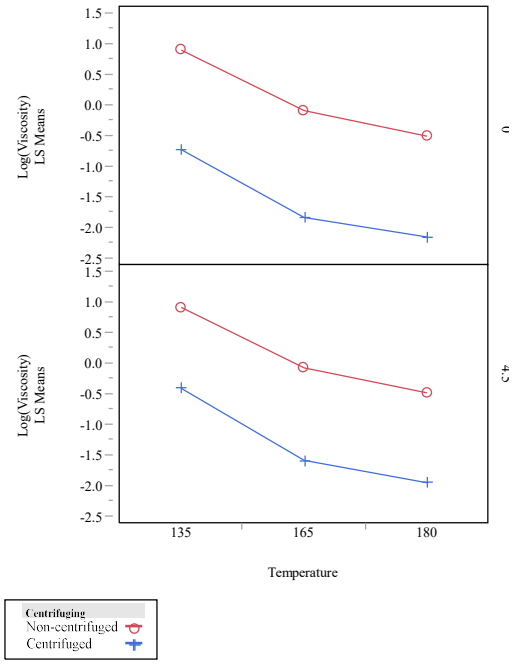

Rubber Type*Polyoctenamer*Centrifuging*Temperature
Effect Test

Sum of Squares	F Ratio	DF	Prob > F
0.01215012	3.1895	2	0.0445*

Denominator MS Synthesis:
Residual

LS Means Plot

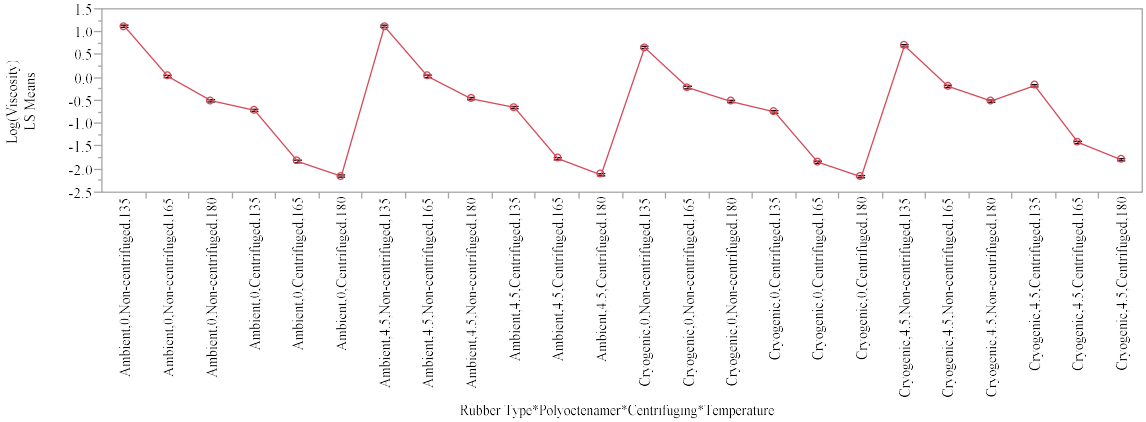

Curing*Centrifuging*Temperature
Effect Test

Sum of Squares	F Ratio	DF	Prob > F
0.27175882	71.3393	2	<.0001*

Denominator MS Synthesis:
Residual

LS Means Plot

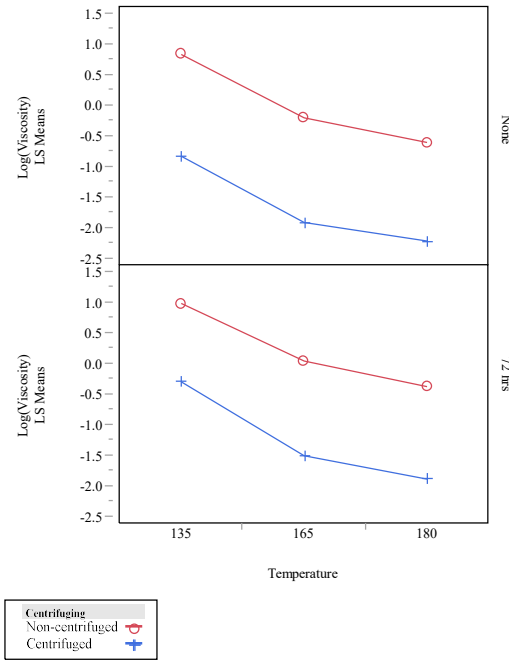

Rubber Type*Polyoctenamer*Curing*Centrifuging*Temperature
Effect Test

Sum of Squares	F Ratio	DF	Prob > F
0.04141479	10.8718	2	<.0001*

Denominator MS Synthesis:
Residual

LS Means Plot

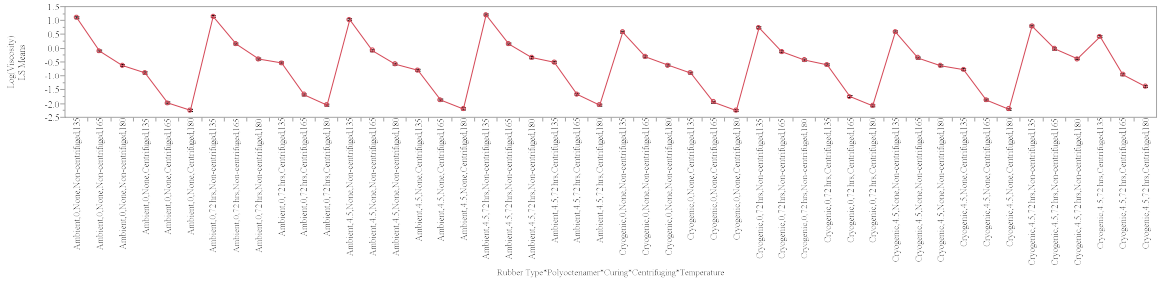

Aging*Temperature
Effect Test

Sum of Squares	F Ratio	DF	Prob > F
0.55574036	145.8871	2	<.0001*

Denominator MS Synthesis:
Residual

Least Squares Means Table

Level	Least Sq Mean	Std Error
Unaged,135	-0.039729	0.00629929
Unaged,165	-1.032034	0.00629929
Unaged,180	-1.377114	0.00629929
RTFOaged,135	0.393700	0.00629929
RTFOaged,165	-0.743784	0.00629929
RTFOaged,180	-1.153847	0.00629929

LS Means Plot

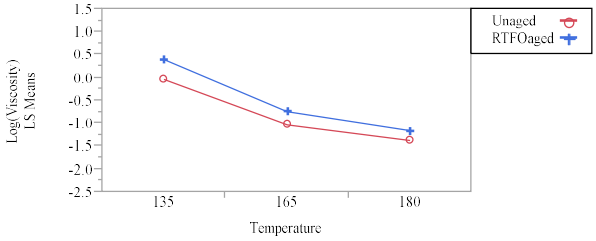

Rubber Type*Aging*Temperature
Effect Test

Sum of Squares	F Ratio	DF	Prob > F
0.16808170	44.1230	2	<.0001*

Denominator MS Synthesis:
Residual

LS Means Plot

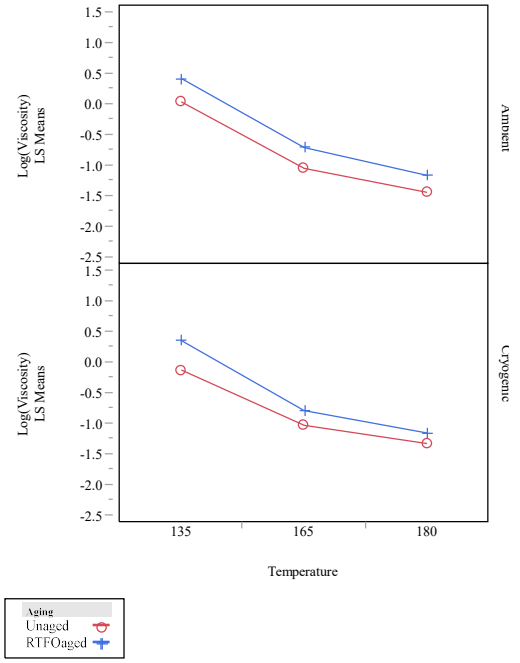

Polyoctenamer*Aging*Temperature
Effect Test

Sum of Squares	F Ratio	DF	Prob > F
0.05078196	13.3307	2	<.0001*

Denominator MS Synthesis:
Residual

LS Means Plot

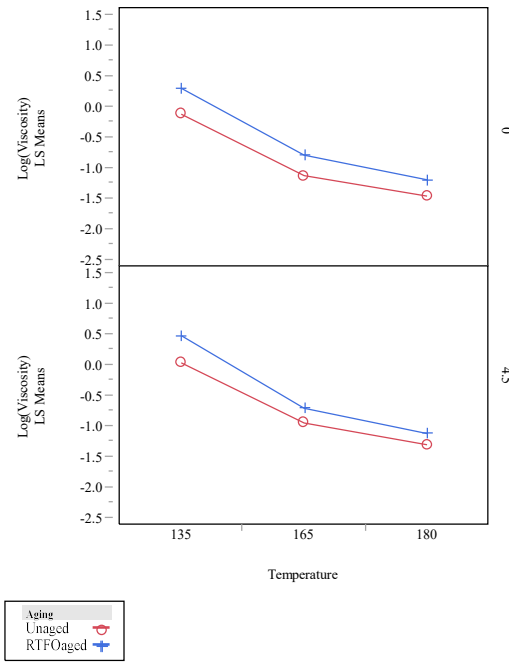

Curing*Aging*Temperature
Effect Test

Sum of Squares	F Ratio	DF	Prob > F
0.04143428	10.8769	2	<.0001*

Denominator MS Synthesis:
Residual

LS Means Plot

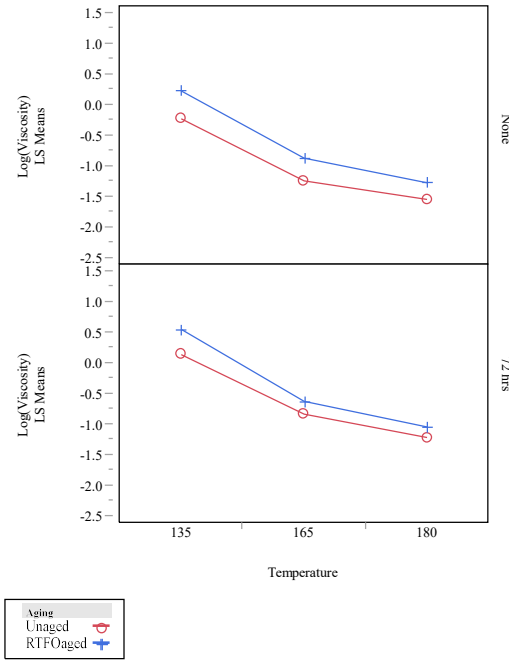

Rubber Type*Polyoctenamer*Curing*Aging*Temperature
Effect Test

Sum of Squares	F Ratio	DF	Prob > F
0.05238692	13.7521	2	<.0001*

Denominator MS Synthesis:
Residual

LS Means Plot

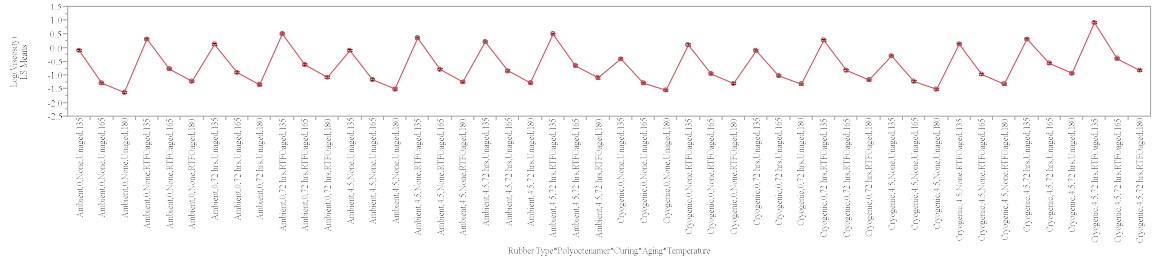

Centrifuging*Aging*Temperature
Effect Test

Sum of Squares	F Ratio	DF	Prob > F
0.05219790	13.7024	2	<.0001*

Denominator MS Synthesis:
Residual

LS Means Plot

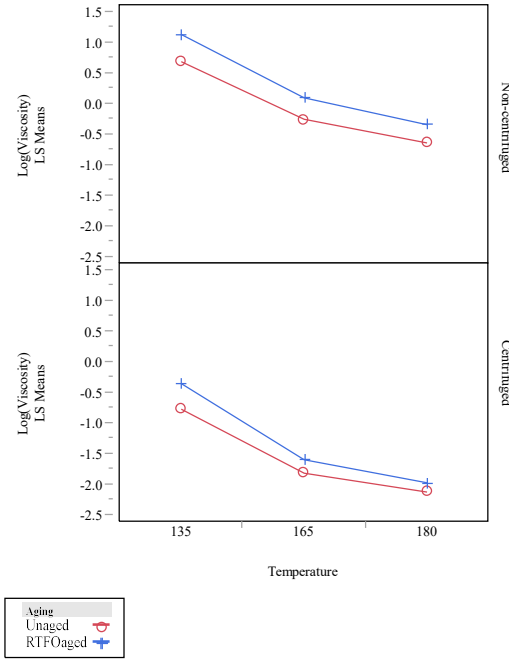

Rubber Type*Curing*Centrifuging*Aging*Temperature
Effect Test

Sum of Squares	F Ratio	DF	Prob > F
0.01512883	3.9715	2	0.0212*

Denominator MS Synthesis:
Residual

LS Means Plot

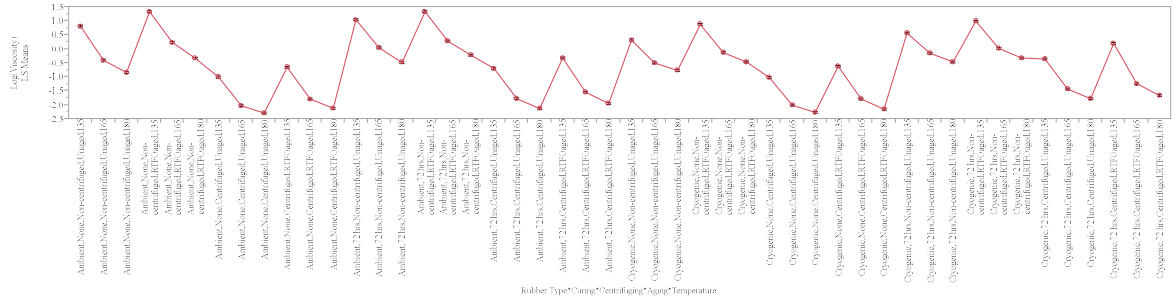

APPENDIX B. MASTER CURVES OF UNAGED MATERIALS

This appendix presents the master curves of the unaged materials tested using different DSR geometries. The CAM and Sigmoidal models were fitted to the master curves.

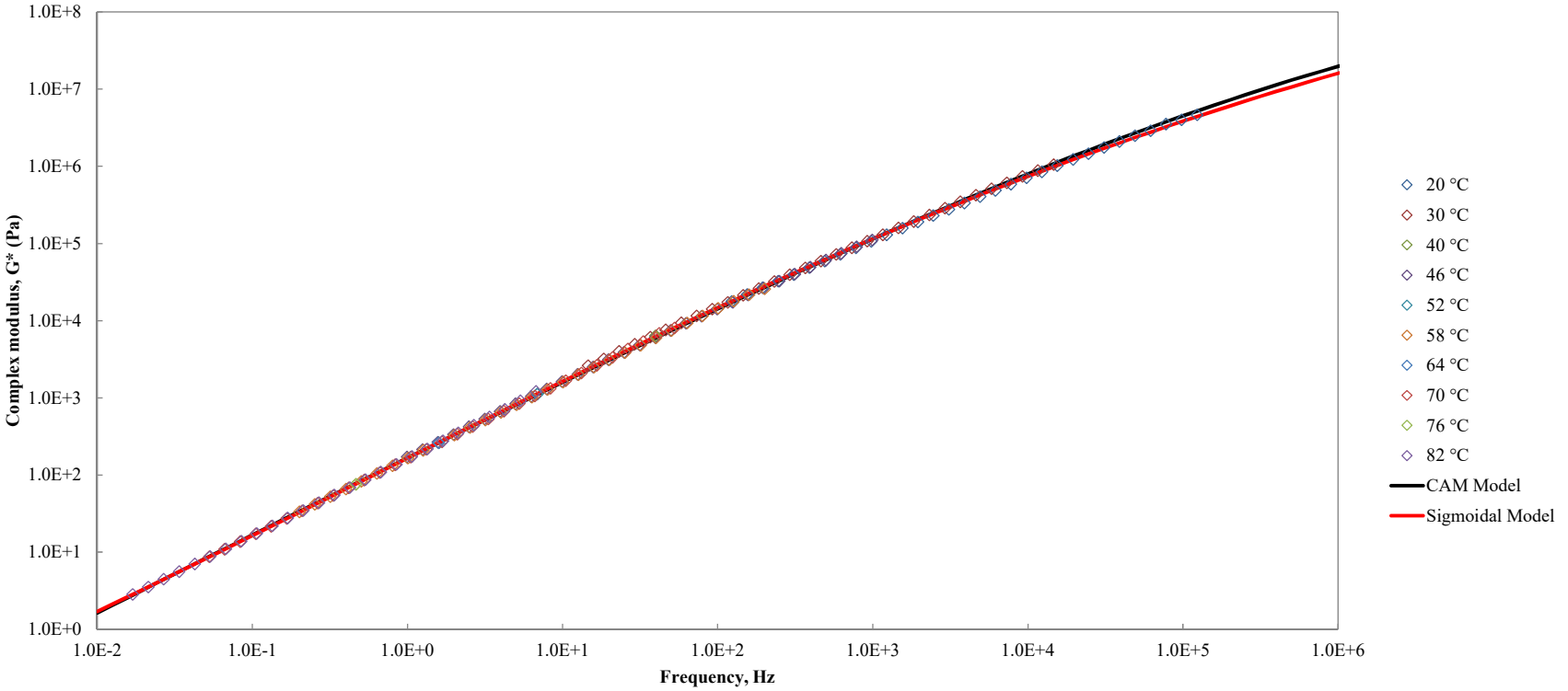

Figure B-1. Master curve of unaged PG52-34 tested with parallel plates – 1 mm gap, T_{ref} = 64 °C

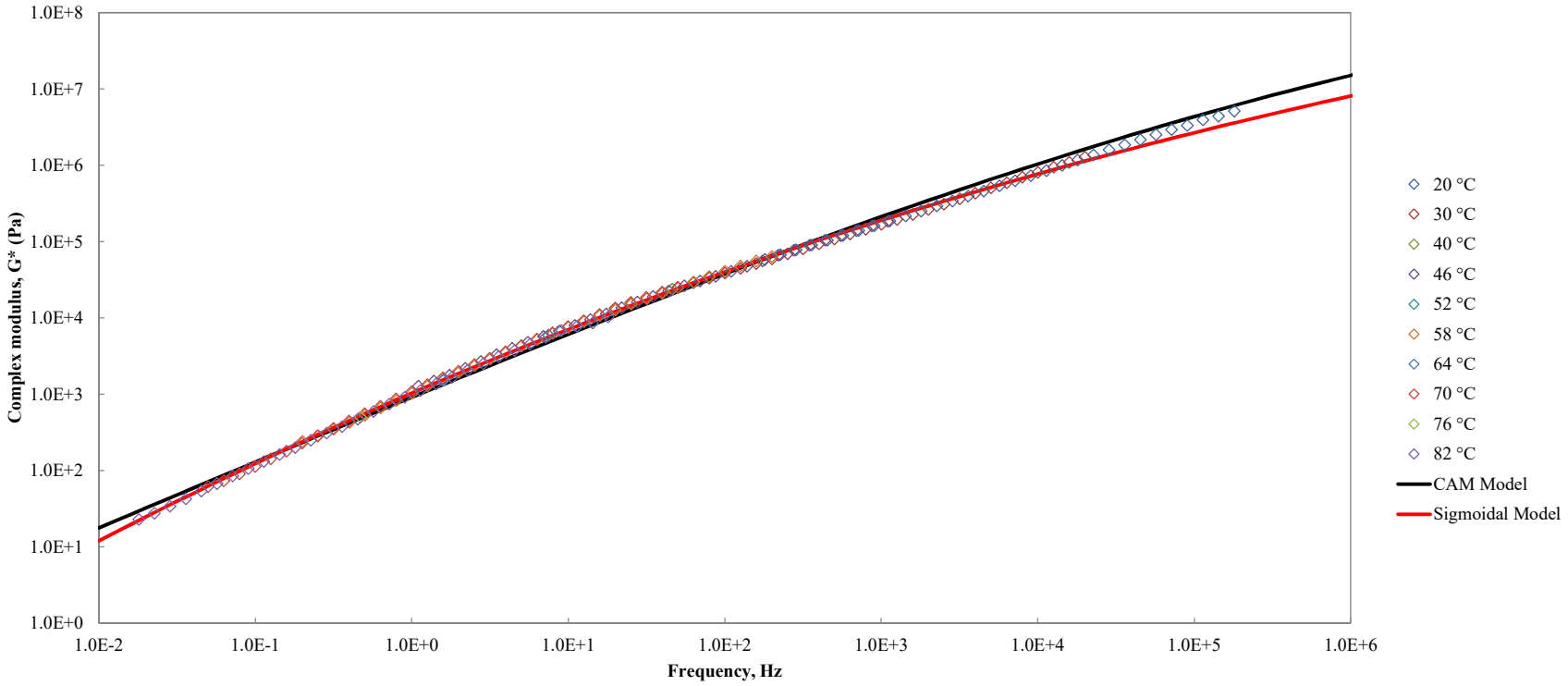

Figure B-2. Master curve of unaged non-centrifuged AMB tested with parallel plates – 1mm gap, T_{ref} = 64 °C

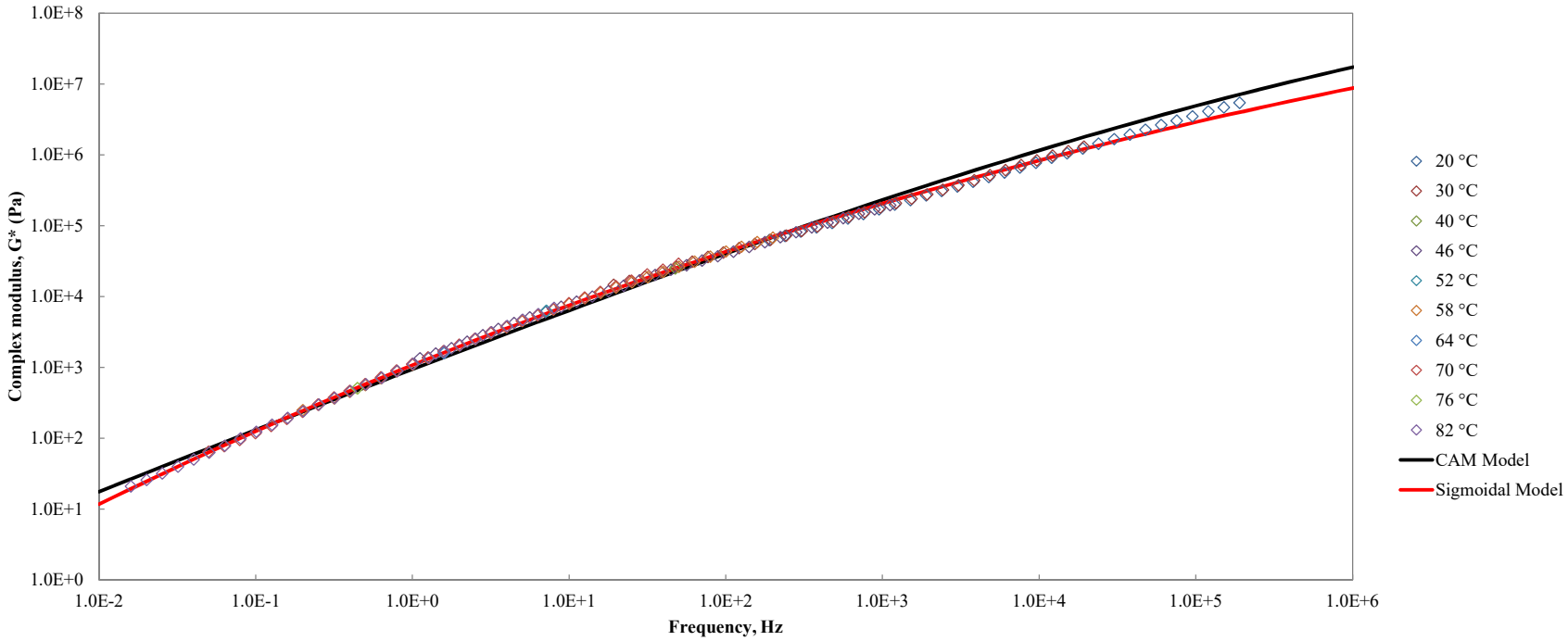

Figure B-3. Master curve of unaged non-centrifuged AMB tested with parallel plates – 2 mm gap, T_{ref} = 64 °C

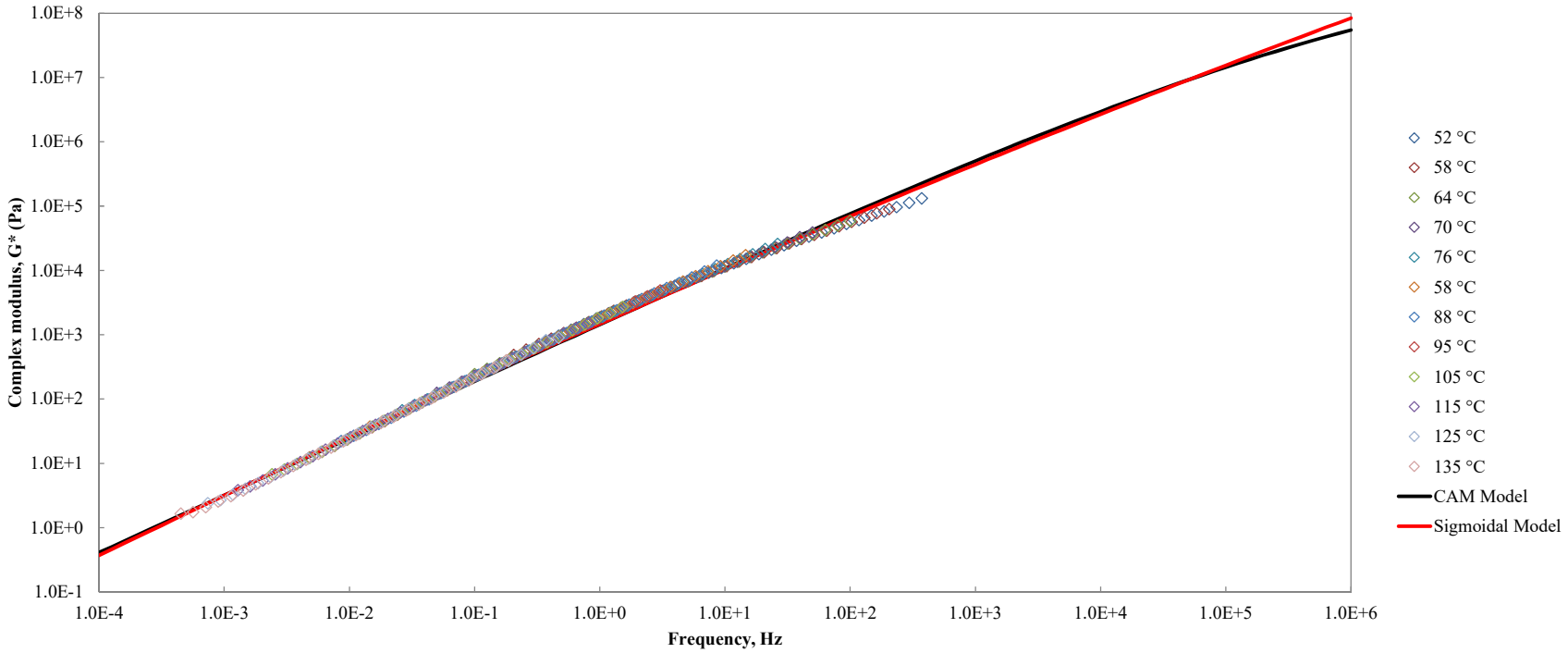

Figure B-4. Master curve of unaged non-centrifuged AMB tested with concentric cylinders, T_{ref} = 64 °C

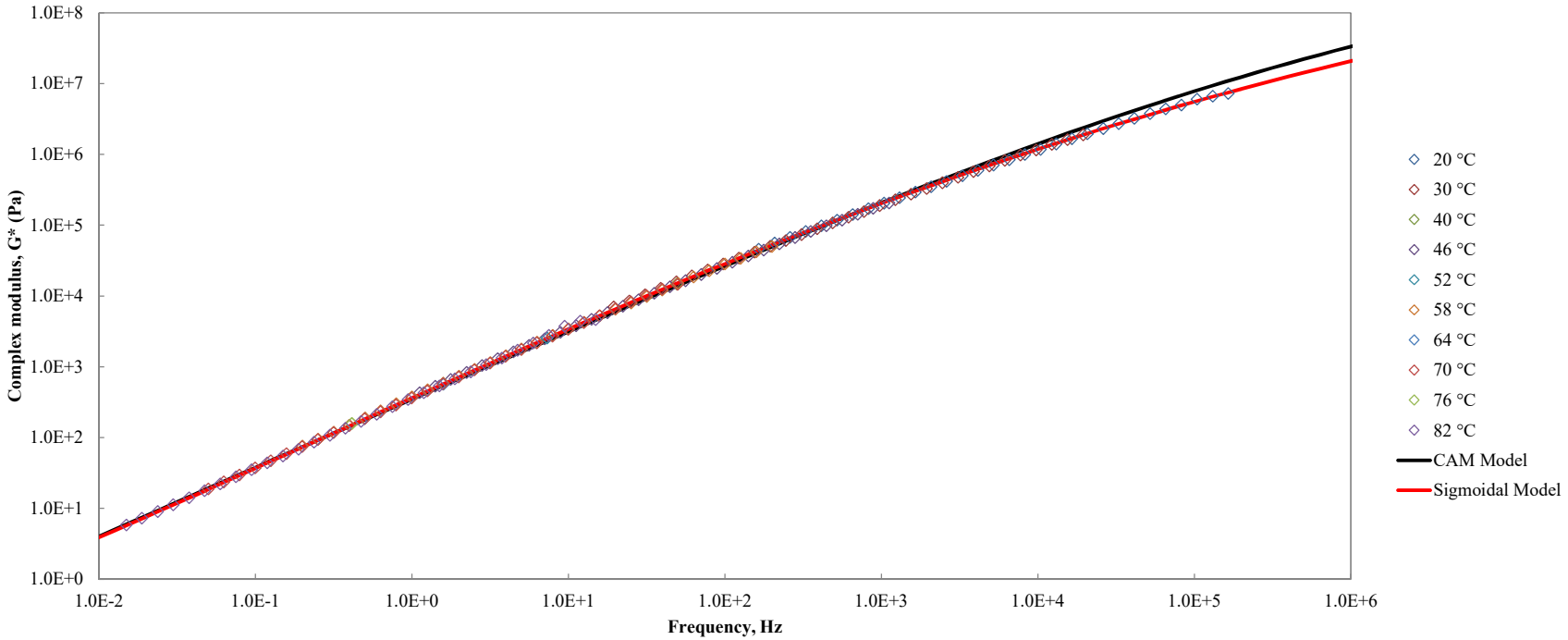

Figure B-5. Master curve of unaged centrifuged AMB tested with parallel plates – 1 mm gap, T_{ref} = 64 °C

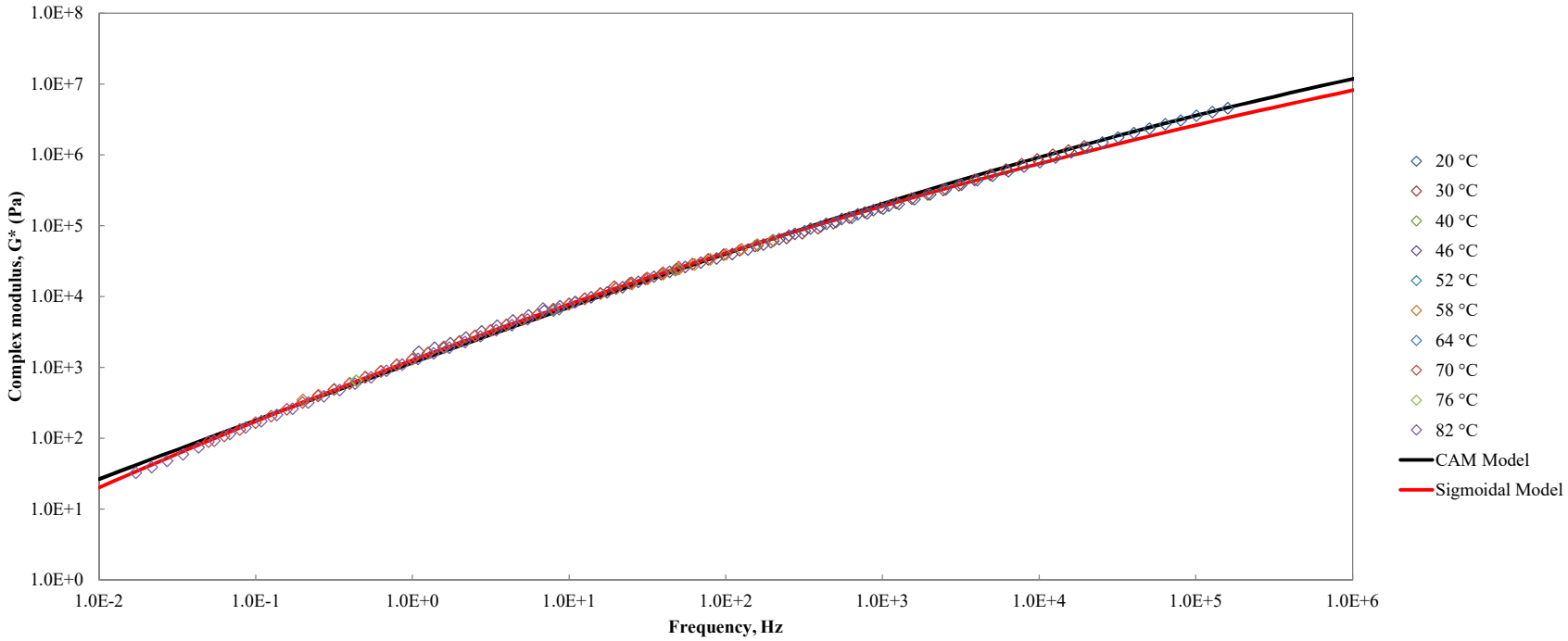

Figure B-6. Master curve of unaged non-centrifuged AMB 72 hrs cure tested with parallel plates – 1 mm gap. T_{ref} = 64°C

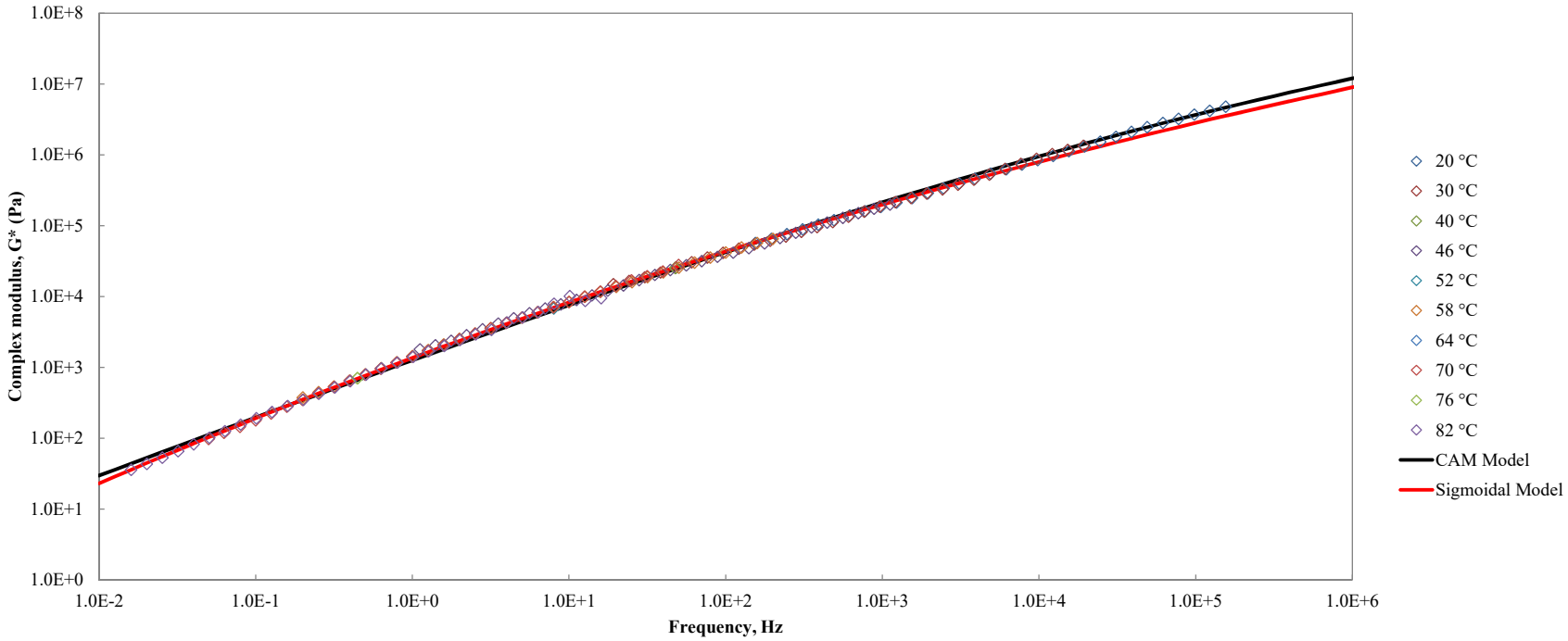

Figure B-7. Master curve of unaged non-centrifuged AMB 72 hrs cure tested with parallel plates – 2 mm gap. T_{ref} = 64 °C

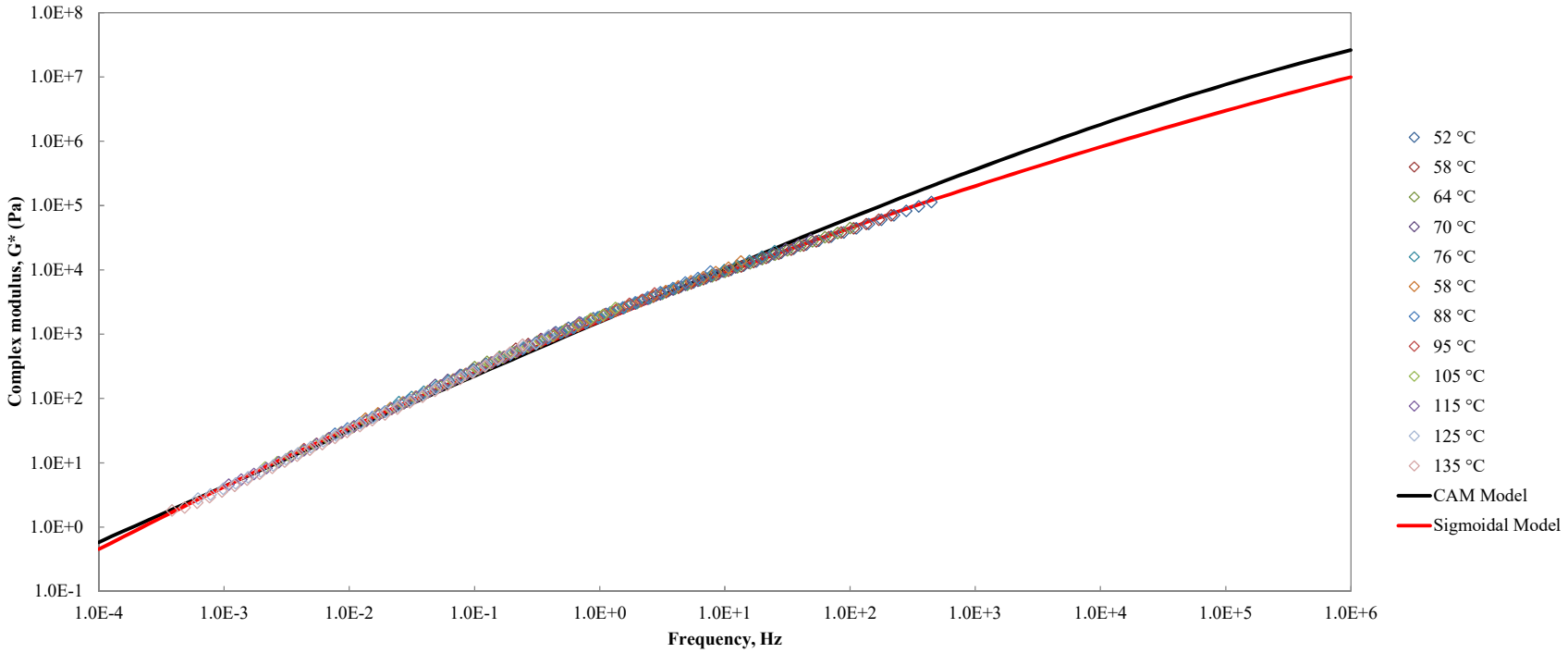

Figure B-8. Master curve of unaged non-centrifuged AMB 72hrs cure tested with concentric cylinders, T_{ref} = 64 °C

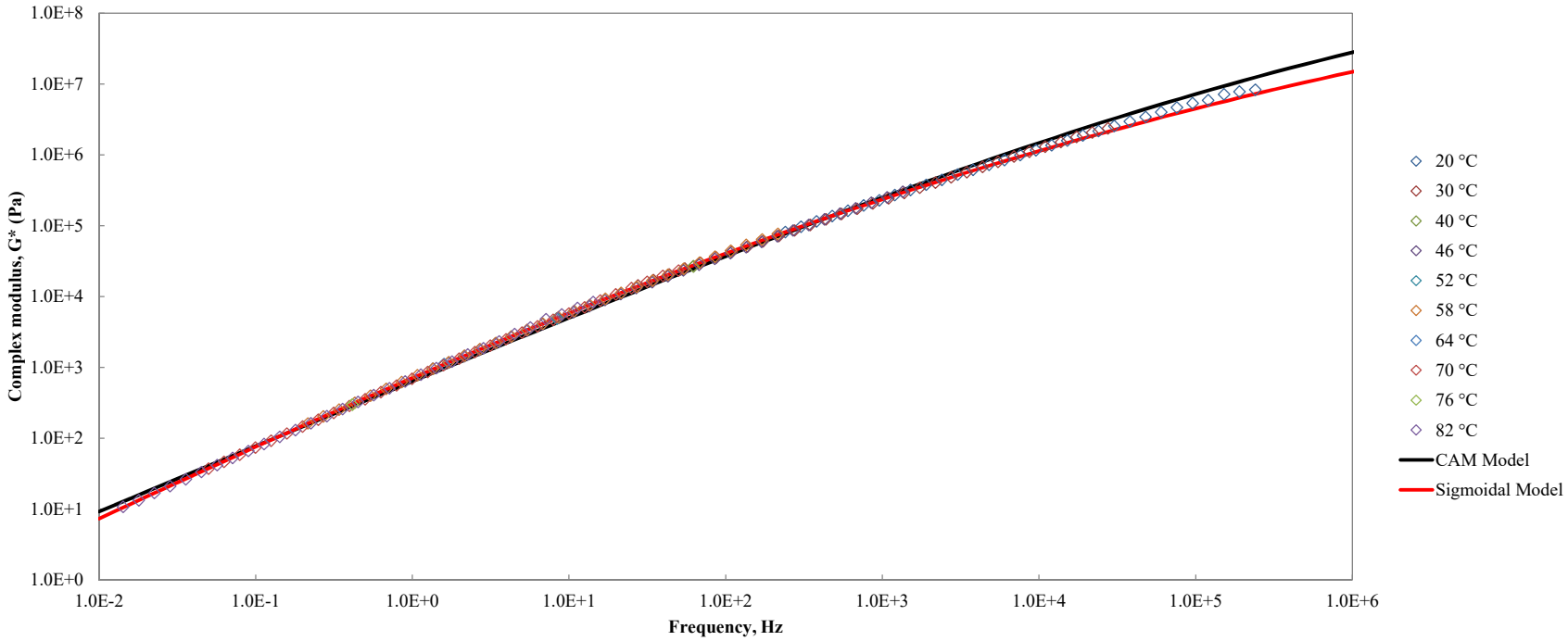

Figure B-9. Master curve of unaged centrifuged AMB 72 hrs cure tested with parallel plates – 1 mm gap. T_{ref} = 64 °C

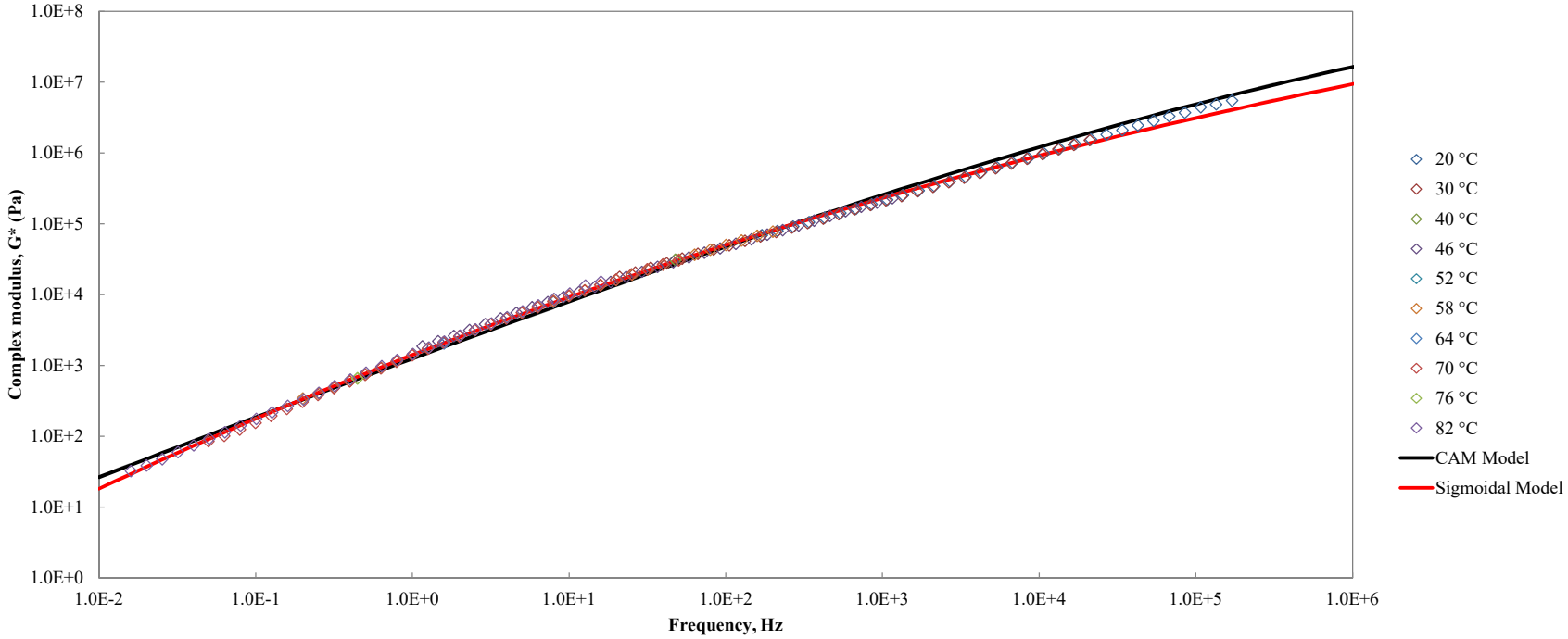

Figure B-10. Master curve of unaged non-centrifuged AP tested with parallel plates – 1 mm gap, T_{ref} = 64 °C

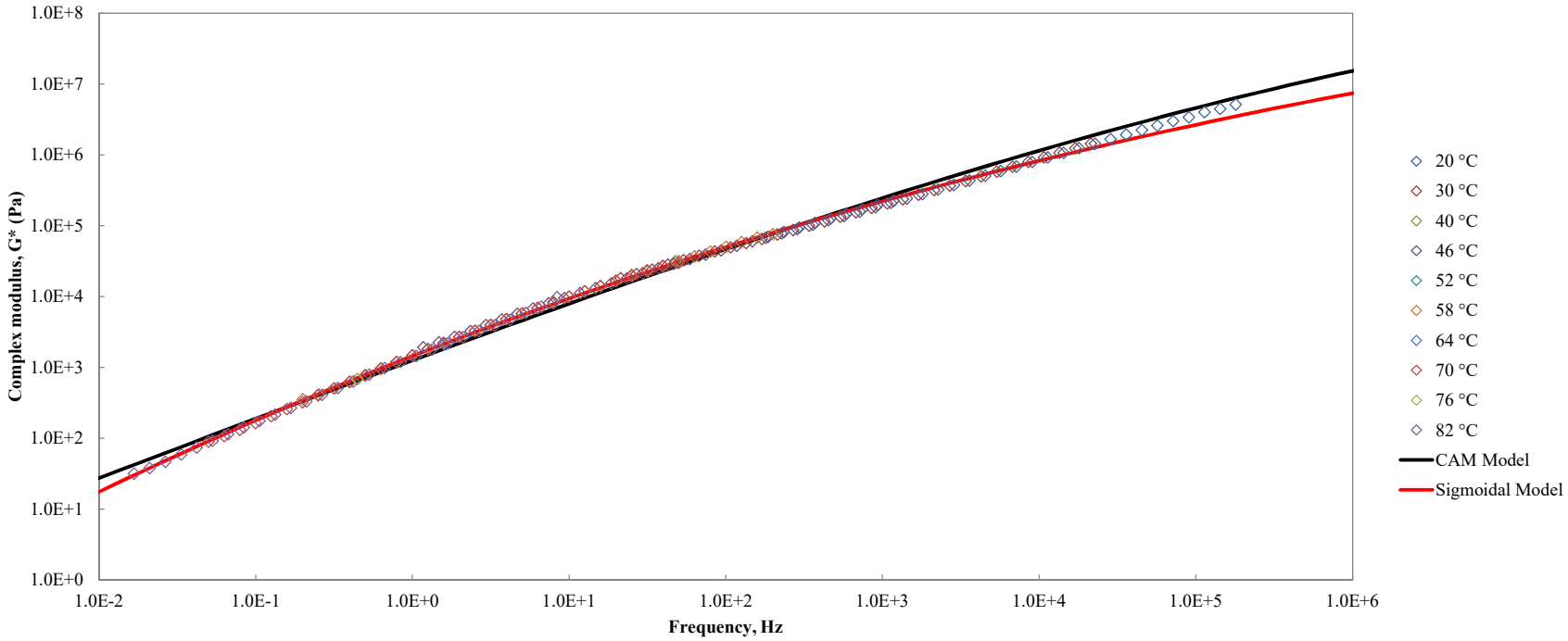

Figure B-11. Master curve of unaged non-centrifuged AP tested with parallel plates – 2 mm gap, T_{ref} = 64 °C

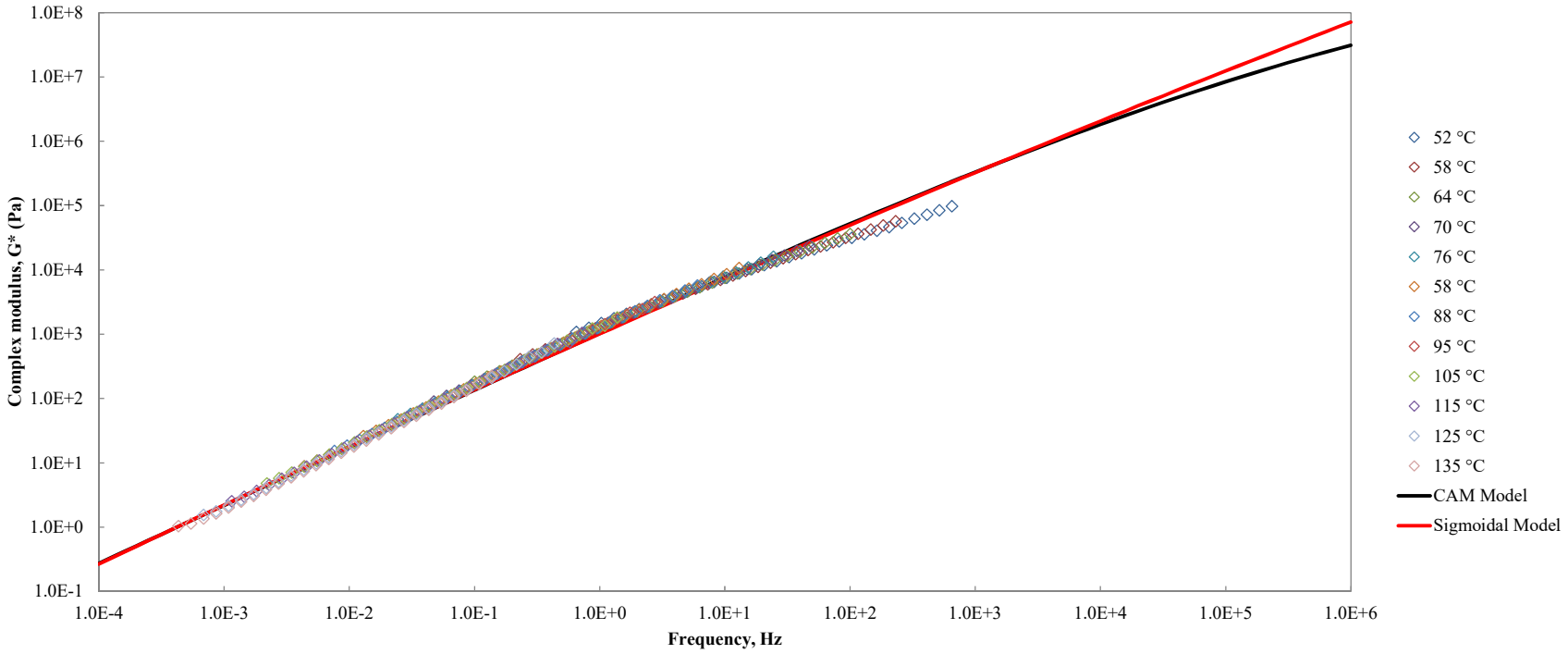

Figure B-12. Master curve of unaged non-centrifuged AP tested with concentric cylinders, T_{ref} = 64 °C

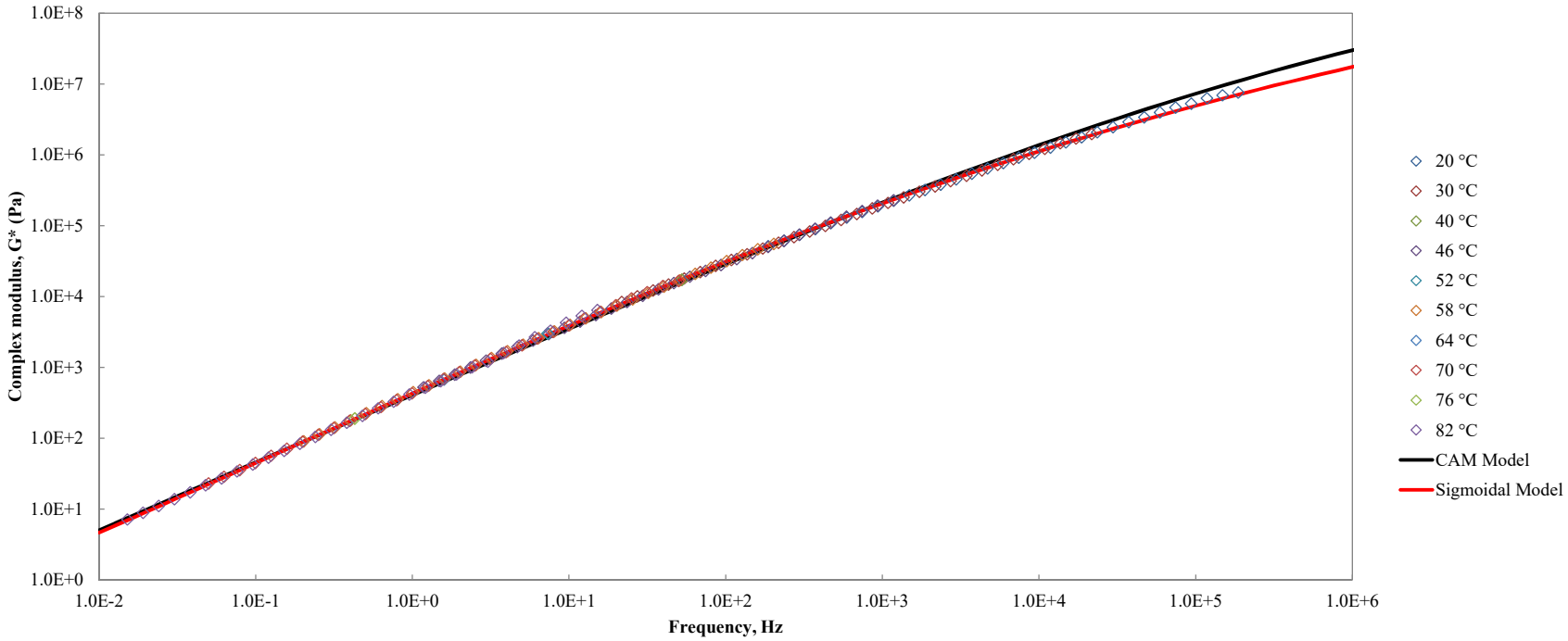

Figure B-13. Master curve of unaged centrifuged AP tested with parallel plates – 1 mm gap, T_{ref} =64 °C

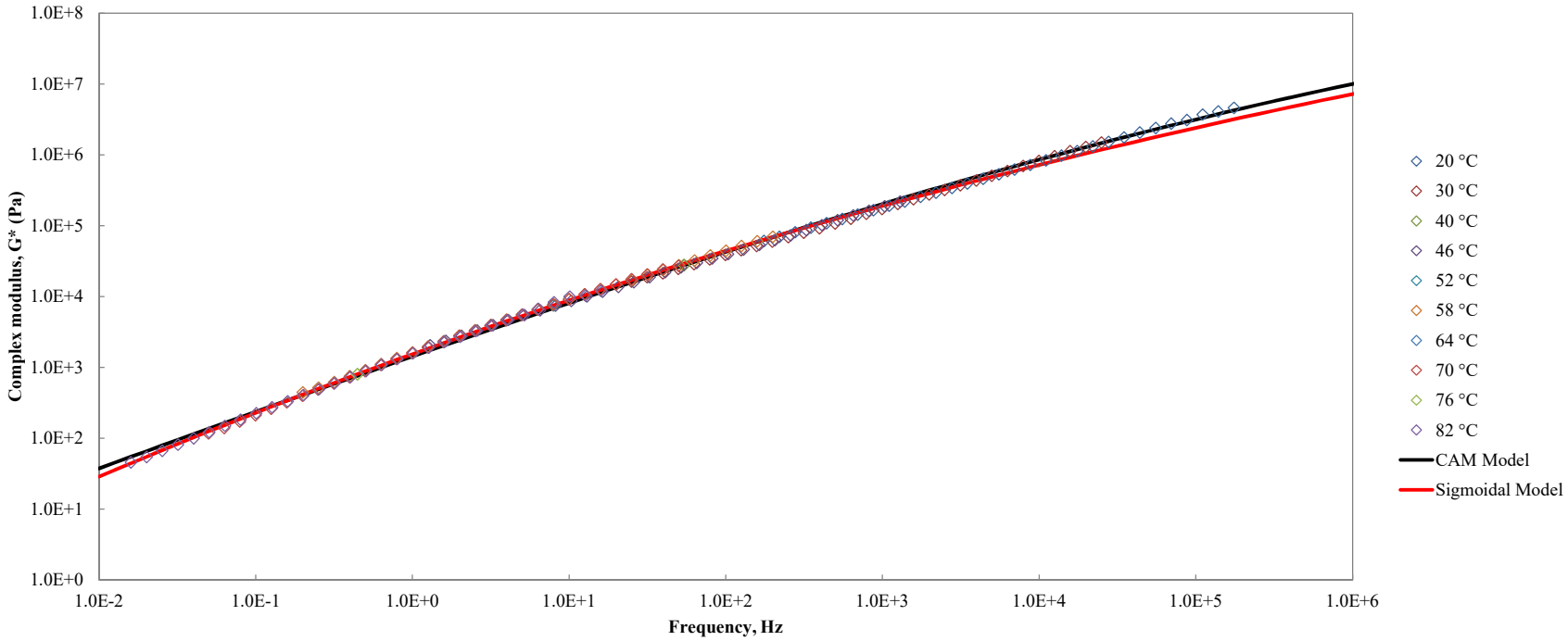

Figure B-14. Master curve of unaged non-centrifuged AP 72 hrs cure tested with parallel plates – 1 mm gap, T_{ref} = 64 °C

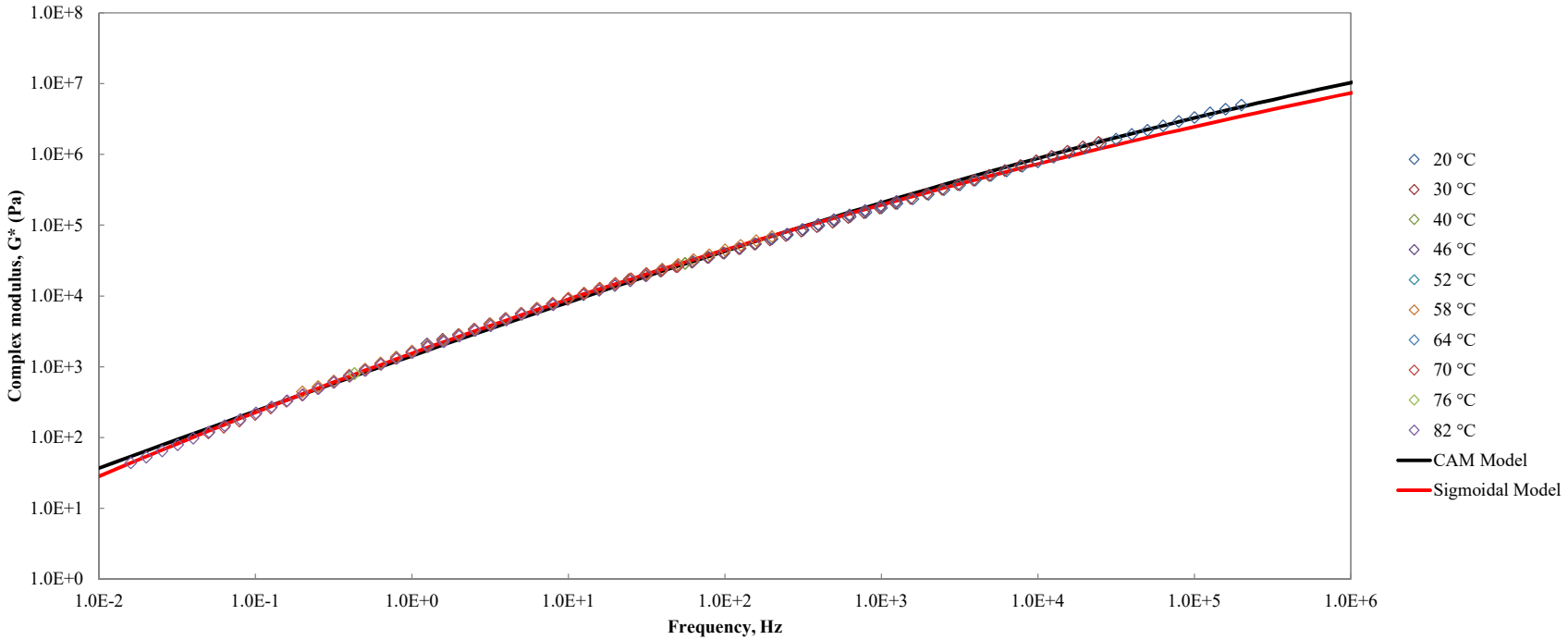

Figure B-15. Master curve of unaged non-centrifuged AP 72 hrs cure tested with parallel plate – 2 mm gap, T_{ref} = 64 °C

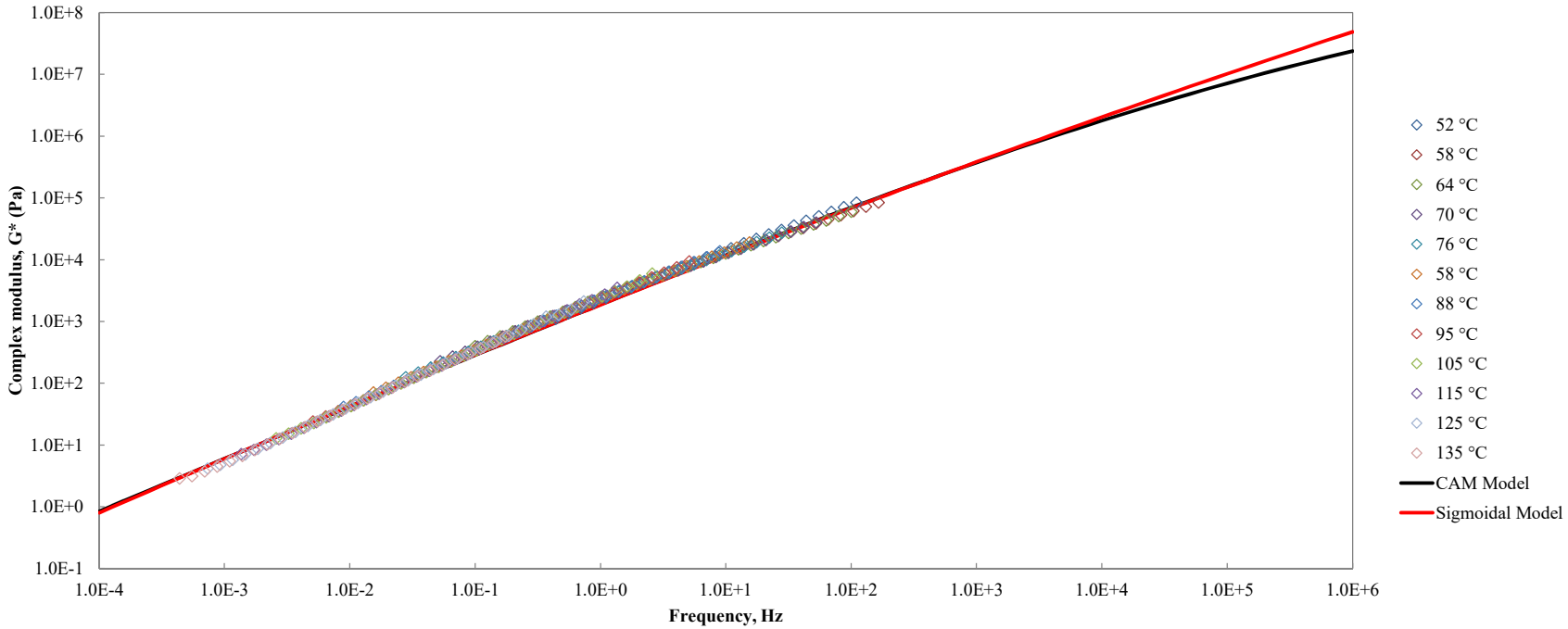

Figure B-16. Master curve of unaged non-centrifuged AP 72hrs cure tested with concentric cylinders, T_{ref} = 64 °C

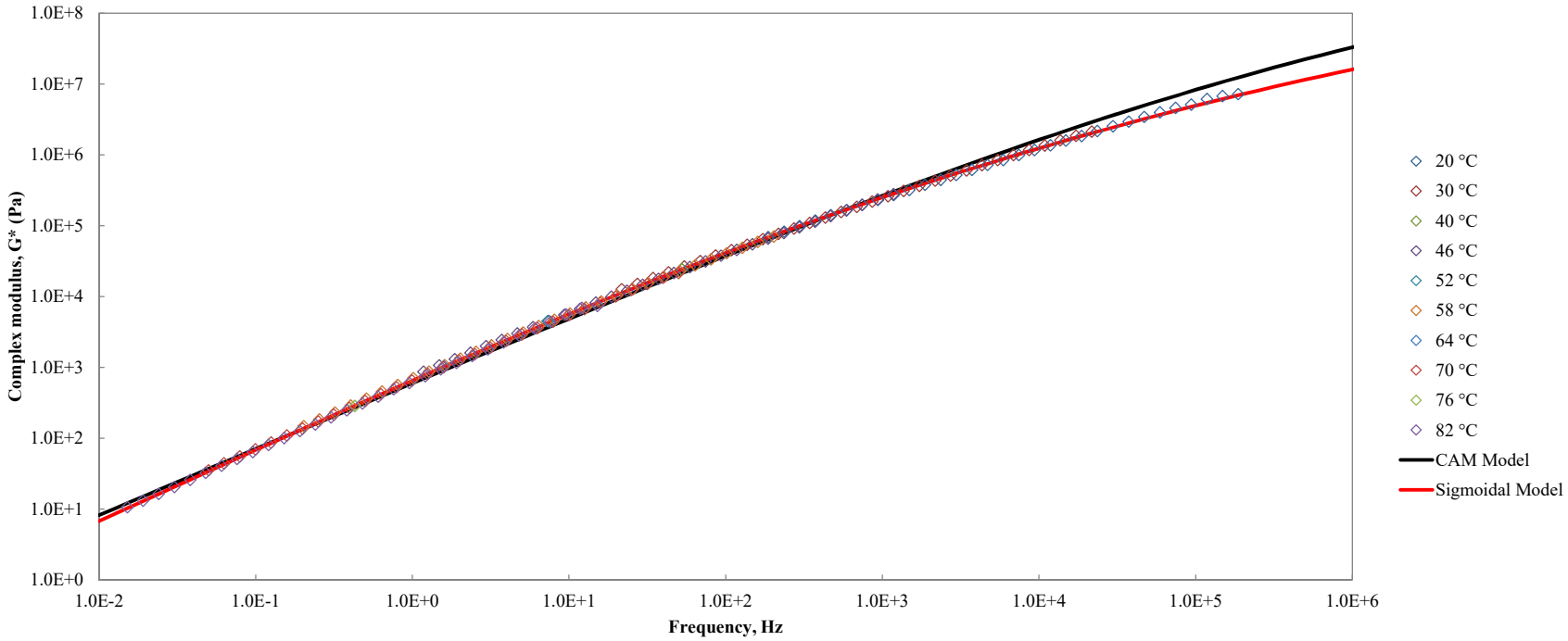

Figure B-17. Master curve of unaged centrifuged AP 72 hrs cure tested with parallel plates – 1 mm gap, T_{ref} = 64 °C

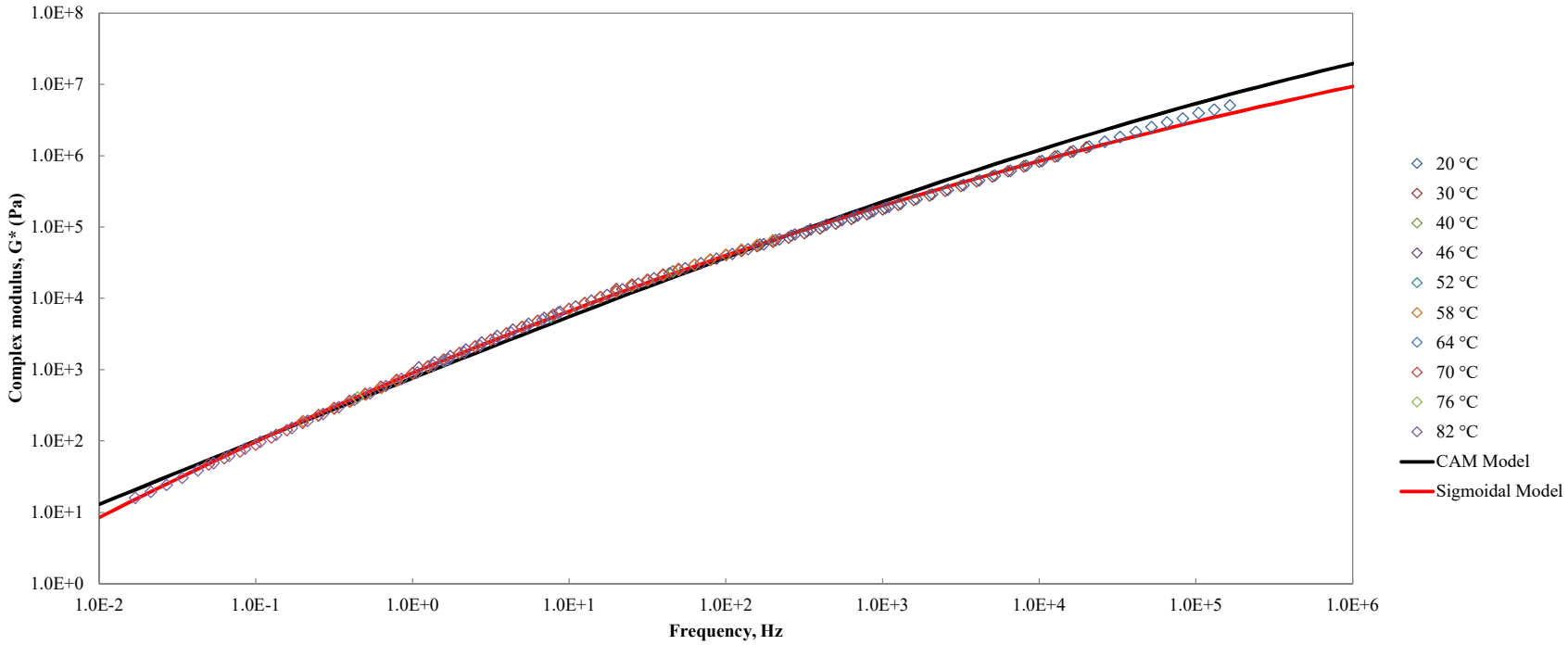

Figure B-18. Master curve of unaged non-centrifuged CRYO tested with parallel plates – 1 mm gap, T_{ref} = 64 °C

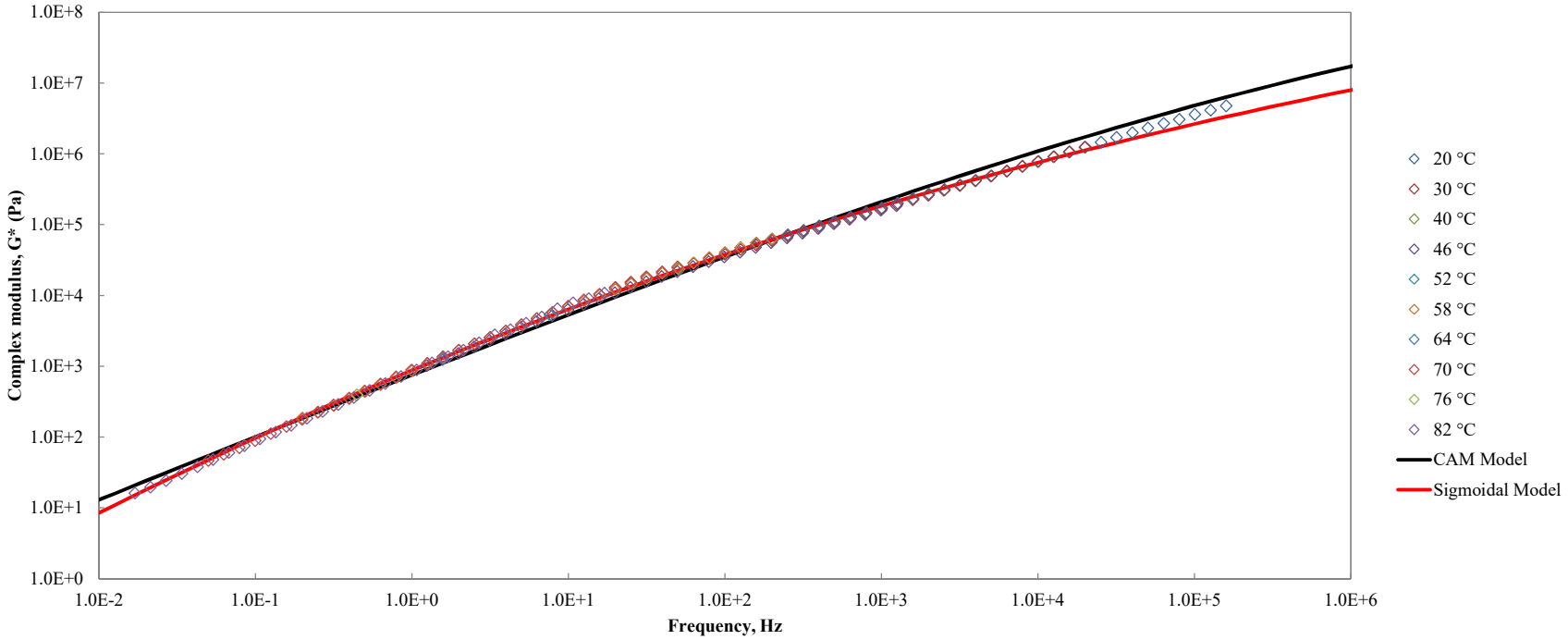

Figure B-19. Master curve of unaged non-centrifuged CRYO tested with parallel plates – 2 mm gap, T_{ref} = 64 °C

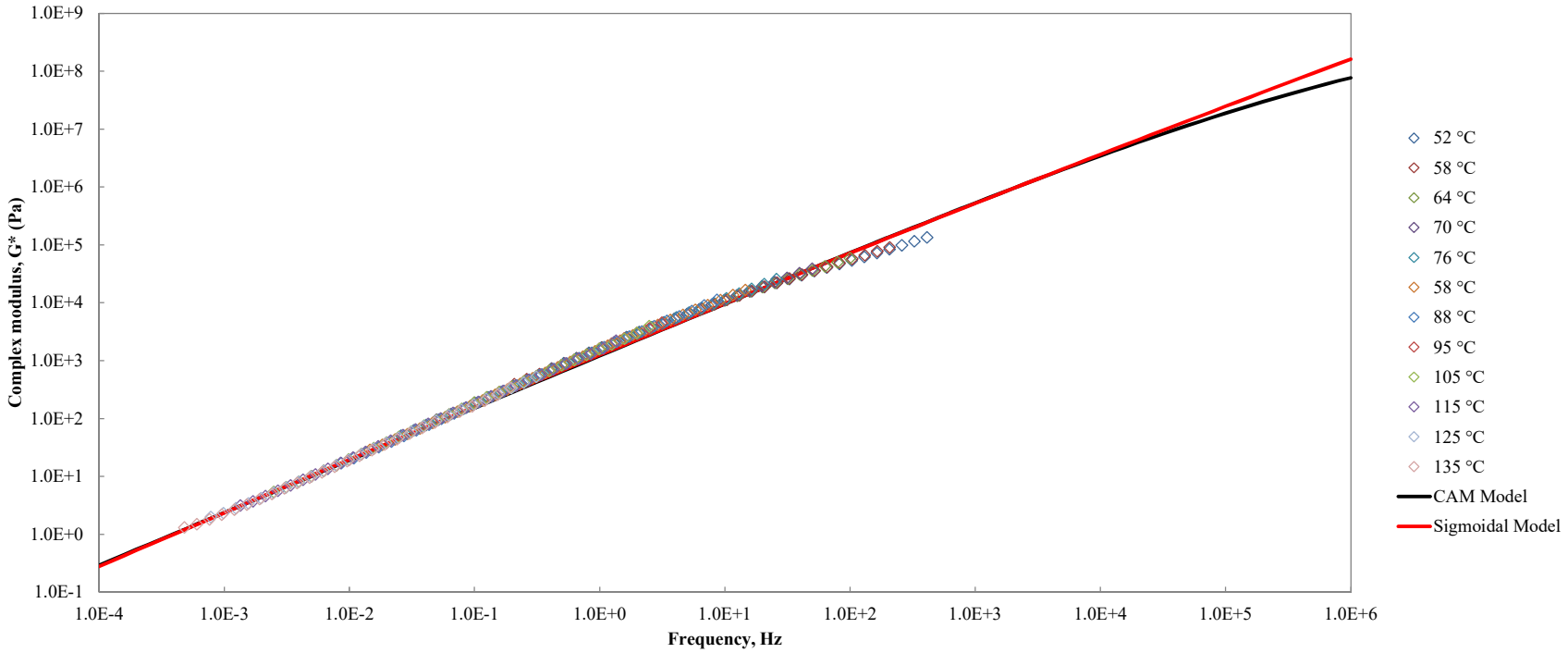

Figure B-20. Master curve of unaged non-centrifuged CRYO tested with concentric cylinders, T_{ref} = 64 °C

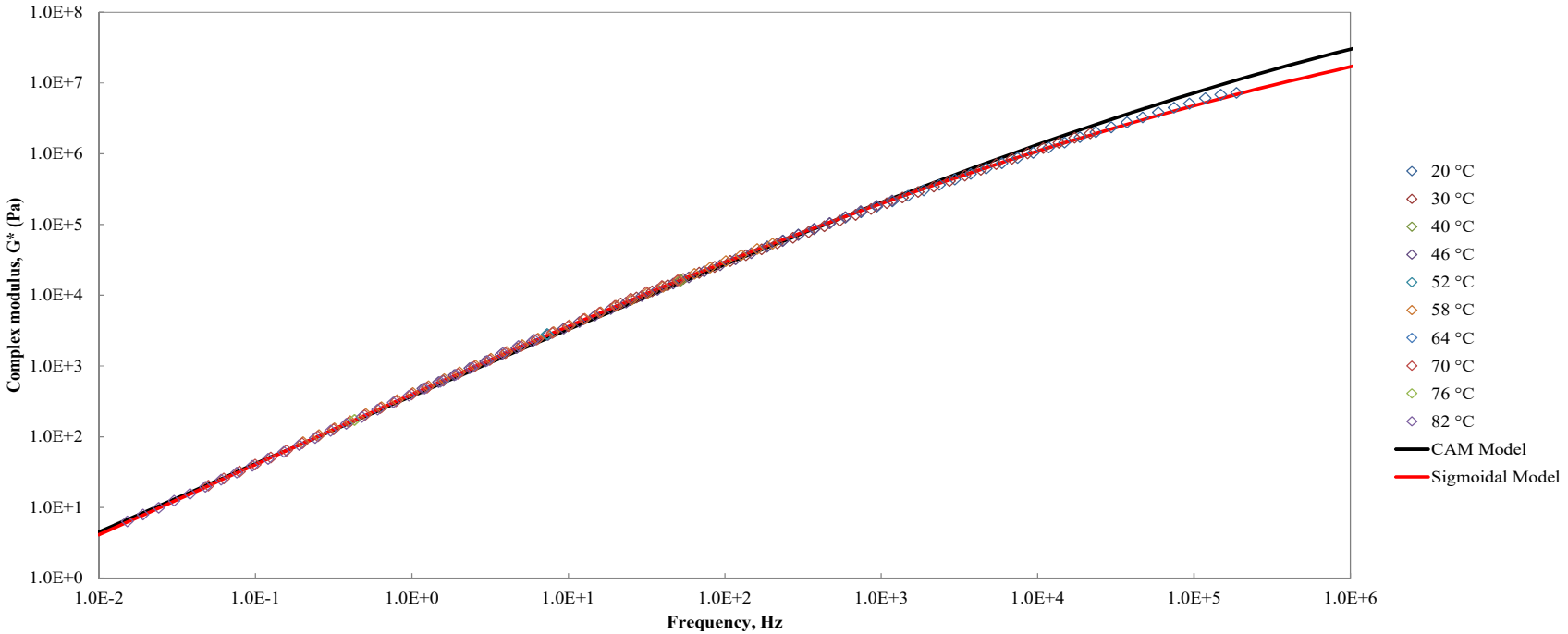

Figure B-21. Master curve of unaged centrifuged CRYO tested with parallel plates – 1 mm gap, T_{ref} = 64 °C

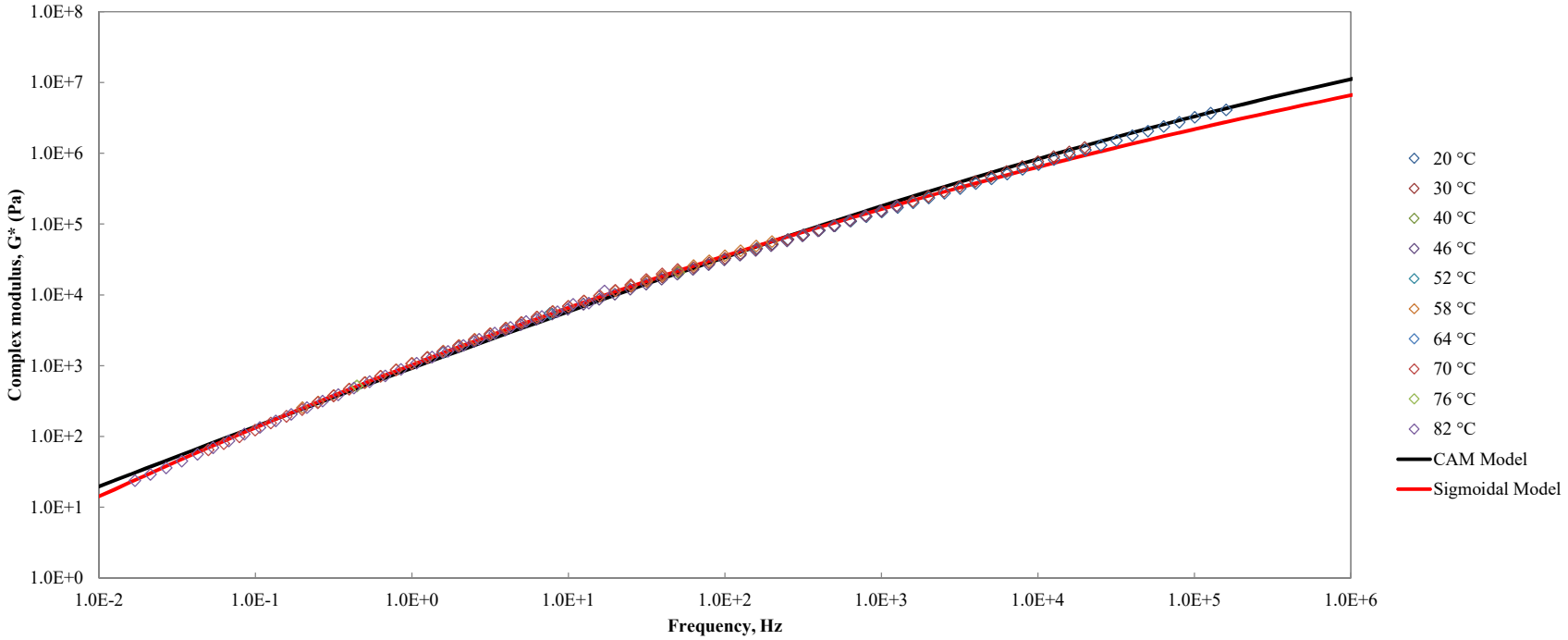

Figure B-22. Master curve of unaged non-centrifuged CRYO 72 hrs tested with parallel plates – 1 mm gap, T_{ref} = 64 °C

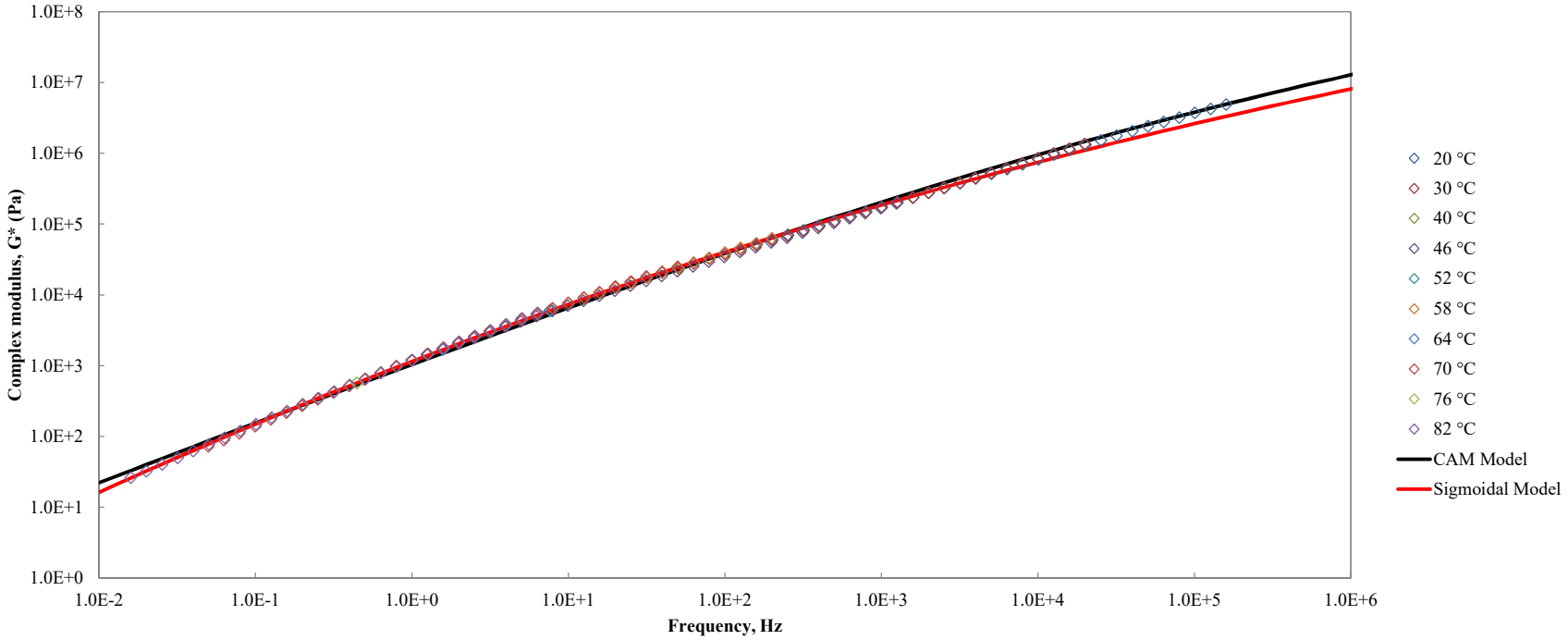

Figure B-23. Master curve of unaged non-centrifuged CRYO 72 hrs cure tested with parallel plates – 2 mm gap, T_{ref} = 64 °C

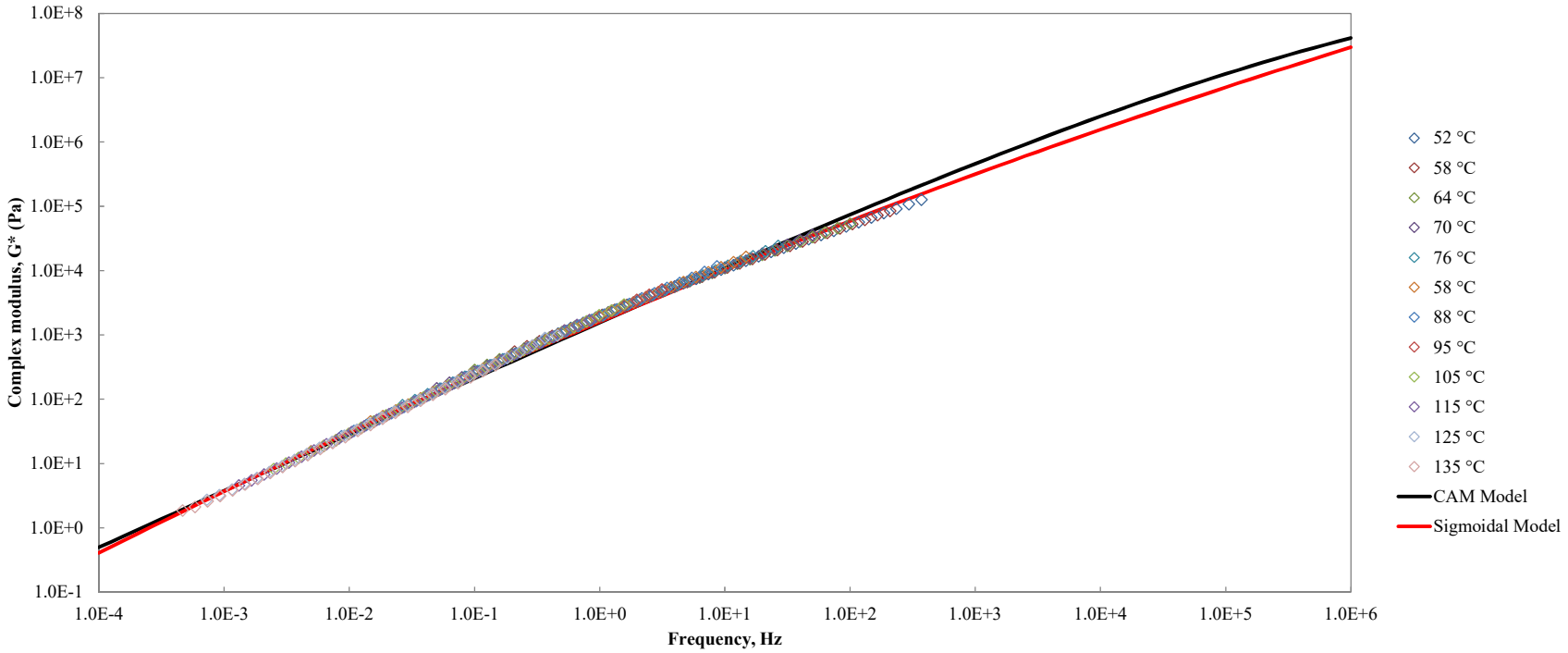

Figure B-24. Master curve of unaged non-centrifuged CRYO 72 hrs tested with concentric cylinders, T_{ref} = 64 °C

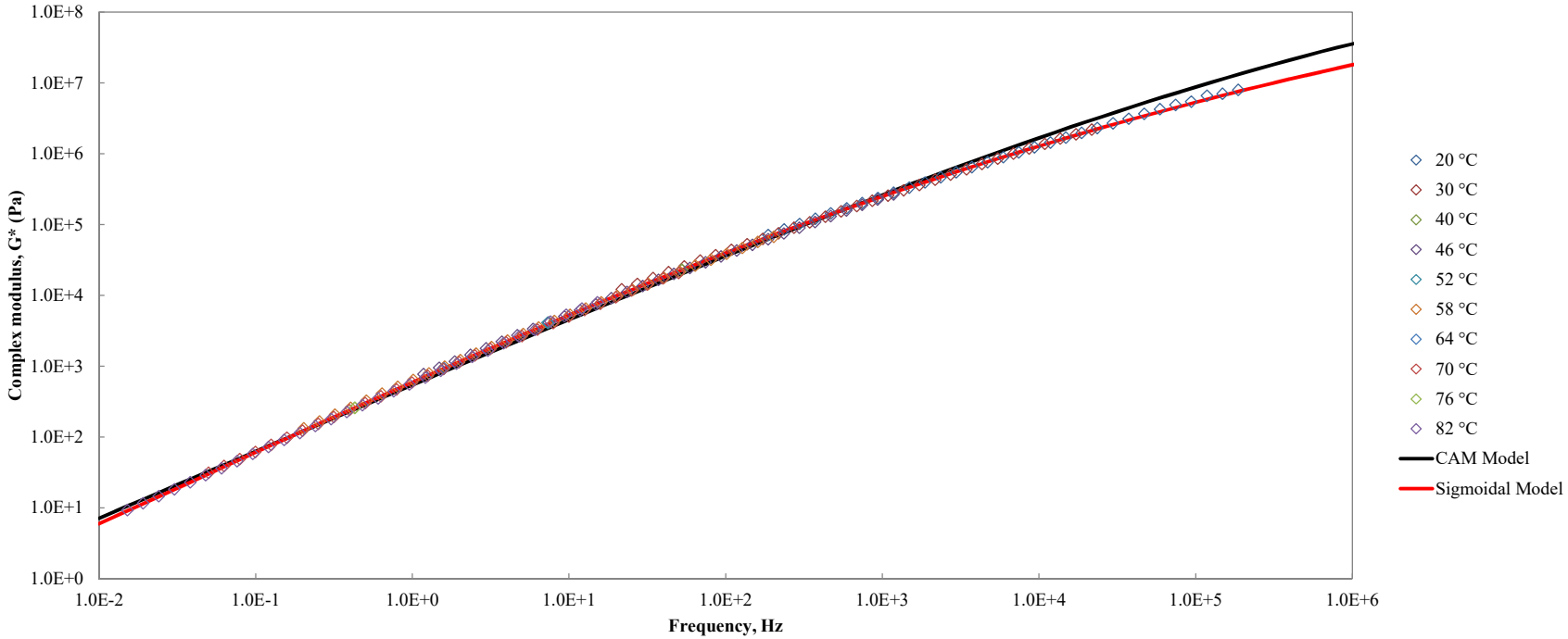

Figure B-25. Master curve of unaged centrifuged CRYO 72 hrs tested with parallel plates – 1 mm gap, T_{ref} = 64 °C

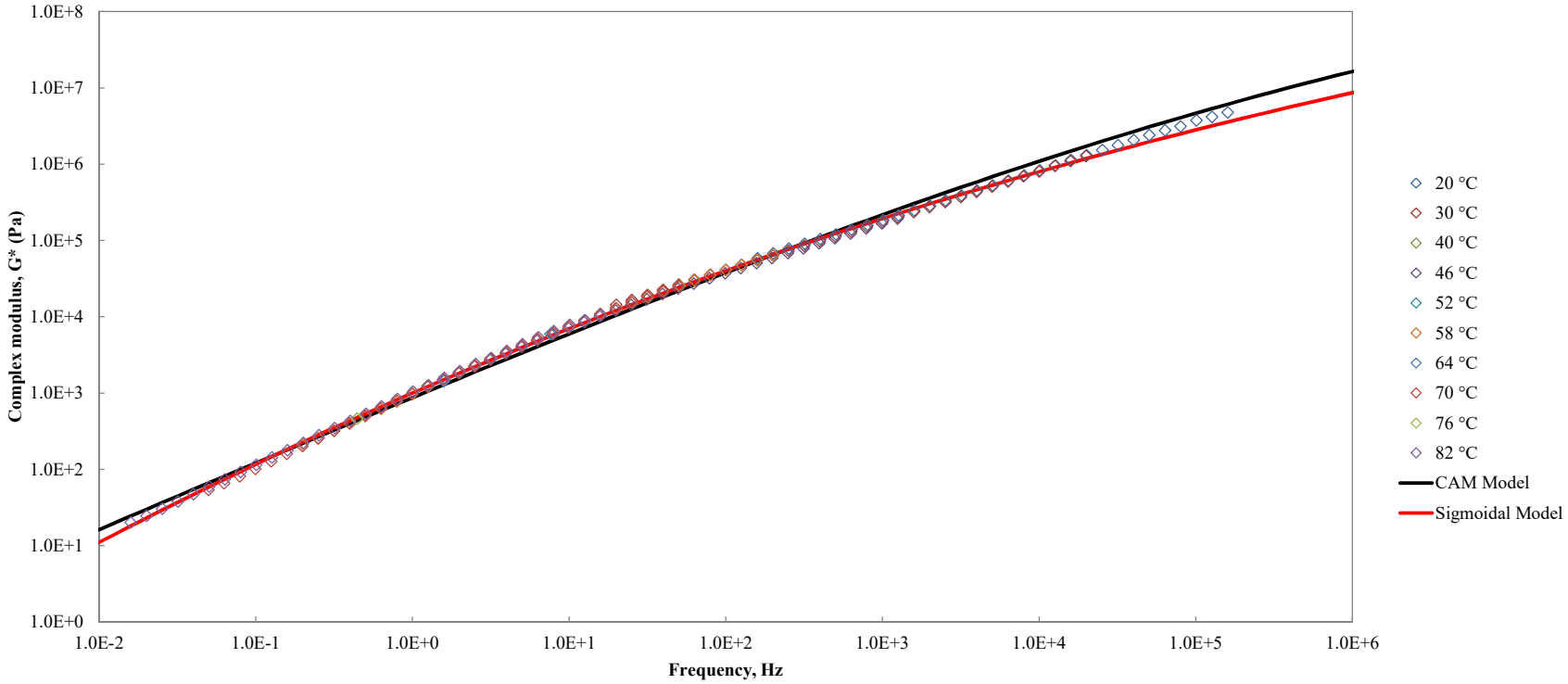

Figure B-26. Master curve of unaged non-centrifuged CP tested with parallel plates – 1 mm gap, T_{ref} = 64 °C

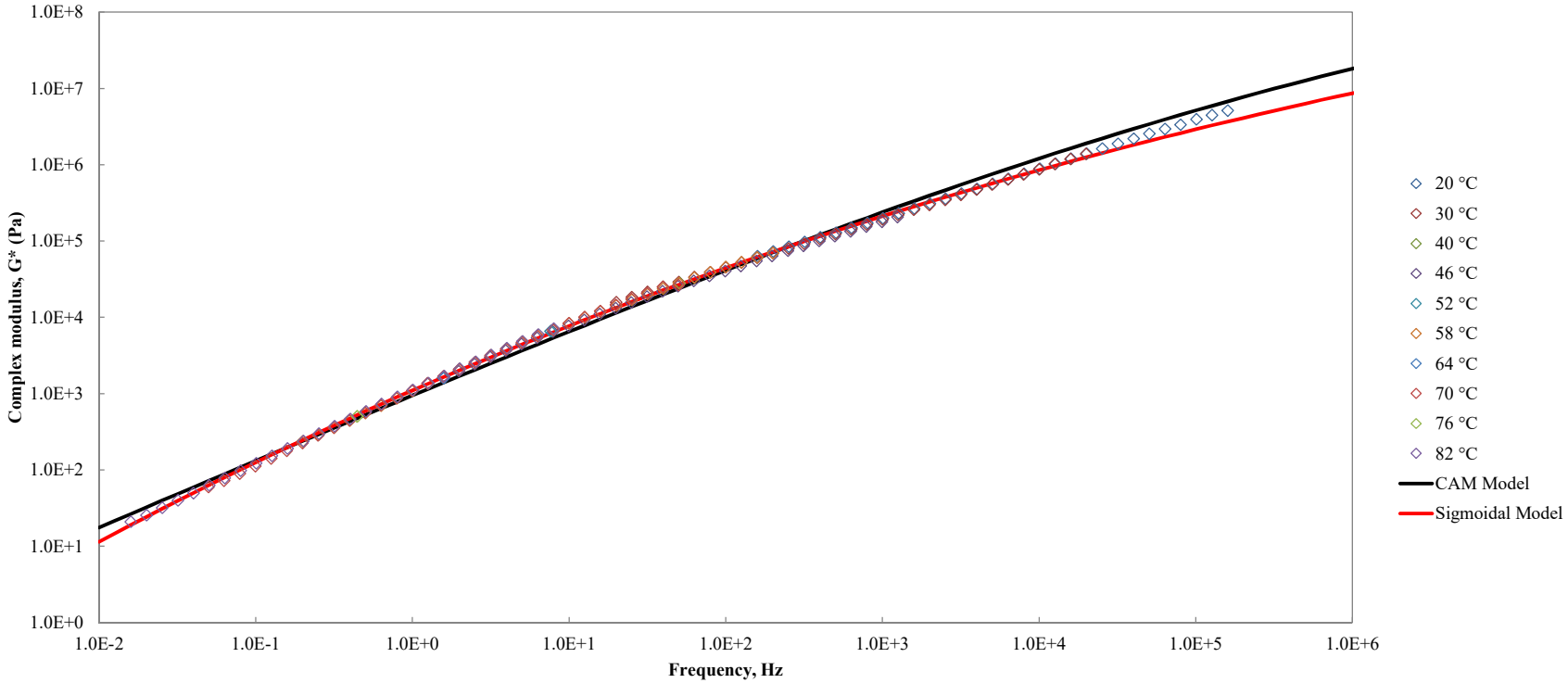

Figure B-27. Master curve of unaged non-centrifuged CP tested with parallel plates – 2 mm gap, T_{ref} = 64 °C

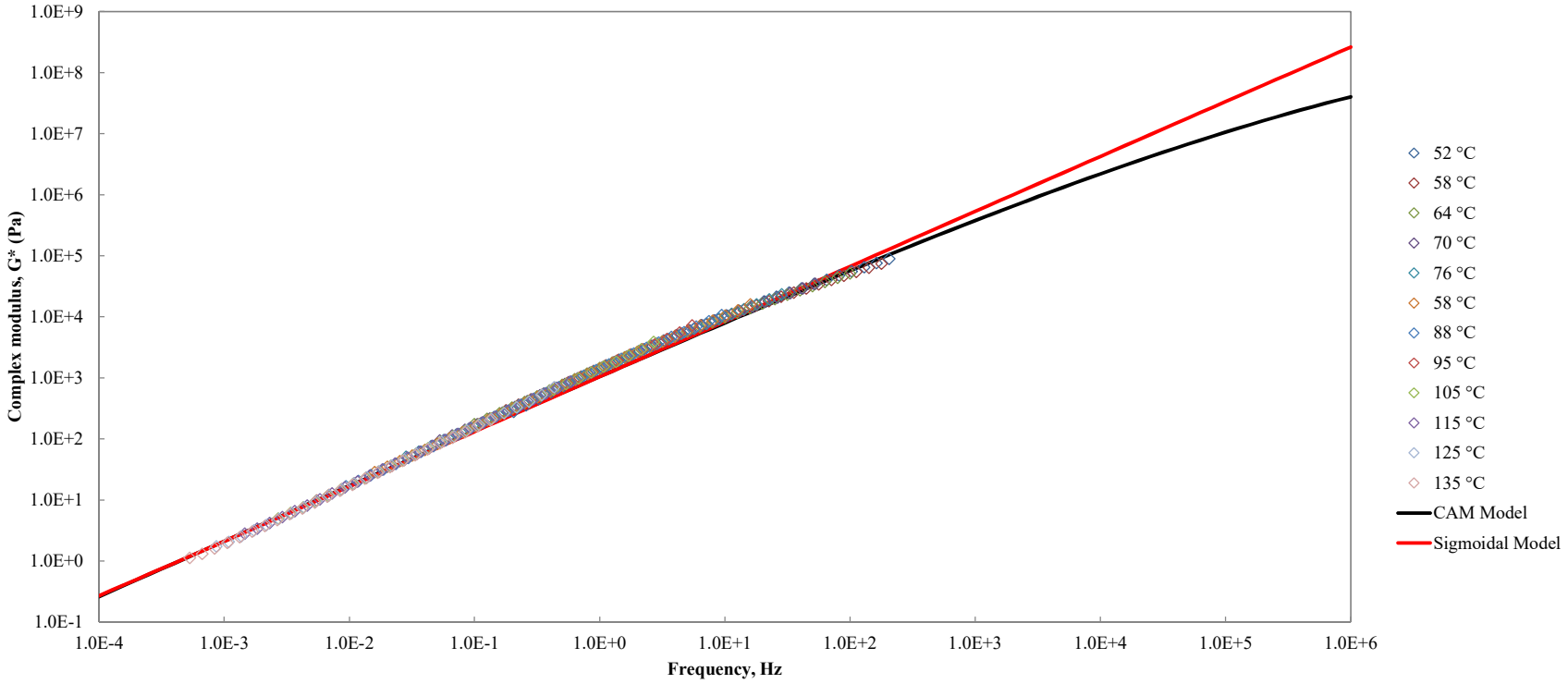

Figure B-28. Master curve of unaged non-centrifuged CP tested with concentric cylinder, T_{ref} = 64 °C

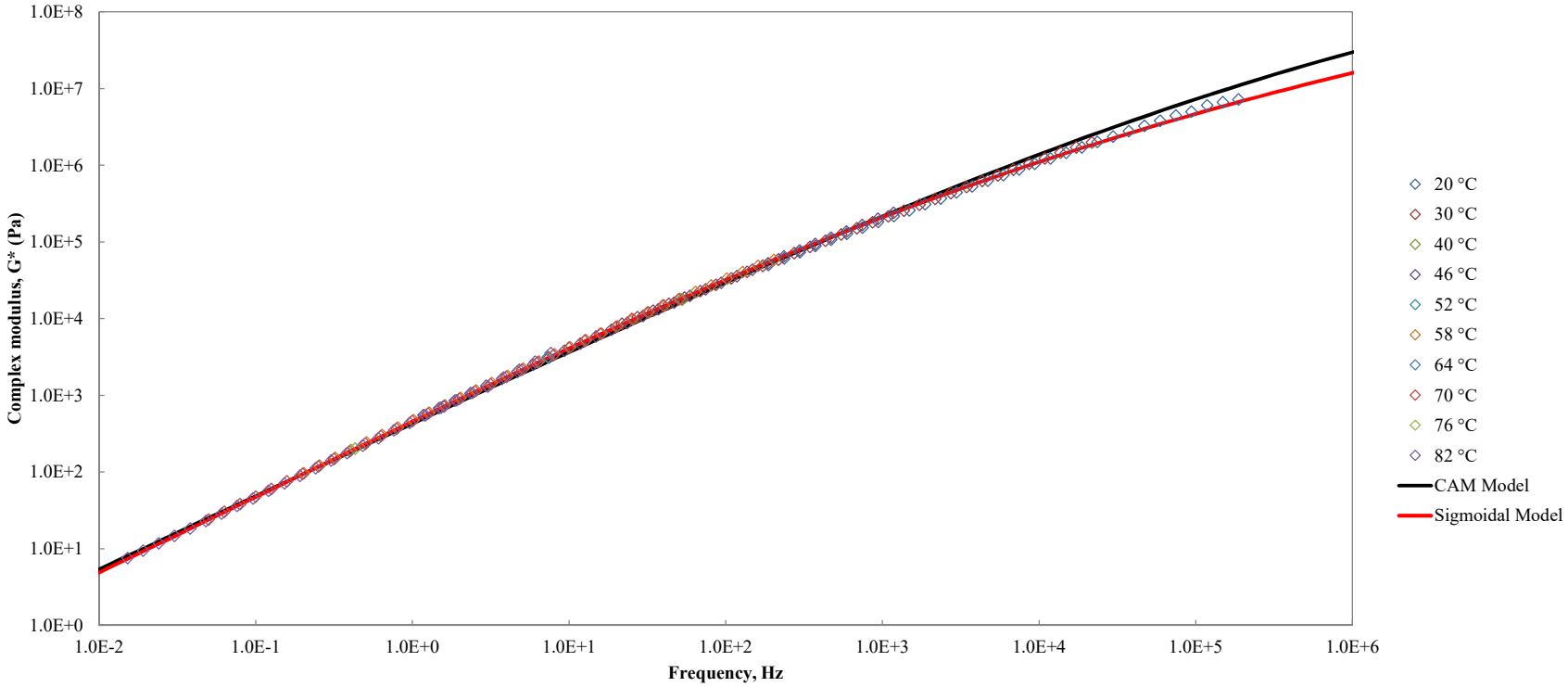

Figure B-29. Master curve of unaged centrifuged CP tested with parallel plates – 1 mm gap, T_{ref} = 64 °C

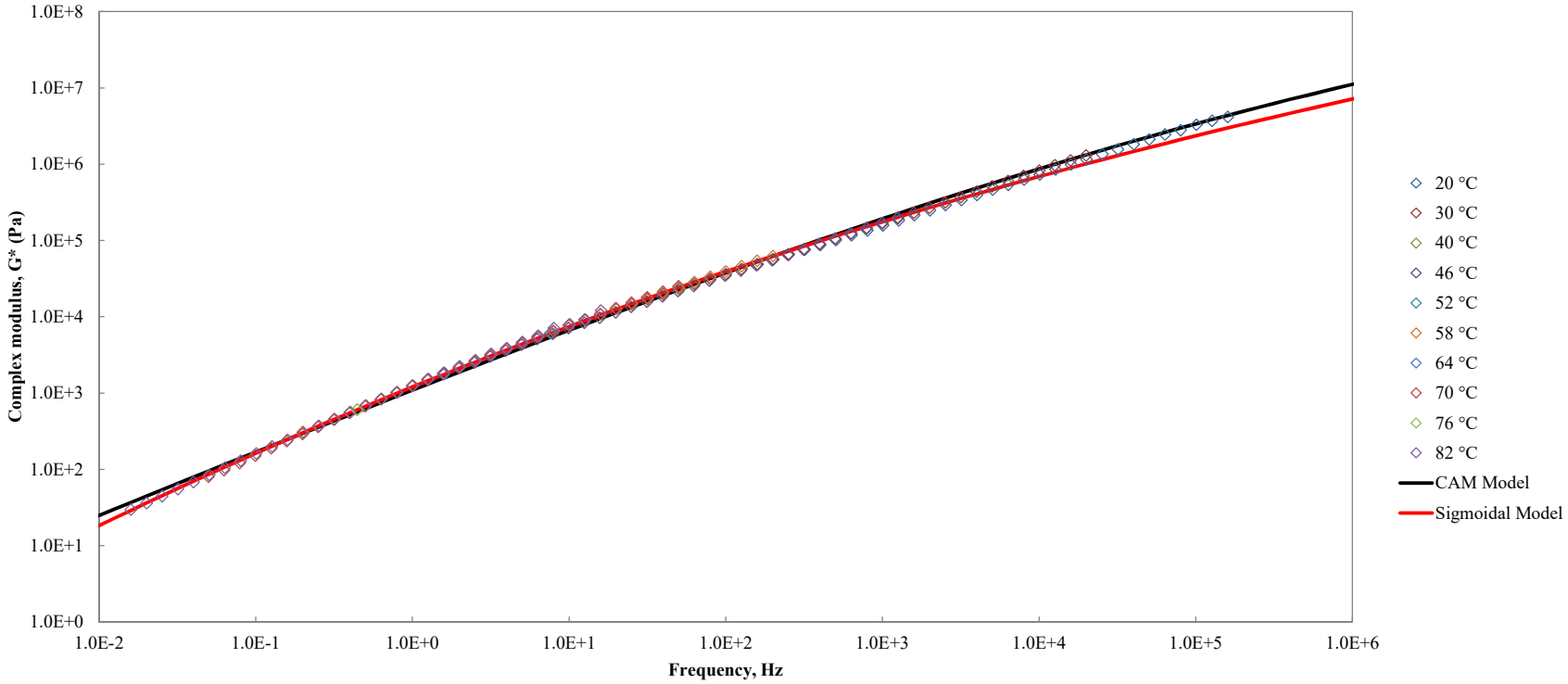

Figure B-30. Master curve of unaged non-centrifuged CP 72hrs cure tested with parallel plates – 1 mm gap, T_{ref} = 64 °C

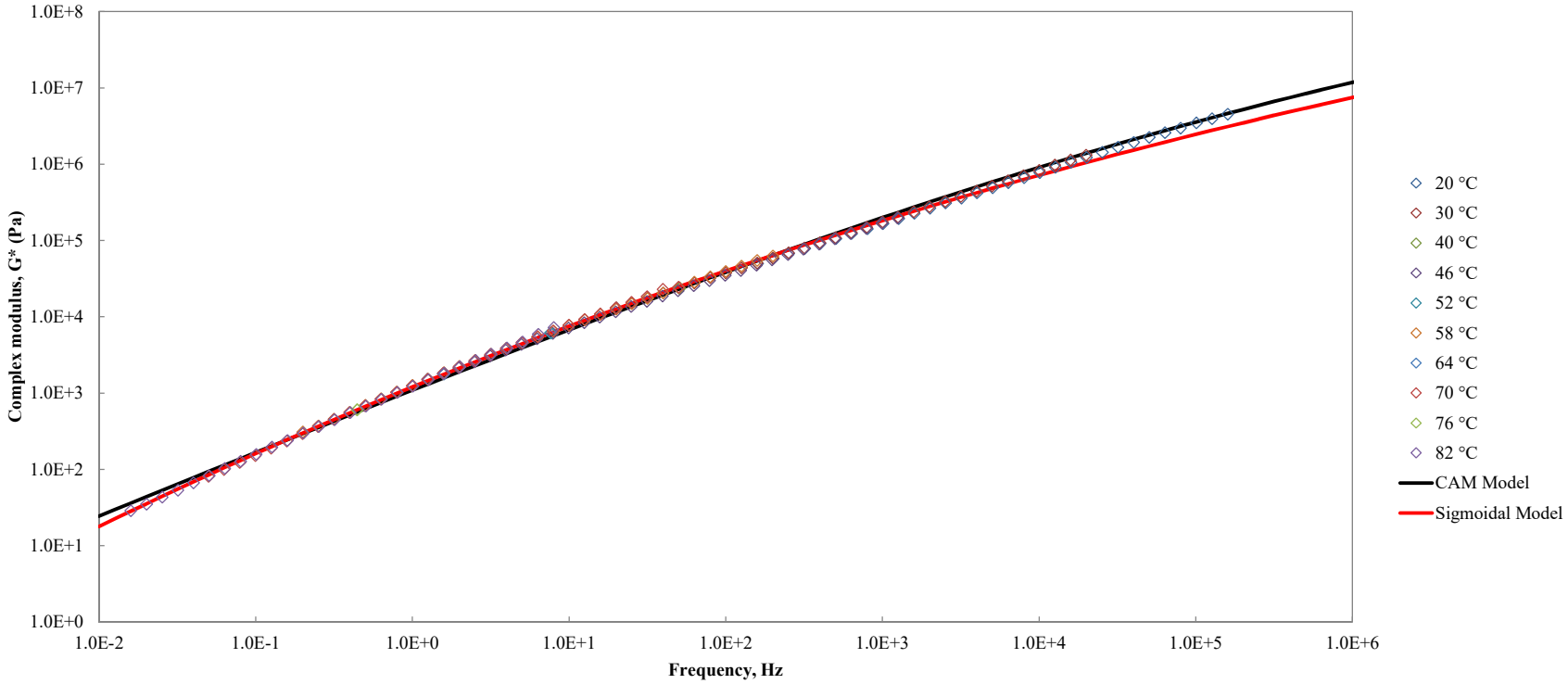

Figure B-31. Master curve of unaged non-centrifuged CP 72hrs cure tested with parallel plates – 2 mm gap, T_{ref} = 64 °C

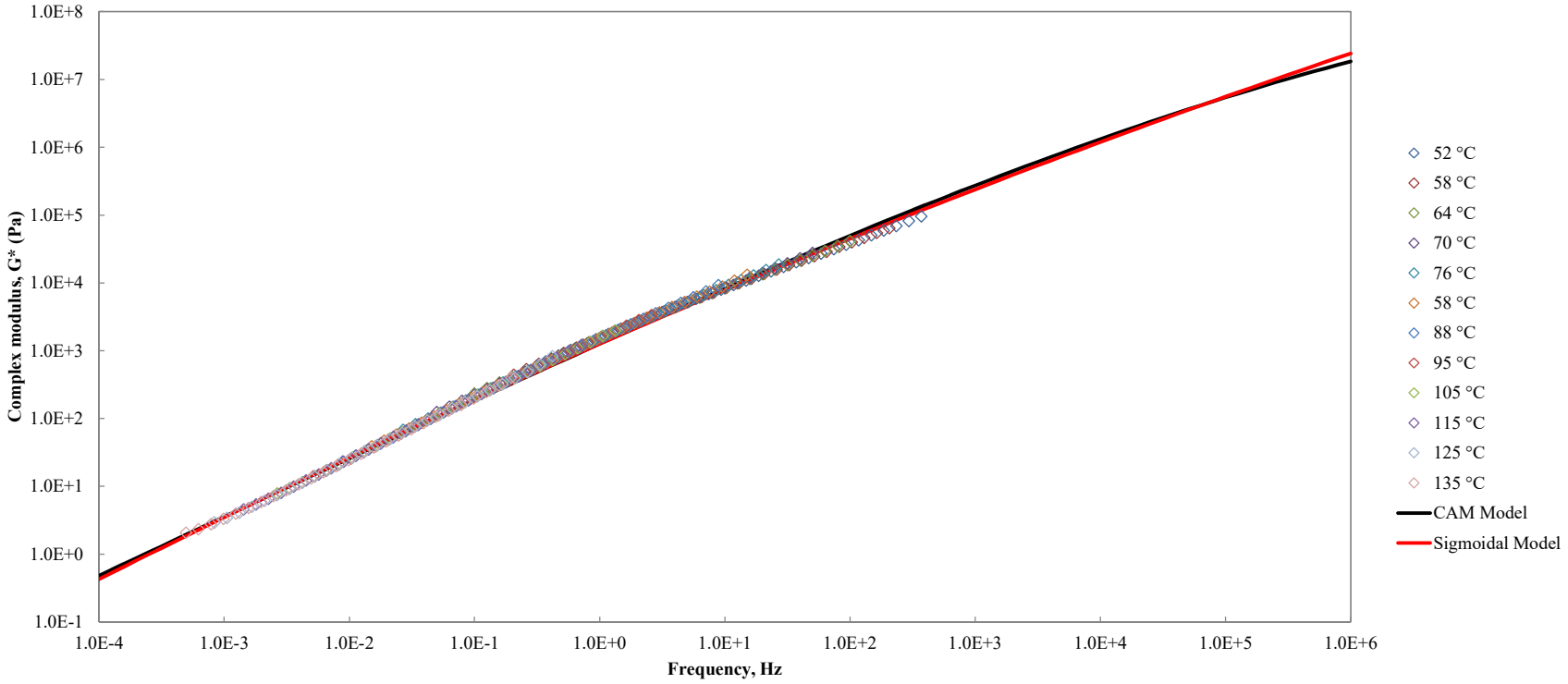

Figure B-32. Master curve of unaged non-centrifuged CP 72 hrs cure tested with concentric cylinders, T_{ref} = 64 °C

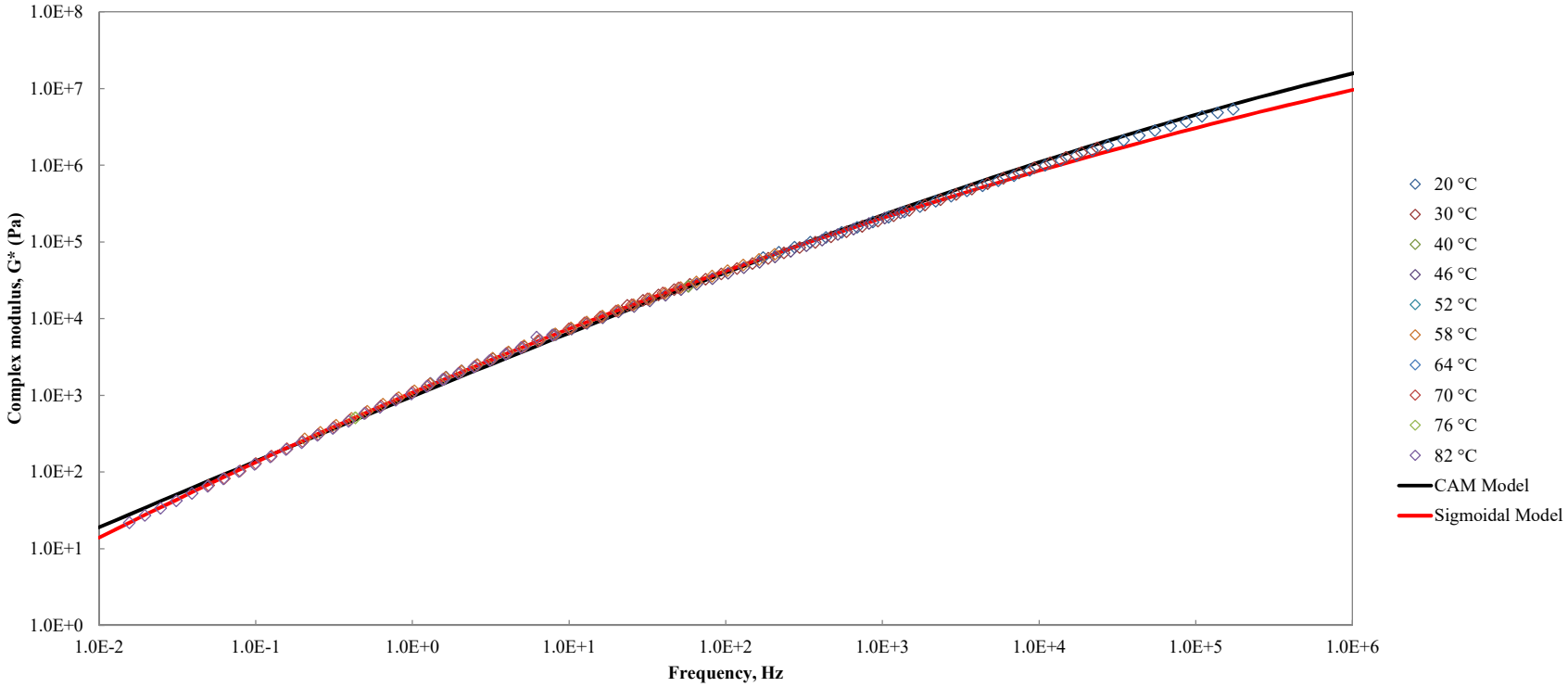

Figure B-33. Master curve of unaged centrifuged CP 72 hrs cure tested with parallel plates – 1 mm gap, T_{ref} = 64 °C

APPENDIX C. MASTER CURVES OF RTFO AGED MATERIALS

This appendix presents the master curves of the RTFO aged materials tested using different DSR geometries. The CAM and Sigmoidal models were fitted to the master curves.

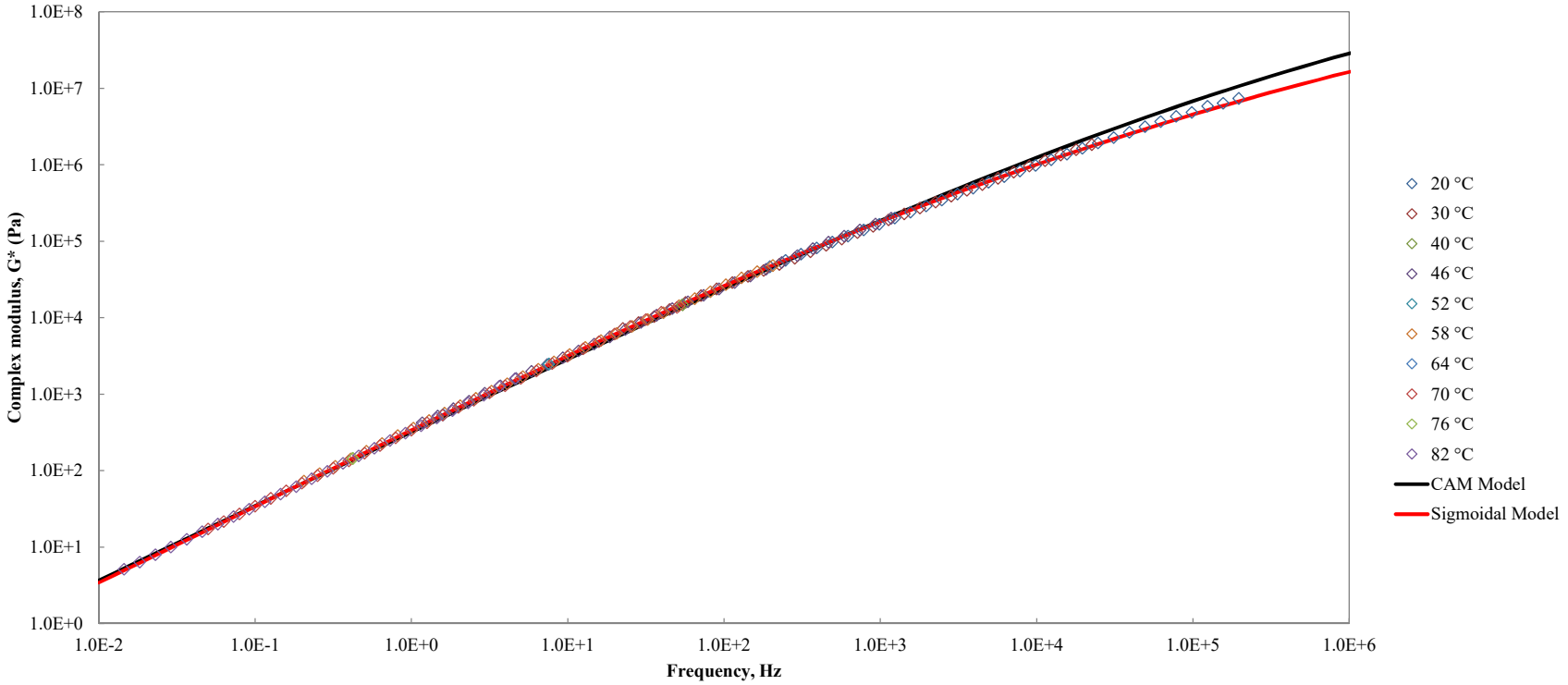

Figure C-1. Master curve of RTFO aged PG52-34 tested with parallel plates – 1 mm gap. T_{ref} = 64 °C

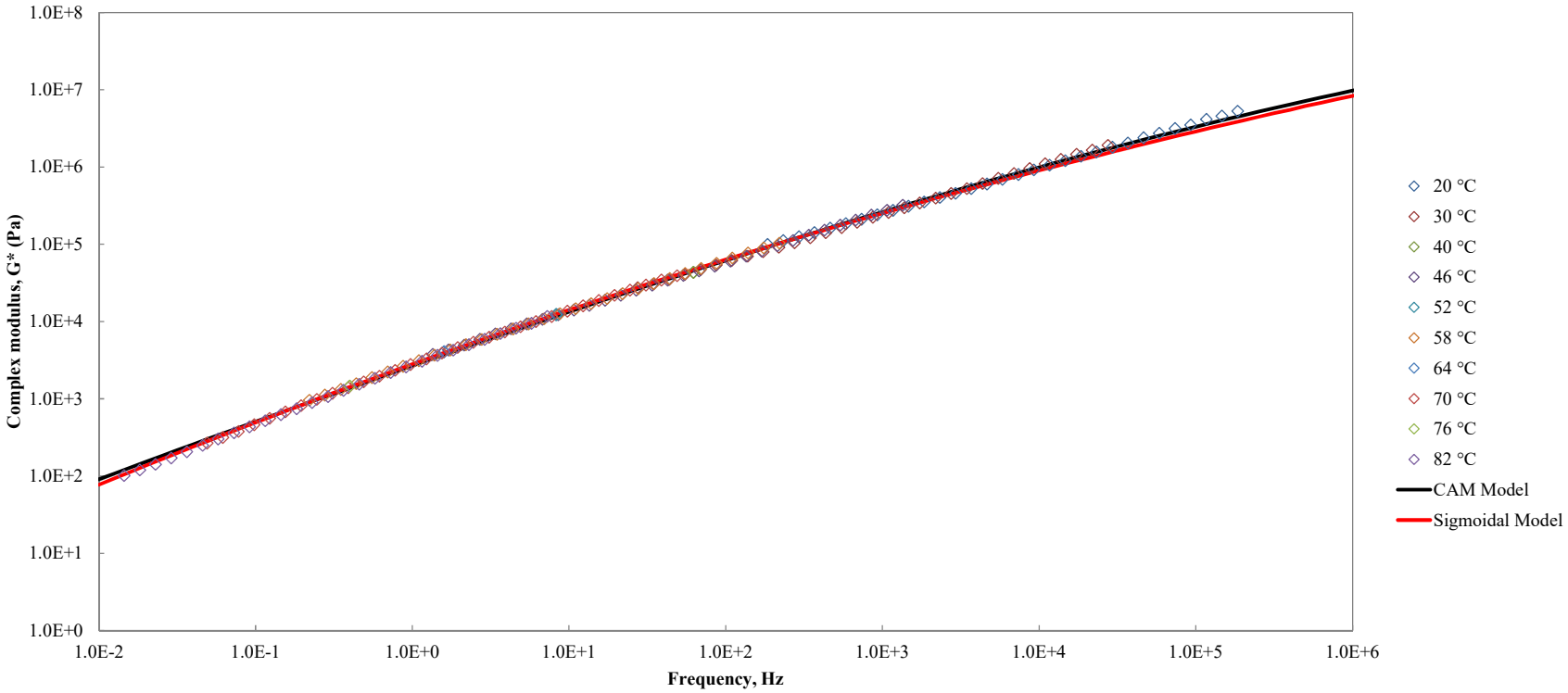

Figure C-2. Master curve of RTFO aged non-centrifuged AMB tested with parallel plates – 1 mm gap, T_{ref} = 64 °C

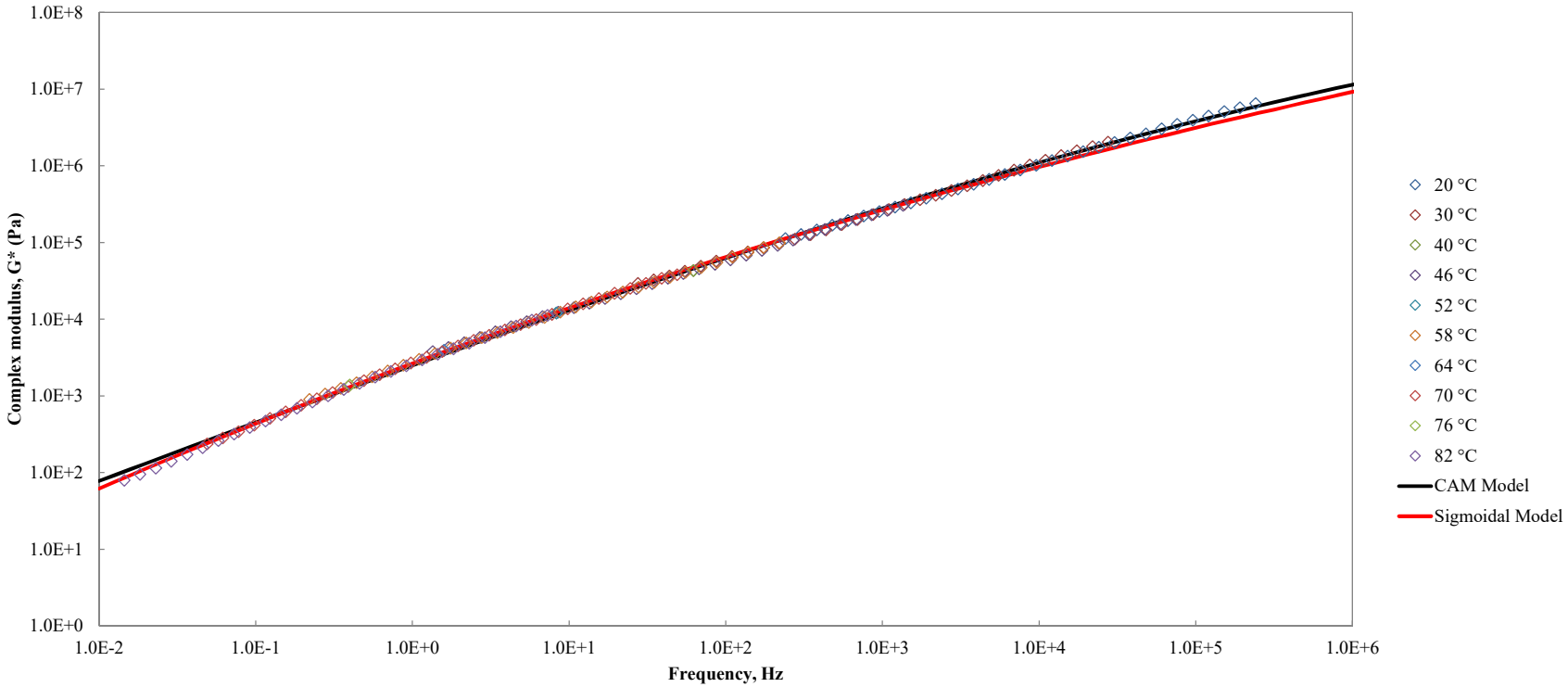

Figure C-3. Master curve of RTFO aged non-centrifuged AMB tested with parallel plates – 2 mm gap, T_{ref} = 64 °C

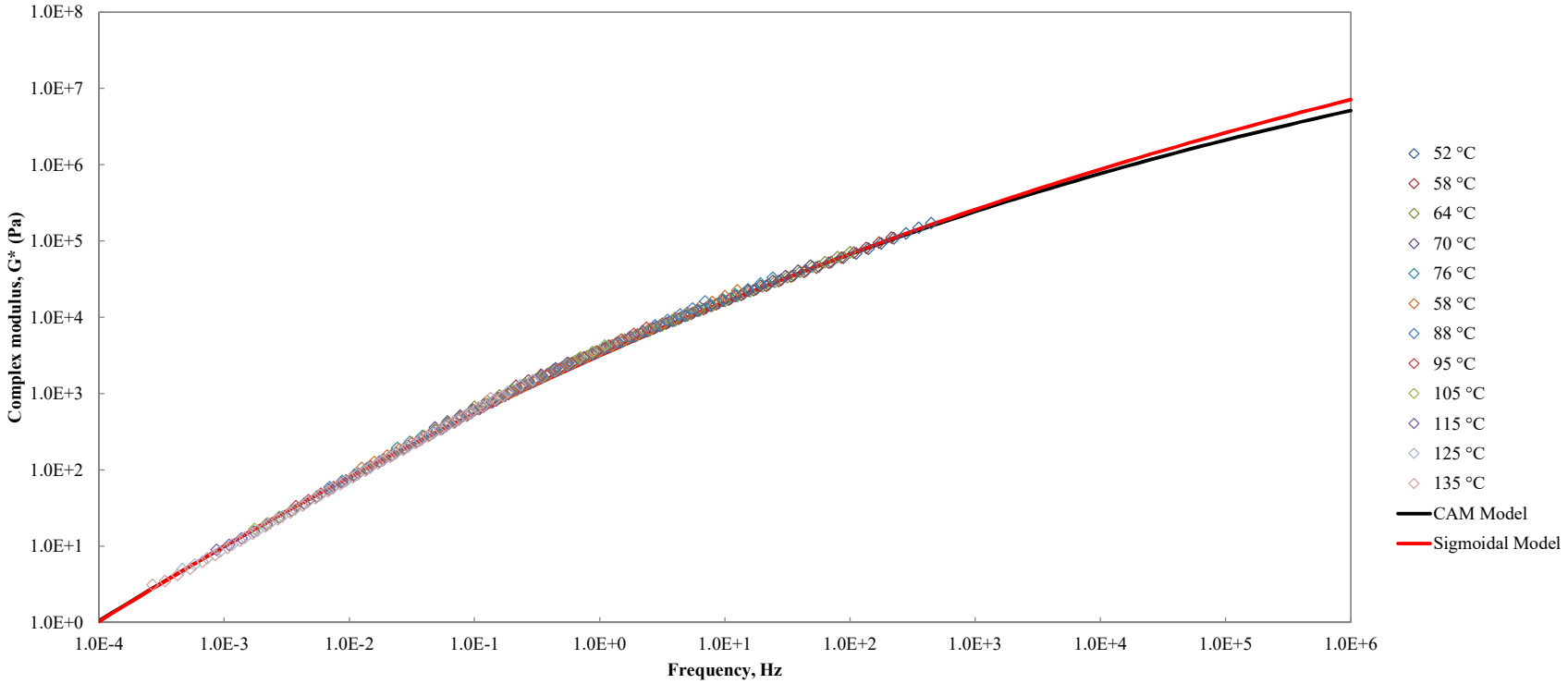

Figure C-4. Master curve of RTFO aged non-centrifuged AMB tested with concentric cylinders, T_{ref} = 64 °C

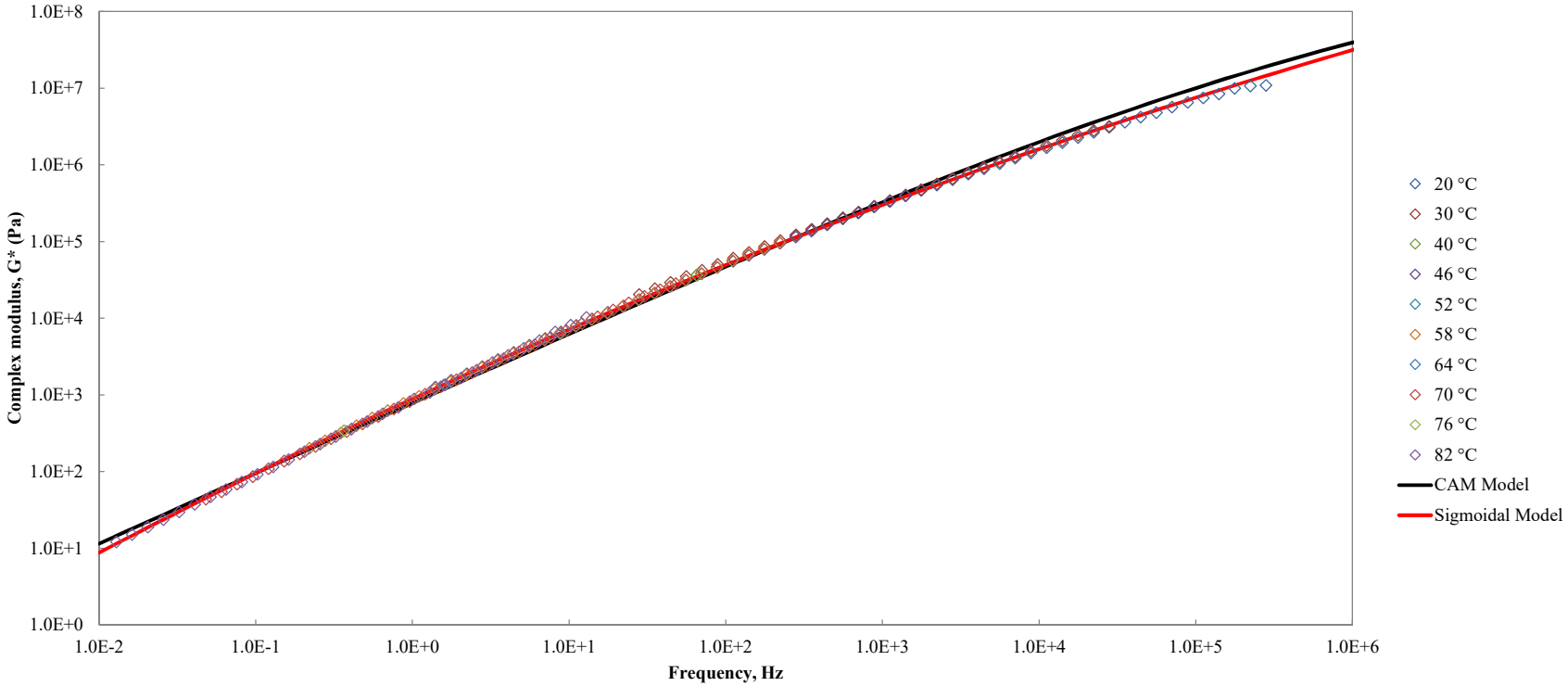

Figure C-5. Master curve of RTFO aged centrifuged AMB tested with parallel plates – 1 mm gap, T_{ref} = 64 °C

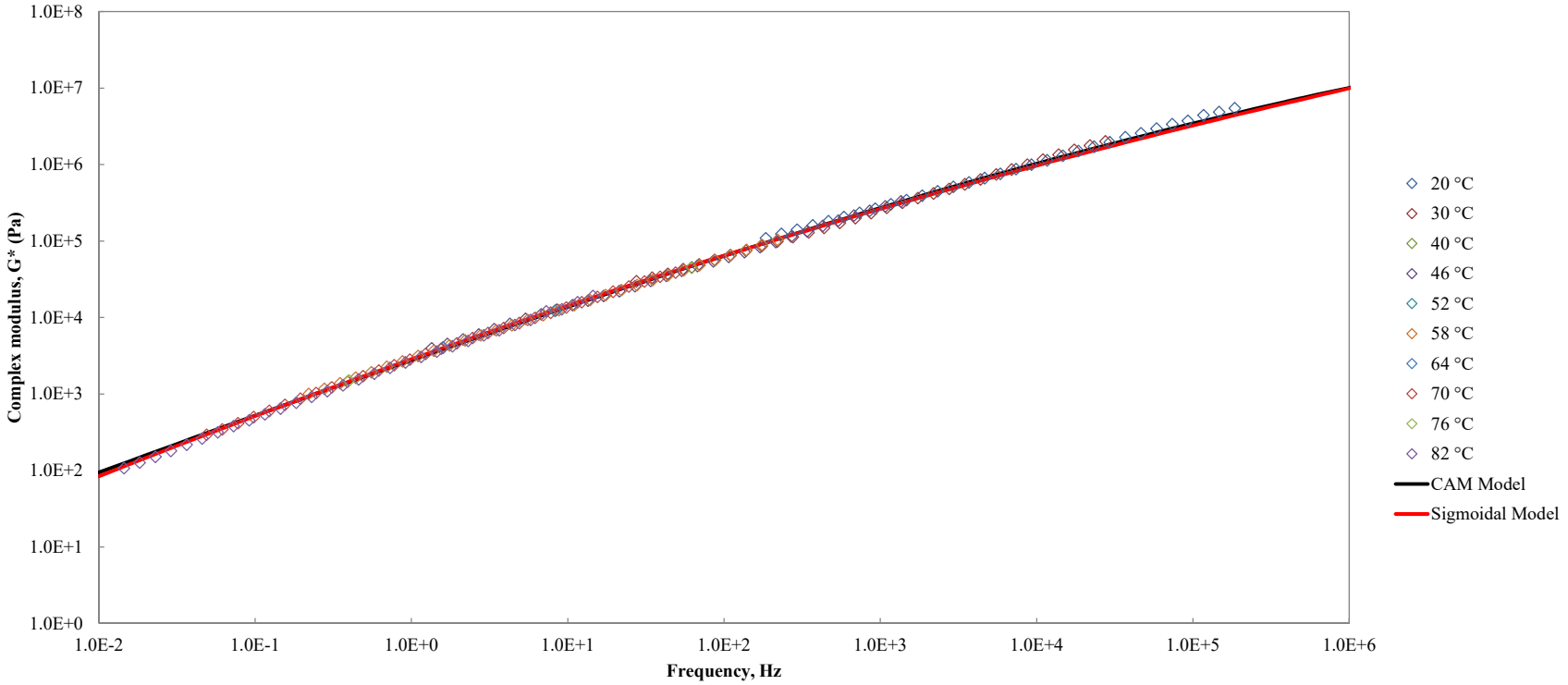

Figure C-6. Master curve of RTFO aged non-centrifuged AMB 72 hrs cure tested with parallel plates – 1 mm gap, T_{ref} = 64 °C

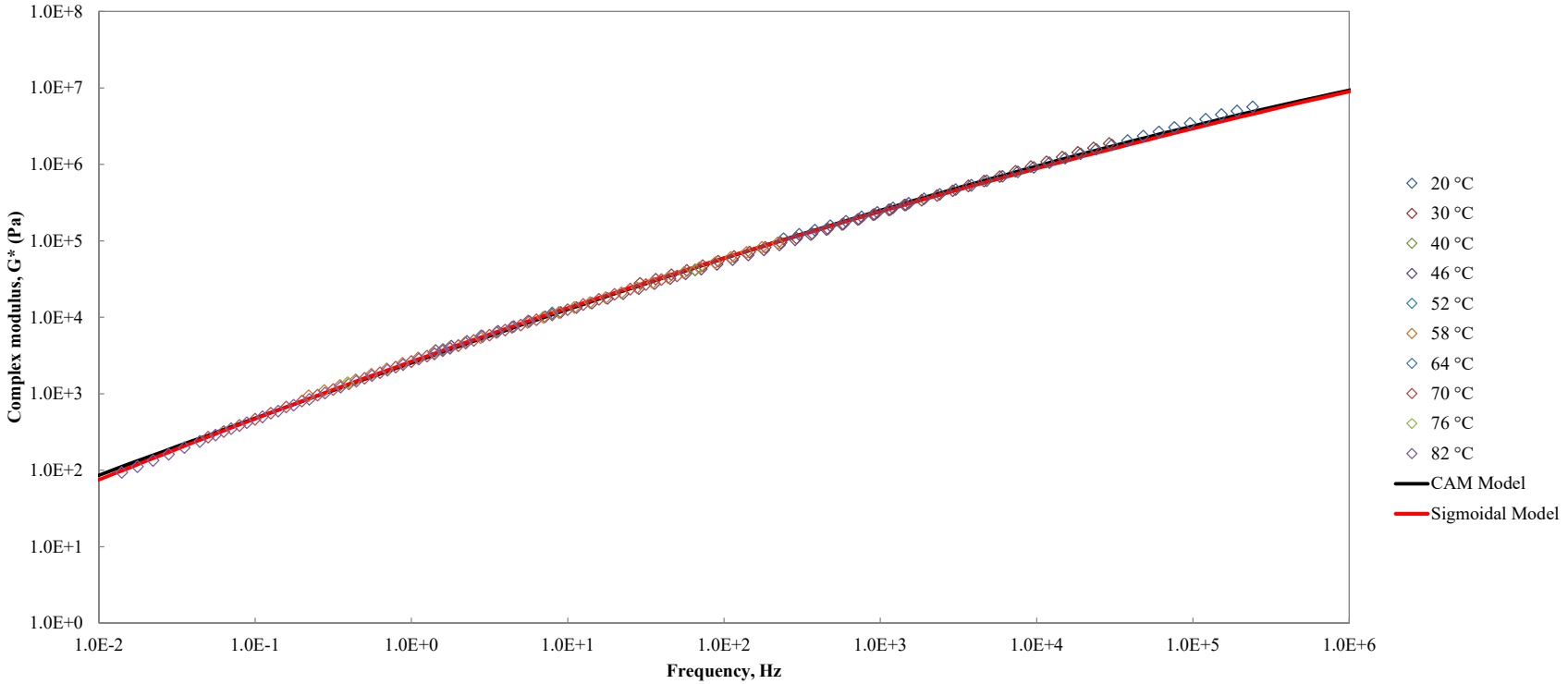

Figure C-7. Master curve of RTFO aged non-centrifuged AMB 72hrs cure tested with parallel plates – 2 mm gap, T_{ref} = 64 °C

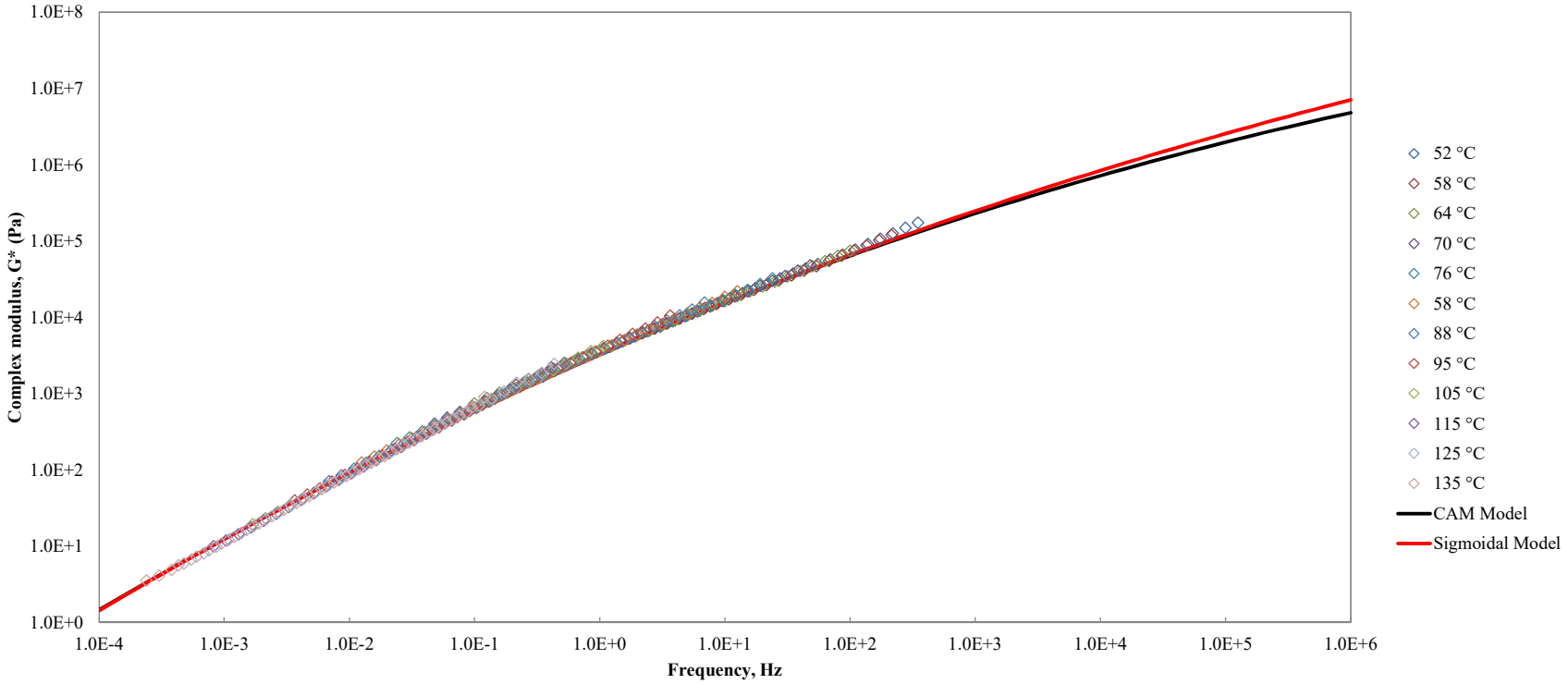

Figure C-8. Master curve of RTFO aged non-centrifuged AMB 72 hrs cure tested with concentric cylinders, T_{ref} = 64 °C

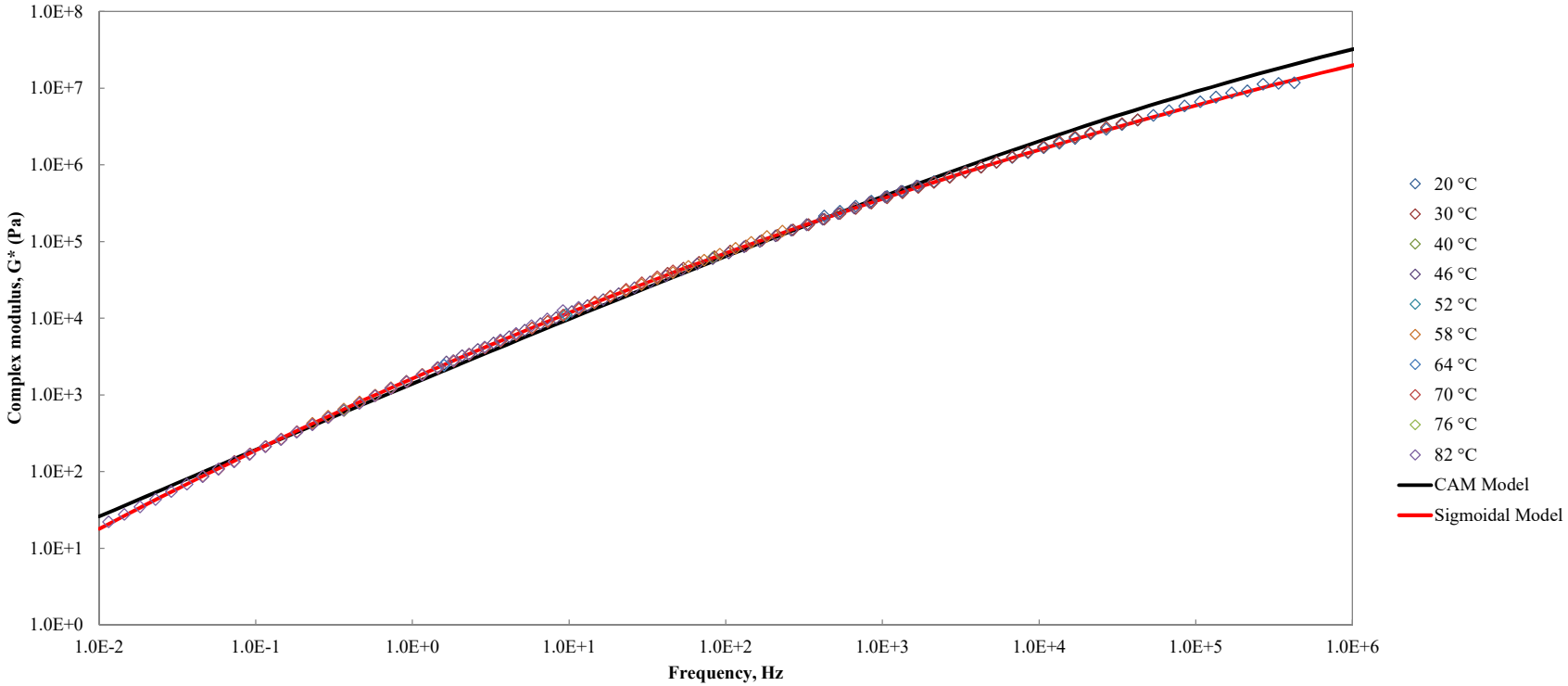

Figure C-9. Master curve of RTFO aged centrifuged AMB 72 hrs cure tested with parallel plates – 1 mm gap, T_{ref} = 64 °C

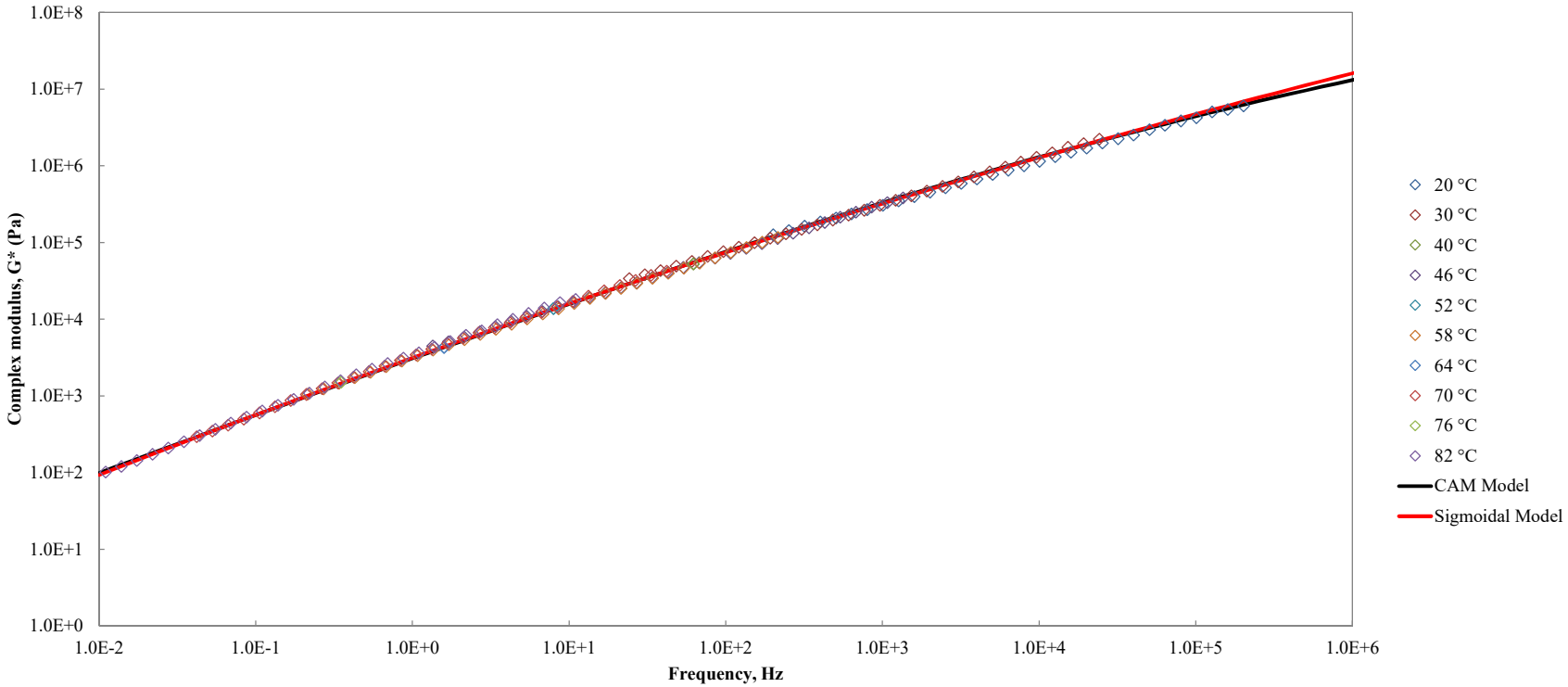

Figure C-10. Master curve of RTFO aged non-centrifuged AP tested with parallel plates – 1 mm gap, T_{ref} = 64 °C

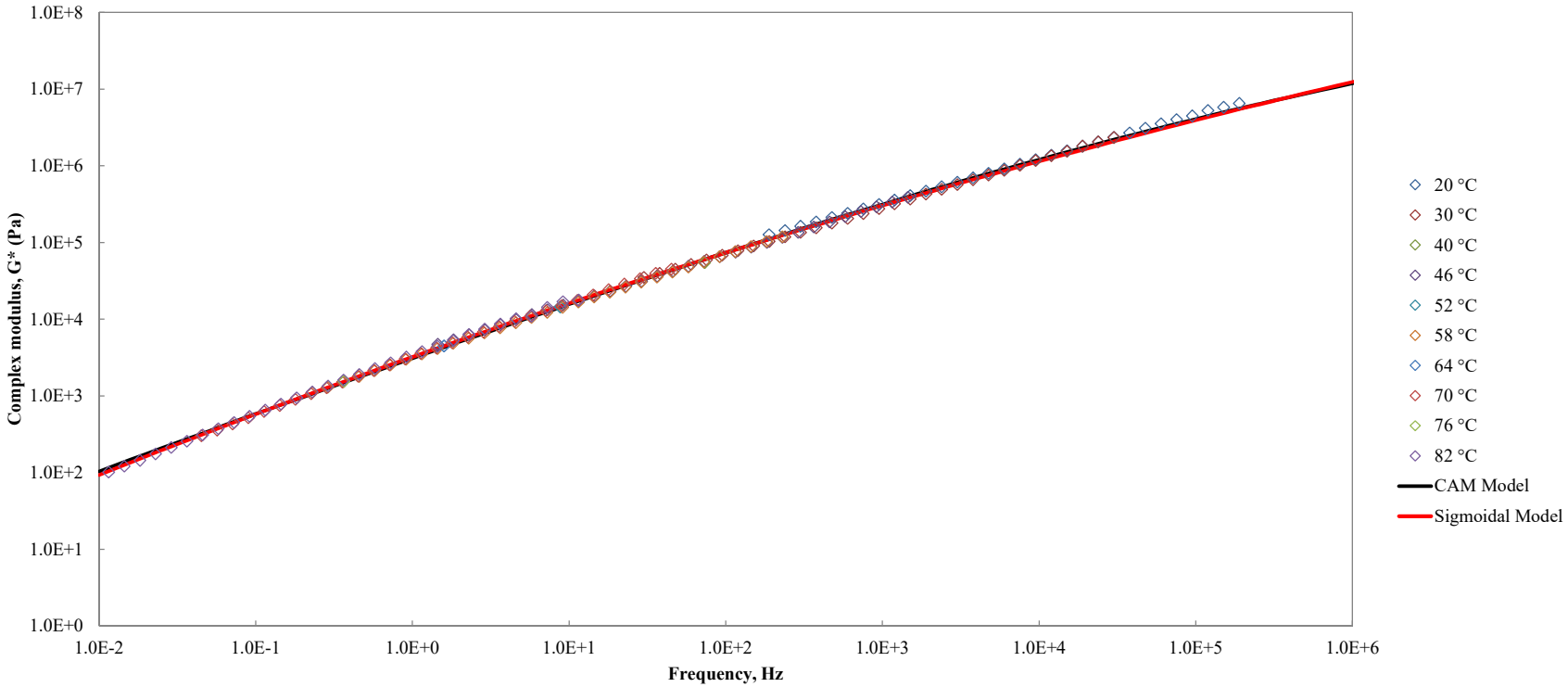

Figure C-11. Master curve of RTFO aged non-centrifuged AP tested with parallel plates – 2 mm gap, T_{ref} = 64 °C

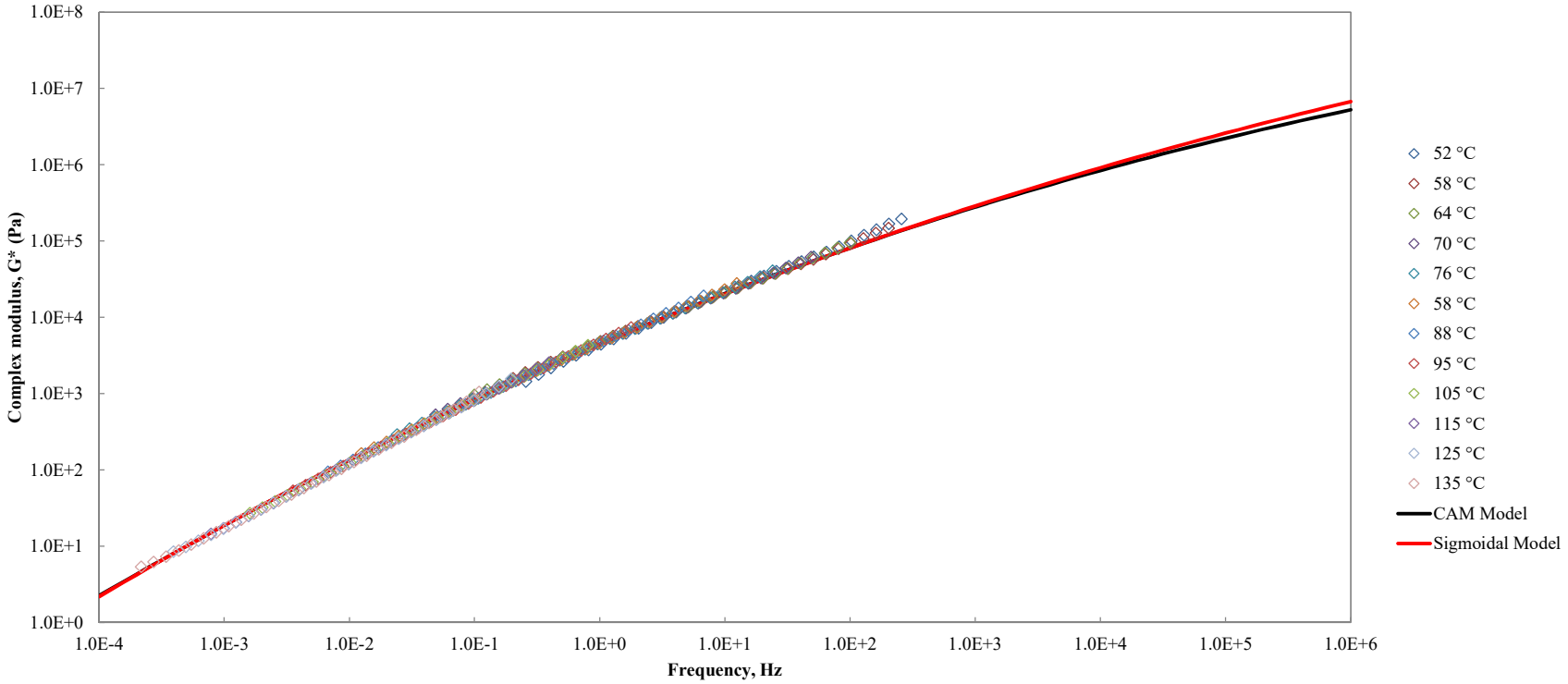

Figure C-12. Master curve of RTFO aged non-centrifuged AP tested with concentric cylinders, T_{ref} = 64 °C

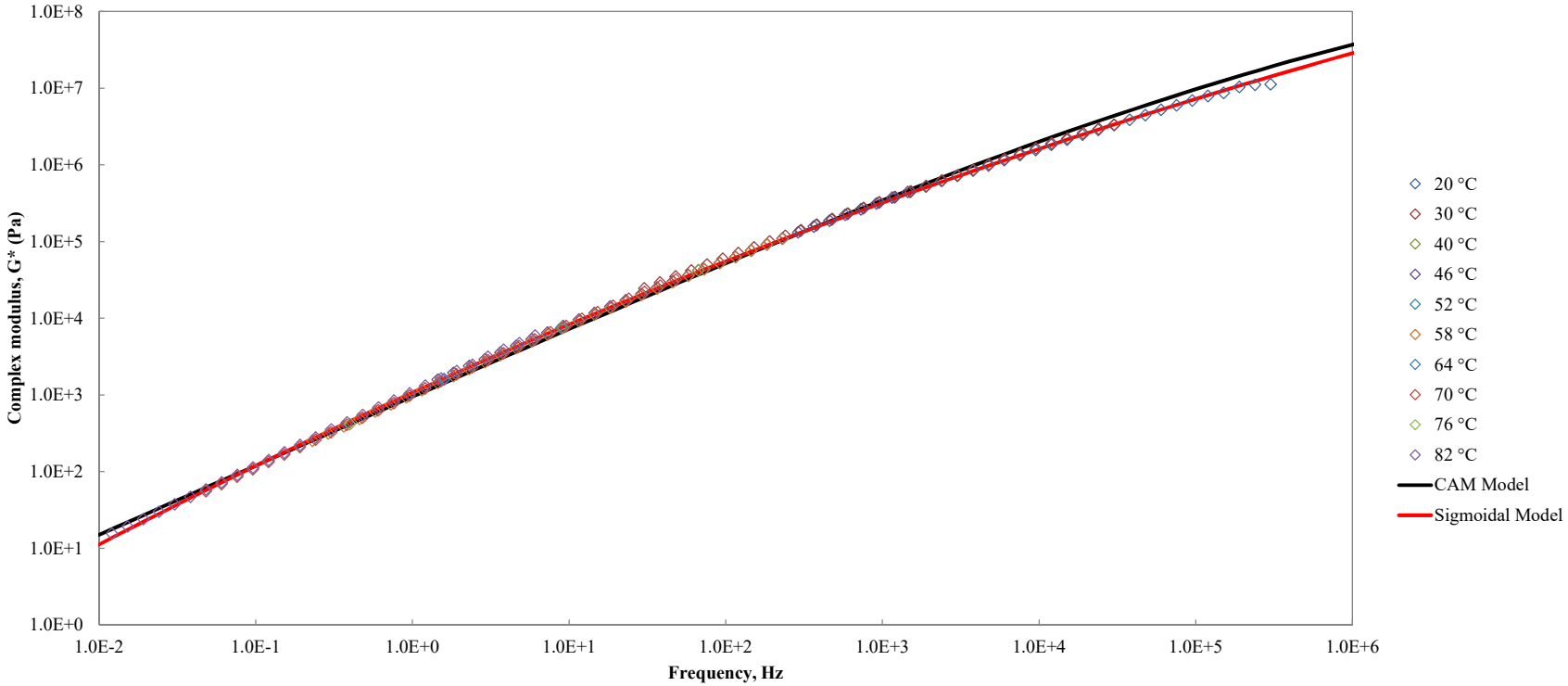

Figure C-13. Master curve of RTFO aged centrifuged AP tested with parallel plates – 1 mm gap, T_{ref} = 64 °C

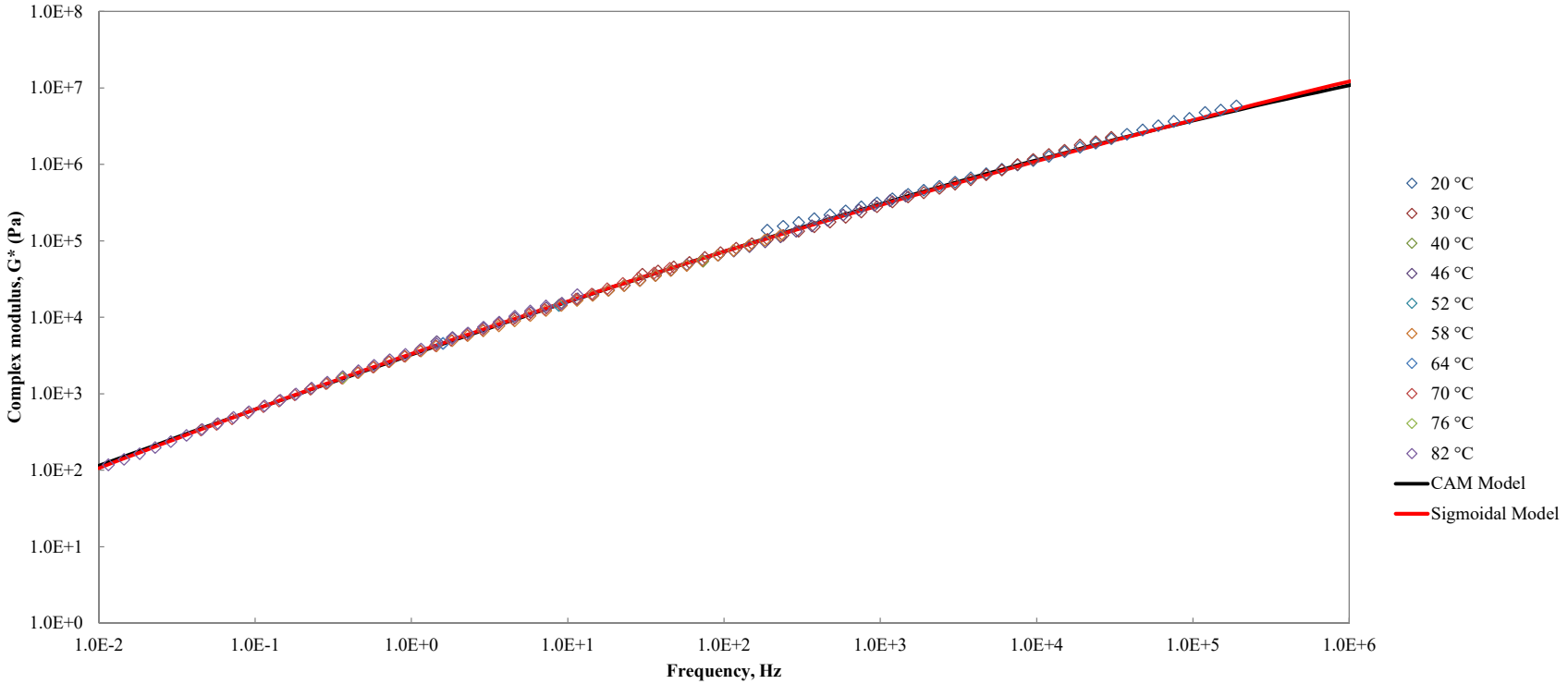

Figure C-14. Master curve of RTFO aged non-centrifuged AP 72 hrs cure tested with parallel plates – 1 mm gap, T_{ref} = 64 °C

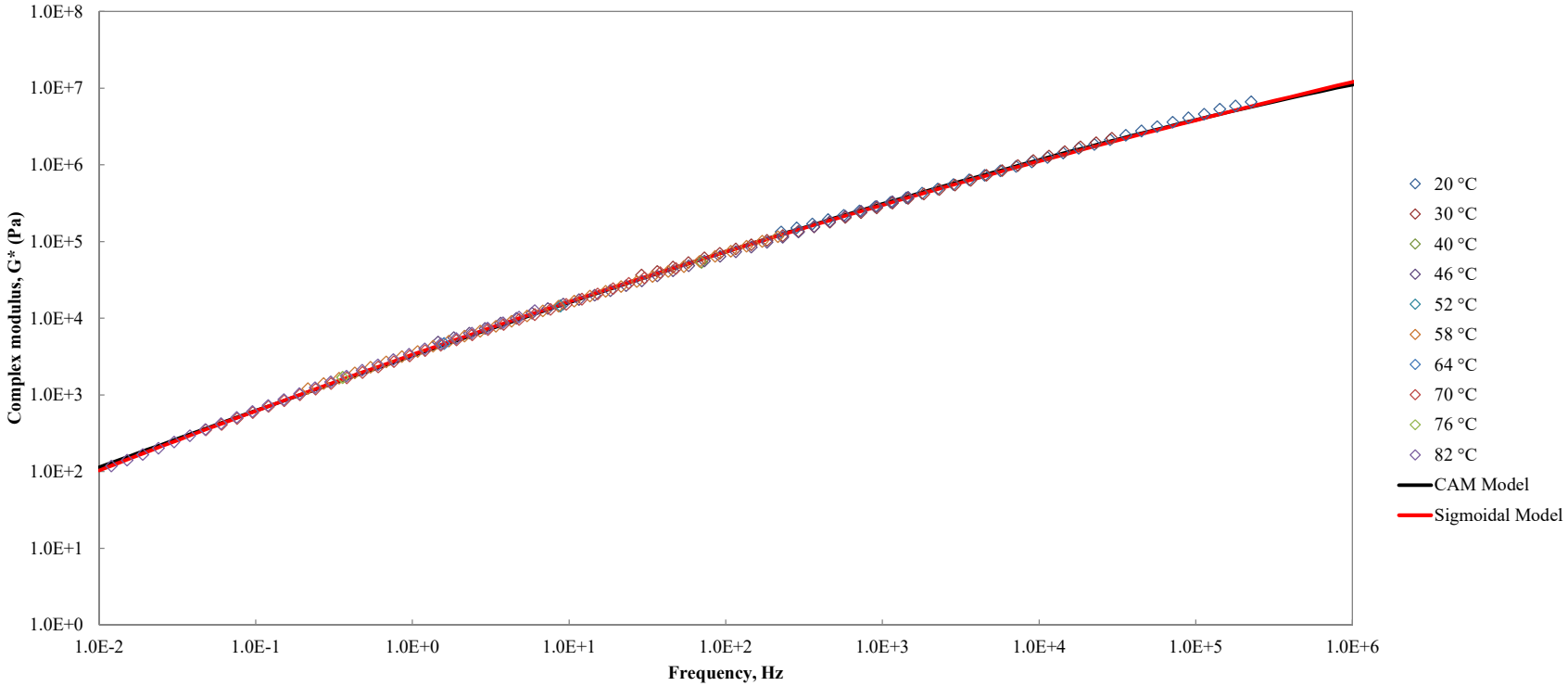

Figure C-15. Master curve of RTFO aged non-centrifuged AP 72 hrs tested with parallel plates – 2 mm gap, T_{ref} = 64 °C

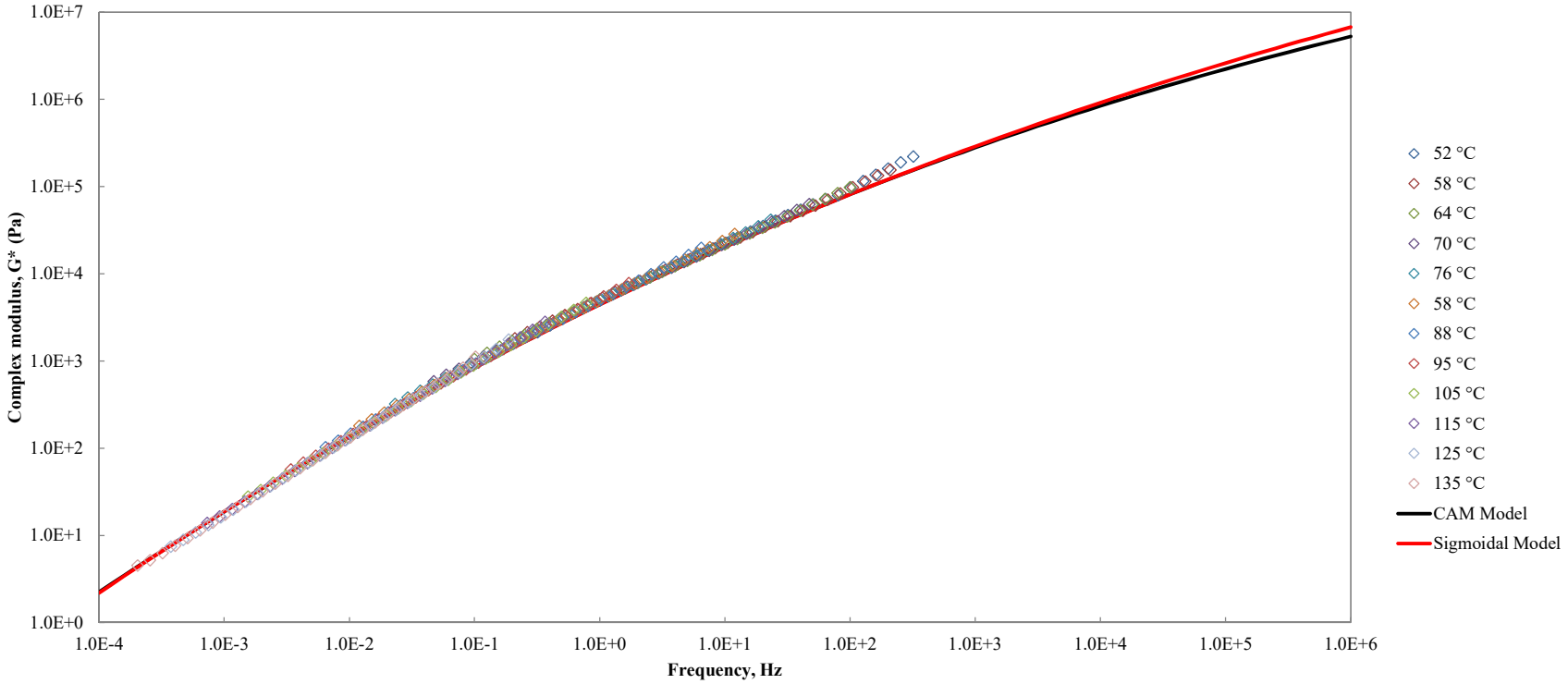

Figure C-16. Master curve of RTFO aged non-centrifuged AP 72 hrs cure tested with concentric cylinders, T_{ref} = 64 °C

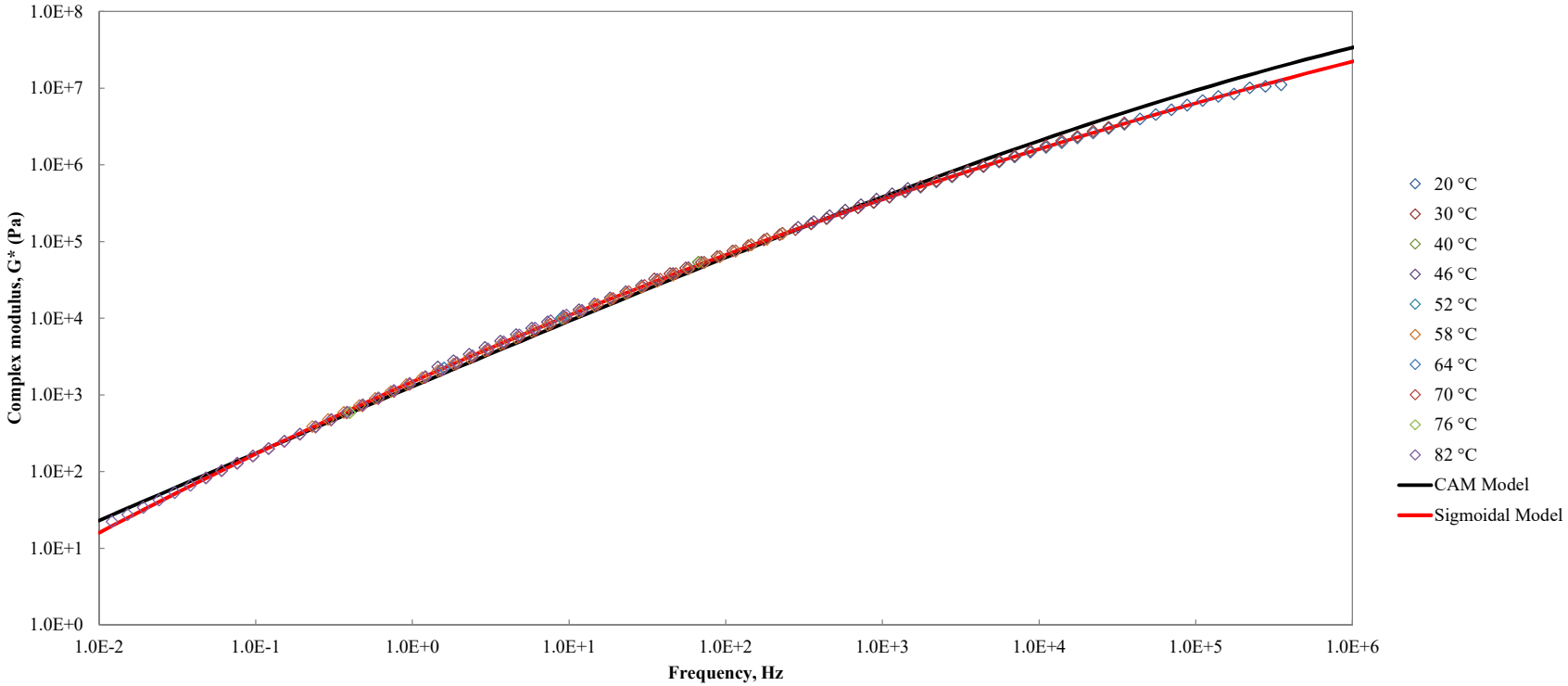

Figure C-17. Master curve of RTFO aged centrifuged AP 72 hrs cure tested with parallel plates – 1 mm gap, T_{ref} = 64 °C

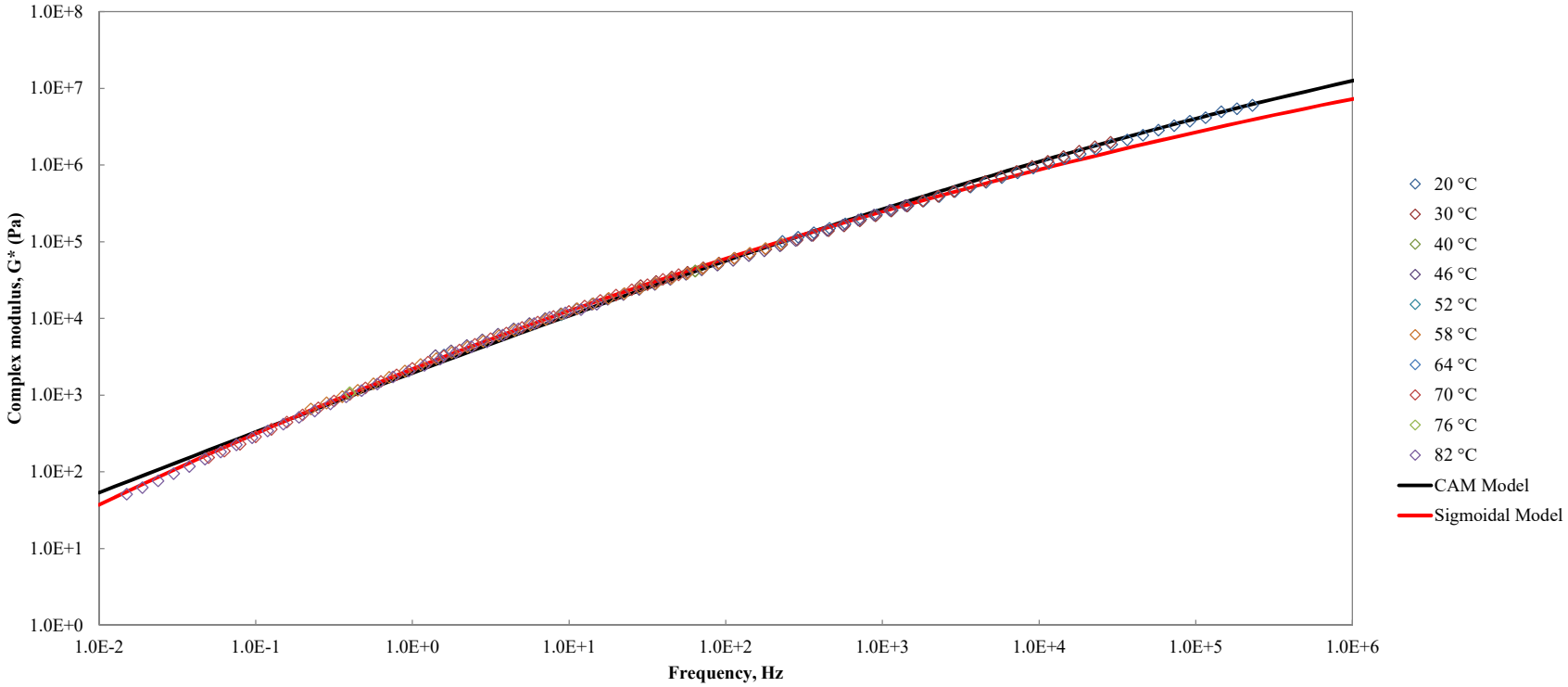

Figure C-18. Master curve of RTFO aged non-centrifuged CRYO tested with parallel plates – 1 mm gap, T_{ref} = 64 °C

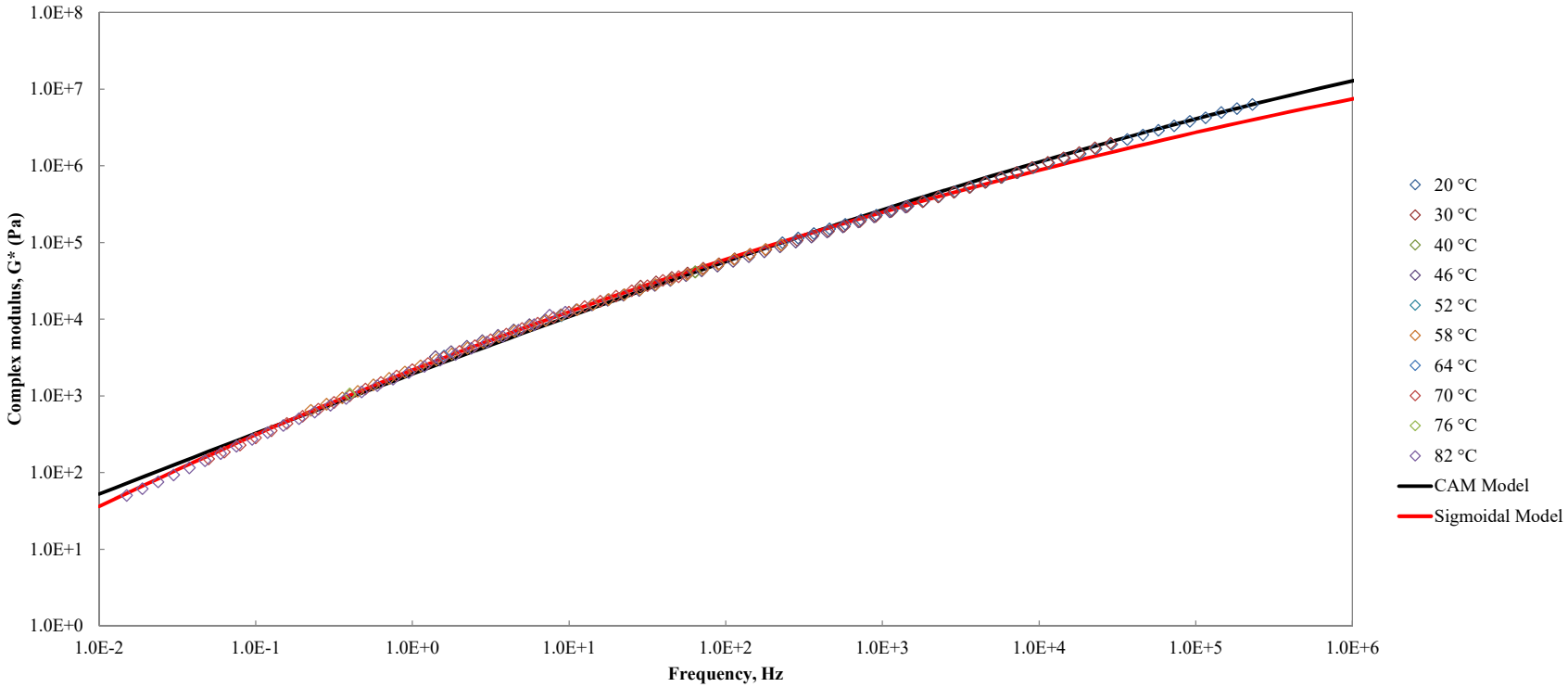

Figure C-19. Master curve of RTFO aged non-centrifuged CRYO tested with parallel plates – 2 mm gap, T_{ref} = 64 °C

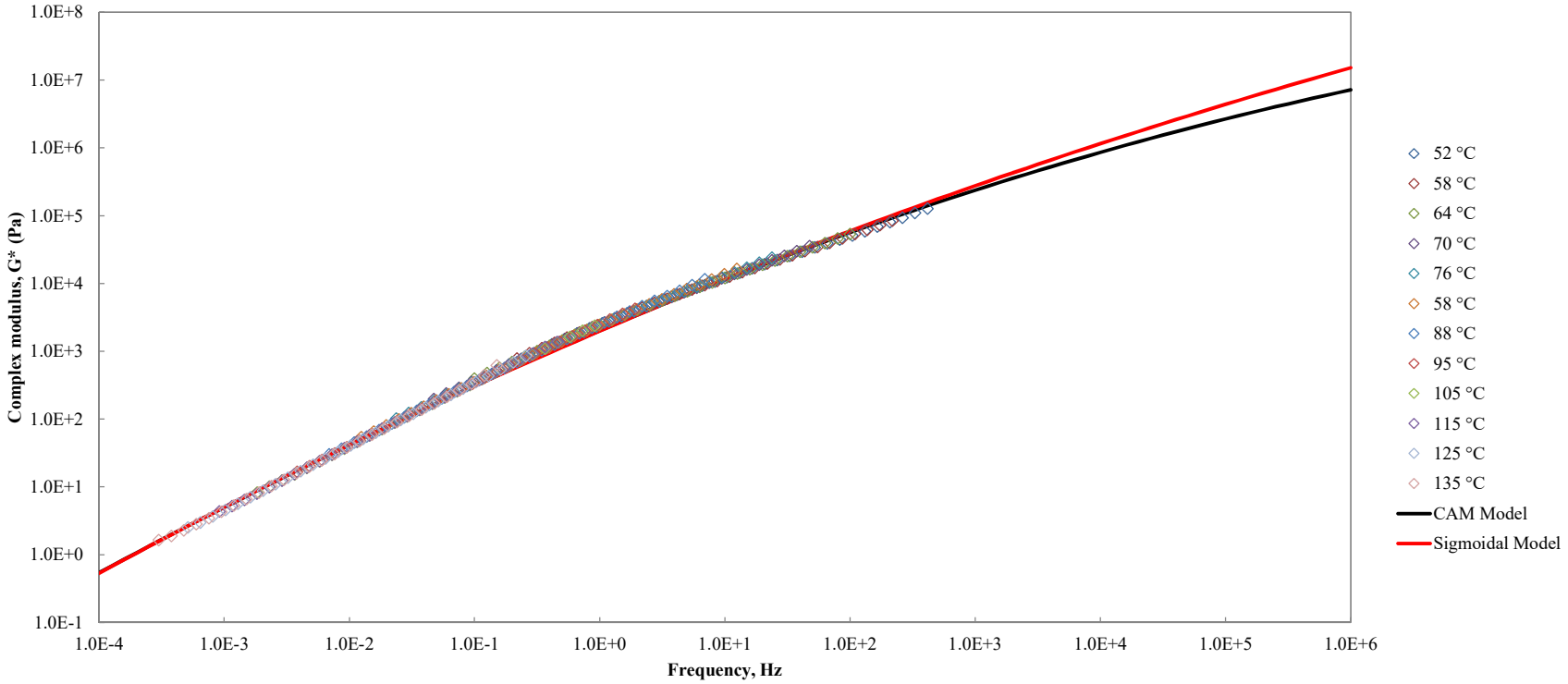

Figure C-20. Master curve of RTFO aged non-centrifuged CRYO tested with concentric cylinders, T_{ref} = 64 °C

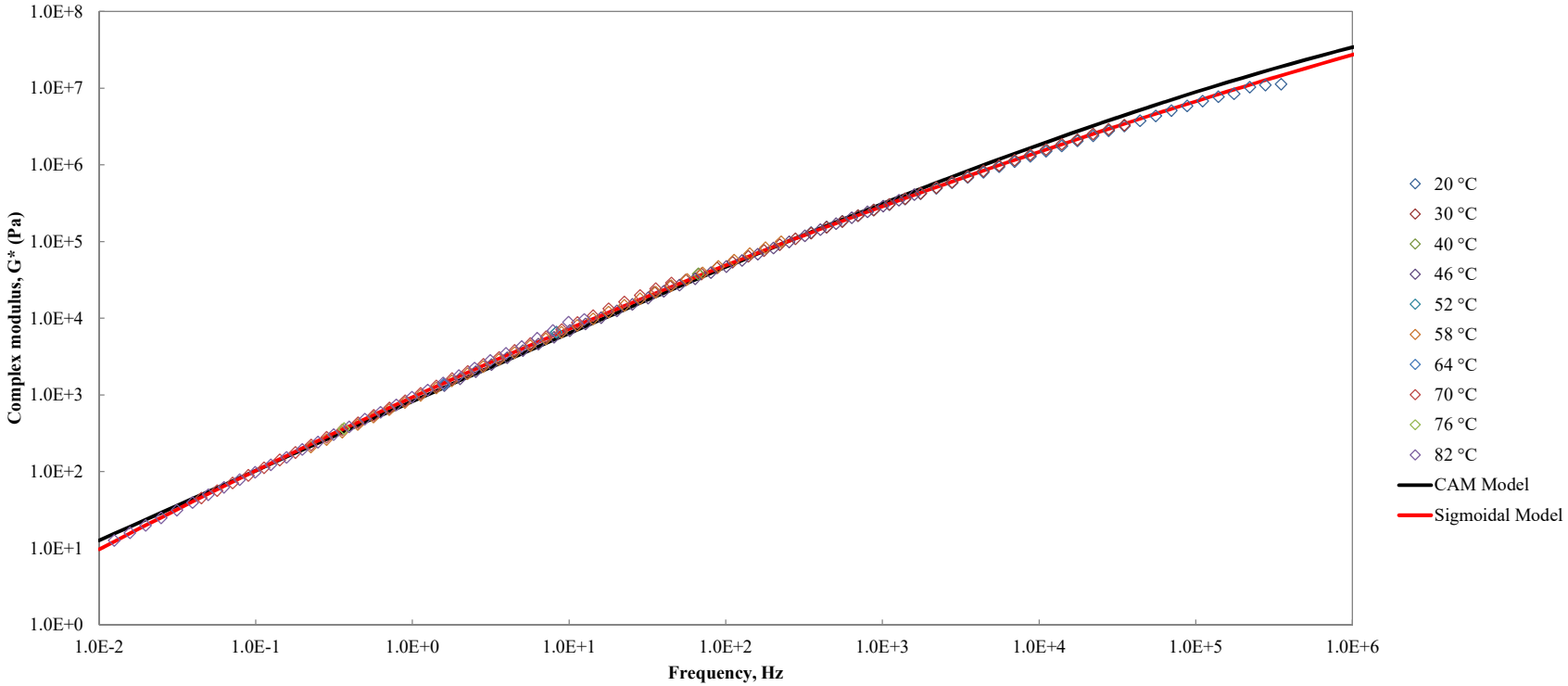

Figure C-21. Master curve of RTFO aged centrifuged CRYO tested with parallel plates – 1 mm gap, T_{ref} = 64 °C

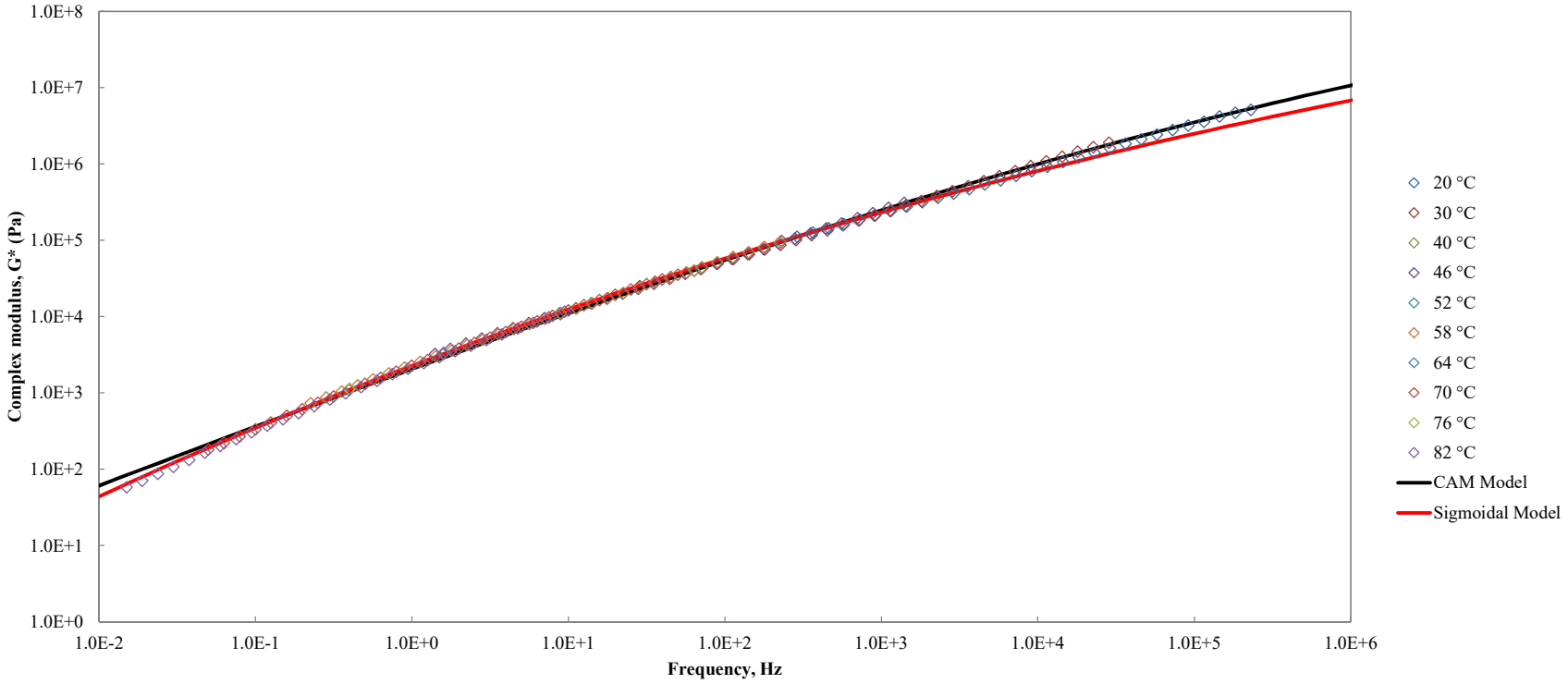

Figure C-22. Master curve of RTFO aged non-centrifuged CRYO 72 hrs cure tested with parallel plates – 1 mm gap, T_{ref} = 64 °C

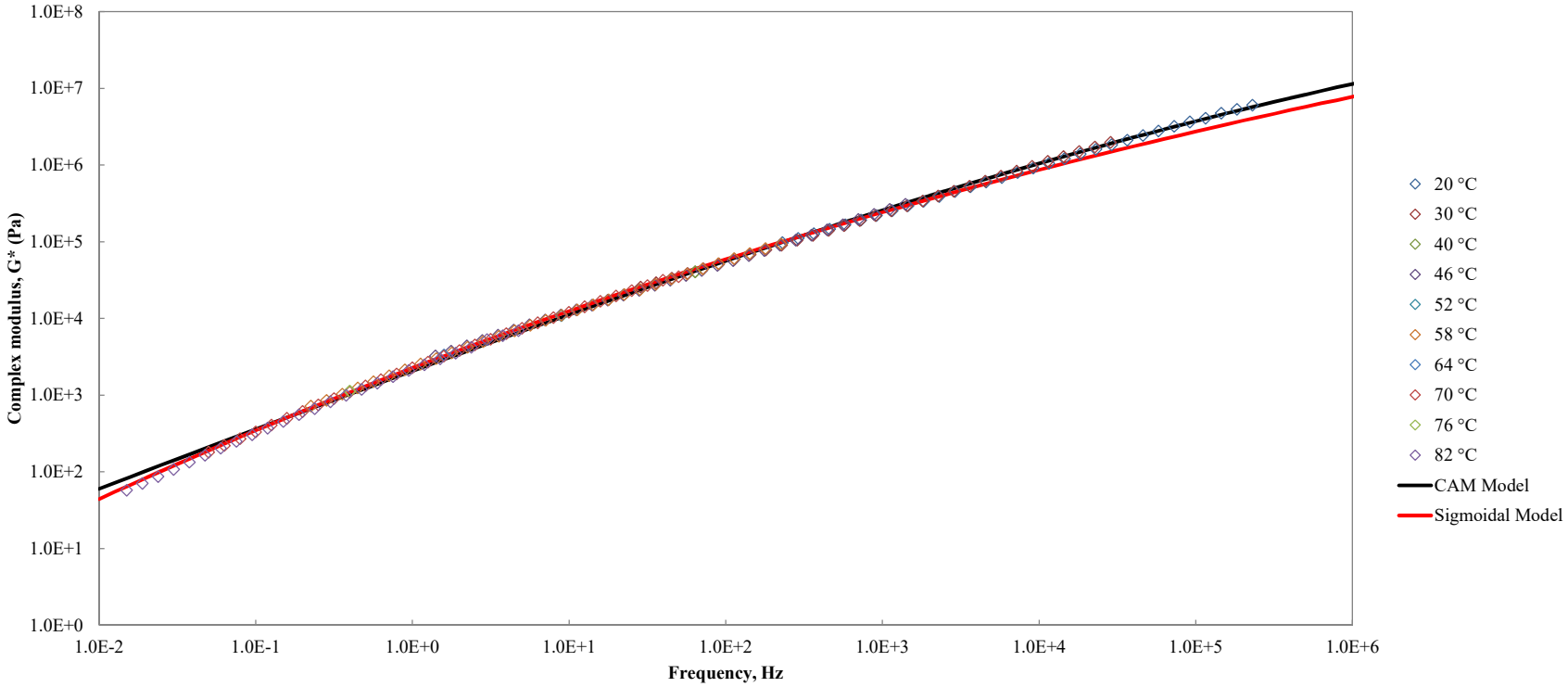

Figure C-23. Master curve of RTFO aged non-centrifuged CRYO 72 hrs cure tested with parallel plates – 2 mm gap, T_{ref} = 64 °C

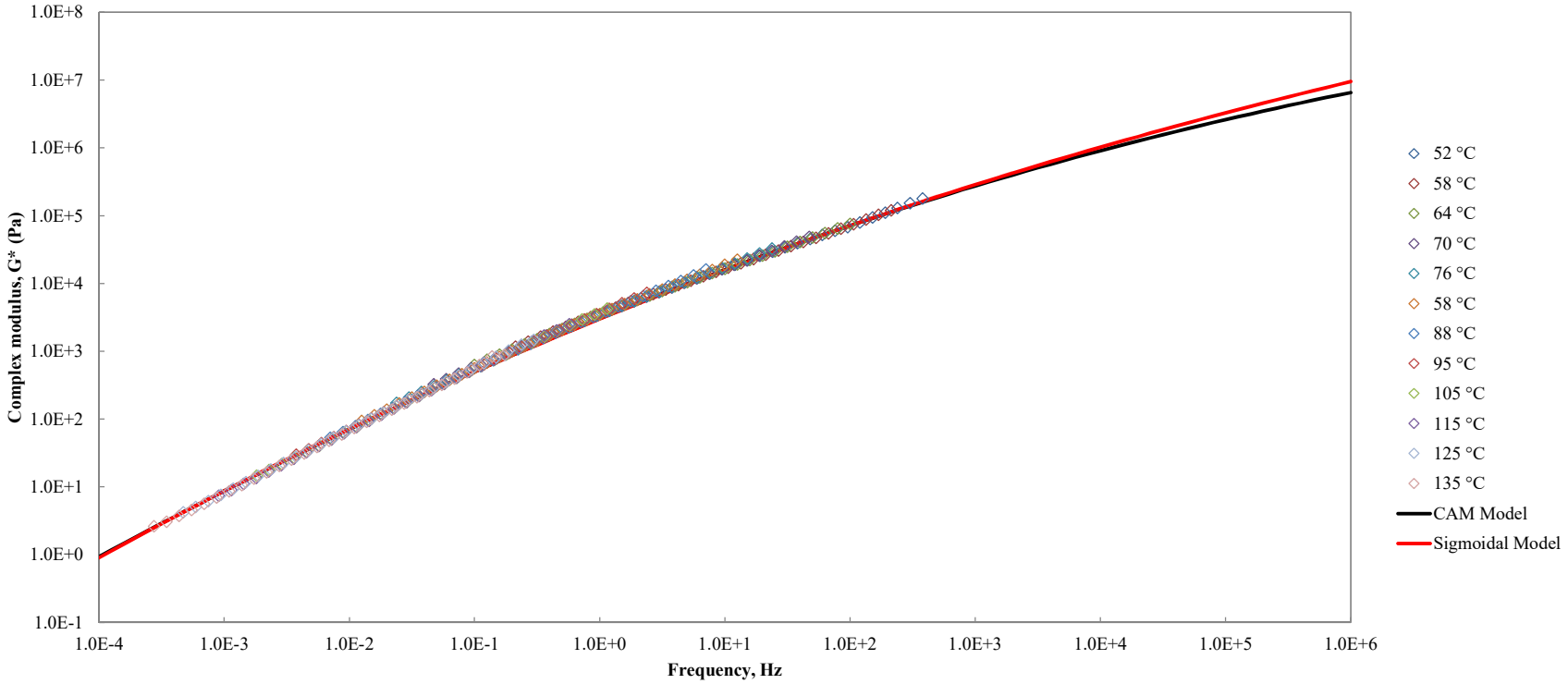

Figure C-24. Master curve of RTFO aged non-centrifuged CRYO 72 hrs cure tested with concentric cylinder, T_{ref} = 64 °C

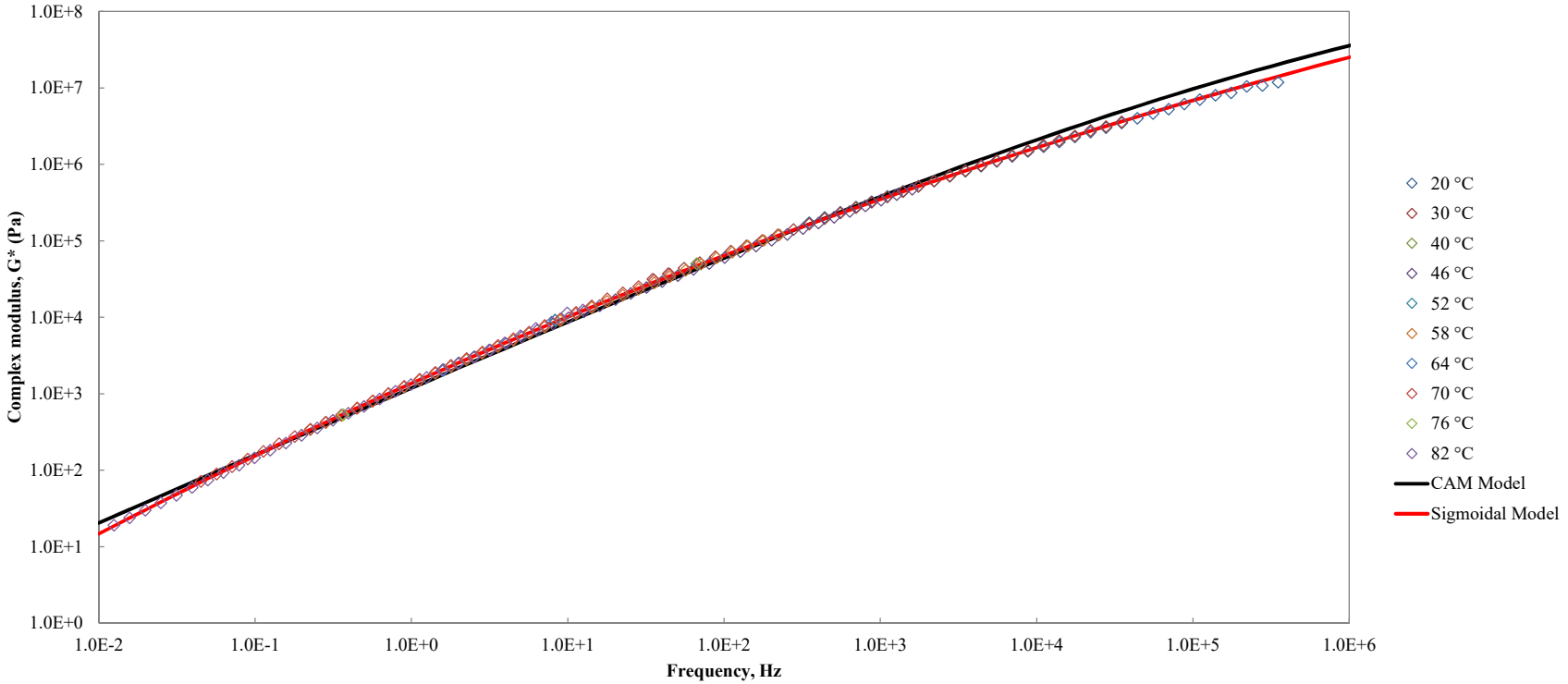

Figure C-25. Master curve of RTFO aged centrifuged CRYO 72 hrs cure tested with parallel plates – 1 mm gap, T_{ref} = 64 °C

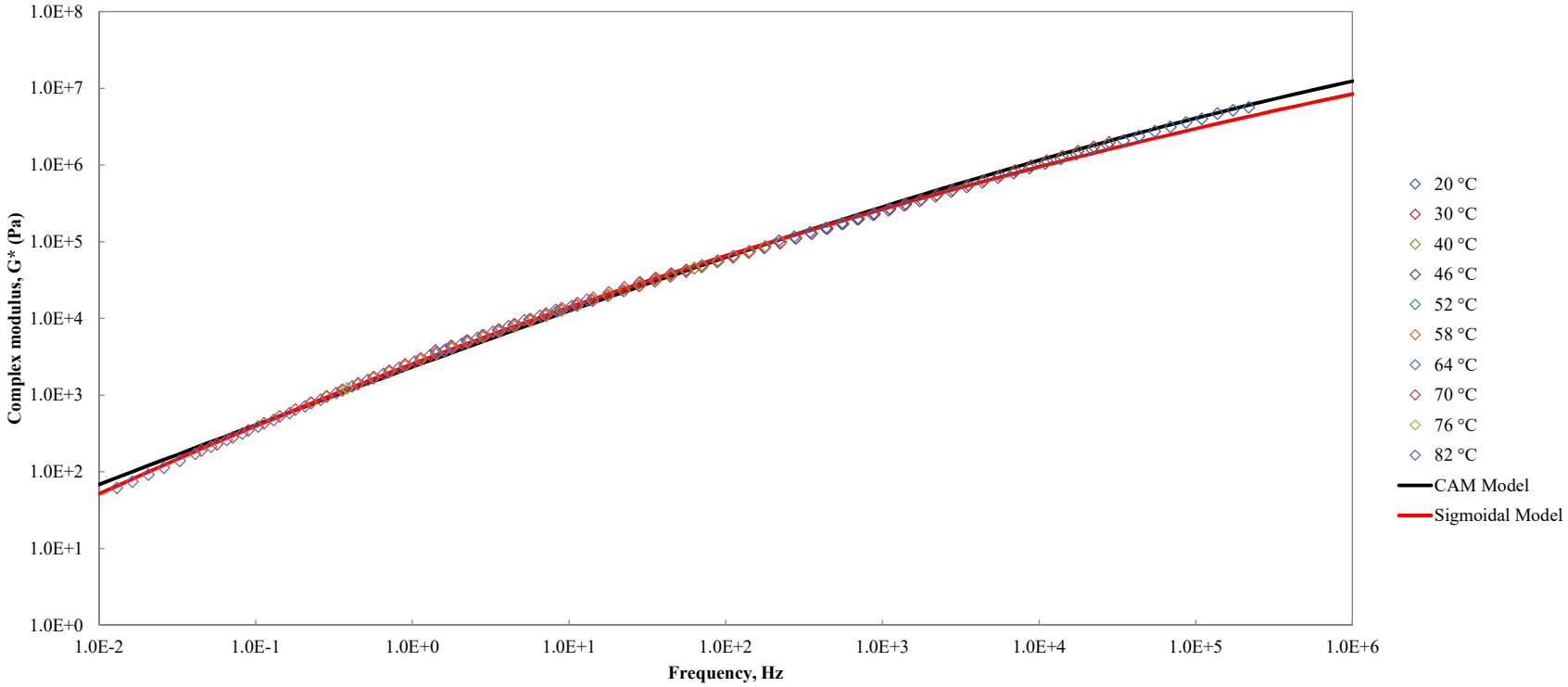

Figure C-26. Master curve of RTFO aged non-centrifuged CP tested with parallel plates – 1 mm gap, T_{ref} = 64 °C

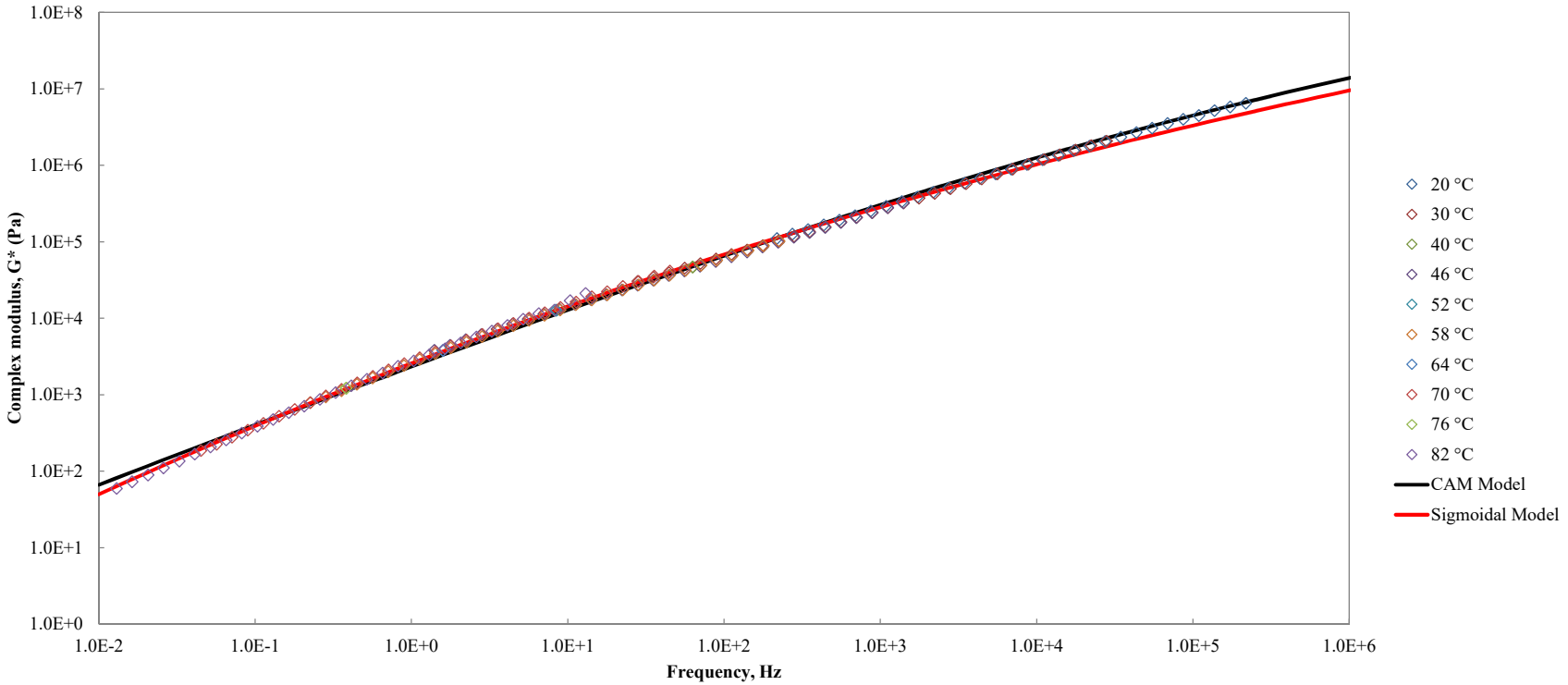

Figure C-27. Master curve of RTFO aged non-centrifuged CP tested with parallel plates – 2 mm gap, T_{ref} = 64 °C

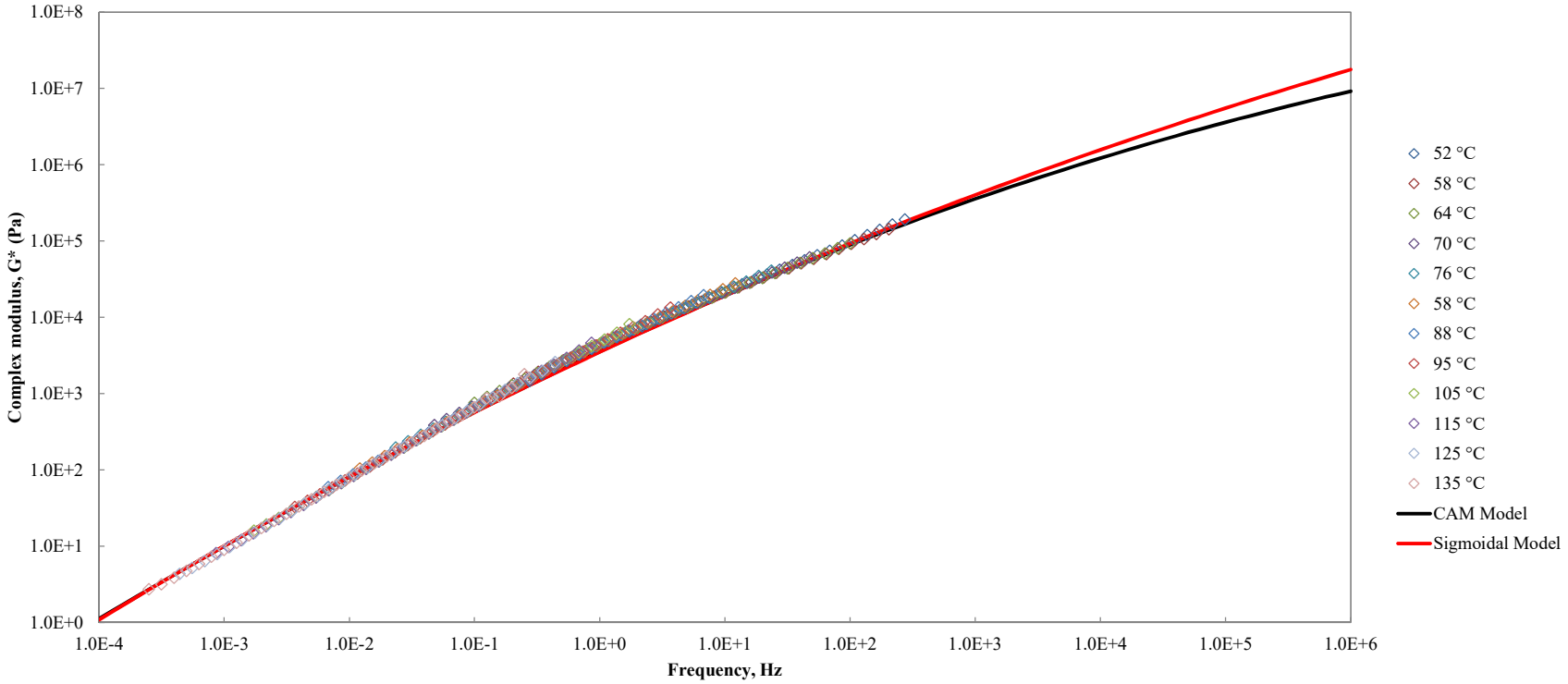

Figure C-28. Master curve of RTFO aged non-centrifuged CP tested with concentric cylinders, T_{ref} = 64 °C

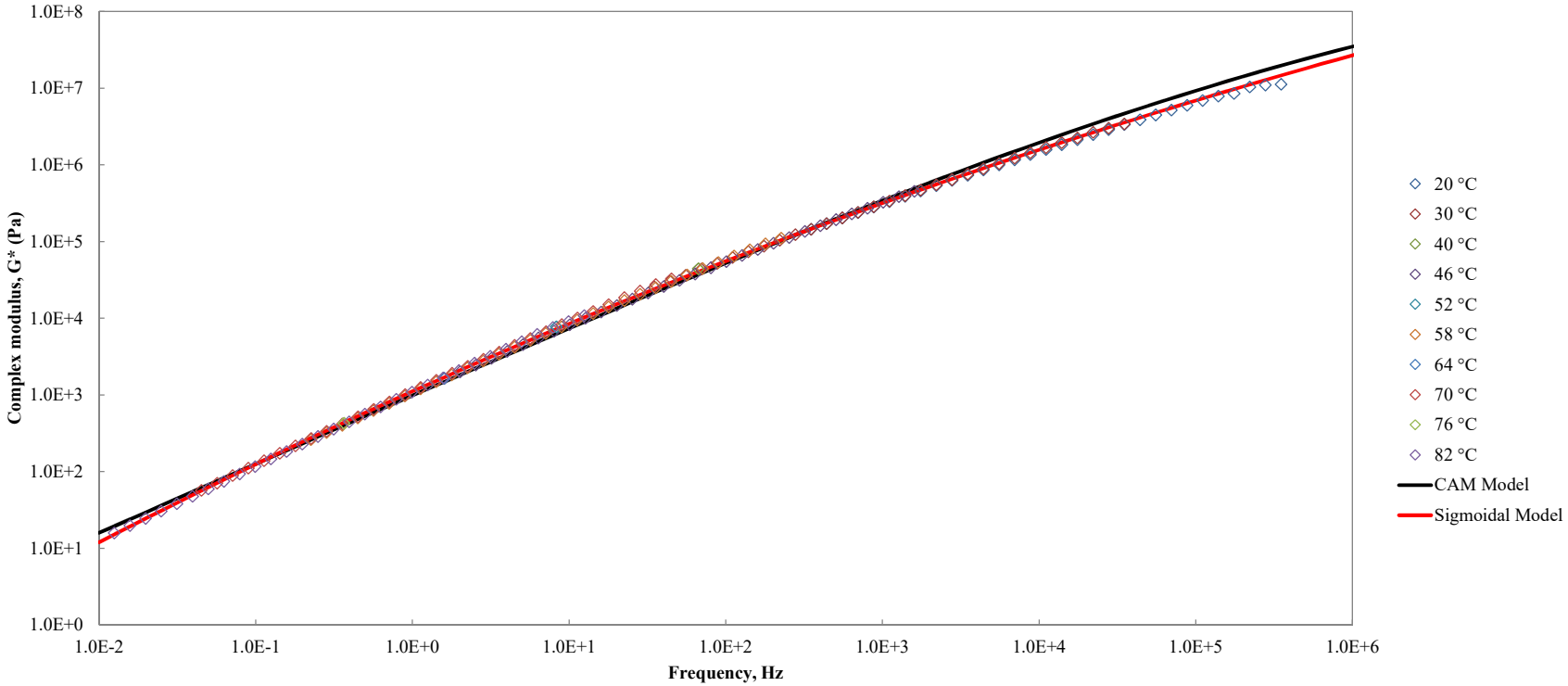

Figure C-29. Master curve of RTFO aged centrifuged CP tested with parallel plates – 1 mm gap, T_{ref} = 64 °C

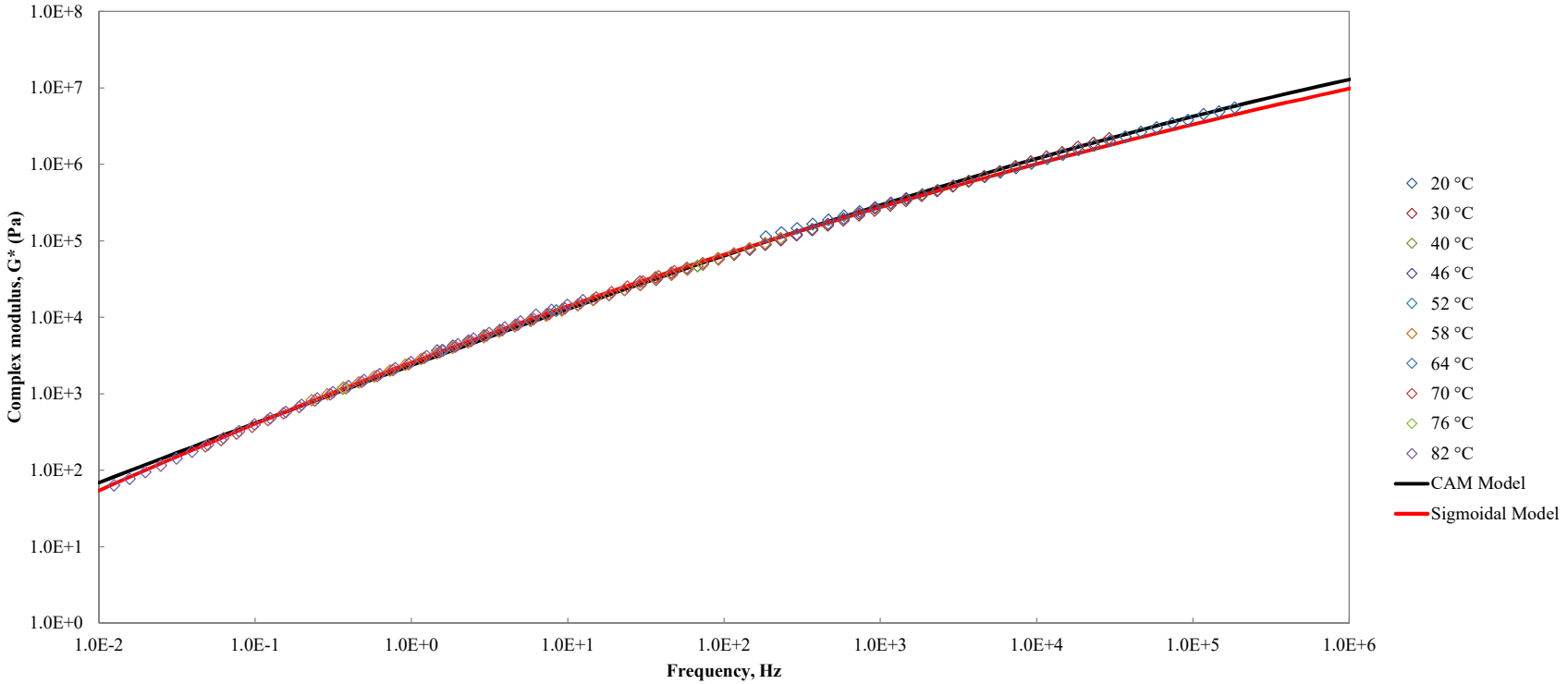

Figure C-30. Master curve of RTFO aged non-centrifuged CP 72 hrs cure tested with parallel plates – 1 mm gap, T_{ref} = 64 °C

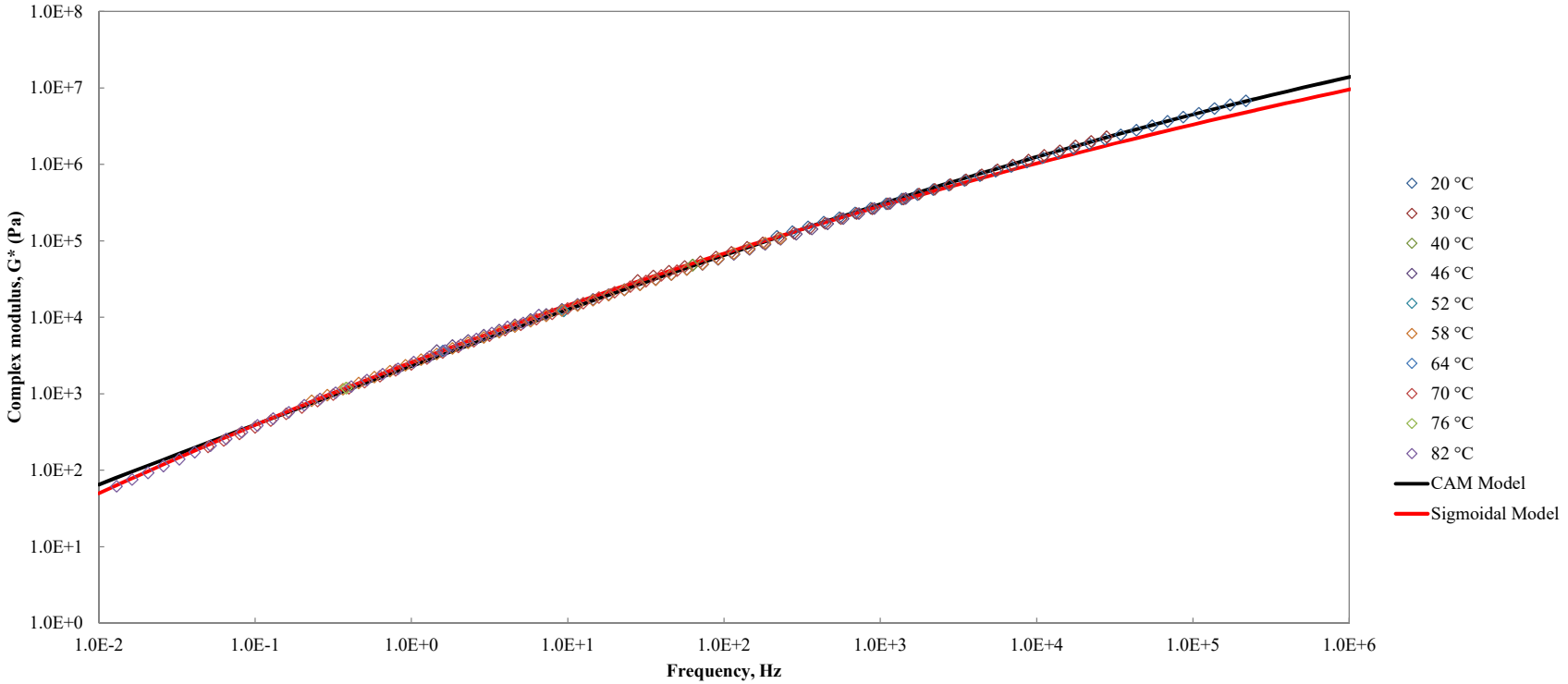

Figure C-31. Master curve of RTFO aged non-centrifuged CP 72 hrs cure tested with parallel plates – 2 mm gap, T_{ref} = 64 °C

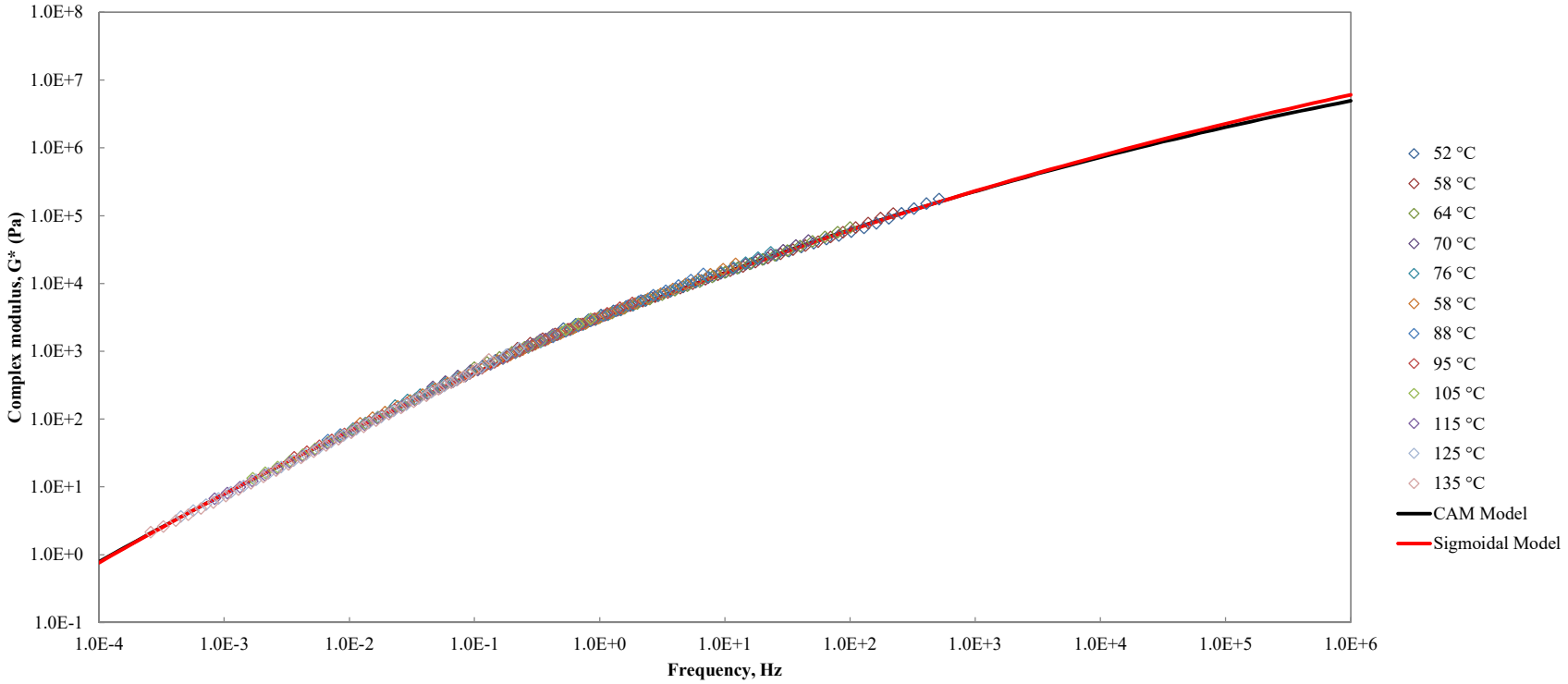

Figure C-32. Master curve of RTFO aged non-centrifuged CP 72 hrs cure tested with concentric cylinders, T_{ref} = 64 °C

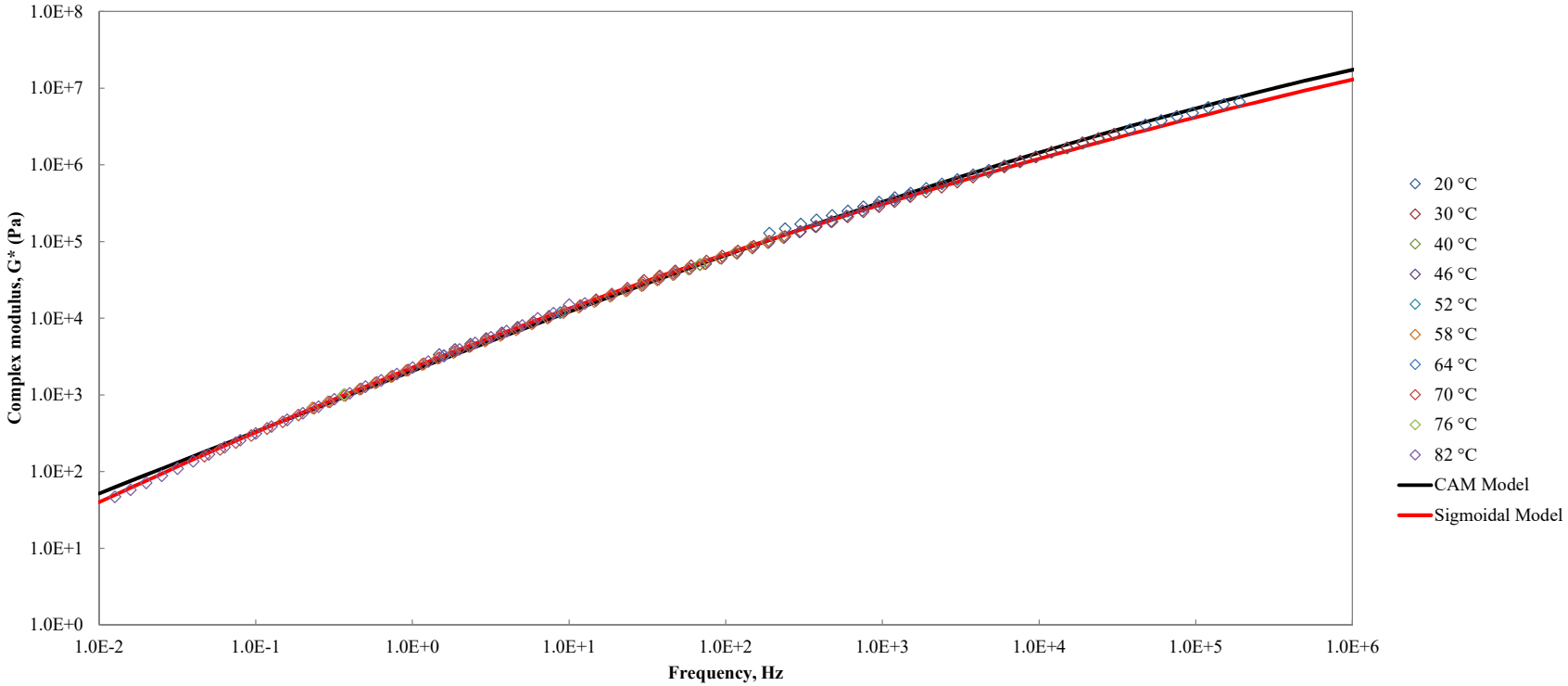

Figure C-33. Master curve of RTFO aged centrifuged CP 72 hrs cure tested with parallel plates – 1 mm gap, T_{ref} = 64 °C